UNIVERSITAT DE BARCELONA

Biomarcadores y genes relacionados con alteraciones en ganglios basales en la infancia

Laura Martí Sánchez

UNIVERSITAT DE BARCELONA

Sant Joan de Déu Research Foundation

Biomarcadores y genes relacionados con alteraciones en ganglios basales en la infancia

Laura Martí Sánchez

2020

Biomarcadores y genes relacionados con alteraciones en ganglios basales en la infancia

Memoria presentada por

Laura Martí Sánchez

para optar al grado de

Doctora

por la **Universitat de Barcelona**

Programa de Medicina i Recerca Translacional

Facultad de Medicina

Tesis realizada bajo la dirección de

la **Dra. Belén Pérez Dueñas** y de la **Dra. Roser Urreizti Frexedas**

y tutorizada por el **Dr**. **Antoni Noguera Julian**

en el **Hospital Sant Joan de Déu**

Barcelona, septiembre del 2020

A mis padres

A mi hermana

Agradecimientos

Tras unos 5 años de doctorado de subidas y bajadas y tras plasmar todos esos experimentos y resultados en un "libro" ahora viene lo complicado, escribir los agradecimientos.

Los que me conocéis sabéis que el don de la palabra no me fue concedido, así que seré breve, y que la música es muy importante en mi vida, por lo tanto, la utilizaré de guía. Agradecer primeramente a la fundación Sant Joan de Déu por su labor investigadora y permitirme la realización de esta tesis, y a los pacientes con alteraciones en los ganglios basales y trastornos del movimiento y familiares por su gran colaboración.

Podríamos decir que durante estos años he conseguido crear una gran banda, cuya obra interpretada ha sido esta tesis. Al fin y al cabo, el genoma humano no deja de ser una partitura que se va interpretando para crear distintas proteínas y elementos funcionales que hacen posible la vida. Mi doctorado ha sido un pequeño análisis de un fragmento de la misma. En esta ocasión, el compositor y solista me ha tocado ser a mí, pero nada hubiera sido posible sin el resto de cuerdas.

Todos los instrumentos de una banda son importantes y hacen que sea única. Por un lado, Metabolopatías ha sido la base de esta partitura, quienes me han ido manteniendo a flote. Sin una base sólida, se desmorona cualquier composición. Dar las gracias a Rafa por aceptarme desde el primer momento en esa pequeña familia. En este caso, tengo que destacar y agradecer personalmente a cada uno de los que formáis parte de ella. Como línea melódica, el grupo de trastornos del movimiento de Neuropediatría han acompañado en todo momento este doctorado. En especial a Dario y a Heidy, que han estado siempre complementando esta tesis con toda la parte clínica. Si a dos corcheas juntas (genética-clínica) le quitas una, el compás se queda incompleto. Por otro lado, está la que considero mi cuerda, el departamento de genética, siempre ayudando en cada bache en los protocolos. Agradecer a Judith toda la ayuda inicial, sin ella hubiera sido muy complicado empezar a componer algo decente. Y todo esto acompañado de toda la armonía que forman Biobanco, Radiología y, como no, el departamento de Gastro, donde he encontrado una segunda casa. Los últimos años también se han incorporado gente nueva a la banda, la gente del VHIR. Sin ellas, la parte funcional hubiera sido más complicada y no hubiera sabido qué es tener un postdoc que te ayude. Destacar por último la gran ayuda de los consejos recibidos por "madres" científicas desde Valencia.

Como en toda obra musical, cada uno ha ido ejerciendo un papel en cada momento del doctorado, que se han ido entrecruzando. A veces, en las partituras encontramos alteraciones accidentales (epigenética lo llaman en el campo de la genética), que no hacen sino modificar e influir en el significado sin quitarle la naturaleza a la nota. Cada una de las personas con las que me he ido cruzando y compartiendo estos años han actuado de una forma parecida. Esto, junto al timbre característico de cada una de ellas, me ha enriquecido mucho en el ámbito profesional y personal.

Tras un ensayo, también es importante desconectar. Te recarga la batería e incluso salen nuevas melodías en esos momentos. No puedo dejar de agradecer a las personas que comprueban como tesis alternativa que una *cerve* post-ensayo, funciona para seguir adelante (a falta de publicar), y aquellas que siempre están cuando bajas a descansar (gaviotas, musas, bandas varias…).

Y toda banda tiene su director. Cuando te pones a escribir frente a una partitura en blanco, se agradece tener alguien que te guie, te anime y te quite el miedo a seguir escribiendo. Agradecer

la labor de Belén y Roser en todo este tiempo. Sin alguien como guía para situar las notas, todo sería una locura.

Compartir la música que creas con un buen público hace que el disfrute sea mayor. Agradecer a Jose, a mis padres, a mi hermana y a mi familia, como reyes del apoyo moral y las críticas constructivas. Como público especial no se han perdido un ensayo y seguro que disfrutan del estreno. Sencillamente, gracias por estar.

Sin las notas de cada uno de vosotros, el resultado no hubiera sido el mismo. No tendría tesis suficiente para este apartado. Simplemente, gracias.

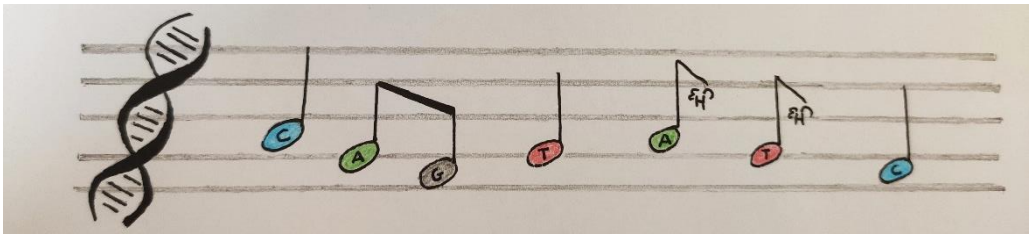

Componentes de la banda, en orden alfabético:

Metabolopatías: Abraham, Adriana, Aida, Aroa, Cristina, Delia, Juan, Judit, Laura Altimira, Mercedes, Montserrat, Rafa, Raquel, Rosa, Tania y Yahel

Gastro: Ana, Carmen Farré, Mari, Marta B, Marta M y Teresa

Genética: Ainhoa, Carlota, Clara, Dani, Dèlia, Jordi, Judith, Laura, Loreto, Núria, Patri, Paola, Sara y Silvia

Biobanco: Anna y Jesús

Neuropediatría: Alejandra, Dario, Heidy, María y Marta

Radiología: Jordi y Mónica

VHIR: Alfons, Anna, Francina, Heidy, Penélope y Silvia

Tesis alternativa (autores): Clara, Delia, Marta B y Marta M

‘‘Antes pensábamos que nuestro futuro estaba en las estrellas. Ahora sabemos que está en nuestros genes.” (James Watson)

Agradecimientos

ABREVIATURAS

ACMG *American College of Medical Genetics*

ADN Ácido desoxirribonucleico

AGS *Aicardi-Goutières síndrome* (síndrome de Aicardi-Goutières)

ALM *Amish lethal microcephaly* (microcefalia letal Amish)

ARN Ácido ribonucleico

CGH *Comparative genomic hibridation* (hibridación de genómica comparativa)

CI Complejo I de la cadena respiratoria mitocondrial

CII Complejo II de la cadena respiratoria mitocondrial

CIII Complejo III de la cadena respiratoria mitocondrial

CIV Complejo IV de la cadena respiratoria mitocondrial

CV Complejo V de la cadena respiratoria mitocondrial

CNV *Copy number variant* (variantes de cambio de copia)

EDTA Ácido etilendiaminotetraacético

FLAIR *Fluid-attenuated inversion recovery* (recuperación de inversión atenuada de fluido)

HGMD *Human Gene Mutation Database*

HIBCH Hidroxyisobutyril-CoA hydratasa

HPLC *High Performance Liquid Chromatography* **(**cromatografía líquida de alta eficacia)

HPO *Human Phenotype Ontology*

ICP-MS *Inductively Coupled Plasma-Mass Spectrometry* (espectrometría de masas con plasma acoplado inductivamente)

IVA *Isovaleric aciduria* (aciduria isovalérica)

LCR Líquido cefalorraquídeo

MLPA *Multiplex Ligation-dependent Probe Amplification* (amplificación de sondas dependiente de ligandos múltiples)

MMA *Methylmalonic aciduria* (aciduria metilmalónica)

MRS *Magnetic resonance spectroscopy* (espectroscopia de resonancia magnética)

NBIA *Neurodegeneration with brain iron accumulation* (neurodegeneración con acúmulos cerebrales de hierro)

NCBI *National centre of biotechnology information* (centro nacional de información biotecnológica)

NEB Necrosis estriatal bilateral

NGS *Next generation sequencing* (secuenciación de nueva generación o secuenciación masiva)

NR No reportado

OMIM *Online Mendelian Inheritance in Man*

PA *Propionic aciduria* (aciduria propiónica)

PCR *Polymerase chain reaction* (reacción en cadena de la polimerasa)

PDH Piruvato deshidrogenasa

PFBC *Primary familiar brain calcifications* **(**calcificaciones cerebrales familiares primarias)

PPI Interacciones proteína-proteína

RMC Resonancia magnética cerebral

RNA-seq Ribonucleica cid sequencing (secuenciación de ARN)

SCEH *Short chain enoyl-coA hydratase*

TC Tomografía computarizada

TFIID *Transciption factor IID* (factor de transcripción IID)

TMP Tiamina monofosfato

TPP Tiamina pirofosfato

TRMA *Thiamine-responsive megaloblastic anemia* (anemia megaloblástica sensible a tiamina)

TSO *TruSight One* (panel exoma clínico de Illumina)

TTP Tiamina trifosfato

WES *Whole exome sequencing* (secuenciación de exoma completo)

WGS *Whole genome sequencing* (secuenciación de genoma completo)

INTRODUCCIÓN

1. Ganglios basales

Los ganglios basales son estructuras cerebrales subcorticales implicadas en el control motor y el aprendizaje. Los componentes del núcleo de los ganglios basales son el globo pálido y el neoestriado, formado por el caudado y el putamen[1] (Figura 1). El núcleo lentiforme está formado por el putamen y el globo pálido y se sitúa lateralmente y en profundidad en los hemisferios, dentro de la sustancia blanca central.

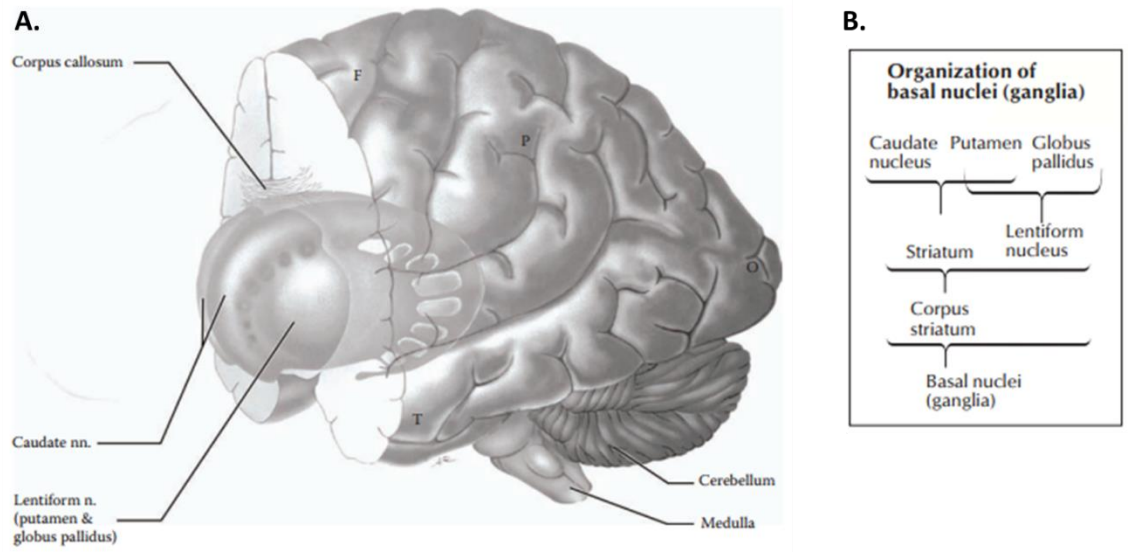

Figura 1: (A): Orientación de los ganglios basales F: lóbulo frontal; P: lóbulo parietal; T: lóbulo temporal; O: lóbulo occipital. (Atlas of Functional Neuroanatomy, 2006[2]).(B): Organización de los ganglios basales (Atlas of Neuroanatomy and Neurophysiology, 2002[3]).

La organización funcional de los ganglios basales está basada en múltiples bucles que forma una red compleja, diseñada para seleccionar e inhibir simultáneamente eventos y señales. En estas redes, las áreas motoras, asociativas y límbicas están implicadas principalmente en el control del movimiento, el comportamiento y las emociones. Sus funciones principalmente son la selección y facilitación de nuevas actividades y tareas, aprendizaje para crear nuevas respuestas habituales automáticas por el circuito motor y capacidad de detener y empezar una nueva actividad en curso[1].

Las lesiones de estas estructuras en la edad pediátrica están asociadas normalmente a un retraso psicomotor y/o regresión de las habilidades adquiridas, trastornos de movimiento, trastornos de la conducta y emocionales, y una notable discapacidad. Estas lesiones pueden observarse en una imagen de resonancia magnética cerebral (RMC) como hiperintensidad en la secuencia T2, edema citotóxico, cavitación, depósitos de elementos

traza, hipomielinización y atrofia[4,5], y en una tomografía computarizada (TC) como hipo o hiperdensidades, sugestivas de edema y/o calcificaciones.

Las lesiones en ganglios basales que afectan a la infancia pueden ser debidas a causas adquiridas. En periodo perinatal destaca la hiperbilirubinemia neonatal, la encefalopatía hipóxico-isquémica y las lesiones vasculares. En época post-natal pueden producirse por procesos tumorales, vasculares, traumáticos, infecciosos o autoinmunes[6].

Asimismo, existe un grupo numeroso y heterogéneo de causas genéticas asociadas a enfermedades neurometabólicas y neurodegenerativas que afectan a los ganglios basales en la infancia. Entre ellas se encuentra el síndrome de Leigh[7,8], la neurodegeneración con acúmulos cerebrales de hierro (NBIA, por sus siglas en inglés)[9], el síndrome de Aicardi-Goutières (AGS, por sus siglas en inglés)[10], los defectos del transporte y metabolismo de la tiamina[11], otros errores congénitos del metabolismo intermediario y lisosomal, los defectos genéticos que causan depósito en ganglios basales de elementos traza como el cobre o el manganeso[12], las enfermedades que cursan con hipomielinización y atrofia[13], etc.

2. Patologías asociadas con lesiones en los ganglios basales

En el siglo XX, las lesiones en el putamen, globo pálido y los núcleos subtalámicos estaban asociados al Parkinson, distonía y espasticidad[14]. Hoy en día, muchas patologías diferentes están asociadas a estas lesiones. En esta propuesta de tesis, hemos trabajado con una clasificación de lesiones en ganglios basales según tres patrones radiológicos: (a) lesiones necróticas y/o edematosas produciendo hiperintensidad en las secuencias T2/FLAIR, (b) calcificaciones con aspecto de hiperintensidad en T1 y/o hiperdensidad en TC, (c) depósitos de sustancias paramagnéticas produciendo hipointensidad en T2/FLAIR y en secuencias de susceptibilidad magnética como SWI/GRE; y (d) lesiones no clasificables en los grupos anteriores. Los genes relacionados con estas patologías están clasificados y esquematizados en la Tabla 1. Los genes y fenotipos asociados a estas patologías están referenciados con su número MIM en la Tabla A1. Los fenotipos clínicos utilizados están correlacionados con su código HPO (*Human Phenotype Ontology*, en inglés) en la Tabla A2.

Fenotipos	Genes
Edema y/o necrosis	
Enfermedades mitocondriales	*AIFM1, BCS1L, BOLA3, BTD, C12ORF65, CLPB, COQ9, COX10, COX15, COX8A, DLAT, DLD, DNM1L, EARS2, ECHS1, ETHE1, FARS2, FBXL4, FOXRED1, GFM1, GFM2, GTPBP3, HIBCH, IARS2, LIAS, LIPT1, LRPPRC, MFN2, MPV17, MRPS34, MRPS39, MTATP6, MTCO3, MTFMT, MTND1, MTND2, MTND3, MTND4, MTND5, MTND6, MTTI, MTTK, MTTL2, MTTL1, MTTV, MTTW, NARS2, NDUFA1, NDUFA10, NDUFA12, NDUFA2, NDUFA4, NDUFA9, NDUFAF2, NDUFAF4, NDUFAF5, NDUFAF6, NDUFAF8 (C17ORF89), NDUFB8, NDUFS1, NDUFS2, NDUFS3, NDUFS4, NDUFS6, NDUFS7, NDUFS8, NDUFV1, NDUFV2, NUBPL, NUP62, PDHA1, PDHB, PDHX, PDSS2, PET100, PNPT1, POLG, POLG2, RANBP2, RNASEH1, RRM2B, SCO2, SDHA, SDHAF1, SDHB, SERAC1, SLC25A4, SLC25A46, SLC39A8, SPG7, SQUOR, SUCLA2, SUCLG1, SURF1, SYNE1, TACO1, TRMU, TSFM, TTC19, TWNK, UQCRQ*
Defectos del transporte y metabolismo de la tiamina	*SLC19A2, SLC19A3, SLC25A19, TPK1*
Otras: acidemia glutárica tipo I, defecto de la dehidrogenasa semialdehido succínica, déficit sulfito oxidasa, defecto NUP62, acidurias orgánicas clásicas, leucodistrofias, enfermedades lisosomales…	*GCDH, ALDH5A1, SUOX, NUP62, PCCA, PCCB, MMA, MMAA, MMAB, MUTACIÓN, IVD, VWL, HLD7, SEMDHL, GLB1*
Calcificaciones	
Calcificaciones cerebrales familiares primarias	*SLC20A2, PDGFRB, PDGFB, XPR1, MYORG, JAM2*
Síndrome de Aicardi-Goutières	*TREX1, RNASEH2B, RNASEH2A, RNASEH2C, SAMHD1, ADAR, IFIH1*
Otros: síndrome Coat, déficit POLG, MELAS, Kearns-Sayre, Moyamoya, hipoparatiroidismo primario, pseudohipoparatiroidismo, síndrome Cockayne, síndrome Keutel, síndrome Raine, enfermedad Nasu Hakola, errores congénitos del metabolismo de folato, ocludina, defectos colágeno IV, disqueratosis congénita...	*CTC1, NDP, POLG, MTTL1, MTTQ, MTTH, MTTK, MTTC, MTTS1, MTND1, MTND5, MTND6, MTTS2,* deleciones en el ADNmt*, ISG15, RNF213, SMARCAL1, PTH, CASR, GNA11, GCM2, GNAS, STX16, DDB2, ERCC1, ERCC2, ERCC3, ERCC4, ERCC5, ERCC6, ERCC8, GTF2H5, MPLKIP, POLH, XPA, XPC, MGP, FAM20C, TYROBP, TREM2, FOLR1, SLC46A1, MTHFR, DHFR, MTFD1, OCLN, COL4A1, COL4A2, DKC1, TERC, TERT, TINF2, NHP2 (NOLA), NOP10 (NOLA3), WRAP53, RTEL1, JAM3, CA2, PANK2, QDPR, CYP2U1, GALC, C1QB, ISG15, FGF23, TBX1, TBCE, FAM111A, NF1, NF2, TSC1, TSC2, FLVCR2, GJA1, HEXA, HEXB, ATN1, GFAP, ARSA, ABCD1, AVP, WFS1, AVPR2, AQP2, SLC12A3, PAH, PSMB8, PCDH12*
Depósitos de sustancias paramagnéticas	
Neurodegeneración con acúmulos cerebrales de hierro	*PANK2, PLA2G6, C19ORF12, FA2H, WDR45, COASY, FTL1, ATP13A2, CP, DCAF17*
Enfermedad de Wilson	*ATP7B*
Hipermanganesemia	*SLC39A14, SLC30A10*
Otras lesiones	
Hipomielinación y atrofia	*TUBB4A, POLR3A, POLR3B*

Tabla 1: Genes asociados a los distintos fenotipos relacionados con alteraciones en los ganglios basales. ADNmt: ADN mitocondrial.

2.1. Enfermedades que cursan con hiperintensidad en los ganglios basales en la secuencia T2

Las causas genéticas más comunes que presentan hiperintensidad bilateral en una secuencia T2 en los ganglios basales son las enfermedades mitocondriales y los defectos del transporte y metabolismo de la tiamina.

El fenotipo más característico que presentan los pacientes con estas patologías es el síndrome de Leigh. Este síndrome fue descrito en 1951 por Denis Leigh como una encefalopatía con lesiones necrotizantes subagudas de forma bilateral, simétrica y focal en los ganglios basales[15]. Se considera una enfermedad rara ya que su prevalencia es de 1:120000 nacidos para mutaciones mitocondriales y 1:40000 para ADN nuclear. Actualmente, el síndrome de Leigh ha sido asociado con más de 110 genes[16–20] y 265 mutaciones patológicas (HGMD Professional 2019.4, acceso mayo 2020).

En esta introducción se ha caracterizado el síndrome de Leigh mediante una revisión incluyendo 385 pacientes de una revisión anterior[21] que engloba cinco estudios[20,22–25] y 10 pacientes de las publicaciones posteriores a dicha revisión[18,19,26–29] (Figura 2). Entre estos pacientes, el 42% eran varones, 31% mujeres y el 27% de casos restantes no estaba especificado el sexo del individuo. En el 77.6% de los pacientes (n=213) el debut de la enfermedad había sido anterior a los 2 años. Un debut en la infancia está desencadenado principalmente por cambios metabólicos en situaciones de mayor estrés (infección, vacunación o traumatismo), produciendo un fallo energético[6,22]. Las características clínicas de estos pacientes están detalladas en la Figura 2A. Radiológicamente, aparte de los ganglios basales, pueden estar afectadas otras estructuras cerebrales (detalladas en la Figura 2B).

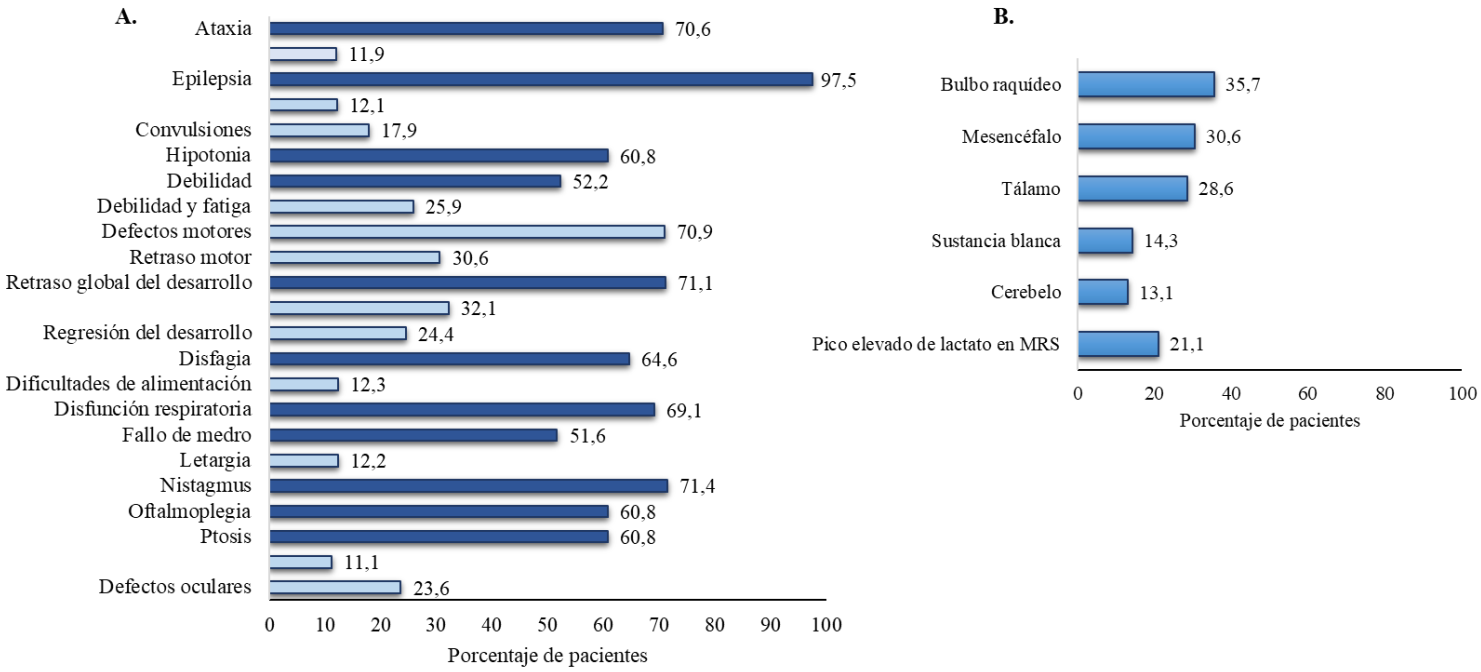

Figura 2: Descripción de los síntomas clínicos y características radiológicas de 395 pacientes con síndrome de Leigh organizados según su prevalencia, basada en una revisión de la literatura médica hasta Julio 2020. (A). Se muestran los síntomas clínicos al debut (barras azul claro) y durante el curso de la enfermedad (barras azul oscuro) indicando el porcentaje de pacientes que los presentan. (B). Se indican las características radiológicas de estos pacientes. MRS: espectroscopia de resonancia magnética, siglas en inglés.

La elevación de lactato en sangre, plasma y/o líquido cefalorraquídeo (LCR) se encuentra en el 62.5% de los pacientes (n=247). Sofou et al[22] asoció la elevación de lactato con un debut agudo anterior a los 6 meses asociado a una alteración del bulbo raquídeo y un curso más severo de la enfermedad. Otra de las características bioquímicas comunes en los pacientes con síndrome de Leigh es el déficit de cadena respiratoria mitocondrial, presentando una deficiencia aislada del complejo I (121/387, 31%), combinada de complejos (79/387, 20%), deficiencia del complejo IV (51/387, 13%) y una deficiencia del complejo V (23/387, 6%)[30]. Un 19% de los pacientes (74/387) presentaron una cadena respiratoria normal.

La aproximación terapéutica utilizada en estos casos es la suplementación de cofactores como tiamina y biotina, compuestos como coenzima Q10, L-carnitina, ácido lipoico o riboflavina y dietas específicas en pacientes con déficit alimenticio o dietas cetogénicas en pacientes con defectos en la piruvato deshidrogenasa (PDH)[31].

Las mutaciones en estos pacientes con síndrome de Leigh en genes nucleares son igual de frecuentes que aquéllas en genes mitocondriales (Figura 3A). Los genes más comunes están representados en la Figura 3B-C.

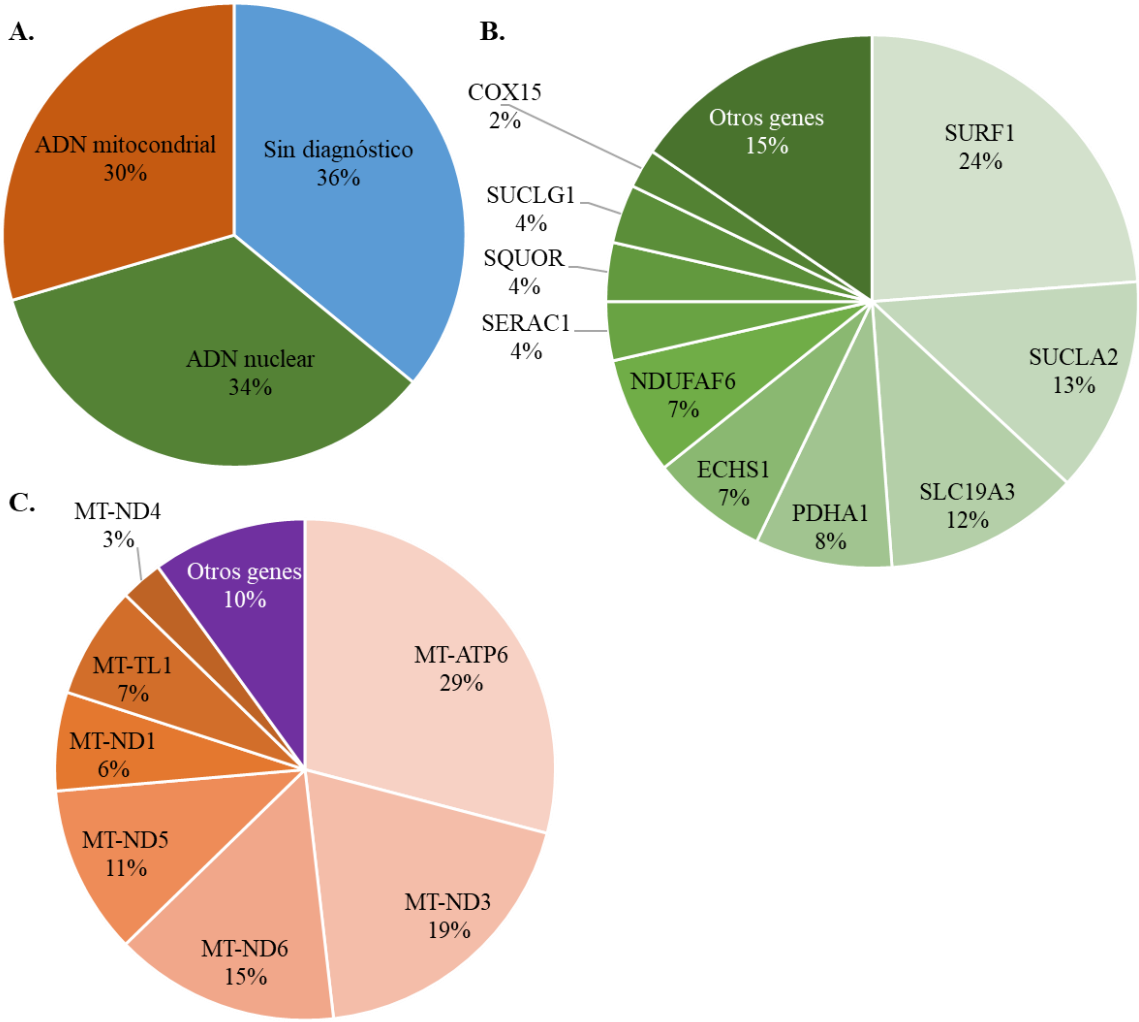

Figura 3: Mutaciones en pacientes con síndrome de Leigh. (A). En 281 pacientes, 84 pacientes (29.9%) portan mutaciones en el ADN nuclear, 83 pacientes (29.5%) portan cambios mitocondriales y 114 (40.6%) continúan sin diagnóstico molecular. (B). De los 84 pacientes con mutaciones nucleares prevalecen aquellos con cambios en el gen *SURF1* (20 pacientes). Aquellos genes mutados en un solo paciente de la cohorte (1.2%) representados en "otros genes" son: *BOLA3, C12orf65, GTPBP3, HIBCH, NDUFA1, NDUFA2, NDUFS4, NDUFS6, NDUFV1, NDUFV2, RRM2B, SCO2* y *SDHB*. (C). En 197 pacientes con síndrome de Leigh y mutaciones

en el ADN mitocondrial (incluyendo los 83 pacientes anteriores y 114 pacientes de artículos con estudios únicamente de secuenciación de ADN mitocondrial) el gen que más prevalece es el *MT-ATP6* (en 32 pacientes). Aquellos genes mutados en un solo paciente de la cohorte (1%) representados en "otros genes" son: *MT-ND2, MT-RN-R1, MT-TK, MT-TE, MT-tRNA-Ala, MT-tRNA-Arg, MT-tRNA-GlnCOXII, MT-tRNA-Glu* y *MT-TW.*

2.1.1. Enfermedades mitocondriales

Las enfermedades mitocondriales son un grupo de patologías genéticas que afectan principalmente la fosforilación oxidativa mitocondrial[32]. La clasificación como enfermedad mitocondrial sigue cuatro criterios establecidos por Morava en 2006[33], y revisados en 2018[34]. La prevalencia de estas enfermedades en pacientes con un debut en la infancia es de unos 5/10000[35], mientras que en adultos es 9.6/100000 para mutaciones de ADN mitocondrial y 2.8/00000 para causas genéticas nucleares[36]. Clínica y radiólogamente, estos niños presentan un síndrome de Leigh (Figura 2A-B). El debut en adultos es menos severo e incluye otros síntomas clínicos como la oftalmoplejia, sordera y diabetes y progresando en una demencia en pacientes que presentas convulsiones y episodios de apoplejía[37].

El diagnóstico de las enfermedades mitocondriales es complicado ya que mutaciones en los mismos genes pueden dar lugar a fenotipos distintos así como un gran número de genes que afectan la función mitocondrial puede causar un mismo cuadro clínico[33]. El 67% de los pacientes mitocondriales presentan mutaciones nucleares mientras que cambios en el ADN mitocondrial están presentes en el 33% de los casos[34]. Se han descrito mutaciones en 36 genes mitocondriales y 295 genes nucleares[38,39]. La genética del ADN mitocondrial es compleja debido a las múltiples copias de ADN mitocondrial que hay en cada célula. Se considera que un cambio patológico en el ADN mitocondrial causa un fenotipo bioquímico cuando se encuentra con una heteroplasmia >70%[37].

2.1.2. Defectos del transporte y metabolismo de la tiamina

La tiamina, o vitamina B1, es una vitamina soluble en agua que se presenta en los humanos como tiamina libre, tiamina monofosfato (TMP), tiamina pirofosfato (TPP) y tiamina trifosfato (TTP). Esta vitamina es sintetizada por plantas, hongos y bacterias[40]. Los humanos obtienen la tiamina de la dieta, leche materna[41] y la microflora[42] como TPP en el intestino donde es defosforilada[43,44] a tiamina libre y transportada con

transportadores específicos. La excreción de tiamina se realiza principalmente por orina[44], pero también puede excretarse en las heces o sudor[45].

Las deficiencias de tiamina pueden ser debidas a causas adquiridas o hereditarias (Tabla 2), ambas con un debut infantil.

Causas	Adquiridas		*SLC19A2*	*SLC19A3*	*SLC25A19*		*TPK1*
Fenotipo	Beriberi infantil	Encefalopatía de Wernicke	Síndrome de Roger	Síndrome de Leigh/Wernicke	Microcefalia letal Amish	Síndrome de disfunción del metabolismo de tiamina 4	Síndrome de Leigh/Encefalopatía episódica
Número de pacientes reportados	>170	>300	>210	>140	61	8	15
Clínica al debut	-	Dolor de cabeza, problemas gástricos, irritabilidad, fatiga	Diabetes, anemia	Dificultades de alimentación, letargia, convulsiones, aflicción respiratoria, encefalopatía	-	Encefalopatía, debilidad	Encefalopatía, distonía
Desencadenante	Ingesta inadecuada de tiamina	Malnutrición o mala absorción de tiamina tras un trasplante o cirugía	-	Infección, traumatismo, ejercicio intenso, vacuna	Fiebre, infección	Enfermedad febril	Infección o deshidratación
Principales características clínicas	Signos neurológicos, sistémicos, cardiovasculares, respiratorios, oftalmoplejia, convulsiones, hipotonía	Ataxia, oftalmoplejia, pérdida de conocimiento	Anemia megaloblástica, diabetes mellitus no autoinmune, sordera sensorineural	Epilepsia, retraso psicomotor, encefalopatía, irritabilidad	Microcefalia, retraso del desarrollo, irritabilidad, convulsiones, encefalopatía	Encefalopatía, neuropatía periférica	Encefalopatía, ataxia, distonía, disartria, convulsiones, oftalmoplejia, nistagmos, regresión psicomotora

Causas	Adquiridas		*SLC19A2*	*SLC19A3*	*SLC25A19*		*TPK1*
Otras características clínicas	Taquipnea, dificultad respiratoria, taquicardia, cardiomegalia, afonia, coreo-atetosis	Hipotensión, taquicardia, hipotermia, convulsiones	Convulsiones, ataxia, retraso del desarrollo, apoplejía, cuadriplejía espástica, atrofia cerebral, alteraciones oftalmológicas, estatura baja, criptorquidia, síndrome de ovario poliquístico, cardiomiopatías, hepatomegalia, reflujo gastroesofágico, trombocitopenia, neutropenia, tiroiditis inmune, nódulos vocales, talipes	Distonía, hipotonía, espasticidad, convulsiones, ataxia, corea, temblor, disartria, disfunción bulbar, oftalmoplejia, diplopía, nistagmo, estrabismo, ptosis, opistótonos, enfermedad hepática, disfagia, ictericia, insuficiencia respiratoria, pérdida de peso, vértigo, rigidez, rabdomiólisis	Polineuropatía axonal, debilidad distal y contracturas, distonía, disfagia, convulsiones, trastorno por déficit de atención	-	-
Radiología	Pálido, tálamo, bulbo raquídeo	Tálamo	Caudado, putamen, áreas cortico / subcorticales, tálamo, sustancia blanca	Caudado, putamen, tálamo, corteza cerebral, tronco encefálico, cerebelo	Hipoplasia en tronco encefálico, cerebelo, cuerpo calloso	Caudado, putamen, neoestriado, cavitación	Cerebelo, núcleos dentados, estriado, globo pálido, médula espinal
Bioquímica	Lactato elevado en suero, déficit de tiamina	-	Déficit de tiamina libre y TMP en plasma	Lactato elevado en sangre / LCR, ácidos orgánicos alterados, disminución de tiamina libre en LCR	Acidosis láctica y excreción de ácido 2-cetoglutarico, lactato elevado en LCR	-	Acidosis láctica, lactato elevado en LCR, ácidos orgánicos alterados, disminución de TPP en sangre

Tabla 2: Características clínicas, bioquímicas y radiológicas de las deficiencias del metabolismo y transporte de tiamina.

Las causas adquiridas agrupan al Beriberi infantil y la encefalopatía de Wernicke. El Beriberi infantil se presenta en lactantes cuyas madres tienen una ingesta inadecuada de tiamina o aquellos que toman una fórmula con bajo contenido en esta vitamina[46], siendo más común en países donde se consume cereales refinados y otras fuentes de tiamina no son consumidas habitualmente (carne, pescado y vegetales)[11,46]. La encefalopatía de Wernicke está causada principalmente tras un trasplante o una cirugía del intestino[47,48]. Los pacientes con enfermedad de Beriberi presentan lesiones principalmente en el pálido[49], sin embargo, en la encefalopatía de Wernicke destacan las lesiones en el tálamo[50,51]. Otras estructuras afectadas son el tálamo medial, los cuerpos mamilares, la placa rectal, y el mesencéfalo[11]. Tradicionalmente, la encefalopatía de Wernicke se ha asociado con tres signos clínicos: alteraciones oculomotoras (nistagmos, movimientos sacádicos), ataxia como el principal trastorno del movimiento y síntomas neuropsiquiátricos[52]. Hoy en día, se conoce que solo el 16.5% de estos pacientes presentan los tres signos guía y el 37.1% no presentan ninguna de esas características[53]. El diagnóstico de esta enfermedad es complicado debido a la heterogeneidad clínica que cursan los pacientes. Además, se han reportado pacientes adultos con ambas enfermedades adquiridas presentes en el mismo paciente[54,55].

Las enfermedades genéticas están causadas por mutaciones en genes que codifican los tres transportadores principales de tiamina (SLC19A2, SLC19A3 y SLC25A19) y la quinasa implicada en la fosforilación de tiamina libre a TPP (TPK1). Los transportadores codificados por los genes *SLC19A2* y *SLC19A3* se localizan en la membrana celular mientras que el transportador SLC25A19 se sitúa en la membrana mitocondrial. Las características clínicas, radiológicas y bioquímicas están detallados en la Tabla 2. Las mutaciones en el transportador mitocondrial causan microcefalia letal Amish (ALM) o una degeneración bilateral del estriado y una polineuropatía progresiva[11]. Hay que remarcar que los 61 pacientes reportados con ALM portan el cambio p.Gly177Ala en homozigosis.

Los pacientes con causas tanto congénitas como adquiridas presentan una mejoría clínica tras ser suplementados con tiamina. El diagnóstico temprano en este caso es esencial para que el tratamiento con altas dosis de tiamina y biotina pueda revertir el fenotipo clínico y radiológico del paciente[56] o prevenir su progresión.

2.1.3. Otras enfermedades que cursan con hiperintensidad en una secuencia T2

La hiperintensidad en la secuencia T2 se presenta también en otras enfermedades como la aciduria glutárica tipo I, la deficiencia de sulfito oxidasa, los defectos de NUP62, las acidurias orgánicas clásicas, enfermedades lisosomales, leucodistrofias, etc.

La aciduria glutárica tipo I es una enfermedad autosómica recesiva con una gran heterogeneidad genética. Su prevalencia general es de 1:40000 nacidos vivos[57]. En la población Amish de Pensilvania esta prevalencia aumenta hasta 1:500 nacimientos, todos ellos portadores de la mutación c.1296C>T en el gen *GCDH*[58]. En el curso clínico de esta enfermedad, destaca la presencia de encefalopatía[57], distonia[59] o deficiencia motora[58], y solo se ha reportado un portador asintomático[58]. Estos pacientes presentan una necrosis en el estriado[57–59], principalmente con lesiones en el putamen y la cabeza del caudado[59]. Como clave diagnóstica de esta patología, la mayoría de estos pacientes presentan una elevación del ácido glutárico y del ácido 3-hidroxiglutárico en orina y de la glutarilcarnitina en sangre seca[60].

La deficiencia de la enzima sulfito oxidasa, codificada por el gen *SUOX*, es una enfermedad metabólica con una presentación clínica principalmente de hipotonía axial, hipertonía periférica, movimientos alterados, retraso psicomotor severo, convulsiones, problemas de alimentación, microcefalia y dislocación lenticular[61]. Radiológicamente, en esta enfermedad destaca una alteración en el globo pálido y la sustancia nigra[62]. Las características bioquímicas que sugieren una deficiencia de sulfito oxidasa son el aumento de los niveles de excreción de sulfito y sulfocisteína en orina y plasma con bajo contenido de ácido úrico en ambos líquidos, bajo nivel de homocisteína total y aumento de los niveles de xantina e hipoxantina en la orina[63].

Se han descrito mutaciones bialélicas en *NUP62* asociadas con coreoatetosis, movimientos oculares alterados, convulsiones y retraso mental. Algunos pacientes presentan un debut desencadenado por una enfermedad febril o vómitos. Estos pacientes presentan una necrosis estriatal con lesiones progresivas principalmente en el núcleo caudado y el putamen y, en algunas ocasiones, en el globo pálido[64].

Las acidurias orgánicas clásicas incluyen la aciduria metilmalónica (MMA, siglas en inglés), la aciduria propiónica (PA, siglas en inglés) y la aciduria isovalérica (IVA, siglas en inglés). La mayoría de los pacientes con estas enfermedades no presentan signos clínicos neurológicos (63% de los pacientes con PA, 76% en pacientes con MMA y el 100% en aquellos con IVA). En aquellos que sí presentan clínica neurológica, destaca el

síndrome extrapiramidal (44%), piramidal (33%) y cerebelar (33%) y necesitan ayuda para andar en el 28% de los casos (44% en PA, 11% en MMA y 0% en IVA). Radiológicamente, presentan lesiones en los ganglios basales un 56% en PA, 36% en MMA y 17% en IVA. Otra de las características comunes de la RMC de estos pacientes es la afectación de la sustancia blanca en el 38% de los casos con PA; 36% en MMA y 50% en IVA. Bioquímicamente, los pacientes con MMA destacan por el incremento del ácido metilmalónico en plasma y orina, mientras que los pacientes con PA tienen una elevación del ácido 3-hidroxi propionato en orina, destacando también una elevación de glicina, alanina y glutamina[65].

2.2. Enfermedades que cursan con calcificaciones en los ganglios basales

Las calcificaciones en los ganglios basales están asociadas a un gran número de enfermedades neurológicas y metabólicas. Los depósitos cerebrales de minerales se detectan principalmente como regiones hipodensas en TC o señales hipo/hiperintensas en la secuencia T2[66]. Las calcificaciones se presentan bilateral y simétricamente en los ganglios basales y, con menos frecuencia, en el núcleo dentado, tálamo, médula espinal, centro semiovalado y sustancia blanca subcortical[66]. La microglia y los astrocitos reactivos se acumulan alrededor de los depósitos de calcio desencadenando un proceso inflamatorio[67], presente en estas enfermedades.

Las calcificaciones en los ganglios basales pueden ser producidas por causas adquiridas como enfermedades metabólicas por causas no genéticas (hipervitaminosis D, hipoparatiroidismo secundario, hiperparatiroidismo, hipotiroidismo, pseudohiperparatiroidismo), exposición a tóxicos (monóxido de carbono, plomo, cobre, radioterapia), infecciones (brucelosis, toxoplasmosis, tuberculosis, cisticercosis, citomegalovirus, inmunodeficiencia humana virus, virus varicela-zoster), enfermedades autoinmunes (síndrome de inmunodeficiencia adquirida, lupus eritematoso sistémico, enfermedad de Behçet, enfermedad celíaca), lesiones cerebrovasculares (accidente cerebrovascular, malformaciones vasculares)[68,69], lesiones accidentales en pacientes asintomáticos o de forma fisiológica en personas mayores de 50 años[70].

Las principales patologías genéticas que cursan con calcificaciones son las calcificaciones cerebrales familiares primarias (o síndrome de Fahr) y el síndrome de Aicardi-Goutières (AGS, siglas en inglés). Otras enfermedades relacionadas con estas calcificaciones son el síndrome de Cockayne, la enfermedad de Coat, la fenilcetonuria[68], la enfermedad de Krabbe, el síndrome de DiGeorge[69] o la enfermedad de Moya-Moya (Tabla 1).

2.2.1. Calcificaciones cerebrales familiares primarias (PFBC, por sus siglas en inglés)

La PFBC es una enfermedad neurodegenerativa con depósitos de calcio principalmente en los ganglios basales, pero puede estar presente en otras regiones cerebrales. Esta patología se ha descrito también como calcificaciones idiopáticas de los ganglios basales, calcinosis bilateral estriopalidodental o síndrome de Fahr[68]. La prevalencia está sobre 4.5/10000-3.3/1000, considerándose una enfermedad rara[71]. Actualmente, hay cinco genes asociados: *SLC20A2, PFGFRB, PDGFB, XPR1, MYORG,* y *JAM2*. Mutaciones en el gen *SLC20A2* son las más frecuentes en esta enfermedad. Recientemente, se han asociado los genes *MYORG*[72] y *JAM2*[73].

Las características clínicas de un total de 425 casos provenientes de tres revisiones[68], 53 pacientes con mutaciones en *MYORG*[72,74,83,75–82] y 11 pacientes con mutaciones en *JAM2*[73,84] reportados hasta el momento están descritas en la Tabla 3.

Calcificaciones cerebrales familiares primarias						
Gen	***SLC20A2***	***PDGFRB***	***PDGFB***	***XPR1***	***MYORG***	***JAM2***
Número de pacientes	218	94	43	6	53	11
Características clínicas principales (%)						
Síntomas psiquiátricos	28,3	39,4	38,9	33,3	26,4	45,5
Parkinsonismo	30,3	13,6	27,8	50	22,6	-
Temblor	27	23,3	18,2	16,7	9,4	-
Distonía	26,2	19,7	5,6	-	5,7	45,5
Deterioro cognitivo	17,2	25,8	16,7	**66,7**	**60,4**	54,5
Corea	13,5	16,2	18,2	16,7	5,7	-
Disartria	13,5	9,3	9,1	33,3	**62,3**	27,3
Dolor de cabeza	11,5	35,1	20,9	-	-	-
Ataxia	9,7	18,2	16,7	16,7	28,3	54,5
Convulsiones	5,5	4,5	-	-	-	18,2
Bradicinesia	-	-	-	-	13,2	**72,7**
Movimientos oculares alterados	-	-	-	-	11,3	45,5
Disfagia	-	-	-	-	5,7	27,3
Otros signos clínicos (%)	-	-	-	-	Signos piramidales (34,0); Síndrome hipertónico acinético (18,9); Hipercinesia (15,1); Signos bulbares (13,2); Dificultades de la marcha (11,3); Dificultades urinarias (5,7)	Habla arrastrada (**63,6**); Reflejos de ausencia (**63,6**); Rigidez (36,4); Marcha inestable (27,3); Hipomimia (18,2); Disquinesia (18,2); Hiperreflexia (18,2); Epilepsia (9,1); Oftalmoplejia (9,1)

Características radiológicas principales (%)						
Ganglios basales	**100**	**100**	**100**	**100**	50,9	**100**
Tálamo	49,3	14	7,7	**66,7**	**75,5**	**81,8**
Cerebelo	49,3	32,6	**69,2**	**100**	54,7	54,5
Núcleo dentado	42,7	9,3	23,1	-	18,9	45,5
Áreas subcorticales	34,7	39,5	38,5	50	11,3	36,4
Corteza	-	-	-	-	43,4	45,5
Mesencéfalo	-	-	-	-	18,9	27,3
Vermis	-	-	-	-	28,3	18,2
Otras áreas afectadas (%)	Áreas corticales (14,7)	Quistes de la sustancia blanca (4,7); Áreas corticales (2,3)	-	Áreas corticales (50,0)	Sustancia blanca (54,7); Tronco encefálico (43,4); Atrofia cerebelosa (35,8); Núcleos lenticulares (28,3); Pons (22,6)	Sustancia gris profunda (45,5)

Tabla 3: Fenotipos asociados a calcificaciones cerebrales familiares primarias. Los signos clínicos y radiológicos comunes (con un porcentaje de pacientes >60%) están marcados en negrita.

La edad de inicio en estas enfermedades tiene un amplio rango, desde la infancia hasta la edad adulta avanzada. Las deficiencias de MYORG aparecen comúnmente en la edad adulta (edad media: 42 años). Curiosamente, el paciente reportado portador de mutaciones en este gen con el inicio más temprano, a los 8 años de edad, únicamente presentó una discinesia paroxística[81], que no es una característica común en este trastorno.

Las enfermedades causadas por mutaciones en los genes *SLC20A2, PFGFRB, PDGFB* y *XPR1* presentan una herencia autosómica dominante, mientras que son necesarias mutaciones bialélicas en *MYORG* y *JAM2* para causar síntomas. Sin embargo, se han reportado casos de portadores heterocigotos en el gen *MYORG* sin presentación clínica, pero con calcificaciones cerebrales[83,85].

2.2.2. Síndrome de Aicardi-Goutières (AGS)

El AGS es una encefalopatía genética con un inicio temprano que se caracteriza por calcificaciones en los ganglios basales, lesiones en la sustancia blanca y una elevación linfocitaria en LCR. Generalmente, esta enfermedad se manifiesta con una encefalopatía subaguda con regresión motora y microcefalia progresiva, progresando a un empeoramiento clínico, un déficit cognitivo y una tetraparesia espasto-distónica[86]. Se han estudiado los datos de 254 pacientes[87–91] y de revisiones anteriores[92–94] para delinear las características clínicas y radiológicas de esta enfermedad. Hay siete subtipos de AGS según el gen mutado: *TREX1, RNASEH2B, RNASEH2A, RNASEH2C, SAMHD1, ADAR* o *IFIH1*. Hasta la fecha, cerca del 99% de los pacientes con características de AGS tienen diagnóstico genético[86]. Aunque los pacientes con AGS comparten las mismas características clínicas y radiológicas, algunos rasgos son más comunes en unos subtipos u otros. La edad de inicio de estos pacientes varía desde el periodo neonatal hasta la adolescencia. Se observa un inicio más temprano en los pacientes con mutaciones en *TREX1* y *RNASEH2C*. Los síntomas sistémicos y el retraso del desarrollo al inicio están presentes en todos los pacientes con mutaciones en *RNASEH2C*; siendo el retraso del desarrollo la característica más común al inicio en los pacientes con defectos en TREX1, RNASEH2B (junto con síntomas sistémicos) y SAMHD1. Los pacientes con mutaciones en *ADAR* e *IFIH1* presentan principalmente síntomas neurológicos al inicio de la enfermedad. En el seguimiento, la mayoría de los pacientes con AGS desarrollan afecciones inflamatorias de la piel (principalmente con la presencia de sabañones), retraso del desarrollo, características autoinmunes, fiebres recurrentes y trombocitopenia. La mayoría de estos pacientes también presentan un glaucoma (excepto los pacientes con

cambios genéticos en *ADAR*), paraparesia espástica (excepto en pacientes con defectos de TREX1) y cardiomiopatía (excepto en pacientes con mutaciones en *SAMHD1* y *ADAR*). Otras características presentadas en estos pacientes son las contracturas (TREX1, SAMHD1, IFIH1), distonía (RNASEH2B/A, ADAR) y epilepsia (TREX1, RNASEH2B). Hay signos clínicos característicos de cada subtipo de AGS como la tiroiditis y pérdida de la audición (TREX1); leucodistrofia y escoliosis (RNASEH2B); leucemia linfocítica (SAMHD1); irritabilidad (ADAR); o pérdida dental prematura, calcificación aórtica y enfermedad renal (IFIH1).

La resonancia magnética de estos pacientes se caracteriza por calcificaciones intracraneales con lesiones en la sustancia blanca y atrofia cerebral. En muchas ocasiones, las calcificaciones solo son visibles mediante TC craneal. Los pacientes con mutaciones en *ADAR* presentan lesiones localizadas principalmente en caudado y putamen, mientras que las lesiones en pacientes con deficiencia de IFIH1 se encuentran en putamen y pálido. Los pacientes con ADAR también presentan una necrosis estriatal bilateral (NEB).

2.3. Enfermedades que cursan con depósitos de sustancias paramagnéticas en los ganglios basales

Existen elementos traza que se acumulan en los ganglios basales como el hierro, magnesio, aluminio, zinc o manganeso[68].

La NBIA agrupa una serie de trastornos hereditarios heterogéneos caracterizados por un síndrome extrapiramidal progresivo[9]. Actualmente, hay diez genes están asociados con este trastorno: *PANK2, PLA2G6, c19orf12, FA2H, WDR45, COASY, FTL1, ATP13A2, CP* y *DCAF17*[9,95].

Otras enfermedades con lesiones de los ganglios basales debido a la acumulación de oligoelementos son la enfermedad de Wilson[96] y la hipermanganesemia[**97**].

2.4. Enfermedades que cursan con otras lesiones en los ganglios basales

La atrofia de los ganglios basales es típica de la enfermedad de Huntington[98]. La atrofia e hipomielinización de los ganglios basales se asocian con el gen *TUBB4A*[13]. Esta hipomielinización se ha reportado en otras leucodistrofias, como los defectos de GJA1 (que también presentan calcificaciones) [99], y POLR3A y POLR3B[100].

3. Biomarcadores en las enfermedades con alteraciones en los ganglios basales

En 2001, el grupo de investigadores pertenecientes al *Biomarkers Definitions Working Group* definió los biomarcadores, o marcadores biológicos, como una característica que puede medirse y evaluarse de forma objetiva como indicador de procesos normales biológicos, procesos patogénicos o respuestas farmacológicas a una intervención terapéutica[101]. La clave de los biomarcadores es determinar la relación entre cualquier biomarcador medible y puntos clínicos relevantes[102].

Debido a la gran heterogeneidad de defectos que engloban las alteraciones de los ganglios basales, es complicado disponer de un biomarcador para un diagnóstico bioquímico de las mismas. Así mismo, algunas de estas enfermedades incluidas disponen de metabolitos biológicos más o menos específicos que ayuden a su diagnóstico.

3.1. Biomarcadores en defectos en el metabolismo y transporte de la tiamina

El contenido de tiamina estimado en el cuerpo humano es 25-30 mg. En sangre, el 80% de la tiamina que encontramos está situada en los eritrocitos como TPP[40], por lo que es la isoforma mayoritaria en ese tejido. Por otro lado, la tiamina libre es capaz de cruzar la barrera hematoencefálica por lo que es la mayoritaria en LCR.

En 2015, nuestro grupo[103] estudió pacientes con síndrome de Leigh observando que aquellos con una deficiencia del transportador 2 de tiamina (codificado por el gen *SLC19A3*) tenían niveles mucho más bajos de tiamina libre en LCR que los pacientes control. El 83% de ellos (5/6) fueron tratados prematuramente con una suplementación de tiamina mostrando una gran mejora clínica[103]. Finalmente, se sugirió que la determinación de tiamina libre en LCR podría ser un biomarcador para la deficiencia del transportador 2 de tiamina.

Mayr et al., 2011[104] demostró una deficiencia de TPP en músculo, sangre y fibroblastos en 7 pacientes con un déficit de tiamina quinasa (*TPK1*), la enzima que transforma la tiamina a TPP, el metabolito activo. Sin embargo, actualmente no existen estudios sobre la determinación de las diferentes isoformas de tiamina en LCR en pacientes con déficit de TPK1 ni en pacientes con una deficiencia en el transportador mitocondrial de la tiamina (gen *SLC25A19*).

3.2. Síndrome de Aicardi-Goutières (AGS)

Rice et al[105] demostraron mediante PCR cuantitativa de retro-transcriptasa que en pacientes con AGS había una sobreexpresión de genes estimulados por la vía del alfa-

interferón. Estos genes incluyen *IFI27, IFI44L, IFIT1, ISG15, RSAD2* y *SIGLEC1*. Por otro lado, el AGS es un trastorno inflamatorio. La neopterina es una pterina liberada por los macrófagos al sistema nervioso central como respuesta directa a la estimulación de los linfocitos por el interferón gamma[106], siendo un indicador sensible en los trastornos inflamatorios e inmunomediados[107]. Varios autores han identificado un aumento de neopterina en el LCR en diversos procesos neurológicos, incluido el AGS[105,107]. Recientemente, la elevación de los niveles de neopterina en LCR se identificó en pacientes con mutaciones *ADAR*, recalcando el papel importante de la neopterina en LCR como biomarcador del AGS[10].

3.3. Acúmulo de elementos traza

La determinación de elementos traza en plasma, orina y sangre total se utiliza de forma rutinaria para control nutricional y evolutivo de pacientes ya diagnosticados en tratamiento dietético, como dietas con restricción de proteínas en pacientes con errores congénitos del metabolismo intermediario, y para el diagnóstico y seguimiento de pacientes con defectos del metabolismo del cobre, como Wilson y Menkes.

En el caso concreto del manganeso, se ha reportado la presencia de acúmulos de este elemento traza en los ganglios basales en trabajadores expuestos largo tiempo a este elemento[108] y en muestras de sangre de pacientes con defectos en el gen *SLC30A10*[109] y *SLC39A14*[12], implicados en el metabolismo del manganeso. Para el estudio bioquímico de los metabolitos a nivel de sistema nervioso central el medio más fiable es el LCR. A pesar de no haberse reportado previamente estudios de manganeso en LCR en estos grupos poblacionales, hay artículos que reportan los niveles de metales en LCR en otras enfermedades como la esclerosis lateral amiotrófica[110].

Por otro lado, el índice palidal es la diferencia entre la intensidad de señal del pálido respecto a la sustancia blanca cortico-frontal en una secuencia T1. Se ha utilizado en pacientes con encefalopatía hepática crónica[111] y en pacientes con exposición a manganeso durante un periodo laboral[108], sugiriéndose como biomarcador en este último caso.

4. Diagnóstico genético de las enfermedades con alteraciones en los ganglios basales

El diagnóstico de las enfermedades que afectan bilateralmente los ganglios basales en niños es un reto en la práctica clínica debido a la amplia variedad de defectos adquiridos

y genéticos que pueden cursar con estas lesiones. La combinación multidisciplinar de diferentes aproximaciones diagnósticas, entre ellas el análisis clínico y radiológico, la secuenciación masiva de nueva generación (NGS, siglas en inglés), la determinación de biomarcadores y los estudios funcionales que permitan confirmar la patogenicidad de las variantes encontradas, es un abordaje holístico y eficaz para establecer el diagnóstico molecular[20,22]. Esta aproximación ha permitido aumentar el número de genes asociados a estas patologías, incrementando la tasa de diagnóstico molecular en los pacientes con alteraciones en los ganglios basales.

Una de las principales cuestiones que debe abordarse a la hora de realizar una prueba genética para el diagnóstico de un paciente es decidir cómo de amplia ha de ser la búsqueda. Si las características fenotípicas sugieren una patología concreta causada por un solo gen el primer paso sería el análisis de dicho gen. Por el contrario, cuando se trata de una patología heterogénea genéticamente o con fenotipos solapantes habría que realizar una búsqueda mayor con otras estrategias de diagnóstico genético. Hay que tener en cuenta que en el ámbito pediátrico el fenotipo del paciente puede ser incompleto.

Mientras que en muchas patologías monogénicas con un diagnóstico claro, la secuenciación Sanger sigue siendo una primera opción, en aquéllas que no disponen de un biomarcador específico o el diagnóstico diferencial no es decisivo esta estrategia puede ser costosa y poco resolutiva. En estos últimos años, las estrategias de NGS han ido desplazando la secuenciación Sanger como herramienta diagnóstica. En las enfermedades con alteraciones en ganglios basales es necesario técnicas de NGS para su diagnóstico debido a la gran heterogeneidad que presentan, tanto clínica como genética.

Existen diferentes plataformas de NGS que van desde paneles de genes que incluyen aquellos genes de interés hasta la secuenciación del genoma completo (WGS). En el ámbito clínico, lo más utilizado son los paneles llamados exoma clínico, constituidos por todos aquellos genes asociados a enfermedades mendelianas. En el campo de la investigación, se utilizan paneles customizados, secuenciación completa de exoma (WES) o WGS. En casos específicos se utilizan otras técnicas como la secuenciación completa del ADN mitocondrial, para detectar cambios en genes mitocondriales, y *arrays* o MLPA (*Multiplex Ligation-dependent Probe Amplification*, en inglés) para identificar reordenamientos genómicos y variantes estructurales de gran tamaño (deleciones/duplicaciones).

4.1. Plataformas de secuenciación masiva

4.1.1. Paneles de genes

Los paneles de genes permiten estudiar de forma simultánea las regiones codificantes y flanqueantes de un número determinado de genes para una enfermedad, por lo que constituye una aproximación intermedia entre el análisis de un solo gen y el análisis del exoma completo. Los paneles son la opción más utilizada en el ámbito clínico ya que aumentan la sensibilidad respecto a otras tecnologías y se estudian únicamente los genes de interés para esa enfermedad, minimizando los hallazgos accidentales en otros genes y la carga de análisis. Se pueden encontrar tanto paneles ya diseñados para patologías concretas de distintos laboratorios diagnósticos o empresas como la posibilidad de diseñar un panel con los genes de interés. Además, también existen distintas tecnologías según los paneles diferentes que hay en el mercado.

Las tecnologías NGS más utilizadas son HaloPlex, SureSelect (Agilent), Nextera y SeqCap (Illumina)[112]. HaloPlex destaca por tener una fragmentación dirigida del ADN mediante enzimas de restricción y el uso de sondas de ADN. El resto de las tecnologías utilizan una fragmentación de ADN aleatoria creando una superposición entre los fragmentos[112]. El problema fundamental de los paneles multigénicos es su limitación a analizar un grupo de genes determinado, sin posibilidad de reanálisis de otros genes de más reciente descripción. El panel dirigido que podemos encontrar con el mayor número de genes asociados es el llamado exoma clínico. Se trata de un panel comercial que ofertan los distintos laboratorios de diagnóstico y empresas e incluye los genes asociados a patología según las tres bases de datos de enfermedades mendelianas HGMD, GeneTest y OMIM.

4.1.2. Secuenciación de exoma completo (WES)

El WES tiene las ventajas de ser una aproximación menos restringida, que permite la identificación de variantes en genes no previamente asociados a la enfermedad y reanalizar genes nuevos asociados a la enfermedad posteriormente. Esta es una gran ventaja en las patologías muy heterogéneas donde nuevos genes se asocian cada año a estas enfermedades, como es el caso de las enfermedades de los ganglios basales. Por otro lado, tiene unas limitaciones como son el gran volumen de datos a la hora de procesarlos e interpretarlos y la mayor probabilidad de obtener variantes de significado incierto y/o hallazgos incidentales[113]. Económicamente, se asume que los paneles son más económicos que la WES, pero no siempre es así[113]. La elección entre WES y paneles

dirigidos también depende del tamaño del panel ya que para paneles pequeños (de unos 50 genes) es posible que el bajo coste de secuenciación haga sopesar los beneficios del WES[114]. Estudios anteriores realizados en cáncer determinan que se deben secuenciar un mínimo de 1Mb de regiones intrónicas y/o exónicas para que os resultados de un panel sean comparables con WES[115].

4.1.3. Secuenciación de genoma completo (WGS)

La WGS cubre el 100% de las regiones del genoma. A pesar de que la cobertura es menor que en la WES, ésta es más uniforme[116]. Otras ventajas que ofrece la WGS, a parte de la cobertura, son la posibilidad de detectar variantes intrónicas profundas y CNVs, incluyendo deleciones de un exón entero[114]. Por otro lado, comparte las ventajas del WES de la reanotación al cabo del tiempo[116]. Las variantes intrónicas profundas pueden alterar el patrón normal de *splicing* o pueden interferir con los dominios reguladores o ARN no codificantes que controlan la expresión de otros genes[117]. Hay algoritmos para estimar el efecto de las variantes intrónicas, además de la combinación de la secuenciación de estas regiones con de transcriptoma en esa región concreta o secuenciación completa del ARN[117]. Sin embargo, una de las limitaciones del WGS es el coste y tiempo de análisis y la obtención de un gran número de variantes de significado incierto y en regiones poco conocidas del genoma difíciles de interpretar.

4.2. Otras técnicas diagnósticas

La presencia de CNV se asocia cada vez más como la causa de enfermedades[118]. A pesar de que hoy en día se pueden analizar estos cambios mediante WES[119] y WGS[116], hay técnicas específicas y más robustas para estos análisis. Un *array* CGH es una técnica de alta resolución que contiene en su superficie una gran cantidad de fragmentos de ADN que permiten la detección de CNV de 200-50 Kb como aneuploidías cromosómicas, amplificaciones y deleciones en todo el genoma. Por otro lado, el MLPA es una técnica utilizada para regiones concretas del genoma.

La RNA-seq, o secuenciación del ARN, es una aproximación altamente precisa para mediar transcripción a través de la secuenciación del transcriptoma con un coste económico y de muestra pequeño. De esta forma te permite determinar isotopos de transcripción, fusiones de genes o variantes de nucleótidos únicos en el ARN[120].

Hay que tener en cuenta que en el síndrome de Leigh, paradigma de enfermedad genética que causa degeneración en ganglios basales en la edad pediátrica, las mutaciones en el

ADN mitocondrial representan una contribución importante, ya que como hemos visto anteriormente se trata mayoritariamente de enfermedades mitocondriales. La secuenciación del ADN mitocondrial se suele llevar a cabo de dos formas: analizando únicamente las mutaciones mitocondriales más comunes relacionadas con enfermedad o secuenciando los 16569 pares de bases que contiene el ADN mitocondrial.

4.3. Herramientas informáticas para la interpretación y clasificación de variantes

A la hora de clasificar las variantes que no están previamente asociadas a patología en función de sus posibles consecuencias (si serán benignas o patológicas), la *American College of Medical Genetics* (ACMG) ha publicado una serie de recomendaciones a seguir[121]. Puesto que no siempre es posible la realización de estudios funcionales para validar dichos cambios genéticos, existen una infinidad de herramientas *in silico*. Las herramientas que siguen las recomendaciones anteriores y son más completas son el InterVar[122] y el Varsome[123], que se basan en un sumatorio de varios algoritmos incluyendo la herencia y posibles estudios funcionales realizados, además de los estudios *in silico* incluidos en otros predictores.

Los predictores que clasifican las variantes en función de su patogenicidad según el cambio de amino ácido producido en la proteína, la conservación de ese residuo a lo largo de la evolución y por la posibilidad de alterar el patrón de *splicing* más utilizados son CADD[124], Mutation Taster[125], SIFT, PROVEAN[126] y PolyPhen-2[127]. Para el estudio de cambios en el patrón de *splicing* hay predictores determinados, el más utilizado en este proyecto ha sido el Human Splicing Finder[128].

Por otro lado, también hay que tener en cuenta a la hora de valorar la patogenicidad de una variante genética su frecuencia poblacional y que exista un número de homozigotos en las bases de datos públicas, como el GnomAD.

Finalmente están las plataformas que permiten compartir datos genómicos de pacientes como el matchmaker Exchange, en las cuales se pueden establecer colaboraciones con otros grupos que hallan identificado variantes genéticas similares en individuos con fenotipos compatibles, con el objetivo de identificar nuevos genes causantes de enfermedad, o nuevos tipos de herencia para un gen conocido.

HIPÓTESIS

La hipótesis de trabajo de este proyecto es que la incorporación de nuevas técnicas de secuenciación masiva, en combinación con la aproximación clínica y radiológica, y la determinación de biomarcadores, permitirá identificar el origen genético de la enfermedad en una mayoría de niños con trastornos del movimiento y alteraciones de ganglios basales de origen desconocido.

La utilización de un algoritmo de diagnóstico genético basado en la secuenciación masiva paralela, mediante paneles personalizados, secuenciación completa de exoma y secuenciación de ADN mitocondrial, posibilitará el diagnóstico genético de la mayoría de estos pacientes. La realización de estudios funcionales en casos en los que encontremos variantes genética con patogenicidad incierta ayudará a la validación del diagnóstico genético del paciente.

Por otro lado, el análisis de biomarcadores permitirá establecer la sospecha diagnóstica de forma precoz y complementará la interpretación de los resultados genéticos obtenidos. Concretamente, la detección de una deficiencia de tiamina en líquido cefalorraquídeo nos orientará hacia un defecto en genes relacionados con el transporte y metabolismo de tiamina, hecho que conllevará un beneficio para los pacientes mediante una suplementación precoz con tiamina. Asimismo, el análisis de metales en plasma y líquido cefalorraquídeo nos ayudará a establecer la sospecha diagnóstica en niños con defectos en el transporte de metales como el manganeso.

OBJETIVOS

El **objetivo principal** de este trabajo es la caracterización genética y el análisis de biomarcadores en pacientes pediátricos con trastornos del movimiento y alteraciones en ganglios basales de origen desconocido.

Dentro de este marco, se han planteado **objetivos específicos**:

1. Establecer un algoritmo diagnóstico mediante diferentes técnicas de secuenciación masiva, con el fin de caracterizar genéticamente la mayoría de pacientes pediátricos con alteraciones en los ganglios basales de causa no filiada.

2. Analizar el fenotipo clínico y el genotipo de una cohorte de pacientes diagnosticados con defectos genéticos en el metabolismo de la valina y estudiar, en concreto, el efecto del cambio c.367C>T en el gen *ECHS1* con el fin de determinar su patogenicidad.

3. Estudiar biomarcadores específicos para las enfermedades que cursan con trastornos del movimiento y alteraciones en los ganglios basales. En concreto, determinación de isoformas de tiamina y elementos traza (manganeso, zinc, selenio, cobre y plomo), en sangre, plasma y líquido cefalorraquídeo de pacientes con posibles defectos genéticos en el metabolismo y/o transporte de dichas moléculas.

RESULTADOS

OBJETIVO 1

OBJETIVO 1: Caracterización genética de pacientes con alteraciones en los ganglios basales.

El objetivo 1 es el resultado de un proyecto multicéntrico, vigente a día de hoy, para el diagnóstico molecular de pacientes pediátricos con trastornos del movimientos y patología en ganglios basales. Dicho diagnóstico se ha realizado a partir de un abordaje clínico-radiológico, seguido de un análisis genético combinado con estudios de biomarcadores (Figura A1). Esta tesis se ha centrado en el análisis genético, estudios funcionales y estudio de biomarcadores.

Este proyecto ha sido financiado con dos Fondos de Investigaciones Sanitarias (FIS PI15/00287, PI18/01319), concedidos por el Instituto de Salud Carlos III de Madrid.

El algoritmo diagnóstico seguido en este proyecto ha sido: estudio clínico y radiológico de los pacientes según los criterios de inclusión explicados anteriormente, análisis genético de ADN nuclear por distintas aproximaciones de nueva generación, posteriormente, estudio completo de ADN mitocondrial en aquellos pacientes cuyos análisis anteriores han sido negativos y, de forma paralela, análisis de biomarcadores con el doble objetivo de realizar un diagnóstico precoz y validar los resultados genéticos (Figura A1).

La cohorte de pacientes con síndrome de Leigh reportada gracias a los resultados de este proyecto (Publicación 1, ver objetivo 2) se engloba dentro de un total de 53 pacientes estudiados con alteraciones en los ganglios basales. Podemos clasificar radiológicamente esta cohorte según la presencia de hiperintensidad en T2 (n=39), la presencia de calcificaciones (n=8), pacientes con ambas lesiones (n=4) u otras lesiones en los ganglios de la base (n=2). Para el estudio de estos pacientes, hemos utilizado: (i) paneles personalizados, (ii) secuenciación completa de exoma (WES) en probandos (WES *singleton*) y en el caso índice junto con ambos padres (WES trío), y (iii) secuenciación completa de ADN mitocondrial; pudiendo comparar entre tecnologías para optimizar el diagnóstico de estas patologías. El porcentaje de diagnóstico ha sido de 37.9% (11/29) mediante distintos paneles de genes (39% panel HaloPlex, 33% panel SureSelect), 45.2% (14/31) mediante WES y 28.6% (6/21) mediante secuenciación de ADN mitocondrial. En los 31 pacientes con diagnóstico molecular definitivo (58.5% del total) se han encontrado cambios en 22 genes distintos (*MT-ATP6, MT-ND1, MT-ND6, ECHS1, HIBCH, PDHA1, SCN2A, COQ2, GFAP, GNAO1, MECR, NDUFAF5, NDUFAF6, PRKRA, SLC25A19,*

SUCLG2, RNF213, ADAR, RNASEH2B, IFIH1, SLC39A14 y *TUBB4A)*, confirmando la gran heterogeneidad de estas enfermedades y pudiendo diagnosticar, además, a tres hermanos afectos.

Cuatro de estos genes (*GNAO1, PRKRA, SCN2A* y *ADAR*) han permitido realizar nuevas asociaciones fenotipo-genotipo, ya que no estaban previamente asociados a síndrome de Leigh.

Los tres pacientes de este proyecto con mutaciones en el gen *ADAR*[129] y el paciente con cambios en el gen *NDUFAF6* junto a sus dos hermanos afectos[130] han sido publicados a través de colaboraciones con otros grupos de investigación.

Cuatro de los 31 pacientes diagnosticados molecularmente, y un hermano afecto, presentaban mutaciones en los genes *ECHS1* y *HIBCH* que participan en el metabolismo de la valina. La historia natural de estos defectos genéticos, así como la correlación fenotipo-genotipo, han sido publicadas junto a una cohorte internacional en el artículo que también cubre el objetivo 2 de esta tesis doctoral (Publicación 1).

OBJETIVO 2

OBJETIVO 2: Análisis del fenotipo y genotipo de una cohorte de pacientes diagnosticados con defectos genéticos en el metabolismo de la valina. Estudio funcional del efecto del cambio c.367C>T en el gen *ECHS1* con el fin de determinar su patogenicidad.

Respecto al objetivo 2, se han estudiado 19 pacientes con mutaciones bialélicas en los genes *ECHS1* o *HIBCH*, que codifican enzimas implicadas en el catabolismo de la valina. Cinco pacientes han sido diagnosticados por nuestro grupo a través del estudio multicéntrico referido en el objetivo 1. Catorce pacientes adicionales han sido reclutados a través de un trabajo colaborativo con distintos hospitales nacionales e internacionales.

Por otro lado, se ha realizado una revisión bibliográfica de los 72 pacientes publicados hasta el momento con defectos en esas dos enzimas con el objetivo de realizar estudios de correlación fenotipo-genotipo y estudios de historia natural y curvas de supervivencia.

Los pacientes con defectos en el SCEH presentan tres fenotipos distintos: síndrome de Leigh (79%), acidosis láctica neonatal (11%) y distonía paroxística (10%). Estos pacientes con síndrome de Leigh presentan signos neurológicos asociados a déficits severos a nivel motor, de habilidades manuales y de comunicación, trastornos del movimiento, convulsiones, microcefalia y defectos visuales y auditivos. Los pacientes que presentan distonía paroxística tienen una clínica más leve con un debut más tardío tras un ejercicio prolongado, ayuno o enfermedad febril. Radiológicamente, predomina la presencia de quistes en el putamen, mientras que los pacientes con distonía paroxística presentan cavitaciones asimétricas en el globo pálido.

Todos los pacientes reportados hasta ahora con mutaciones en el gen *HIBCH* presentan un síndrome de Leigh. Destacan los episodios con un deterioro agudo tras una enfermedad febril, la presencia de convulsiones en un 33% de los pacientes y la falta de características sistémicas, que sí son comunes en otros defectos genéticos con síndrome de Leigh incluyendo el SCEH. Radiológicamente, predominan los quistes en el globo pálido.

Bioquímicamente, los metabolitos de metacrilato y el ácido 2,3-dihidroxi-2-metilbutirato se encuentran elevados con más frecuencia en pacientes con defectos en SCEH que en pacientes HIBCH. Por otro lado, la carnitina 3-hidroxiisobutiril está elevada únicamente en pacientes con un déficit en HIBCH.

Se han utilizado estudios de patrón de *splicing* y de expresión proteica para validar el cambio c.367C>T en el gen *ECHS1*. De esta forma se ha conseguido confirmar su patogenicidad a pesar de la caracterización de los predictores y el leve fenotipo del paciente.

Por último, este estudio nos ha permitido hacer varias correlaciones fenotipo-genotipo. Se ha observado que los pacientes con mutaciones en el *HIBCH* tienen una mayor supervivencia que aquéllos con cambios genéticos en *ECHS1*. En el caso de los pacientes con distonía paroxística y un defecto en SCEH, se han podido correlacionar con la mutación c.518C>T en heterozigosis. En los pacientes con mutaciones en el HIBCH se ha observado una correlación según la localización de la mutación portadora en la proteína en pacientes homozigotos, teniendo una mayor supervivencia aquellos que portan cambios en la superficie de la proteína.

Publicación 1

Título:

Delineating the neurological phenotype in children with defects in the *ECHS1* or *HIBCH* gene

Autores:

L Marti-Sanchez, H Baide-Mairena, A Marcé-Grau, R Pons, A Skouma, E López-Laso, M Sigatullina, C Rizzo, M Semeraro, D Martinelli, R Carrozzo, C Dionisi-Vici, L González-Gutiérrez-Solana, M Correa-Vela, JD Ortigoza-Escobar, A Sánchez-Montañez, E Vazquez, I Delgado, S Aguilera-Albesa, ME Yoldi, A Ribes, F Tort, L Pollini, S Galosi, V Leuzzi, M Tolve, L Pérez-Gay, L Aldamiz-Echevarría, M Del Toro, A Arranz, F Roelens, R Urreizti, R Artuch, A Macaya, B Pérez-Dueñas

Referencia:

Marti-Sanchez L, Baide-Mairena H, Marcé-Grau A, et al. Delineating the neurological phenotype in children with defects in the ECHS1 or HIBCH gene [published online ahead of print, 2020 Jul 17]. *J Inherit Metab Dis*. 2020;10.1002/jimd.12288. doi:10.1002/jimd.12288

Resumen:

Se han estudiado 42 pacientes con síndrome de Leigh según un algoritmo de diagnóstico genético que combina distintos métodos de secuenciación de nueva generación (NGS), identificando cinco pacientes con deficiencias de SCEH o HIBCH. Se han reclutado catorce pacientes adicionales a través de colaboraciones con otros centros. En total, se han analizado las características neurológicas y el espectro genético de 19 nuevos pacientes con mutaciones en los genes *ECHS1* o *HIBCH*. Para los estudios de historia natural y las asociaciones fenotipo-genotipo también incluimos 72 pacientes reportados previamente. Los 19 casos recientemente identificados presentaron un síndrome de Leigh (SCEH n = 11; HIBCH n = 6) y distonía paroxística (SCEH n = 2). Las lesiones de los ganglios basales (18 pacientes) se asociaron con quistes pequeños en el putamen/pálido en la mitad de los casos, una característica radiológica a tener en cuenta para el diagnóstico. Dieciocho variantes patogénicas fueron identificadas, 11 de ellas noveles. Entre los 91 casos publicados hasta la fecha, observamos una supervivencia más larga en los pacientes con déficit de HIBCH en comparación con pacientes con una deficiencia de

SCEH, y en pacientes con HIBCH portadores de mutaciones en homozigosis en la superficie de la proteína en comparación con aquellos con variantes dentro o cerca de la región catalítica. El cambio SCEH p.Ala173Val se asoció con una forma más leve de distonía paroxística desencadenada por el aumento de las demandas de energía. Este cambio se ha estudiado en un paciente con el cambio ya reportado p.Ala173Val y el nuevo cambio p.Leu123Phe en SCEH, observando una reducción del 83,6% de la proteína en los fibroblastos. Los defectos de SCEH y HIBCH en la vía de valina catabólica fueron una causa frecuente del síndrome de Leigh en nuestra cohorte. Las asociaciones de fenotipo y genotipo realizadas pueden ayudar a predecir el resultado y mejorar el manejo clínico.

Received: 3 April 2020 | Revised: 3 July 2020 | Accepted: 14 July 2020

DOI: 10.1002/jimd.12288

ORIGINAL ARTICLE

JIMD SSIEM WILEY

Delineating the neurological phenotype in children with defects in the *ECHS1* or *HIBCH* gene

Laura Marti-Sanchez[1,2] | Heidy Baide-Mairena[3,4,5] | Anna Marcé-Grau[3] | Roser Pons[6] | Anastasia Skouma[7] | Eduardo López-Laso[8,9,10] | Maria Sigatullina[3] | Cristiano Rizzo[11] | Michela Semeraro[11] | Diego Martinelli[11] | Rosalba Carrozzo[11] | Carlo Dionisi-Vici[11] | Luis González-Gutiérrez-Solana[10,12] | Marta Correa-Vela[3,4] | Juan Dario Ortigoza-Escobar[13] | Ángel Sánchez-Montañez[14] | Élida Vazquez[14] | Ignacio Delgado[14] | Sergio Aguilera-Albesa[15] | María Eugenia Yoldi[15] | Antonia Ribes[10,16] | Frederic Tort[10,16] | Luca Pollini[17] | Serena Galosi[17] | Vincenzo Leuzzi[17] | Manuela Tolve[18] | Laura Pérez-Gay[19] | Luis Aldamiz-Echevarría[20] | Mireia Del Toro[3] | Antonio Arranz[3] | Filip Roelens[21] | Roser Urreizti[1,10] | Rafael Artuch[1,10] | Alfons Macaya[3,4,10] | Belén Pérez-Dueñas[3,4]

[1]Department of Clinical Biochemistry, Institut de Recerca Sant Joan de Déu, Barcelona, Spain

[2]Universitat de Barcelona, Barcelona, Spain

[3]Pediatric Neurology Research Group, Hospital Vall d'Hebrón, Barcelona, Spain

[4]Universitat Autònoma de Barcelona, Barcelona, Spain

[5]Department of Paediatrics, Hospital General de Granollers, Granollers, Spain

[6]Department of Paediatric Neurology, Hospital Agia Sofia, Athens, Greece

[7]Institute of Child Health, Agia Sofia Children's Hospital, Athens, Greece

[8]Unit of Paediatric Neurology, Department of Pediatrics, University Hospital Reina Sofía, Córdoba, Spain

[9]Instituto Maimónides de Investigación Biomédica de Córdoba (IMIBIC), Córdoba, Spain

[10]CIBERER-ISCIII, Centro de Investigaciones Biomédicas en Red de Enfermedades Raras, Madrid, Spain

[11]Division of Metabolism, Bambino Gesù Children's Hospital, Rome, Italy

[12]Department of Pediatric Neurology, Hospital Infantil Universitario Niño Jesús, Madrid, Spain

[13]Department of Paediatric Neurology, Hospital Sant Joan de Déu, University of Barcelona, Barcelona, Spain

[14]Department of Neuroradiology, Hospital Vall d'Hebron – Institut de Recerca (VHIR), Barcelona, Spain

[15]Unit of Paediatric Neurology, Department of Pediatrics, Complejo Hospitalario de Navarra, Navarrabiomed, Pamplona, Spain

[16]Secció d'Errors Congènits del Metabolisme -IBC, Servei de Bioquímica i Genètica Molecular, Hospital Clínic, IDIBAPS, CIBERER, Barcelona, Spain

Abbreviations: CFCS, communication function classification system; GMFCS E&R, gross motor function classification system expanded and revised; HIBCH, 3-hydroxyisobutyryl-CoA hydrolase; LS, Leigh syndrome; MACS, manual ability classification system; MRI, magnetic resonance imaging; MRS, magnetic resonance spectroscopy; NGS, next generation sequencing; PDHc, pyruvate dehydrogenase complex; SCEH, short-chain enoyl-CoA hydratase; WES, whole exome sequencing.

L. Marti-Sanchez and H. Baide-Mairena contributed equally to the work.

[17]Department of Neurology and Psychiatry, Sapienza University of Rome, Rome, Italy
[18]Department of Experimental Medicine, Sapienza University, Rome, Italy
[19]Unit of Paediatric Neurology, Hospital Universitario Lucus Augusti, Lugo, Spain
[20]Department of Pediatric Metabolism, University Cruces Hospital, Barakaldo, Spain
[21]Pediatric Neurology, AZ Delta, Roeselare, Belgium

Correspondence
Belén Pérez-Dueñas, Department of Pediatric Neurology. Pediatric Neurology Research Group (Laboratory 122) Edifici Mediterrània, Hospital Vall d'Hebron - Institut de Recerca (VHIR), Passeig Vall d'Hebrón 119-129, 08035 Barcelona, Spain.
Email: belen.perez@vhir.org

Funding information
Instituto de Salud Carlos III, Grant/Award Number: PI18/01319; CERCA Programme/Generalitat de Catalunya; Agència de Gestió d'Ajuts Universitaris i de Recerca (AGAUR); Centro de Investigación Biomédica en Red de Enfermedades Raras (CIBERER); Instituto de Salud Carlos III (ISCIII), Grant/Award Numbers: PI19/01310, PI16/01048

Communicating Editor: David Cassiman

Abstract

The neurological phenotype of 3-hydroxyisobutyryl-CoA hydrolase (HIBCH) and short-chain enoyl-CoA hydratase (SCEH) defects is expanding and natural history studies are necessary to improve clinical management. From 42 patients with Leigh syndrome studied by massive parallel sequencing, we identified five patients with SCEH and HIBCH deficiency. Fourteen additional patients were recruited through collaborations with other centres. In total, we analysed the neurological features and mutation spectrum in 19 new SCEH/HIBCH patients. For natural history studies and phenotype to genotype associations we also included 70 previously reported patients. The 19 newly identified cases presented with Leigh syndrome (SCEH, n = 11; HIBCH, n = 6) and paroxysmal dystonia (SCEH, n = 2). Basal ganglia lesions (18 patients) were associated with small cysts in the putamen/pallidum in half of the cases, a characteristic hallmark for diagnosis. Eighteen pathogenic variants were identified, 11 were novel. Among all 89 cases, we observed a longer survival in HIBCH compared to SCEH patients, and in HIBCH patients carrying homozygous mutations on the protein surface compared to those with variants inside/near the catalytic region. The SCEH p.(Ala173Val) change was associated with a milder form of paroxysmal dystonia triggered by increased energy demands. In a child harbouring SCEH p.(Ala173Val) and the novel p.(Leu123Phe) change, an 83.6% reduction of the protein was observed in fibroblasts. The SCEH and HIBCH defects in the catabolic valine pathway were a frequent cause of Leigh syndrome in our cohort. We identified phenotype and genotype associations that may help predict outcome and improve clinical management.

KEYWORDS
basal ganglia cavitation, *ECHS1*, *HIBCH*, Leigh syndrome, methacrylate metabolites, paroxysmal dystonia, valine catabolism

1 | INTRODUCTION

Leigh syndrome (LS; MIM#256000) is a childhood-onset neurodegenerative disorder characterised by impaired neurodevelopment and brainstem and basal ganglia dysfunction.[1] More than 80 mitochondrial and nuclear genes related to LS have been described.[2,3] Due to the broad genetic heterogeneity and lack of specific neurological and biochemical features, next generation sequencing (NGS) is the technique of choice for the diagnosis of LS, achieving molecular confirmation in 38-50% of the cases.[4,5] An early genetic diagnosis is important to avoid unnecessary investigations, provide genetic counselling, and offer early intervention for treatable conditions.[6,7]

LS has emerged as the main clinical phenotype described in 3-hydroxyisobutyryl-CoA hydrolase (HIBCH; crotonase EC3.1.2.4) and short-chain enoyl-CoA hydratase (SCEH; EC4.2.1.17) deficiencies.[8-11] These enzymes, which are encoded by *HIBCH* (MIM*610690) and *ECHS1*

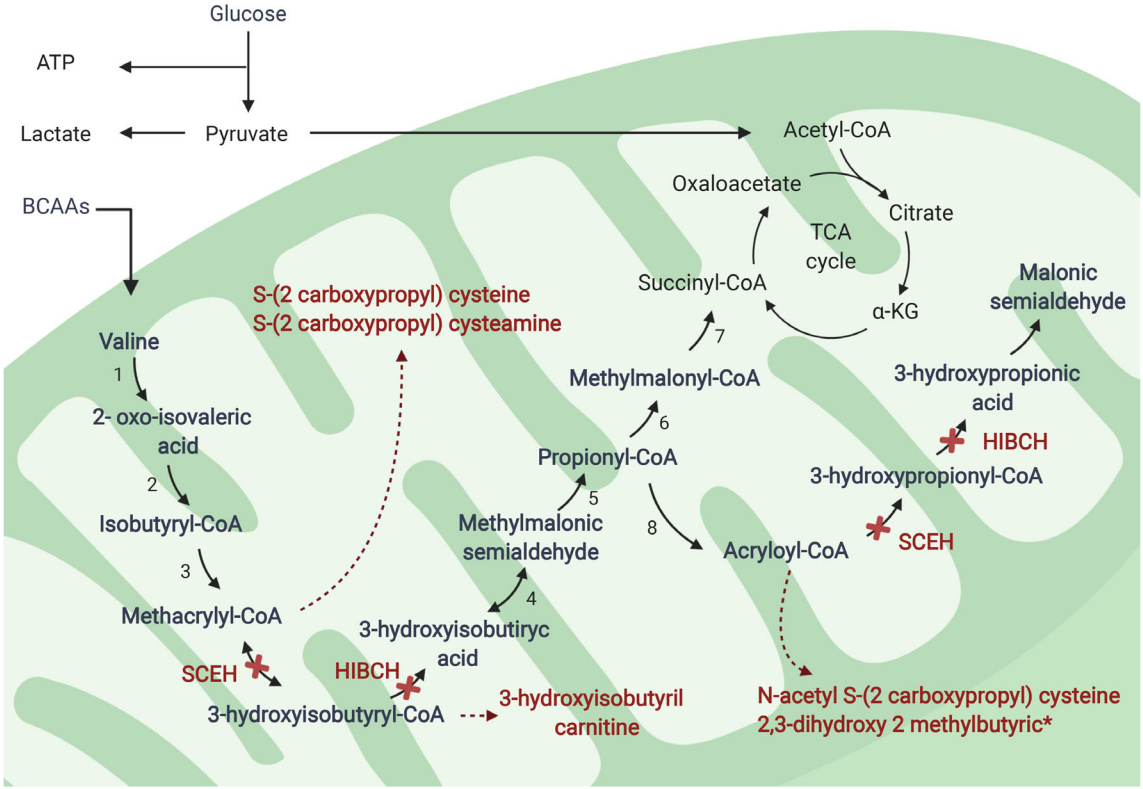

FIGURE 1 Valine catabolism pathway showing the formation of metabolites in SCEH/HIBCH deficiencies. *, The origin of 2,3-dihydroxy-2-methylmutyric from acryloyl-CoA is indirectly inferred.[9] Enzymes are numbered: 1, branched-chain aminotransferase; 2, branched-chain 2-keto acid dehydrogenase; 3, isobutyryl-CoA dehydrogenase; 4, 3-hydroxyisobutyric acid dehydrogenase; 5, methylmalonic semi-aldehyde dehydrogenase; 6, proponyl-CoA carboxylase; 7, (R)-methylmalonyl-CoA mutase; 8, propionyl-CoA dehydrogenase. Created with BioRender.com

(MIM*602292), play a major role in the valine catabolic pathway[8] and produce secondary deficiencies in the mitochondrial oxidative phosphorylation system and pyruvate dehydrogenase complex (PDHc).[8,12] SCEH is involved in mitochondrial fatty acid β-oxidation[9,13-15] and in the fourth step of valine catabolism[16] by converting methacrylyl-CoA to 3-hydroxyisobutyryl-CoA and acryloyl-CoA to 3-hydroxypropionyl-CoA[17] (Figure 1). HIBCH catalyses the fifth step of valine catabolism from 3-hydroxyisobutyryl-CoA to 3-hydroxyisobutyric acid[17] (Figure 1). HIBCH deficiency leads to an accumulation of 3-hydroxyiso butyrylcarnitine.[14]

In view of the wide clinical variability and growing number of children with mutations in *ECHS1* and *HIBCH*, our aim was to delineate the neurological phenotype and search for phenotype-genotype correlations that may help predict prognosis and optimise clinical management. For this purpose, we analysed 19 newly identified patients with biallelic pathogenic variants in *ECHS1* or *HIBCH* and compared them with 72 patients previously reported. Furthermore, we analysed HIBCH and SCEH proteins in silico to study the missense changes location and searched for phenotype-to-genotype correlations. Finally, in an SCEH patient with paroxysmal dystonia in compound heterozygous for the novel [p.(Leu123Phe)] and the known [p.(Ala173Val)] variants we conducted functional studies and provided data that support pathogenicity.

2 | PATIENTS AND METHODS

For a detailed description of methods, see Data S1.

2.1 | Patients

Participants or their legal guardians provided informed consent for their inclusion in the study. Procedures followed the Helsinki Declaration of 1975 as revised in 2013. The Ethic Committees of the participating centres approved the study.

A multi-centre cohort of 42 patients with clinical evidence of basal ganglia dysfunction, psychomotor delay or regression, and symmetric lesions affecting the basal

ganglia and/or brainstem were studied using NGS techniques. Among them, 33 cases fulfilled the diagnostic criteria established by Rahman for LS,[21] while nine patients featured other clinical presentations.

Within this cohort, four patients (plus one sibling) were identified as having *ECHS1* or *HIBCH* mutations. Fourteen additional SCEH/HIBCH patients were recruited through collaborations from centres in Spain, Greece, Italy, and Belgium. The responsible clinician at each collaborating centre collected clinical, biochemical, and genetic data via a 102-item questionnaire.

We searched the PubMed database (accessed January 2020) for patients with SCEH/HIBCH deficiencies. Thirty-six publications reported a total of 50 SCEH patients and 22 HIBCH patients. Tables S1 and S2 and Figure 2A summarise these data.

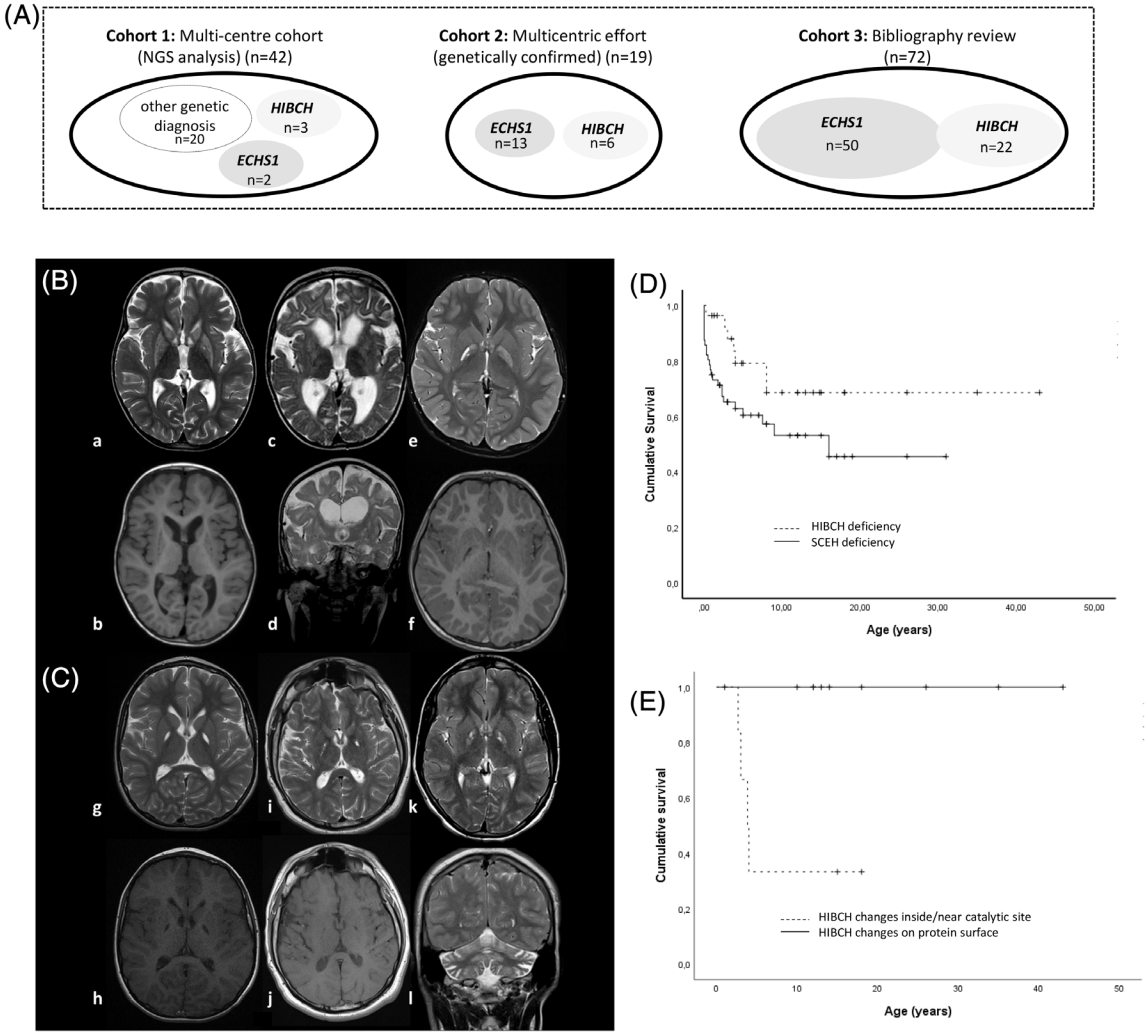

FIGURE 2 Cohort from this report, A, brain lesions on magnetic resonance imaging in SCEH and HIBCH patients, B and C, and Kaplan–Meier survival curves in SCEH and HIBCH patients, D and E. A, Schematic structure of the three cohorts used in this study. B, Brain MRI of SCEH-related LS patients. P11 with LS at 22 months, a and b, shows T2-WI hyperintensity affecting both caudate and putamen nuclei and T1-WI hypointensity foci. P3 with LS at 20 months, c and d, shows caudate and putamen T2-WI hyperintensity and thalamic and pallidal involvement. Global atrophy associated with dilated ventricles and thinning of the corpus callosum is also observed. P2 with paroxysmal dystonia at 5 years, e and f, shows exclusive but asymmetric involvement of the globus pallidus, with hyper-T2-WI and hypo-T1-WI signals suggesting cavitation. C, Brain MRI of HIBCH LS patients depicting an almost exclusive involvement of the globus pallidus. In P15 at 8 years, g and h, and P14 at 33 years, i and j, we observed T2-WI hyper- and T1-WI hypointensity, signifying small cysts cavitation. In P16 (16 years), k and l, globus pallidus involvement is associated with cerebellar atrophy and T2-WI hyperintensity involving the dentate nucleus. D, Comparison between HIBCH (n = 27; 20 [74.1%] censured cases) vs SCEH (n = 56; 32 [57.1%] censured cases) deficient patients showed that differences reached statistical significance (Breslow test, $P = .036$). We used Breslow test because the majority of patients died within the first 10 years of life. E, Comparison between patients who carried homozygous mutations in *HIBCH* gene located inside or near the catalytic region (mutations p.(Ala96Asp), p.(Tyr122Cys), and p.(Gly317Ser); n = 6; 2 [33%] censured cases) vs those with mutations on the surface of the protein (mutations p.(Arg66Trp), p.(Phe259Leu), p.(Ser270Gly), and p.(Thr305Ala); n = 10; 10 [100%] censured cases) in HIBCH protein. When comparing both groups, differences reach statistical significance (log-rank test, $P = .004$)

2.2 | Neuroimaging studies

For the 19 newly identified SCEH/HIBCH patients, at least one brain MRI study was available. Since the images were obtained from different centres, the quality and applied pulse sequences varied. MRI underwent systematic analysis by paediatric neurologists and neuroradiologists from the coordinating centre following an established protocol.

2.3 | Biochemical studies

In SCEH/HIBCH patients, urine organic acids were analysed by gas chromatography mass spectrometry of their trimethylsilyl derivatives.[18] Plasma acyl-carnitine profiles were studied by tandem mass spectrometry with or without derivatization depending on each individual laboratory. Before next generation sequencing testing, mitochondrial respiratory chain activities were analysed in frozen muscle of eight patients (P3-4, P6-7, P9, and P16-18). PDHc activity was performed in frozen muscle, fibroblasts or lymphocytes in P4, P7, P9, P11, P14, and P18. All these SCEH/HIBCH patients had a suspicion of mitochondrial disorder.[19,20] Some years ago our protocol for the biochemical/genetic diagnosis started with the measurement of enzyme activities in muscle and fibroblasts. At present, whole exome sequencing (WES) is the method of choice, and we only measure the enzymatic activities in some specific cases.

2.4 | Genetic analysis

Peripheral blood DNA samples from the multi-centre cohort of 42 patients were analysed either using customised panels of genes related to infantile basal ganglia diseases (HaloPlex Panel, version E.0; and SureSelect Panel, version D1, Agilent technologies) or WES (SureSelect Human All Exon V6, Agilent). In negative cases, complete mitochondrial DNA sequencing was performed. Variants were prioritised following in-house pipelines. The 14 patients from the collaborating centres were also analysed via WES.

Missense change location affecting the homohexamer SCEH and HIBCH were analysed in silico in an X-ray crystal structure (PDB 2HW5 and 3BPT, respectively) using the PyMOL Molecular Graphics System (Version 2.2.3. Schrödinger, LLC).

P1 with a milder phenotype of paroxysmal dystonia was compound heterozygous for a known mutation c.518C>T [p.(Ala173Val)] in *ECHS1* and a novel variant c.367C>T [p.(Leu123Phe)] classified as tolerated/benign by in silico predictors, but the Human Splicing Finder predicted a possible alteration in the splicing pattern. This novel variant is located 48 base-pairs from the 3′ end in exon 3. Therefore, we conducted splicing analysis and protein expression assay to confirm pathogenicity. RNA was extracted and retrotranscription was performed. Different PCRs covering exons 2–4 of *ECHS1* were analysed in cDNA (Figure S1). All of the PCR fragments underwent Sanger sequencing for confirmation. We also analysed SCEH protein in fibroblasts from P1 and four controls using Western-blotting.

2.5 | Statistical analysis

The chi-squared test was used to analyse the association between the c.518C>T [p.(Ala173Val)] variant and the paroxysmal dystonia phenotype in the group of 63 SCEH-deficient patients. Kaplan-Meier survival curves were used (a) to compare the survival rates between SCEH and HIBCH patients and (b) to compare patients carrying homozygous *HIBCH* mutations according to the protein location of the pathogenic variants.

3 | RESULTS

The clinical, radiological, and genetic data of the 19 newly identified SCEH and HIBCH patients are reported in Table 1.

Table 2 includes clinical, biochemical and radiologic features that may suggest the diagnosis of HIBCH vs SCEH deficiency.

Figure 2A represents the three studied cohorts: (a) multi-centre cohort of 42 patients with basal ganglia dysfunction, (b) multicentric effort (n = 19), and (c) literature review on previous published patients (n = 72).

Tables S1 and S2 summarise data on previously reported ECHS1 and HIBCH patients, including clinical, radiological, biochemical, and genetic characteristics (Table S1) and the distribution of brain MRI abnormalities (Table S2).

3.1 | SCEH deficiency

3.1.1 | Clinical phenotype and management

We identified 13 new SCEH patients. Two (P7-8) had affected LS siblings who died before achieving the molecular diagnosis. The mean age at onset was 11.5 (1-35) months. The clinical phenotype was characterised as LS (n = 11) and paroxysmal dystonia (P1-2).

The 11 patients with LS fulfilled the four criteria established by Rahman,[21] except for P11, who did not show mitochondrial energy impairment parameters. At onset, the patients manifested developmental delay or regression, feeding difficulties, episodes of acute

TABLE 1 Clinical, radiological, and genetic features of patients with SCEH and HIBCH deficiency

	Impairment in the fourth step of valine catabolism: SCEH deficiency													Impairment in the fifth step of valine catabolism: HIBCH deficiency					
Patient	**1**	**2**	**3**	**4**	**5**	**6**	**7**	**8**	**9**	**10**	**11**	**12**	**13**	**14**	**15**	**16**	**17**	**18**	**19**
Geographic origin	Spain	Belgium	Greece	Greece	Greece	Spain	Morocco	Romania	Albany	Italy	Portugal	Morocco	Spain	Italy	Greece	Spain	Spain	Spain	Spain
Allele 1/allele 2	c.518C>T/ c.367C>T	c.239C>T/ c.817A>G	c.476A>G/ c.476A>G	c.476A>G/ c.542G>T	c.476A>G/ c.542G>T	c.123_124 delAG/ c.830C>T	c.476A>G/ c.476A>G	c.476A>G/ c.817A>G	c.476A>G/ c.476A>G	c.371C>T/ c.371C>T	c.123_124 delAG/ c.713C>T	c.404A>G/ c.404A>G	c.740C>T/ c.740C>T	c.777T>A/ c.777T>A	c.913A>G/ c.913A>G	c.365A>G/ c.365A>G	c.365A>G/ c.365A>G	c.517+1G>A/ c.353T>C	c.353T>C/ c.488G>T
Protein change	p.(Ala173Val)/ p.(Leu123Phe)	p.(Pro80Leu)/ p.(Lys273Glu)	p.(Gln159Arg)	p.(Gln159Arg)/ p.(Arg181Leu)	p.(Gln159Arg)/ p. (Arg181Leu)	p.(Gly42Glufs*3)/ p.(Thr277Ile)	p.(Gln159Arg)	p.(Gln159Arg)/ p.(Lys273Glu)	p.(Gln159Arg)	p.(Thr124Ile)	p.(Gly42Glufs*3)/ p. (Ala238Val)	p.(Asn135Ser)	p.(Ala247Val)	p.(Phe259Leu)	p.(Thr305Ala)	p.(Tyr122Cys)	p.(Tys122Cys)	./p.(Phe188Ser)	p.(Phe188Ser)/ p. (Cys163Phe)
Reported in	[10,25,29,a]	[a,25,32,34]	[19,23,24,32,34]	[19,23,24,32,34,a]	[19,23,24,32,34,a]	[a,a]	[19,23,24,32,34]	[19,23,24,32,34,] [25,32,34]	[19,23,24,32,34]	[a]	[a,a,39]	[a]	[a]	[a]	[37,50]	[36]	[36]	[39,a]	[a,a]
Disease onset																			
Sex/Age at onset (m)	M/18	M/35	F/2.5	F/8	F/8	M/15	F/1	F/3	M/4	M/28	F/10	M/4.5	M/5mo	M/3	M/16	M/4	F/6	M/4	M/0
Phenotype	PD	PD	LS	LS	LS	LS	LS	LS	LS	LS	LS	LS	LS	LS	LS	LS	LS	LS	LS
Feeding difficulties	Yes	No	Yes	Yes	Yes	No	Yes	Yes	Yes	No	No	No	Yes	No	No	No	N/A	No	Yes
Neurological features	Lower limbs PD	Lower limbs PD	E	E, RI	EOEE: WS	D, A, Dysart	E	H, S, Spas	E,V	A, Spas, Dysart, Dysph	DD, D, At, Spas	E	E, DD, D, S, Dysph	Hypok and DD	E, A	DD, Pt, Stra	DD	E, H, D	H, Dysk
Seizures (age onset)	No	No	Focal seizures (2y)	No	WS (8mo)	No	No	Infantile Spasms mioclonic (3mo)	Infantile Spasms (4mo)	No	No	Status Epilepticus (5mo)	Clonic seizures (5mo)	Febrile Status Epilepticus (8mo)	No	No	No	WS (5mo)	No
Outcome																			
Death (age)/Alive (current age)	Alive: 3y	Alive: 6y	Alive: 4y	Death: 9y	Alive: 12y	Alive: 12y	Death: 2.5y	Alive: 3.3y	Alive: 1.3y	Alive: 7.8y	Alive: 2.3y	Death: 0.5y	Death: 16y	Alive: 35y	Alive: 10y	Alive: 18y	Alive: 15y	Alive: 8y	Alive 1.6y
Recurrent episodes of neurological involvement	3–4 PD episodes/ mo	3–4 PD episodes/ mo Stroke-like episode (4,5y)	No	No	No	D, motor regression	No	No	No	No	E, D and motor regression	No	Stroke-like episode (5y)	Motor regression	No	No	Acute E	Acute E and respiratory distress	No
Movement disorder	D	D, Spas	D	D	D, Hypok	D, A	D, Hypok, Spas	D, Hypok	No	D, A, Spas	D, Spas	D	D, Spas	D, A, Spas	D, A, Spas	A	D, A, Spas	Spas	Spas
Hearing loss	No	No	No	Yes	Yes	No	Yes	Yes	Yes	No	ND	Yes	No	No	No	No	No	Yes	No
Optic atrophy	No	No	Yes	Yes	Yes	No	Yes	Yes	Yes	No	No	ND	Yes	Yes	No	No	No	No	No
Nystagmus	No	No	Yes	Yes	No	No	Yes	Yes	Yes	Yes	Yes	No	No	No	No	Yes	Yes	No	Yes
Microcephaly	No	No	Yes	Yes	Yes	No	Yes	Yes	No	No	No	No	Yes	No	No	No	No	Yes	Yes
Non-neurological features	No	No	HC	No	HC	No	No	HC	HC, CRF, Hep	No	No	HC	No	Retinitis	No	No	No	Hypothyroidism, CRF	No
Developmental impairment	No	Mild	Severe	Severe	Severe	Mild	Severe	Severe	Severe	Mild	Moderate - Severe	Severe	Severe	Severe	Moderate	Severe	Severe	Severe	Severe
GMFCS	I	I	V	V	V	III	V	V	V	ND	V	V	V	V	IV	IV	IV	ND	V
MACS	ND[b]	I	V	V	V	III	ND[b]	ND[b]	ND[b]	ND	ND[b]	ND[b]	V	V	III	IV	IV	ND	ND[b]
CFCS	I	I	V	V	V	I	V	V	ND	ND	V	ND	V	III	I	II	IV	ND	ND
Radiological findings																			
BG T2 hyperintensity	GP	GP	C, P, GP	C, GP	C, P	C, P	C, P	P	No	P, C	C,P, GP	C, P,GP	C, P, GP	GP	GP	GP	C,P, GP,	P	GP
BG Cavitation	GP	GP	P	No	No	No	P	P	No	No	P	No	P, GP	GP	GP	GP	No	No	No
Dentate T2-w hyperintensity	No	No	No	No	No	No	No	No	No	No	No	Yes	No	Yes	No	Yes	Yes	Yes	No
Cerebellar atrophy	No	No	Yes	No	Yes	No	No	No	No	No	No	No	Yes	No	No	Yes	Yes	Yes	No
Brain atrophy	No	No	Yes	No	Yes	No	Yes	Yes	Yes	No	No	Yes	Yes	Yes	Yes	No	No	No	No
White matter involvement	No	No	Volume loss	No	Leukodystrophy	No	Leukodystrophy	Leukodystrophy	Leukodystrophy	Gliosis	No	Yes	Volume loss	No	No	Yes	No	No	No
Biochemical features																			
Plasma lactate	Normal	Normal	Elevated	Elevated	Elevated	Elevated	Elevated	Elevated	Elevated	Elevated	Elevated	Normal	Normal	Elevated	Normal	Elevated	Normal	Elevated	Elevated
Alpha-alanine	Normal	Normal	Normal	Normal	Normal	ND	Normal	Normal	Elevated	Elevated	Elevated	Normal	Elevated	Elevated	Normal	Normal	Normal	Elevated	Elevated
Acyl-carnitines	ND	Normal	Normal	Normal	ND	Normal	ND	Normal	Normal	Normal	↑ C2	ND	ND	↑ C4-OH	Normal	↑ C4-OH	↑ C4-OH	↑C2, ↑C3	Normal

TABLE 1 (Continued)

Patient	Impairment in the fourth step of valine catabolism: SCEH deficiency												Impairment in the fifth step of valine catabolism: HIBCH deficiency						
	1	2	3	4	5	6	7	8	9	10	11	12	13	14	15	16	17	18	19
2-Methyl-2, 3-hydroxybutyrate acid	Normal	Normal	Normal	Normal	Normal	Normal	Normal	Elevated	Elevated	Normal	Elevated	Elevated	ND	Normal	Normal	Normal	Normal	Normal	Elevated
RCC	ND	ND	Normal	Normal	ND	↓ CI	↓ CII, CI+III	ND	Normal	ND	ND	ND	ND	ND	ND	↓ CI	↓ CI	↓ CI, CII, CIII	ND
PDHc activity	ND	ND	ND	Normal	ND	ND	Decrease	ND	Normal	ND	Decrease	ND	ND	Normal	ND	ND	ND	Decreased	ND

Abbreviations: A, ataxia; At, athetosis; CRF, chronic respiratory failure; C, caudate; D, dystonia; Dysk, dyskinesia; Dysart, dysarthria; Dysph, dysphagia; EOEE, early onset epileptic encephalopathy; E, encephalopathy; GP, globus pallidus; Hep, hepatomegaly; H, hypotonia; HC, hypertrophic cardiomyopathy; Hypok, hypokinesia; LS, Leigh syndrome; ND, not determined; PD, paroxysmal dystonia; Pt, ptosis; Stra, strabismus; P, putamen; Spas, spasticity; RI, respiratory insufficiency; RN, red nuclei; RCC, respiratory chain complex; T, thalamus; S, seizures; SN, substantia nigra; V, vomiting; WS, West Syndrome; WM, white matter; C4-OH, 3-hydroxyisobutyrylcarnitine.

[a]Novel mutations.

[b]Younger than 4 years of age.

encephalopathy, and infantile spasms. Five patients developed cardiac ventricular hypertrophy. Four patients died between 0.5 and 16 years of age. Neurological examination of seven surviving patients at a mean age of 5.7 (1.3-12) years showed movement disorders (dystonia, hypokinesia, ataxia, and spasticity), epilepsy, hearing loss, microcephaly, nystagmus, and optic atrophy. Eight patients were severely impaired according to gross motor function (GMFCS), manual ability (MACS), and communication function classification system (CFCS) (levels IV-V); whereas two children with a later onset (P6 and P10) had mild developmental delay and GMFCS levels I-III.

P1 and P2 presented at 18 and 35 months with 3-4 monthly episodes of paroxysmal dystonia, lasting 15-40 minutes, affecting asymmetrically one lower limb and occasionally the upper limb. In P1, these episodes were triggered by fever and infection. On follow-up, P1 was a normally developing child at 3 years of age; P2 presented a stroke-like event with acute hemidystonia at 4.5 years followed by residual spastic-dystonic hemiparesis and learning and speech difficulties. Brain MRI in both cases (P1 at 22 months; P2 at 5 years) showed bilateral T2-WI hyperintensity, restricted diffusion, and asymmetric cavitation of globus pallidus (Figure 2B,C).

P12 was diagnosed on newborn screening after abnormal acyl-carnitine profile, elevated urinary excretion of 2,3-dihydroxy-2-methylbutyrate acid, and genetic confirmation. P12 died at 5 months from LS and respiratory infection.[23] The severe clinical deterioration by the time of genetic confirmation precluded any therapeutic intervention in this patient.

Some patients received valine restricted and low protein formula (P1, P3, P5-6, and P8-P11) and/or supplementation of thiamine (n = 8), biotin (n = 4), riboflavin (n = 6), CoQ (n = 9), and carnitine (n = 8). P6 presented a mild improvement in lower limb dystonia while receiving valine restricted formula (ELL's personal observation). No neurological improvement was observed for the rest of patients.

3.1.2 | Neuroradiological findings

Brain MRI showed T2-WI hyperintense lesions in the basal ganglia in 12/13 SCEH patients. Cavitation was observed in the putamen in 5/11 LS patients and in the globus pallidus in 2/2 paroxysmal dystonia patients. Less frequent abnormalities were brain and cerebellar atrophy, T2-WI dentate hyperintensities, and white matter, brainstem and thalamus involvement (Figure 2B). P13 suffered from recurrent stroke-like episodes in both cerebral hemispheres. Magnetic resonance spectroscopy (MRS) showed elevated lactate peak in 5/9 patients.

TABLE 2 Clinical, biochemical and radiologic features that may suggest the diagnosis of HIBCH vs SCEH deficiency

HIBCH	*ECHS1*
Onset before 10 years of age	Onset before 10 years of age
Clinical phenotype: Leigh syndrome (#256000) (100%)	*Clinical phenotype*: Leigh syndrome (#256000) 79% Fatal neonatal lactic acidosis 11% Paroxysmal dystonia triggered by high metabolic demands (exercise, fever, and low caloric intake) 10%
Main features (present in >50%): Developmental delay/arrest/regression Acute episodes of encephalopathy and neurological deterioration Movement disorders **(**dystonia, ataxia, and spasticity)	*Main features (present in >50%)*: Developmental delay/arrest/regression Acute episodes of encephalopathy and neurological deterioration Movement disorders **(**dystonia, ataxia, and spasticity)
Less common neurological features: Ocular abnormalities (optic atrophy and nystagmus) Seizures Microcephaly	*Less common neurological features*: Sensorineural hearing loss Ocular abnormalities: optic atrophy and nystagmus Seizures (infantile spasms maybe present)Microcephaly Paroxysmal dystonia Stroke-like episodes *Non-neurological symptoms*: Dilated or hypertrophic cardiomyopathy, and hepatomegaly
Main biochemical features (present in >50%): Elevated plasma levels of 3-hydroxyisobutyryl carnitine *Less common findings*: ↓PDH activity (muscle/fibroblasts) ↓RCC activities (muscle/fibroblasts) ↑Plasma lactate and pyruvate levels	*Main biochemical features (present in >50%)*: ↑plasma lactate levels Elevated S-(2-carboxypropyl)cysteine and N-acetyl-S-(2-carboxypropyl) cysteine ↑urinary excretion of organic acids (↑2,3-dihydroxy-2-methylbutyric acid, 3-MGA, 3-HIVA, and EMA) **Less common findings:** ↓PDH activity (muscle/fibroblasts) ↓RCC activities (muscle/fibroblasts)
Main neuroradiological features (present in >50%): Bilateral globus pallidus T2-WI hyperintensities (cytotoxic, vasogenic, or STE oedema and/or cavitation may be present) *Less common findings*: Bilateral caudate/putamen T2-WI hyperintensities (cytotoxic, vasogenic, or STE oedema and/or cavitation may be present) Brainstem lesions Brain atrophy White matter involvement Dentate T2-WI hyperintensity	*Main neuro radiological features (present in >50%)*: Bilateral putamen, caudate, and/or globus pallidus T2-WI hyperintensity (cytotoxic, vasogenic, or STE oedema and/or cavitation may be present) *Less common findings*: White matter involvement Brainstem lesions Brain atrophy Thinning of corpus callosum

Abbreviations: EMA, ethylmalonic acid; 3-HIVA, 3-hydroxyisovaleric acid; 3-MGA, methylglutaconic acid; PDHc, pyruvate dehydrogenase complex; RCC, respiratory chain complex; STE, shine through effect.

3.1.3 | Biochemical findings

We observed elevated levels of plasma lactate (9/12), pyruvate (4/9), alpha-alanine (4/11), C2 acetylcarnitine (1/9), and CSF lactate (2/8). Urinary organic acids showed high excretion of 2,3-dihydroxy-2-methylbutyrate acid (P8-9, P11-12), 3-hydroxyisovaleric (P4, P7), 3-methylglutaconic (P9, P12), and ethylmalonic acid (P4). Other biochemical abnormalities were: elevated methacrylate metabolites (P8-9, P11), mitochondrial respiratory chain complex I (CI) (P6) and combined CI-CII + CIII (P7) deficiencies, and decreased PDHc activity (P7 and P11). Four patients had normal pathology and immunohistochemistry on muscle biopsies.

3.2 | HIBCH deficiency

3.2.1 | Clinical phenotype and management

Six HIBCH patients had their onset of symptoms at 7.7 (0-19) months of age. Insidious onset in four children showed developmental delay and neurological

features (ptosis, strabismus, hypo- and hyperkinetic movements, and hypotonia). Two patients had acute onset triggered by infection, causing encephalopathy and ataxia (P14) and West Syndrome (P18). On follow-up, three patients developed recurrent episodes of acute encephalopathy and neurological deterioration triggered by infection (P14, and P17-18). On last examination (14.6 [1.67-35] years) patients had ataxia (4), dystonia (3), pyramidal signs (5), epilepsy (2), abnormal ocular movements (3), visual (1) and hearing loss (1), central apnoea, and moderate to severe functional impairment.

HIBCH patients received treatment with carnitine (n = 4), CoQ10 (n = 2), riboflavin (n = 2), thiamine (n = 1), a valine-restricted diet (P15-P19), and/or low protein intake diet (P14-15 and P18-19). In P14, a mild improvement in vigilance and environmental participation was observed under carnitine supplementation and protein restriction. However, no standardised follow up was designed to evaluate the clinical response of these patients.

3.2.2 | Neuroradiological findings

Brain MRI of HIBCH patients was characterised by bilateral globus pallidus involvement (T2-WI hyperintensities, cavitation, and/or atrophy) in 5/6 patients and T2-WI hyperintensity in the dentate nucleus (4/6). Cerebellar and brain atrophy was also observed (Figure 2C). MRS was available for one patient with normal pattern.

3.2.3 | Biochemical findings

We observed elevated levels of 3-hydroxyisobutyrylcarnitine (3/4), plasma lactate (4/6), pyruvate (2/3), and alpha-alanine (3/6). Abnormal urine organic acids (3/6) included 2-hydroxybutyric and 2-ketobutyric acids (P14), 3-methylglutaconic (P17), and 2,3-dihydroxy-2-methylbutyrate acid (P17-18). Other abnormalities were deficiencies of CI (P16-17), combined CI-CII-CIII (P18), and PDHc (P18). Histopathology of muscle biopsy was normal in three patients.

3.3 | Genetic results

Twenty-five out of 42 patients from the multi-centre cohort had a genetic confirmation. Among them, we identified four unrelated patients harbouring biallelic mutations in ECHS1 (n = 2) or HIBCH (n = 2); sixteen patients were found to have pathogenic variants in other genes causing LS, and five cases had genetic defects not related to mitochondrial metabolism but with clinical evidence of basal ganglia dysfunction (data not shown). Overall, genetic defects in the valine catabolic pathway represented 4/20 (20%) of all genetically confirmed LS patients.

We also diagnosed P17, the sister of P16 from the multi-centre cohort with a similar phenotype, as having a HIBCH genetic defect.

In the newly identified patients with SCEH (n = 13) and HIBCH (n = 6) deficiency, we reported 18 variants, and 11 were novel (Table S3). Segregation was confirmed in all cases. Regarding the novel *ECHS1* c.367C>T [p.(Leu123Phe)] variant, we did not observe an alteration of the splicing pattern in P1 fibroblasts compared with a control sample. An 83.6% reduction in SCEH was confirmed by Western-blotting analysis (Figure 3F).

Figure 3 shows the location of novel missense variants in the protein structure. Table S3 details prioritisation parameters of pathogenicity for novel mutations. Table S4 shows the 52 *ECHS1* and *HIBCH* missense variants reported, including secondary structure and protein location.

3.4 | Phenotype-genotype correlations

We observed a longer survival in 27 HIBCH patients compared to 56 SCEH patients (mean age of survival: 30.9 vs 16.4 years; Breslow test, $P = .036$) (Figure 2D).

In HIBCH patients, we observed a longer survival in patients with homozygous mutations located on the protein surface than in those with variants inside or near the catalytic site (log-rank test $P = .004$, Figure 2E). The same analysis could not be conducted in the SCEH patients due to the low number of homozygous cases.

In SCEH patients, the missense *ECHS1* variant c.518C>T [p.(Ala173Val)] in compound heterozygosity was present in 5/6 patients with paroxysmal dystonia (5/12 alleles) compared to 1/56 patients (1/112 alleles) with LS or fatal neonatal lactic acidosis (chi-squared, $P < .0001$, risk estimate 80.71).

4 | DISCUSSION

In this report, we describe the phenotype and genotype spectrum of 19 SCEH/HIBCH patients from a multicentre study. We compare them with 72 previously reported patients (Table S1) and summarise the main clinical, biochemical and radiologic features that may suggest the diagnosis of HIBCH vs SCEH deficiency in Table 2.

To date, 63 SCEH patients are described, all presenting between 0 and 18 years of age.[2,4,26-35,8,

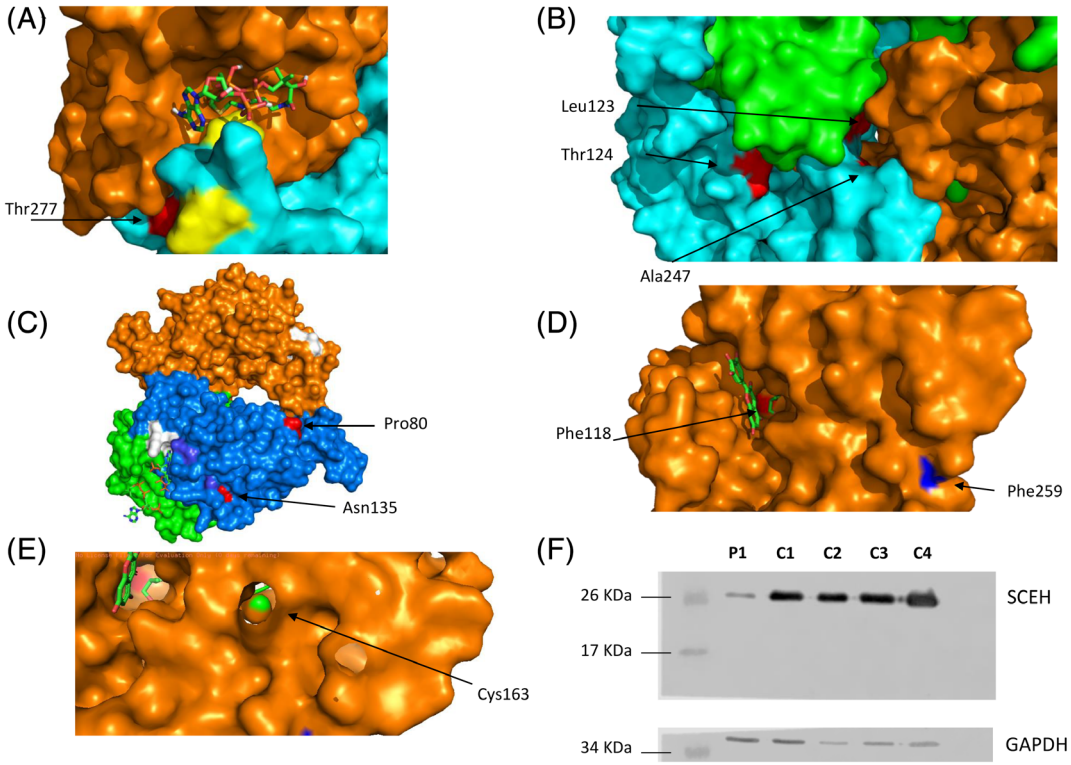

FIGURE 3 PyMol representation of SCEH, A, B, and C, HIBCH, D and E, proteins, and Western-blotting analysis, F. A, Location of the novel variant Thr277 (in red) and reported mutations (Phe279 and Glu281, in yellow). Binding site with the ligand crotonyl-CoA is also represented. Different monomers are represented in different colours (orange and blue). The interaction between the novel variant and the binding site are shown. B, Location of the novel variants Leu123, Thr124, and Arg181 (in red). Different monomers are represented with different colours (blue, green, and orange). These three mutations are located in the inter-phase between monomers. C, Location of Pro80 (red) on the surface of the protein. The novel change Asn135 (red) is located inside the protein. D, Location of variant Phe118 (red) and Phe259 (blue). Ligands quercetin and 3-hydroxyisobutyrate are represented. Phe118 is located in the binding site while Phe259 is in the periphery of the protein. E, Location of Cys163 (green) in the inner part of the protein. F, Western blotting analysis of fibroblasts from P1 and four normal controls using antibodies specific for SCEH protein (upper panel) or GAPDH (lower panel)

[36,10-13,22,24,25,59] Three distinct clinical phenotypes are reported: LS (79%), paroxysmal dystonia (10%), and fatal neonatal lactic acidosis (11%) (Table S1). Kaplan-Meier survival curves showed that half of the patients died before 10 years of age.

In our series, the SCEH patients developed LS within the first 3 years of life. We observed infantile spasms in 33% of SCEH-LS patients, a rare LS feature reported in other molecular defects.[37,38] Neurological outcome was associated with severe impairment on gross motor, manual ability and communication function, as well as movement disorders, seizures, microcephaly, and hearing and visual involvement. Cardiomyopathy, previously reported in 21% of SCEH patients with severe neonatal forms,[10,13,25,27] was identified in 5/13 patients.

On the opposite side of the severity spectrum, the SCEH-related paroxysmal dystonia phenotype was identified in two patients from our cohort and in four previous cases. All six patients were normally developing children who presented with paroxysmal dystonia at 3.4 (1.7-8) years.[11,32,36] Two clinical scenarios were identified: (a) paroxysmal and asymmetric dystonic episodes in the lower limbs lasting a few minutes, and normal neurological examination in between episodes (P1,[11,32]); and (b) stroke-like events with acute hemydystonia and residual pyramidal and extra-pyramidal signs (P2,[32]). Prolonged exercise, fasting, and febrile illness were frequent triggers in these children. Thus, paroxysmal dystonia triggered by situations with increased energy demands should lead to the suspicion of SCEH-related disease. Patients received a vitamin cocktail with no improvement in the episodes, in contrast to the improvement reported in two patients taking a vitamin cocktail[32] or ketogenic diet.[39]

Currently, 28 HIBCH patients are described presenting with LS from 0 to 5 years of age. In our series, early signs of developmental delay were observed, together with insidious onset of hypotonia, feeding difficulties, pyramidal signs, dystonia, and ataxia. Episodes of acute deterioration were common during febrile illness, as in 50% of reported patients.[9,14,40-44] Seizures were

reported in 27%-33%.[40,45,46] Systemic features, such as those observed in SCEH and in other LS genetic defects, were not common in the HIBCH patients. Although early death may occur, survival up to 43 years of age has been reported.[41] Remarkably, we found a significant longer survival in the HIBCH patients compared to the SCEH patients (25.9% vs 43.4% of deceased cases).

Brain MRI analysis in this study identified basal ganglia cavitation in half of the patients. A phenotype-genotype association was observed, with small cysts predominating either in the putamen (SCEH-LS patients) or in the globus pallidus (HIBCH-LS patients). Moreover, in SCEH-paroxysmal dystonia patients asymmetric globus pallidus cavitation was observed in our series and in the literature.[36] Basal ganglia cavitation was initially described in anatomo-pathological studies of LS patients[1,49] and later as a specific MRI feature located in the putamen in *SLC19A3*,[50] *NDUFAF6*,[51] and *NDUFV1*,[52] or in the globus pallidum in PDHc deficiency.[53] White matter demyelination and brain atrophy, dilated ventricles, and thinning of the corpus callosum was commonly observed in our SCEH patients, as in other causes of LS.[47] Stroke-like events were observed in one patient from our cohort and one previously reported patient[36] Finally, dentate T2-WI hyperintensity and cerebellar atrophy was observed in 4/6 patients with HIBCH, similar to LS patients with *MT-ATP6* and *SURF1* genetic defects.[43,47,48]

Biochemical features in our 19 patients suggested mitochondrial energy dysfunction, with elevated plasma lactate and alanine levels, respiratory chain complex and PDHc deficiencies, as described for other patients.[3,4,13,16,5-12] MRS lactate peak was most frequently observed in the SCEH patients than HIBCH patients. On the other hand, high levels of urinary lactate and 3-methylglutaconate (a biomarker of mitochondrial dysfunction), methacrylyl-CoA and acryloyl-CoA related metabolites, as well as 2,3-dihydroxy-2-methylbutyrate, a metabolite derived from acryloyl-CoA[29] (Figure 1) were more often recorded in SCEH than in HIBCH patients from our series. Methacrylate metabolites (S-2-carboxypropyl cysteamine, S-2-carboxypropyl cysteine and N-acetyl-S-2-carboxypropyl) were detected in 80% of our SCEH patients and 75% of previous reports,[8,11,12,26,27] even in the milder forms of paroxysmal dystonia.[12,28] Therefore, it seems that mitochondrial dysfunction and metabolite alterations are more severe in SCEH deficiency than in HIBCH deficiency, but more studies are necessary to corroborate this appreciation as metabolite abnormalities are essentially the same in both diseases, with the exception of 3-hydroxyisobutyryl carnitine (only present in HIBCH), that can be useful for the differential diagnosis. This metabolite was found in 75% of HIBCH cases in our study and in previous series.[4,9,26,27,40,41,45,54]

Forty-three different *ECHS1* mutations in 63 SCEH patients from 54 families have been described[2,4,26-35,8,36,10-13,22,24,25,59] (Figure S2). Overall, 73% of the variants were present exclusively in one or two alleles, confirming the wide genetic heterogeneity of *ECHS1*. The SCEH p.(Ala173Val) variant was detected in compound heterozygosity in 5/6 patients with a milder form of paroxysmal dystonia triggered by increased energy demands. The only patient harbouring this variant with LS phenotype was the older sibling of a patient with paroxysmal dystonia who manifested with acute neurological regression after a major surgery at 3.5 years of age.[11] Statistical analysis confirmed a strong association between p.(Ala173Val) variant and the paroxysmal dystonia phenotype, thus providing evidence for outcome prediction in these patients. P1 with paroxysmal dystonia carried the c.518C>T [p.(Ala173Val)] and the novel c.367C>T [p.(Leu123Phe)] in compound heterozygosity. We observed an 83.6% reduction of SCEH expression in the patient's fibroblasts, suggesting loss-of-function and hypomorphic effect. Because no splicing alteration was demonstrated for the c.367C>T [p.(Leu123Phe)], other molecular mechanisms can be postulated, such as protein instability or misfolding.

In *HIBCH*, 22 different pathogenic variants were reported in 28 patients (Figure S2).[9,14,55-58,40-46,54] Overall, 50% of the total *HIBCH* variants were unique mutations showing a wide heterogeneity. Remarkably, 17% of missense variants were located in the SCEH mitochondrial signal peptide while no variants were detected in the shorter HIBCH mitochondrial peptide (Table S4).

We observed a genotype-phenotype correlation in the homozygous HIBCH patients according to the protein location: the patients with mutations on the protein surface had longer survival than those with variants inside/near the catalytic site, as suggested in previous reports.[41] Thus, an early genetic diagnosis might be relevant to better predict outcome.

In conclusion, the SCEH and HIBCH defects in the catabolic valine pathway were a frequent cause of LS in our cohort. According to these results and previous literature, LS is a major phenotype in both genetic defects. The SCEH patients showed a broader spectrum of severity including children with isolated paroxysmal dystonia triggered by situations of increased energy demands, most of them harbouring the c.518C>T [p.(Ala173Val)] variant. Brain MRI analysis showed that the presence of small cysts in the putamen and the globus pallidus might be candidate radiological hallmarks for the diagnosis of both defects. Finally, genetic analysis led to the

identification of novel variants and allowed the establishment of phenotype-genotype correlations.

CONFLICT OF INTEREST

Laura Marti-Sanchez, Heidy Baide-Mairena, Anna Marcé-Grau, Roser Pons, Anastasia Skouma, Eduardo López-Laso, Maria Sigatullina, Critiano Rizzo, Michela Semeraro, Diego Martinelli, Rosalba Carrozzo, Carlo Dionisi-Vici, Luis González-Gutiérrez-Solana, Marta Correa-Vela, Juan Dario Ortigoza-Escobar, Angel Sánchez-Montañez, Elida Vázquez, Ignacio Delgado, Sergio Aguilera-Albesa, Maria Eugenia Yoldi, Antonia Ribes, Frederic Tort, Luca Pollini, Serena Galosi, Vincenzo Leuzzi, Manuela Tolve, Laura Pérez-Gay, Luis Aldamiz-Echevarría, Mireia Del Toro, Antonio Arranz, Filip Roelens, Roser Urreizti, Rafael Artuch, Alfons MAcaya, and Belén Perez-Dueñas declare that they have no conflict of interest.

AUTHORS CONTRIBUTIONS

L. Marti-Sanchez, H. Baide-Mairena, and B. Pérez-Dueñas participated in the study design, acquisition, analysis, and data interpretation, and drafting of the manuscript. L. Marti-Sanchez, H. Baide-Mairena, A. Marcé-Grau, R. Pons, A. Skouma, E. López-Laso, M. Sigatullina, C. Rizzo, M. Semeraro, D. Martinelli, R. Carrozzo, C. Dionisi-Vici, L. González-Gutiérrez-Solana, M. Correa-Vela, J.D. Ortigoza-Escobar, S. Aguilera-Albesa, M.E. Yoldi, A. Ribes, F. Tort, L. Pollini, S. Galosi, V. Leuzzi, M. Tolve, L. Pérez-Gay, L. Aldamiz-Echevarría, M. Del Toro, A. Arranz, F. Roelens, and A. Macaya were responsible for the collection of clinical data. L. Marti-Sanchez, R. Urreizti, and R. Artuch participated in the analysis and interpretation of the biochemical and molecular genetic studies. A. Sánchez-Montañez, I. Delgado, and E. Vazquez participated in the analysis and interpretation of brain MRIs. B. Pérez-Dueñas conceived the idea for the study, designed the study, supervised the study, interpreted the data, and drafted and revised the manuscript content. All of the authors read and approved the final manuscript.

ETHICAL APPROVAL

The ethics committee at Sant Joan de Déu Hospital (PIC-158-15) and at Vall d'Hebrón Hospital (PR(AG)430/2019) approved the study, and parents gave written informed consent for study participation.

This study does not contain any animal studies conducted by any of the authors. Participants or their legal guardians provided informed consent for their inclusion in the study. All procedures followed the Helsinki Declaration of 1975 as revised in 2013.

ORCID

Belén Pérez-Dueñas https://orcid.org/0000-0002-4979-2788

REFERENCES

1. Lake NJ, Bird MJ, Isohanni P, Paetau A. Leigh syndrome: neuropathology and pathogenesis. *J Neuropathol Exp Neurol*. 2015;74(6):482-492.
2. Aretini P, Mazzanti CM, La Ferla M, et al. Next generation sequencing technologies for a successful diagnosis in a cold case of Leigh syndrome. *BMC Neurol*. 2018;18(1):99.
3. Rahman J, Noronha A, Thiele I, Rahman S. Leigh map: a novel computational diagnostic resource for mitochondrial disease. *Ann Neurol*. 2017;81(1):9-16.
4. Ogawa E, Shimura M, Fushimi T, et al. Clinical validity of biochemical and molecular analysis in diagnosing Leigh syndrome: a study of 106 Japanese patients. *J Inherit Metab Dis*. 2017;40(5):685-693.
5. Kohda M, Tokuzawa Y, Kishita Y, et al. A comprehensive genomic analysis reveals the genetic landscape of mitochondrial respiratory chain complex deficiencies. *PLoS Genet*. 2016;12(1):e1005679.
6. Murayama K, Shimura M, Liu Z, Okazaki Y, Ohtake A. Recent topics: the diagnosis, molecular genesis, and treatment of mitochondrial diseases. *J Hum Genet*. 2019;64(2):113-125.
7. El-Hattab AW, Zarante AM, Almannai M, Scaglia F. Therapies for mitochondrial diseases and current clinical trials. *Mol Genet Metab*. 2017;122(3):1-9.
8. Peters H, Buck N, Wanders R, et al. ECHS1 mutations in Leigh disease: a new inborn error of metabolism affecting valine metabolism. *Brain*. 2014;137(Pt 11):2903-2908.
9. Peters H, Ferdinandusse S, Ruiter JP, Wanders RJ, Boneh A, Pitt J. Metabolite studies in HIBCH and ECHS1 defects: implications for screening. *Mol Genet Metab*. 2015;115(4):168-173.
10. Ganetzky RD, Bloom K, Ahrens-Nicklas R, et al. ECHS1 deficiency as a cause of severe neonatal lactic acidosis. *JIMD Rep*. 2016;30:33-37.
11. Olgiati S, Skorvanek M, Quadri M, et al. Paroxysmal exercise-induced dystonia within the phenotypic spectrum of ECHS1 deficiency. *Mov Disord*. 2016;31(7):1041-1048.
12. Huffnagel IC, Redeker EJW, Reneman L, Vaz FM, Ferdinandusse S, Poll-The BT. Mitochondrial encephalopathy and transient 3-methylglutaconic aciduria in ECHS1 deficiency: long-term follow-up. *JIMD Rep*. 2018;39:83-87.
13. Nair P, Hamzeh AR, Mohamed M, Malik EM, Al-Ali MT, Bastaki F. Novel ECHS1 mutation in an Emirati neonate with severe metabolic acidosis. *Metab Brain Dis*. 2016;31(5):1189-1192.
14. Ferdinandusse S, Waterham HR, Heales SJ, et al. HIBCH mutations can cause Leigh-like disease with combined deficiency of multiple mitochondrial respiratory chain enzymes and pyruvate dehydrogenase. *Orphanet J Rare Dis*. 2013;8:188.
15. Sharpe AJ, McKenzie M. Mitochondrial fatty acid oxidation disorders associated with short-chain enoyl-CoA hydratase (ECHS1) deficiency. *Cell*. 2018;7(6):46.
16. Janssen U, Davis EM, Le Beau MM, Stoffel W. Human mitochondrial enoyl-CoA hydratase gene (ECHS1): structural

organization and assignment to chromosome 10q26.2-q26.3. *Genomics*. 1997;40(3):470-475.
17. Wanders RJ, Duran M, Loupatty FJ. Enzymology of the branched-chain amino acid oxidation disorders: the valine pathway. *J Inherit Metab Dis*. 2012;35(1):5-12.
18. Christou C, Gika HG, Raikos N, Theodoridis G. GC-MS analysis of organic acids in human urine in clinical settings: a study of derivatization and other analytical parameters. *J Chromatogr B Anal Technol Biomed Life Sci*. 2014;964:195-201.
19. Rustin P, Chretien D, Bourgeron T, et al. Biochemical and molecular investigations in respiratory chain deficiencies. *Chim Acta*. 1994;228(1):35-51.
20. Sutendra G, Dromparis P, Bonnet S, et al. Pyruvate dehydrogenase inhibition by the inflammatory cytokine TNFα contributes to the pathogenesis of pulmonary arterial hypertension. *J Mol Med*. 2011;89(8):771-783.
21. Rahman S, Blok RB, Dahl HH, et al. Leigh syndrome: clinical features and biochemical and DNA abnormalities. *Ann Neurol*. 1996;39(3):343-351.
22. Tetreault M, Fahiminiya S, Antonicka H, et al. Whole-exome sequencing identifies novel ECHS1 mutations in Leigh syndrome. *Hum Genet*. 2015;134(9):981-991.
23. Pajares S, López RM, Gort L, et al. An incidental finding in newborn screening leading to the diagnosis of a patient with ECHS1 mutations. *Mol Genet Metab Reports*. 2020;22:100553.
24. Sakai C, Yamaguchi S, Sasaki M, Miyamoto Y, Matsushima Y, Goto Y. ECHS1 mutations cause combined respiratory chain deficiency resulting in leigh syndrome. *Hum Mutat*. 2015;36(2):232-239.
25. Haack TB, Jackson CB, Murayama K, et al. Deficiency of ECHS1 causes mitochondrial encephalopathy with cardiac involvement. *Ann Clin Transl Neurol*. 2015;2(5):492-509.
26. Yamada K, Aiba K, Kitaura Y, et al. Clinical, biochemical and metabolic characterisation of a mild form of human short-chain enoyl-CoA hydratase deficiency: significance of increased n-acetyl-s-(2-carboxypropyl)cysteine excretion. *J Med Genet*. 2015;52(10):691-698.
27. Ferdinandusse S, Friederich MW, Burlina A, et al. Clinical and biochemical characterization of four patients with mutations in ECHS1. *Orphanet J Rare Dis*. 2015;10:79.
28. Al Mutairi F, Shamseldin HE, Alfadhel M, Rodenburg RJ, Alkuraya FS. A lethal neonatal phenotype of mitochondrial short-chain enoyl-CoA hydratase-1 deficiency. *Clin Genet*. 2017;91(4):629-633.
29. Bedoyan JK, Yang SP, Ferdinandusse S, et al. Lethal neonatal case and review of primary short-chain enoyl-CoA hydratase (SCEH) deficiency associated with secondary lymphocyte pyruvate dehydrogenase complex (PDC) deficiency. *Mol Genet Metab*. 2017;120(4):342-349.
30. Balasubramaniam S, Riley LG, Bratkovic D, et al. Unique presentation of cutis laxa with Leigh-like syndrome due to ECHS1 deficiency. *J Inherit Metab Dis*. 2017;40(5):745-747.
31. Fitzsimons PE, Alston CL, Bonnen PE, et al. Clinical, biochemical, and genetic features of four patients with short-chain enoyl-CoA hydratase (ECHS1) deficiency. *Am J Med Genet Part A*. 2018;176(5):1115-1127.
32. Mahajan A, Constantinou J, Sidiropoulos C. ECHS1 deficiency-associated paroxysmal exercise-induced dyskinesias: case presentation and initial benefit of intervention. *J Neurol*. 2017;264(1):185-187.
33. Carlston CM, Ferdinandusse S, Hobert JA, Rong M, Longo N. Successful screening for Gaucher disease in high-prevalence population in Tabuleiro do Norte. *JIMD Rep*. 2018;1:73-78.
34. Uchino S, Iida A, Sato A, et al. A novel compound heterozygous variant of ECHS1 identified in a Japanese patient with Leigh syndrome. *Hum Genome Var*. 2019;6:6-9.
35. Stark Z, Tan TY, Chong B, et al. A prospective evaluation of whole-exome sequencing as a first-tier molecular test in infants with suspected monogenic disorders. *Genet Med*. 2016;18(11):1090-1096.
36. Korenke G, Nuoffer JM, Alhaddad B, et al. Paroxysmal dyskinesia in ECHS1 defect with globus pallidus lesions. *Neuropediatrics*. 2016;47:518.
37. Vona B, Maroofian R, Bellacchio E, et al. Expanding the clinical phenotype of IARS2-related mitochondrial disease. *BMC Med Genet*. 2018;19(1):196.
38. Takada R, Tozawa T, Kondo H, et al. Early infantile-onset Leigh syndrome complicated with infantile spasms associated with the m.9185 T>C variant in the MT-ATP6 gene: expanding the clinical spectrum. *Brain Dev*. 2020;42(1):69-72.
39. Sofou K, De Coo IF, Isohanni P, et al. A multicenter study on Leigh syndrome: disease course and predictors of survival. *Orphanet J Rare Dis*. 2014;9:52.
40. Loupatty FJ, Clayton PT, Ruiter JP, et al. Mutations in the gene encoding 3-hydroxyisobutyryl-CoA hydrolase results in progressive infantile neurodegeneration. *Am J Hum Genet*. 2007;80(1):195-199.
41. Schottmann G, Sarpong A, Lorenz C, et al. A movement disorder with dystonia and ataxia caused by a mutation in the HIBCH gene. *Mov Disord*. 2016;31(11):1733-1739.
42. Yamada K, Naiki M, Hoshino S, et al. Clinical and biochemical characterization of 3-hydroxyisobutyryl-CoA hydrolase (HIBCH) deficiency that causes Leigh-like disease and ketoacidosis. *Mol Genet Metab Reports*. 2014;1:455-460.
43. Soler-Alfonso C, Enns GM, Koenig MK, Saavedra H, Bonfante-Mejia E, Northrup H. Identification of HIBCH gene mutations causing autosomal recessive Leigh syndrome: a gene involved in valine metabolism. *Pediatr Neurol*. 2015;52(3):361-365.
44. Yang HY, Wu LW, Deng XL, Yin F, Yang LF. Diagnosis and treatment of 3-hydroxyisobutyryl-CoA hydrolase deficiency: a case report and literature review. *Chinese J Contemp Pediatr*. 2018;20(8):647-651.
45. Reuter MS, Sass JO, Leis T, et al. HIBCH deficiency in a patient with phenotypic characteristics of mitochondrial disorders. *Am J Med Genet Part A*. 2014;164A(12):3162-3169.
46. Reuter MS, Tawamie H, Buchert R, et al. Diagnostic yield and novel candidate genes by exome sequencing in 152 consanguineous families with neurodevelopmental disorders. *JAMA Psychiat*. 2017;74(3):293-299.
47. Bonfante E, Koenig MK, Adejumo RB, Perinjelil V, Riascos RF. The neuroimaging of Leigh syndrome: case series and review of the literature. *Pediatr Radiol*. 2016;46(4):443-451.
48. de Beaurepaire I, Grévent D, Rio M, et al. High predictive value of brain MRI imaging in primary mitochondrial respiratory chain deficiency. *J Med Genet*. 2018;55(6):378-383.
49. Cavanagh JB, Harding BN. Pathogenic factors underlying the lesions in Leigh's disease. Tissue responses to cellular energy

deprivation and their clinico-pathological consequences. *Brain*. 1994;117 (Pt 6:1357-1376.
50. Alfadhel M, Almuntashri M, Jadah RH, et al. Biotin-responsive basal ganglia disease should be renamed biotin-thiamine-responsive basal ganglia disease: a retrospective review of the clinical, radiological and molecular findings of 18 new cases. *Orphanet J Rare Dis*. 2013;8:83.
51. Bianciardi L, Imperatore V, Fernandez-Vizarra E, et al. Exome sequencing coupled with mRNA analysis identifies NDUFAF6 as a Leigh gene. *Mol Genet Metab*. 2016;119(3):214-222.
52. Lal D, Becker K, Motameny S, et al. Homozygous missense mutation of NDUFV1 as the cause of infantile bilateral striatal necrosis. *Neurogenetics*. 2013;14(1):85-87.
53. van Dongen S, Brown RM, Brown GK, Thorburn DR, Boneh A. Thiamine-responsive and non-responsive patients with PDHC-E1 deficiency: a retrospective assessment. *JIMD Rep*. 2015;15:13-27.
54. Stiles AR, Ferdinandusse S, Besse A, et al. Successful diagnosis of HIBCH deficiency from exome sequencing and positive retrospective analysis of newborn screening cards in two siblings presenting with Leigh's disease. *Mol Genet Metab*. 2015;115(4):161-167.
55. Brown GK, Hunt SM, Scholem R, et al. Beta-Hydroxyisobutyryl coenzyme a Deacylase deficiency: a defect in valine metabolism associated with physical malformations. *Pediatrics*. 1982;70(4):532-538.
56. Tan H, Chen X, Lv W, Linpeng S, Liang D, Wu L. Truncating mutations of HIBCH tend to cause severe phenotypes in cases with HIBCH deficiency: a case report and brief literature review. *J Hum Genet*. 2018;63(7):851-855.
57. Karimzadeh P, Saberi M, Sheidaee K, Nourbakhsh M, Keramatipour M. 3-Hydroxyisobutyryl-CoA hydrolase deficiency in an Iranian child with novel HIBCH compound heterozygous mutations. *Clin Case Reports*. 2019;7(2):375-380.
58. Candelo E, Cochard L, Caicedo-Herrera G, et al. Syndromic progressive neurodegenerative disease of infancy caused by novel variants in HIBCH: report of two cases in Colombia. *Intractable Rare Dis Res*. 2019;8(3):187-193.
59. Yang H, Yu D. Clinical, biochemical and metabolic characterization of patients with short-chain enoyl-CoA hydratase (ECHS1) deficiency: two case reports and the review of the literature. *BMC Pediatr*. 2020;20(1):50.

SUPPORTING INFORMATION

Additional supporting information may be found online in the Supporting Information section at the end of this article.

How to cite this article: Marti-Sanchez L, Baide-Mairena H, Marcé-Grau A, et al. Delineating the neurological phenotype in children with defects in the *ECHS1* or *HIBCH* gene. *J Inherit Metab Dis*. 2020;1–14. https://doi.org/10.1002/jimd.12288

Supplementary material:

Delineating the neurological phenotype in children with *ECHS1* and *HIBCH* genetic defects.

L Marti-Sanchez[1,2*], H Baide-Mairena[3,4,5*], A Marcé-Grau[3], R Pons[6], A Skouma[7], E López-Laso[8,9,21], M Sigatullina[3], C Rizzo[10], M Semeraro[10], D Martinelli[10], R Carrozzo[10], C Dionisi-Vici[10], L González-Gutiérrez-Solana[11,21], M Correa-Vela[3,4], JD Ortigoza-Escobar[12], A Sánchez-Montañez[13], E Vazquez[13], I Delgado[13], S Aguilera-Albesa[14], ME Yoldi[14], A Ribes[15,21], F Tort[15,21] , L Pollini[16], S Galosi[16], V Leuzzi[16], M Tolve[17], L Pérez-Gay[18], L Aldamiz-Echevarría[19], M Del Toro[3], A Arranz[3], F Roelens[20], R Urreizti[1,21], R Artuch[1,21], A Macaya[3,4,21], B Pérez-Dueñas[3,4]

Supplementary methods

Patients

Physical and neurological examination was performed by paediatric experts in inborn errors of metabolism from the coordinator centre (Hospital Universitari Vall d'Hebron; HUVH) in six patients, and by experts from collaborating centres in 12 cases.

The questionnaire from the responsible clinician at each collaborating centre included demographic data, genetic studies, early developmental milestones, age of disease onset, trigger events, clinical and biochemical data, multi-systemic evaluation, clinical follow-up, and management. Functional capability was assessed at the last examination according to GMFCS E&R (Gross Motor Function Classification System - Expanded & Revised) in all ages, MACS (Manual Ability Classification System) in patients older than four years, and CFCS (Communication Function Classification System) in patients older than two years.

Neuroimaging studies

MRI from 13 of 19 patients underwent systematic analysis by two paediatric neurologists and two paediatric neuroimaging experts from HUVH. The MRI analysis included the location and presence of T2-WI/FLAIR hyperintensity, T1-WI hypointensity, atrophy, and DWI/ADC hyper/hyposignal. Cavitation was described when T1-WI and FLAIR hypointensity was present. Neuroradiologists from the collaboration centres following the same protocol conducted the MRI analysis of the remaining six patients. MRI spectroscopy was available in 16 cases to analyse the presence/absence of lactate peak.

Biochemical studies

Biochemical studies included plasma and CSF lactate, pyruvate, and plasma amino acids. Urine organic acids were also analysed, including the acryloyl-CoA metabolite 2,3-dihydroxy-2-methylbutyrate acid (P8, P9, P11, P12, and P18). Methacrylate metabolites S-(2-carboxypropyl) cysteine and S-(2-carboxypropyl) cysteamine were studied (P8, P9, P11, P17, and P18). Acyl-carnitines analysis was assessed, considering C4OH carnitine in the HIBCH patients. In the patients with suspected OXPHOS impairment PDHc activity and mitochondrial respiratory chain enzymes were analysed. Histopathology of muscle biopsies were analysed in P3, P7, P9, P15, P16, and P17.

Genetic analysis

Patients from the LS cohort at HUVH underwent whole exome sequencing (WES). Genomic DNA samples were extracted from the peripheral blood using standard methods. Sequencing (SureSelect Human All Exon V6, Agilent) and bioinformatics analysis was performed by Centogene (Rostock, Germany). Variant annotation and analysis was done using VarAFT software[1]. Variants were filtered by minimum allele frequency <0.01 in the Genome Aggregation Database[2] (GnomAD, accessed January 2020) and variant type. We considered *in silico* bioinformatics prediction tools (Mutation Taster[3], SIFT, PROVEAN[4] and Human Splicing Finder[5]) and reported mutations in Human Gene Mutation Database (HGMD professional 2019.2) and ClinVar database[6]. All of the inheritance Mendelian patterns were considered. All of the selected variants were validated by Sanger sequencing. Whenever possible, segregation studies were conducted for candidate variants in family members, including other affected siblings.

Splicing analysis and protein expression studies

Skin fibroblasts from P1 and the normal controls were maintained in Dulbecco Modified Eagle's Minimal essential medium (DMEM; Biowest) supplemented with 10%

inactivated foetal bovine serum (FBS) and 1% sodium pyruvate and incubated at 37ºC with 5% of CO_2.

For splicing analysis of the c.367C>T variant in *ECHS1* gene, cycloheximide (1 mg/mL in DMEM) (Sigma-Aldrich, St. Louis, MO, USA) treatment was performed in P1 and one paediatric control fibroblasts for 6 hours. Afterwards, RNA was extracted from confluent fibroblast plates both in the presence and absence of cycloheximide, using TRIzol (NZYTech, Lisbon, Portugal). RNA quantity and quality was assessed via 1% agarose gel electrophoresis and spectrometry with a NanoDrop ND-100 spectrophotometer (Nanodrop Technologies Inc; Thermo Fisher Scientific, Waltham, MA, USA). Retrotranscription was performed using SuperScript™ III Reverse Transcriptase (Invitrogen, Thermo Fisher Scientific, Waltham, MA, USA). Exons 2 to 4 were amplified in overlapping fragments as indicated in Figure S1. Moreover, exons 1 to 5 were sequenced (primers not shown). PCR was performed in P1, a cDNA control, and a genomic control. All of the PCR fragments were sequenced for confirmation.

For Western-blotting studies, protein was extracted by lysing P1 and four normal control fibroblasts overnight with RIPA buffer. The protein concentration was determined using the Bradford method with a Bio-Rad Protein Assay (Bio-Rad, Hercules, CA, USA) using bovine serum albumin (BSA) as a standard. The proteins were electrophoresed on 10% polyacrylamide gel and transferred to polyvinylidene fluoride membrane (PVDF; Thermo Fisher Scientific, Waltham, MA, USA). The membrane was incubated with anti-SCEH (1:3000; AB153732, Abcam) at 4ºC overnight and anti-GAPDH (1:5000; 60004-1; Proteintech) for 2 hours at room temperature. Secondary anti-rabbit or anti-mouse IgG antibodies were used (1:5000, Dabco, Cusabio), respectively, and was developed using an Amersham ECL Prime kit (GE Healthcare).

Statistical analysis

Statistical analyses were conducted using IBM SPSS Statistics 23 software (IBM Corp., Armonk, NY, USA). The quantitative variables were reported in terms of the normal distribution mean, standard error of the mean (SEM), and the range.

Different statistical methods were used to analyse phenotype to genotype correlations. Paroxysmal dystonia phenotype in SCEH-deficient patients correlated to c.518C>T variant was analysed using the chi-squared test. The Kaplan–Meier survival curve was used to compare the survival rates between SCEH and HIBCH deficiencies. Differences in survival between both groups were evaluated using the Breslow test because the majority of patients died within the first 10 years of life. The Kaplan-Meier curve was also used to compare patients who were homozygous for *HIBCH* mutations located inside or near the catalytic region of the protein vs those with mutations on the surface of the protein. Differences were evaluated using the log-rank test. All of the statistical tests were two-sided and conducted at a 0.05 significance level.

Table S1: **Clinical, radiological, biochemical, and genetic characteristics of 91 patients with genetic defects in *ECHS1* and *HIBCH***

Gene	***HIBCH***	***ECHS1***
Patients	28	63
References	[7,8,17–20,9–16], our report	[21,22,31–40,23,41,24–30,42], our report
First described in	1989	2014
Sex	19M/9F	27M/32F/4NR
Parental consanguinity	6	12
Affected siblings	2	17
Age at onset, median (range)	12,4 (0-65) months	10.6 (0-96) months
Current age, median (range)	14 (1,3- 43) years	9 (1.3-31) years
Alive/death/Not Reported	19/7/2NR	34/25/4NR
Age of death, median (range)	4,2 (0,25-8)years	2,3 (0-16) years
Phenotype		
LS (#256000)	28	50
Fatal neonatal lactic acidosis	0	7
Paroxysmal Dystonia	0	6
Clinical features at onset	n=28	n=59
Trigger	11 (39%)	7 (12%)
Encephalopathy	12 (43%)	20 (34%)
Respiratory insufficiency	2 (7%)	16 (27%)
Poor feeding	14 (50%)	16 (27%)
Hypotonia	22 (78%)	31 (53%)
Clinical features on follow up	n=28	n=59
Neurological features		
Developmental delay	19 (68%)	41 (69%)
Developmental regression	12 (43%)	25 (42%)
Hypotonia	22 (78%)	23 (39%)
Nystagmus	6 (21%)	12 (20%)
Seizures	8 (28%)	16 (27 %)
Microcephaly	6 (21%)	16 (27%)
Sensorineural hearing loss	0	21 (36%)
Optic atrophy	9 (32%)	17 (29%)
Movement disorders		
Dystonia	10 (36%)	31 (53%)
Ataxia	10 (36%)	8 (14%)
Spasticity	8 (28%)	12 (20%)
Rigidity	2 (7%)	6 (10%)
Chorea	0	4 (7%)
Tremor	1 (4%)	0
Extraneurological features		
Cardiomyopathy	0	12 (20%)
Hepatomegaly	0	6 (10%)
Dysmorphic features	5 (18%)	7 (12%)
Biochemical Features		
Elevated plasma lactate levels	10/24 (42%)	41/52 (79%)
Elevated plasma pyruvate levels	3/7 (43%)	6/19 (32%)
Elevated alanine levels	3/ 26 (11%)	17/41 (41%)
Abnormal urine organic acids	5 /26 (19%)	32/48 (67%)
Elevated 2,3-dihydroxy-2-methylbutyric acid	3 /26 (11%)	21/48 (44%)
Elevated S-(2-carboxypropyl)cysteine; N-acetyl-S-(2-carboxypropyl)cysteine	1 /26 (4%)	11/13 (85%)
Elevated C4OH acyl carnitine	15/20 (75%)	8/38 (21%)
Low PDH activity	4/9 (44%)	10/24 (42%)
RCC deficiency (muscle/fibroblasts)	7/16 (44%)	12/40 (30%)
Radiological features	n=23	n=50
Age at reported Brain MRI	4,17 (0,2-26) years	3,1 (0-16) years
Basal Ganglia lesions		
Putamen	7 (30%)	33 (66%)
Caudate	8 (35%)	30 (60%)
GP	23 (100%)	32 (64%)
Other affected structures:		
Thalamus	3 (13%)	9 (18%)
Brainstem	14 (61%)	16 (32%)
Substantia Nigra	1 (4%)	8 (16%)
White matter	9 (36%)	25 (50%)
Cerebellum	6 (26%)	11 (22%)
Medulla	0	4 (8%)
Other findings		
MRS lactate peak	2 (8%)	19/36 (53%)
Brain atrophy	18 (78%)	15 (30%)
Genetics		
Missense	64% (14/22)	84% (38/45)
Intron variant	23% (5/22)	7% (3/45)
Stop/Frameshift	14% (3/22)	9% (4/45)
Homozygous	68% (19/28)	32% (20/63)
Heterozygous	32% (9/28)	68% (43/63)

References	No. of patients with described Brain MRI	Age at assessment	T2-WI hyperintensity			Thalamus	Brainstem	Cerebellar involvement	White matter involvement	Brain atrophy
			Caudate	Putamen	Globus Pallidus					
ECHS1										
Peters, 2014	2	2 (0-4) months	0	1 (50%)	1 (50%)	1 (50%)	1 (50%)	0	2 (100%)	1 (50%)
Tetreault, 2015	4	6,6 (0,5-12) years	4(100%)	4 (100%)	4 (100%)	0	2 (50%)	1 (25%)	2 (50%)	0
Sakai, 2015	1	NR	0	1 (100%)	0	0	0	0	0	0
Haack, 2015	10	2,4 (0-15) years	3 (30%)	5 (50%)	3 (30%)	0	0	0	6 (60%)	2 (20%)
Yamada, 2015	2	15 (14-16) months	2 (100%)	2 (100%)	1 (50%)	0	0	0	0	0
Ferdinandusse, 2015	3	8(0-12)months	0	1 (33%)	1 (33%)	1 (33%)	1 (33%)	0	1 (33%)	1 (33%)
Olgiati, 2016	2	4,2 (3,5-5) years	0	0	1 (50%)	0	1 (50%)	0	0	0
Mahajan, 2016	1	NR	0	0	1 (100%)	0	0	0	0	0
Bedoyan, 2017	1	NR	0	0	0	0	0	0	1 (100%)	1 (100%)
Huffnagel 2017	1	1,4 and 12 years	1 (100%)	1 (100%)	0	0	0	1 (100%)	1 (100%)	1 (100%)
Balasubramaniam 2017	1	15months	1 (100%)	1 (100%)	1 (100%)	0	0	0	0	0
Fitzsimons, 2018	4	11 (1,2-35)months	4 (100%)	4 (100%)	4 (100%)	1(25%)	4 (100%)	2 (50%9	3 (75%)	2 (50%)
Aretini, 2018	1	16m and 12 years	1 (100%)	1 (100%)	1 (100%)	1 (100%)	0	0	0	0
Uchino, 2018	1	1 year	1 (100%)	1 (100%)	1 (100%)	0	1 (100%)	0	1 (100%)	1 (100%)
Carlston, 2019	1	1 years	1 (100%)	1 (100%)	1 (100%)	0	1 (100%)	0	0	0
Yang, 2020	2	NR	0	0	2 (100%)	0	0	0	0	0
Total	37		18 (51%)	23 (66%)	20 (57%)	4 (11%)	11 (31%)	4 (11%)	17 (48%)	9(26%)
HIBCH										
Loupatty, 2007	1	14 months	0	0	1 (100%)	0	1 (100%)	0	0	0
Ferdinandusse, 2013	2	9 months	0	0	2 (100%)	0	0	0	1 (50%)	0
Yamada, 2014	2	17,5 (14-24) months	1 (50%)	0	2 (100%)	0	0	0	0	1 (50%)
Reuter, 2014	1	9months, 3 and 3,5 years	1 (100%)	1 (100%)	1 (100%)	0	0	0	0	1 (100%)
Peters, 2015	1	10 months	1 (100%)	1 (100%)	1 (100%)	1 (100%)	1 (100%)	0	1 (100%)	0
Soler-Alfonso, 2015	1	13 months, 16 months and 4,9 years	1 (100%)	1 (100%)	1 (100%)	0	1 (100%)	1 (100%)	0	0
Stiles, 2015	2	6,8 (1,6-12) years	1 (50%)	0	2 (100%)	0	2 (100%)	0	2 (100%)	0
Schottmann, 2016	5	8,5 (1-26) years	0	0	5 (100%)	0	1 (25%)	0	0	0
Tan, 2018	1	3 months	0	0	0	0	0	0	0	1 (100%)
Karimzadeh, 2019	1	2 years	0	0	1 (100%)	0	0	0	0	0
Candelo, 2019	2	9.5 (9-10) years	1(100%)	1(100%)	1(50%)	0	1(50%)	0	0	2(100%)

Total	19	6 (31%)	4 (21%)	17 (89%)	1 (5%)	7 (36%)	1 (6%)	4 (21%)	5 (26%)

Table S2. Literature review on brain MRI abnormalities from 56 patients with SCEH and HIBCH deficiency according to PubMed

Table S3: Pathogenicity data of novel variants reported in our series

	cDNA	Protein	Patient number	Protein *in silico* software			Conservation	Population frequency databases
				MT (score)	PROVEAN (score)	SIFT (score)	Clustal Omega	GnomAD frequency
ECHS1	c.367C>T	p.(Leu123Phe)	P1	P (22)	N (-2.43)	T (0.07)	conserved	NR
	c.239C>T	p.(Pro80Leu)	P2	D (98)	D (-3.87)	D (0.025)	not conserved	0,00006924
	c.542G>T	p.(Arg181Leu)	P4, P5	D (102)	D (-6.22)	D (0.006)	highly conserved	NR
	c.123_124delAG	p.(Gly42Glufs*3)	P6, P11	D	.	.	.	NR
	c.830C>T	p.(Thr277Ile)	P6	P (89)	D (-4.26)	D (0.022)	not conserved	0.000007954
	c.371C>T	p.(Thr124Ile)	P10	P (89)	D (-3,37)	D (0.012)	not conserved	NR
	c.404A>G	p.(Asn135Ser)	P12	D (46)	D (-4.64)	T (0.425)	highly conserved	0.00001062
	c.740C>T	p.(Ala247Val)	P13	D (64)	D (-3.48)	D (0.009)	highly conserved	0.000003986
HIBCH	c.777T>A	p.(Phe259Leu)	P14	D (22)	D (-5.28)	D (0.0007)	highly conserved	NR
	c.353T>C	p.(Phe118Ser)	P18, P19	D (155)	N (-0.78)	P (0.227)	highly conserved	0.000003978
	c.488G>T	p.(Cys163Phe)	P19	P (205)	N (-1.20)	D (0.001)	not conserved	0.000003985

In silico studies of novel mutations reported in this study. MT: mutation taster; NR: not reported; P: polymorphism; D: damaging; N: neutral; T; tolerated. Clustal omega has done comparing human protein with different species: anole lizard, zebrafish, mouse, pig, sheep, macaque, rat and drosophila melanogaster (flycatcher in *HIBCH*). No homozygous individuals have been reported in population frequency databases for the novel variants. All novel missense variants were classified as likely pathogenic according to ACMG guidelines. *ECHS1* (NM_004092.3) *HIBCH* gene (NM_014362.3).

Table S4: Location of previously reported and new pathogenic variants in the SCEH and HIBCH

Nt change in cDNA	Effect on coding region	Change of polarity/charge	Secondary structure	Location in the protein	First described in
			ECHS1		
c.1A>G	p.(Met1Val)	sulfur-> aliphatic chain		mitochondrial signal peptide	Ogawa, 2018
c.2T>G	p.(Met1Arg)	no polar->+ charge		mitochondrial signal peptide	Sakai, 2015
c.5C>T	p.(Ala2Val)	-		mitochondrial signal peptide	Sakai, 2015
c.8C>A	p.(Ala3Asp)	no polar->neutral polar		mitochondrial signal peptide	Ganetzky, 2016
c.23T>C	p.(Leu8Pro)	aliphatic->cyclic chain		mitochondrial signal peptide	Uchino, 2019
c.74G>A	p.(Arg25His)	-		mitochondrial signal peptide	Yang, 2020
c.79T>G	p.(Phe27Val)	aromatic ring->aliphatic		mitochondrial signal peptide	Carlston, 2018
c.98T>C	p.(Phe33Ser)	no polar->neutral polar	coil	on the surface	Haack, 2015
c.160C>T	p.(Arg54Cys)	+ charge->neutral polar	coil	on the surface, near substrate binding site	Stark, 2016
c.161G>A	p.(Arg54His)	-	coil	on the surface, near substrate binding site	Haack, 2015
c.176A>G	p.(Asn59Ser)	acid->hydroxylic group	coil	inner part, outside the catalytic site	Haack, 2015
c.197T>C	p.(Ile66Thr)	no polar->neutral polar	alpha-helix	inner part, near the catalytic site	Haack, 2015
c.229G>C	p.(Glu77Gln)	- charge->neutral	alpha-helix	inner part, outside the catalytic site	Haack, 2015
c.239C>T	p.(Pro80Leu)	cyclic->aliphatic chain	alpha-helix	on the surface, near interaction regions	this report
c.268G>A	p.(Gly90Arg)	neutral->+ charge	coil	on the surface	Haack, 2015
c.367C>T	p.(Leu123Phe)	aliphatic->aromatic ring	alpha-helix	Inner part near monohexamer interaction regions and substrate binding site	this report
c.371C>T	p.(Thr124Ile)	polar->no polar	alpha-helix	monohexamer interaction regions	this report
c.389T>A	p.(Val130Asp)	no polar->-charge	alpha-helix	monohexamer interaction regions	Ganetzky, 2016
c.394G>A	p.(Ala132Thr)	no polar->neutral polar	beta-sheet	inner part, outside the catalytic site	Haack, 2015
c.404A>G	p.(Asn135Ser)	acid->hydroxylic group	coil	inner part, outside the catalytic site	this report
c.413C>T	p.(Ala138Val)	-	beta-sheet	inner part, near the catalytic site	Yamada, 2015
c.433C>T	p.(Leu145Phe)	aliphatic->aromatic ring	alpha-helix	inner part, near the catalytic site	Ferdinandusse, 2015
c.449A>G	p.(Asp150Gly)	- charge-> neutral	coil	monohexamer interaction regions	Haack, 2015
c.473C>A	p.(Ala158Asp)	no polar-> - charge	coil	inner part, near the catalytic site	Peters, 2014
c.476A>G	p.(Gln159Arg)	neutral->+ charge	beta-sheet	on the surface, near substrate binding site	Tetreault, 2015
c.518C>T	p.(Ala173Val)	-	coil	inner part, near interaction regions and inside catalytic site	Olgiati, 2016
c.538A>G	p.(Thr180Ala)	polar->no polar	alpha-helix	monohexamer interaction regions	Tetreault, 2015
c.542G>T	p.(Arg181Leu)	+ charge-> no polar	alpha-helix	monohexamer interaction regions	this report
c.563C>T	p.(Ala188Val)	-	alpha-helix	inner part, near interaction regions and substrate binding site	Huffnagel, 2017

c.583G>A	p.(Gly195Ser)	aliphatic->hydroxylic chain	alpha-helix	inner part, near interaction regions and substrate binding site	Haack, 2015
c.673T>C	p.(Cys225Arg)	neutral->+ charge	alpha-helix	monohexamer interaction regions	Haack, 2015
c.674G>C	p.(Cys225Ser)	sulfur-> hydroxylic chain	alpha-helix	monohexamer interaction regions	Ferdinandusse, 2015
c.713C>T	p.(Ala238Val)	-	alpha-helix	monohexamer interaction regions	Tetreault, 2015
c.740C>T	p.(Ala247Val)	-	alpha-helix	inner part, near catalytic site	this report
c.817A>G	p.(Lys273Glu)	+ -> - charge	alpha-helix	on the Surface in monohexamer interaction regions	Haack, 2015
c.830C>T	p.(Thr277Ile)	polar->no polar	alpha-helix	on the surface in monohexamer interaction regions and near substrate binding site	this report
c.836T>C	p.(Phe279Ser)	no polar-> neutral polar	alpha-helix	on the surface forming substrate binding site	Bedoyan, 2017
c.842A>G	p.(Glu281Gly)	- charge -> neutral	alpha-helix	on the surface, near monohexamer interaction region and substrate binding site	Nair,2016
			HIBCH		
c.173A>G	p.(Asn58Ser)	acid->hydroxylic group	coil	inner part, near the catalytic site	Candelo, 2019
c.196C>T	p.(Arg66Trp)	+ charge-> no polar	alpha-helix	on the surface	Stiles, 2015
c.287C>A	p.(Ala96Asp)	no polar-> - charge	coil	inside the catalytic site	Yamada, 2014
c.353T>C	p.(Phe118Ser)	no polar-> neutral polar	alpha-helix	3 amino acids far from a substrate binding site, forming the catalytic core	this report
c.365A>G	p.(Tyr122Cys)	hydroxylic -> sulfur chain	alpha-helix	Forming catalytic core, adjacent amino acid	Loupatty, 2007
c.410C>T	p.(Ala137Val)	-	beta-sheet	inner part, outside the catalytic site	Soler-Alfonso, 2015
c.488G>T	p.(Cys163Phe)	neutral polar-> no polar	coil	linking two beta-sheets near to catabolic region	this report
c.641C>T	p.(Thr214Ile)	neutral polar-> no polar	coil	on the surface	Karimzadeh, 2019
c.777T>A	p.(Phe259Leu)	aromatic ring->aliphatic	coil	linking two alpha helixes, on the surface	this report
c.808A>G	p.(Ser270Gly)	hydroxylic ->aliphatic chain	alpha-helix	on the surface	Candelo, 2019
c.913A>G	p.(Thr305Ala)	neutral polar-> no polar	alpha-helix	on the surface	Schottmann, 2016
c.950G>A	p.(Gly317Glu)	neutral-> - charge	alpha-helix	inner part, near catalytic site	Ferdinandusse, 2013
c.1027C>G	p.(His343Asp)	+ -> - charge	alpha-helix	on the surface	Ya Yang, 2018
c.1033G>A	p.(Gly345Ser)	aliphatic-> hydroxylic chain	alpha-helix	inner part, near catalytic site	Peters, 2015

Figure S1: Primers designed for RNA expression analysis

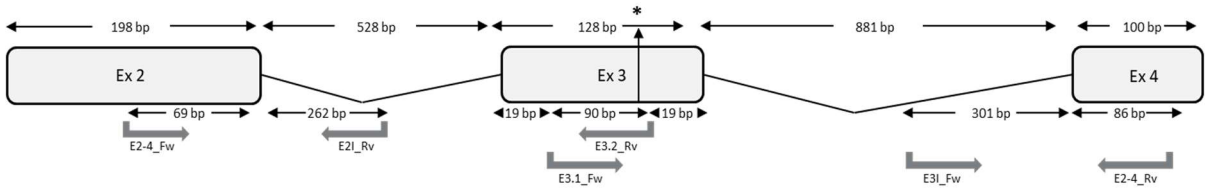

E2-4_Fw: TGAAGACCTTCGAGGAGGA	**E3.1_Fw:** AATGCAGAACCTGAGTTTCC
E2I_Rv: tgacacacacaaagcctgac	**E3I_Fw:** cacccacctgtgcaccta
E3.2_Rv: GCGATGACTGGCTTCTTGA	**E2-4_Rv:** ATTAAGATCTCCGGCTGTGC

Primers design for RNA expression analysis of c.367C>T from fibroblast from P1 and a normal control. The genetic variant is represented with an asterisk in the scheme. PCRs design were done combining all forward and reverse primers.

Figure S2: Schematic representation of *ECHS1* and *HIBCH* genes with reported mutations

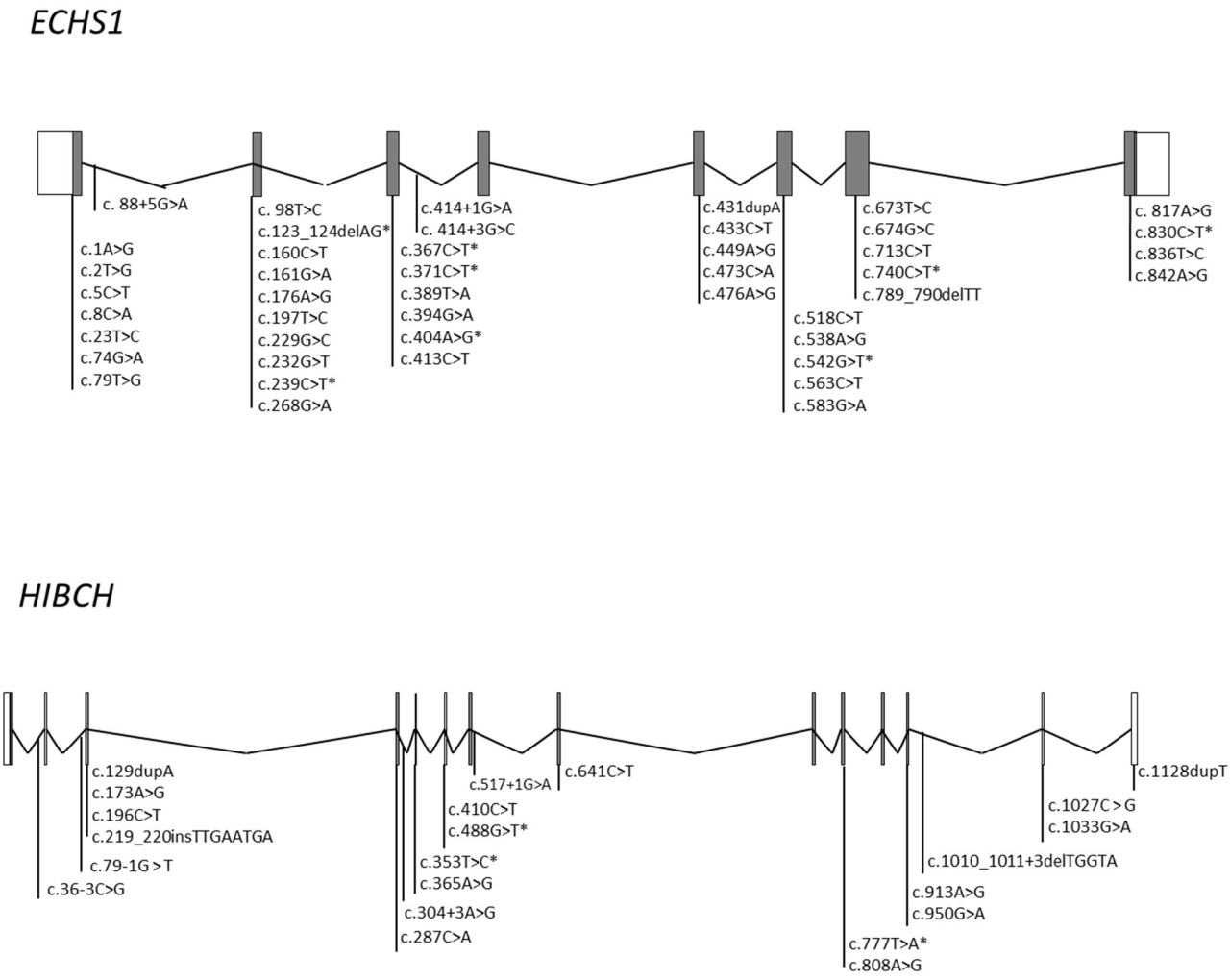

Figure shows all reported mutations to date including novel changes from this report (*).

References

1. Desvignes JP, Bartoli M, Delague V, et al. VarAFT: A variant annotation and filtration system for human next generation sequencing data. *Nucleic Acids Res.* 2018;46(W1):W545–W553.

2. Karczewski KJ, Francioli LC, Tiao G, et al. Variation across 141,456 human exomes and genomes reveals the spectrum of loss-of-function intolerance across human protein-coding genes. *bioRxiv.* 2019;531210.

3. Schwarz JM, Cooper DN, Schuelke M, Seelow, D. Mutationtaster2: Mutation prediction for the deep-sequencing age. *Nat. Methods.* 2014;11(4):361–362.

4. Choi Y, Chan AP. PROVEAN web server: A tool to predict the functional effect of amino acid substitutions and indels. *Bioinformatics.* 2015;31(16):2745–2747.

5. Desmet FO, Hamroun D, Lalande M, Collod-Béroud G, Claustres M, Béroud C. Human Splicing Finder: An online bioinformatics tool to predict splicing signals. *Nucleic Acids Res.* 2009;37(9):e67.

6. Landrum MJ, Lee JM, Benson M, et al. ClinVar: Improving access to variant interpretations and supporting evidence. *Nucleic Acids Res.* 2018;46(D1):D1062–D1067.

7. Brown GK, Hunt SM, Scholem R, et al. beta-Hydroxyisobutyryl Coenzyme A Deacylase Deficiency : A Defect in Vali ne Metabolism Associated with Physical Malformations. *Pediatrics*. 1982;70(4):532-8.

8. Loupatty FJ, Clayton PT, Ruiter JP, et al. Mutations in the gene encoding 3-hydroxyisobutyryl-CoA hydrolase results in progressive infantile neurodegeneration. *Am. J. Hum. Genet.* 2007;80(1):195–199.

9. Ferdinandusse S, Waterham HR, Heales SJ, et al. HIBCH mutations can cause Leigh-like disease with combined deficiency of multiple mitochondrial respiratory chain enzymes and pyruvate dehydrogenase. *Orphanet J. Rare Dis.* 2013;8:188.

10. Yamada K, Naiki M, Hoshino S, et al. Clinical and biochemical characterization of 3-hydroxyisobutyryl-CoA hydrolase (HIBCH) deficiency that causes Leigh-like disease and ketoacidosis. *Mol. Genet. Metab. Reports*. 2014;1:455–460.

11. Reuter MS, Sass JO, Leis T, et al. HIBCH deficiency in a patient with phenotypic characteristics of mitochondrial disorders. *Am. J. Med. Genet. Part A*. 2014;164A(12**)**:3162–3169.

12. Yang HY, Wu LW, Deng XL, Yin F, Yang LF. Diagnosis and treatment of 3-hydroxyisobutyryl-CoA hydrolase deficiency: A case report and literature review. *Chinese J. Contemp. Pediatr.* 2018;20(8):647–651.

13. Peters H, Ferdinandusse S, Ruiter JP, Wanders RJ, Boneh A, Pitt J. Metabolite studies in HIBCH and ECHS1 defects: Implications for screening. *Mol Genet Metab.* 2015;115(4):168–73.

14. Soler-Alfonso C, Enns GM, Koenig MK, Saavedra H, Bonfante-Mejia E, Northrup H. Identification of HIBCH gene mutations causing autosomal recessive Leigh syndrome: A gene involved in valine metabolism. *Pediatr. Neurol.* 2015;52(3):361–365.

15. Stiles AR, Ferdinandusse S, Besse A, et al. Successful diagnosis of HIBCH deficiency from exome sequencing and positive retrospective analysis of newborn screening cards in two siblings presenting with Leigh's disease. *Mol. Genet. Metab.* 2015;115(4):161–167.

16. Schottmann G, Sarpong A, Lorenz C, et al. A movement disorder with dystonia and

ataxia caused by a mutation in the HIBCH gene. *Mov. Disord.* 2016;31(11):1733–1739.

17. Reuter MS, Tawamie H, Buchert R, et al. Diagnostic yield and novel candidate genes by exome sequencing in 152 consanguineous families with neurodevelopmental disorders. *JAMA Psychiatry.* 2017;74(3):293–299.

18. Tan H, Chen X, Lv W, Linpeng S, Liang D, Wu L. Truncating mutations of HIBCH tend to cause severe phenotypes in cases with HIBCH deficiency: A case report and brief literature review. *J. Hum. Genet.* 2018;63(7):851–855.

19. Karimzadeh P, Saberi M, Sheidaee K, Nourbakhsh M, Keramatipour M. 3-Hydroxyisobutyryl-CoA hydrolase deficiency in an Iranian child with novel HIBCH compound heterozygous mutations. *Clin. Case Reports.* 2019;7(2):375–380.

20. Candelo E, Cochard L, Caicedo-Herrera G, et al. Syndromic progressive neurodegenerative disease of infancy caused by novel variants in HIBCH: Report of two cases in Colombia. *Intractable Rare Dis. Res.* 2019;8(3):187–193.

21. Tetreault M, Fahiminiya S, Antonicka H, et al. Whole-exome sequencing identifies novel ECHS1 mutations in Leigh syndrome. *Hum. Genet.* 2015;134(9):981–991.

22. Peters H, Buck N, Wanders R, et al. ECHS1 mutations in Leigh disease: A new inborn error of metabolism affecting valine metabolism. *Brain.* 2014;137(Pt11):2903–2908.

23. Sakai C, Yamaguchi S, Sasaki M, Miyamoto Y, Matsushima Y, Goto Y. ECHS1 mutations cause combined respiratory chain deficiency resulting in leigh syndrome. *Hum. Mutat.* 2015;36(2):232–239.

24. Haack TB, Jackson CB, Murayama K, et al. Deficiency of ECHS1 causes

mitochondrial encephalopathy with cardiac involvement. *Ann. Clin. Transl. Neurol.* 2015;2(5):492–509.

25. Yamada K, Aiba K, Kitaura Y, et al. Clinical, biochemical and metabolic characterisation of a mild form of human short-chain enoyl-CoA hydratase deficiency: Significance of increased n-acetyl-s-(2-carboxypropyl)cysteine excretion. *J. Med. Genet.* 2015;52(10):691–698.

26. Ganetzky RD, Bloom K, Ahrens-Nicklas R, et al. ECHS1 Deficiency as a Cause of Severe Neonatal Lactic Acidosis. *JIMD Rep.* 2016;30:33-37.

27. Ferdinandusse S, Friederich MW, Burlina A, et al. Clinical and biochemical characterization of four patients with mutations in ECHS1. *Orphanet J. Rare Dis.* 2015;10:79.

28. Nair P, Hamzeh AR, Mohamed M, Malik EM, Al-Ali MT, Bastaki F. Novel ECHS1 mutation in an Emirati neonate with severe metabolic acidosis. *Metab. Brain Dis.* 2016;31(5):1189–1192.

29. Olgiati S, Skorvanek M, Quadri M, et al. Paroxysmal exercise-induced dystonia within the phenotypic spectrum of ECHS1 deficiency. *Mov. Disord.* 2016;31(7):1041–1048.

30. Al Mutairi F, Shamseldin HE, Alfadhel M, Rodenburg RJ, Alkuraya FS. A lethal neonatal phenotype of mitochondrial short-chain enoyl-CoA hydratase-1 deficiency. *Clin. Genet.* 2017;91(4):629–633.

31. Bedoyan JK, Yang SP, Ferdinandusse S, et al. Lethal neonatal case and review of primary short-chain enoyl-CoA hydratase (SCEH) deficiency associated with secondary lymphocyte pyruvate dehydrogenase complex (PDC) deficiency. *Mol. Genet. Metab.*

2017;120(4):342–349.

32. Huffnagel IC, Redeker EJW, Reneman L, Vaz FM, Ferdinandusse S, Poll-The BT. Mitochondrial Encephalopathy and Transient 3Methylglutaconic Aciduria in ECHS1 Deficiency: Long-Term Follow-Up. *JIMD Rep.* 2018;39:83-87.

33. Balasubramaniam S, Riley LG, Bratkovic D, et al. Unique presentation of cutis laxa with Leigh-like syndrome due to ECHS1 deficiency. *J. Inherit. Metab. Dis.* 2017;40(5):745–747.

34. Fitzsimons PE, Alston CL, Bonnen PE, et al. Clinical, biochemical, and genetic features of four patients with short-chain enoyl-CoA hydratase (ECHS1) deficiency. *Am. J. Med. Genet. Part A.* 2018;176(5):1115–1127.

35. Aretini P, Mazzanti CM, La Ferla M, et al. Next generation sequencing technologies for a successful diagnosis in a cold case of Leigh syndrome. *BMC Neurol.* 2018;18(1):99.

36. Mahajan A, Constantinou J, Sidiropoulos C. ECHS1 deficiency-associated paroxysmal exercise-induced dyskinesias: case presentation and initial benefit of intervention. *J. Neurol.* 2017;264(1):185–187.

37. Ogawa E, Shimura M, Fushimi T, et al. Clinical validity of biochemical and molecular analysis in diagnosing Leigh syndrome: a study of 106 Japanese patients. *J. Inherit. Metab. Dis.* 2017;40(5):685–693.

38. Carlston CM, Ferdinandusse S, Hobert JA, Rong M, Longo N. Successful screening for Gaucher Disease in High-prevalence population in Tabuleiro do Norte. *JIMD Rep.* 2018;1:73–78.

39. Uchino S, Iida A, Sato A, et al. A novel compound heterozygous variant of ECHS1

identified in a Japanese patient with Leigh syndrome. *Hum. Genome Var.* 2019;6:6–9.

40. Stark Z, Tan TY, Chong B, et al. A prospective evaluation of whole-exome sequencing as a first-tier molecular test in infants with suspected monogenic disorders. *Genet. Med.* 2016;18(11):1090–1096.

41. Korenke G, Nuoffer JM, Alhaddad B, et al. Paroxysmal Dyskinesia in ECHS1 Defect with Globus Pallidus Lesions. *Neuropediatrics.* 2016;47:518.

42. Yang H, Yu D. Clinical, biochemical and metabolic characterization of patients with short-chain enoyl-CoA hydratase(ECHS1) deficiency: two case reports and the review of the literature. *BMC Pediatr*. 2020;20(1):50.

OBJETIVO 3

OBJETIVO 3: Estudio de biomarcadores en pacientes con enfermedades que cursan con trastornos del movimiento y alteraciones en los ganglios basales, en concreto, determinación de isoformas de tiamina y metales, en sangre y líquido cefalorraquídeo.

La disponibilidad de biomarcadores en una enfermedad incrementa notablemente la tasa de éxito diagnóstico, permite establecer un diagnóstico más precoz y monitorizar el curso clínico de la enfermedad. Haciendo referencia al objetivo 3 de esta tesis, se han analizado biomarcadores para los defectos del transporte y metabolismo de la vitamina B1 (tiamina) (Publicación 2) y el oligoelemento manganeso (Publicación 3).

Nuestro grupo ha contribuido a la estandarización de un método de análisis mediante cromatografía líquida de alta eficacia (HPLC, siglas en inglés) para la determinación de tres isoformas de la tiamina presentes en el cuerpo humano (tiamina libre, tiamina monofosfato y tiamina difosfato) tanto en sangre total como en líquido cefalorraquídeo de pacientes con defectos en el transporte y metabolismo de la tiamina. El resultado de estos estudios ha sido publicado en revistas de alto impacto, en los que la doctoranda ha participado realizando la determinación de las isoformas de tiamina en el laboratorio[131,132].

En la cohorte de pacientes analizada en este proyecto de tesis, uno de los pacientes portaba mutaciones en el gen *SLC25A19*, causante del síndrome de disfunción del metabolismo de tiamina tipo 4 (polineuropatía progresiva; MIM#613710). En esta paciente no pudimos realizar la determinación de tiamina libre en LCR ya que presentaba una clínica estable y no estaba justificada la realización de una punción lumbar.

En este proyecto de tesis, se ha realizado una revisión de estos defectos con el fin de profundizar en la clínica, radiología, bioquímica y genética de los mismos (Publicación 2).

Por otro lado, hemos podido analizar y poner a punto el estudio de manganeso en LCR en un paciente con mutaciones en el gen *SLC39A14*, siendo este paciente y su hermano afecto el segundo grupo de pacientes publicados con este defecto (Publicación 3).

En esta publicación se ha determinado la concentración de manganeso mediante espectrometría de masas con plasma acoplado inductivamente (ICP-MS, siglas en inglés) en plasma y LCR, observando 10 veces más manganeso en plasma y 30 veces más en

LCR en el paciente respecto a los controles. Por otro lado, se observó el acúmulo de manganeso en el pálido mediante el índice palidal y comparando con controles normales observando un mayor acúmulo conforme avanzaba la edad del paciente.

Tras dos dosis del tratamiento con el quelante $Na_2CaEDTA$, el paciente disminuyó sus niveles de manganeso disminuyeron un 57% en el plasma del paciente, pero no presentando ninguna mejoría clínica. Destacar que junto a la disminución de manganeso hubo un descenso de los niveles de selenio y zinc, habiendo que suplementar al paciente.

Publicación 2

Título:

Genetic defects of thiamine transport and metabolism: a review of clinical phenotypes, genetics and functional studies.

Autores:

A Marcé-Grau, L Marti-Sanchez, H Baide-Mairena, JD Ortigoza-Escobar, B Pérez-Dueñas

Referencia:

Marcé-Grau A, Martí-Sánchez L, Baide-Mairena H, Ortigoza-Escobar JD, Pérez-Dueñas B. Genetic defects of thiamine transport and metabolism: A review of clinical phenotypes, genetics, and functional studies. *J Inherit Metab Dis*. 2019;42(4):581-597. doi:10.1002/jimd.12125

Resumen:

La tiamina es un cofactor que participa en el mantenimiento del metabolismo de los carbohidratos y en múltiples procesos metabólicos celulares dentro del citosol, las mitocondrias y los peroxisomas. Actualmente, se han descrito cuatro defectos genéticos que causan deterioro del transporte y el metabolismo de la tiamina: la disfunción SLC19A2 conduce a diabetes mellitus, anemia megaloblástica y pérdida auditiva sensorial-neural, mientras que los trastornos relacionados con SLC19A3, SLC25A19 y TPK1 resultan en encefalopatía recurrente, necrosis de los ganglios basales, distonía generalizada, discapacidad grave y muerte prematura. Para lograr un diagnóstico y tratamiento tempranos, los biomarcadores juegan un papel importante. Los pacientes con SLC19A3 presentan una disminución notable de tiamina libre en el LCR y fibroblastos. Los pacientes con TPK1 muestran concentraciones disminuidas de tiamina pirofosfato en la sangre y músculo. Se ha demostrado que la administración de suplementos de tiamina mejora el control de la diabetes y la anemia en pacientes con síndrome de Rogers debido a la deficiencia de SLC19A2. En un número significativo de pacientes con SLC19A3, la tiamina mejora el curso clínico y la supervivencia, y previene de la aparición de nuevas crisis metabólicas. En los defectos SLC25A19 y TPK1, la tiamina también ha llevado a la estabilización clínica en casos únicos. Además, la suplementación con tiamina normaliza las concentraciones de tiamina libre en el LCR de pacientes con SLC19A3

Genetic defects of thiamine transport and metabolism: a review of clinical phenotypes, genetics and functional studies.

Anna Marcé-Grau[1*], Laura Martí-Sánchez[2,4*], Heidy Baide-Mairena[1], Juan Dario Ortigoza-Escobar[3], Belén Pérez-Dueñas[1,5].

[1]Pediatric Neurology Research Group. Hospital Vall d'Hebron and Research Institute – VHIR Barcelona, Spain.

[2]Department of Clinical Biochemistry and [3]Child Neurology, Hospital Sant Joan de Déu Barcelona, Spain.

[4]Universitat de Barcelona, Barcelona, Spain

[5]Centre for Biochemical Research in Rare Diseases – CIBERER.

*These authors made an equal contribution

Corresponding author:

Belén Pérez Dueñas

Pediatric Neurology Research Group

Edifici Mediterrània

Passeig Vall d'Hebrón 119-129a

08035 Barcelona

email: belen.perez@vhir.org

This article has been accepted for publication and undergone full peer review but has not been through the copyediting, typesetting, pagination and proofreading process which may lead to differences between this version and the Version of Record. Please cite this article as doi: 10.1002/jimd.12125

Word Count (text and summary): 7303

Number of figures and tables: 5 figures and 3 tables

Summary

Thiamine is a crucial cofactor involved in the maintenance of carbohydrate metabolism and participates in multiple cellular metabolic processes within the cytosol, mitochondria and peroxisomes. Currently, four genetic defects have been described causing impairment of thiamine transport and metabolism: SLC19A2 dysfunction leads to diabetes mellitus, megaloblastic anaemia and sensory-neural hearing loss, whereas SLC19A3, SLC25A19 and TPK1-related disorders result in recurrent encephalopathy, basal ganglia necrosis, generalized dystonia, severe disability and early death. In order to achieve early diagnosis and treatment, biomarkers play an important role. *SLC19A3* patients present a profound decrease of free-thiamine in CSF and fibroblasts. *TPK1* patients show decreased concentrations of thiamine pyrophosphate in blood and muscle. Thiamine supplementation has been shown to improve diabetes and anaemia control in Rogers' syndrome patients due to SLC19A2 deficiency. In a significant number of patients with *SLC19A3*, thiamine improves clinical outcome and survival, and prevents further metabolic crisis. In *SLC25A19* and *TPK1* defects, thiamine has also led to clinical stabilization in single cases. Moreover, thiamine supplementation leads to normal concentrations of free-thiamine in the CSF of SLC19A3 patients. Herein we present a literature review of the current knowledge of the disease including related clinical phenotypes, treatment approaches, update of pathogenic variants, as well as *in*

vitro and *in vivo* functional models that provide pathogenic evidence and propose mechanisms for thiamine deficiency in humans.

Synopsis: Inherited defects of thiamine transport and metabolism are amenable to thiamine supplementation, which may prevent further encephalopathic episodes and improve clinical outcome when initiated early in the disease course.

Authors contribution: All authors contributed to drafting and critically reviewing the manuscript.

Corresponding author: Belén Pérez Dueñas

Details of funding: This work was supported by Fundació La Marató de TV3 (Grant 20143130) and by the Instituto de Salud Carlos III (ISCIII) - Subdirección General de Evaluación y Fomento de la Investigación within the framework of the National R+D+I Plan co-funded with FEDER funds [Grant PI15/00287 and PI18/01319].

Conflicts of interest:

Anna Marcé Grau declares that she has no conflict of interest.

Laura Martí Sanchez declares that she has no conflict of interest

Heidy Baide-Mairena declares that she has no conflict of interest

Juan Darío Origoza Escobar declares that he has no conflict of interest

Belén Pérez Dueñas declares that she has no conflict of interest

Informed consent and animal rights: this review does not contain any human or animal studies performed by any of the authors

Key words: Thiamine; SLC19A2; SLC19A3; SLC25A19; TPK1; Leigh syndrome; thiamine transporter 2 deficiency; thiamine responsive megaloblastic anemia; Roger's syndrome.

1. Biochemistry of thiamine in humans.

1.a. Biochemical function.

Thiamine, also known as vitamin B1 or aneurine, is a water-soluble essential vitamin that is present in humans as free thiamine, thiamine monophosphate (TMP), thiamine pyrophosphate (TPP) and thiamine triphosphate (TTP), depending on functional activity in different tissues. TPP, which accounts for 80% of total body thiamine (Losa et al 2005), participates in multiple metabolic processes in the cytosol, mitochondria and peroxisome (**Figure 1**). In the cytosol, it is involved in the pentose phosphate pathway, as a cofactor of transketolase enzyme (Ortigoza-Escobar et al 2016). In the mitochondria, TPP is a cofactor of several complexes: (1) pyruvate dehydrogenase complex, which catalyses the conversion of pyruvate into acetyl-CoA; (2) oxoglutarate dehydrogenase complex, which catalyses the decarboxylation of alpha-ketoglutarate in the Krebs cycle; and (3) branched-chain alpha-keto acid dehydrogenase complex, which

catalyzes the decarboxylation of branched, short-chain alpha-ketoacids. (Tittmann 2009, Ortigoza-Escobar et al 2017). In the peroxisome, TPP acts as a cofactor of 2-hydroxyacyl-CoA lyase (HACL1) which has a role in fatty acids degradation (Fraccascia et al 2007, Ortigoza-Escobar et al 2016). Oxoglutarate dehydrogenase complex intervenes in the production of succinyl-coenzyme A, which is the substrate of the enzyme delta-aminolevulinate synthase 2, an enzyme that catalyzes the first step of the synthesis of the heme group. The role of TPP as a cofactor of this enzyme complex may explain the megaloblastic anaemia that is observed in Rogers' syndrome (Fujiwara et al 2013, Beshlawi et al 2014, Bergmann et al 2009).

TTP accounts for 5-10% of total whole body thiamine (Losa et al 2005). This isomer is implicated in the activation of chloride channels and in the phosphorylation reactions of energy metabolism, acting as a phosphate donor (Mkrtchyan et al 2015).

Free-thiamine and TMP represents a low percentage of total thiamine in humans (Losa et al 2005). Free-thiamine is mostly found in the central nervous system (CNS), where it is implicated in the generation of acetylcholine (Manzetti et al 2014), in the uptake of serotonin (Vigil et al 2010) and GABA (Ferreira-Vieira et al 2016), and as an antioxidant for reactive species of nitrogen and oxygen (Huang et al 2010). Thiamine is also implicated in the regulation and activation of brain immune cells and the expression of antibodies (Ottinger et al 2012), immunoglobulins and CD40L-mediated immune system (Ke et al 2005, Manzetti et al 2014). Apart from this, thiamine acts as an antioxidant for neutrophil cells (Jones and Anderson 1983), inhibits the reactive

oxygen species in macrophages (Yadav et al 2010) and inhibits p53 during the replication and apoptosis (Bennett et al 1994).

1.b. Chemistry and dietary sources.

Chemically, thiamine is defined as 3-[(4-amino-2-methyl-5-pyrimidinyl) methyl]-5-(2-hydroxyethyl)-4-methyl-1,3-thiazol-3-ium ($C_{12}H_{17}N_4OS$). It has a molecular weight of 265.35 Da (Turk et al 2016) and it is composed of a pyrimidine and a thiazole ring linked by a methylene group, which forms a sulphur-containing structure (Manzetti et al 2014).

Thiamine can be synthesized by bacteria (Burkholder and McVeigh 1942), fungi (Manzetti et al 2014) and plants (Goyer 2010) but not by mammals. Therefore, thiamine, as an essential vitamin for humans, is obtained from the intestinal microflora and dietary sources (Burkholder and McVeigh 1942). Thiamine is present in all plants (free-thiamine) and animal tissues (phosphorylated forms). The principal thiamine sources for humans are whole grains, puls, meat, liver and fish. Food sources of thiamine are meat and meat products (28.2%), followed by cereals and grains (23.2%), vegetables (11.6%), milk and dairy products (9.5%) and fruits (6.4%) (Mielgo-Ayuso et al 2018). In humans, thiamine half-life is 9 to 18 days (Manzetti et al 2014).

The daily recommended dietary allowances (RDAs) of thiamine according to age and gender are listed in Table 1. Almost 28% of the population does not meet the daily intake recommendation for this vitamin (Mielgo-Ayuso et al 2018).

1.c. Proteins involved in thiamine transport and metabolism.

Thiamine is obtained from the diet as phosphorylated thiamine vitamers and from bacteria and plants in the form of free-thiamine in a proportion of 50% (Turck et al 2016, Said et al 2004). Thiamine is absorbed in the proximal part of the large intestine, where phosphatases hydrolyse thiamine phosphate esters and convert them into free-thiamine (Said et al 2004, Turck et al 2016). Free-thiamine uptake is done by thiamine transporter 1 (ThTR-1) and 2 (ThTR-2), encoded by *SLC19A2* (MIM*603941) and *SLC19A3* (MIM*606152), respectively (**Figure 1**). Both transporters are transmembrane proteins with 12 transmembrane domains and they are expressed in small and large intestines. Human ThTR-1 (hThTR-1) is expressed in the apical and basolateral membrane domains of polarized enterocytes and ThTR-2 is expressed in the apical brush-border membrane domain (Said et al 2004). Human ThTR-2 is supposed to have an important role in intestinal absorption because deficiency of hThTR1 does not affect plasma thiamine levels.

Regulation of thiamine uptake in the intestine depends on concentrations and request of thiamine. Dietary deficiency of thiamine induces the synthesis of ThTR-2 via transcriptional mechanisms (Reidling and Said 2005). Also, transcription of both carriers is regulated during development, with high expression in early stages of life and a reduction with maturation. This pattern occurs in the intestine and kidneys according to mouse models (Reidling et al 2006). Said et al 1999, studied the thiamine uptake regulation in an intestinal epithelial cell line showing that temperature, energy and Ca^{2+}/calmodulin intracellular pathway are involved.

A high-affinity carrier (TPPT) for TPP encoded by *SLC44A4* gene also regulates thiamine uptake. *SLC44A4* gene (MIM*606107) is located on chromosome 6p21.33. This carrier consists of 710 amino acids and is highly expressed in epithelial cells of the colon, prostate, trachea and lungs. TPPT has an important role in TPP absorption from microbiota and contributes to cellular nutrition of the local colonocytes (Nabokina et al 2015).

The whole body content of thiamine is estimated in 25-30 mg, mostly located in skeletal muscles, heart, brain, liver and kidneys. In the blood, 80% of thiamine is located in erythrocytes as TPP (Manzetti et al 2014). Free-thiamine crosses the cell membranes and can be present in extracellular fluids, including the cerebrospinal fluid.

Once free-thiamine enters the bloodstream, it is transported by high affinity free-thiamine carries into erythrocytes, where it is phosphorylated into TPP. In cells, two enzymes phosphorylate thiamine: thiamine pyrophosphokinase, which catalyses the formation of TPP from free thiamine using adenosine triphosphate (ATP), and TTP-ATP-phosphoryltransferase, which catalyses the conversion from TPP to TTP, also with ATP (Turck et al 2016). The most abundant thiamine kinase is thiamine pyrophosphokinase (encoded by *TPK1*) (**Figure 1**). *TPK1* (MIM*606370) is located on chromosome 7q34-q35 and it is highly expressed in small intestine (related to thiamine absorption) and kidney (implicated in thiamine re-absorption) but also in brain, liver, placenta and spleen (Zhao et al 2001).

ThTR-1 and ThTR-2 are involved in the active transport of free-thiamine in all tissues due to their ubiquitous expression (Labay et al 1999, Zeng et al 2005). A minority of

phosphorylated thiamine forms (TMP, TPP and TTP) is also carried by folate carrier-1 (encoded by *SLC19A1*) (Manzetti et al 2014, Turck et al 2016).

Intake of thiamine into the mitochondria occurs by mitochondrial TPP carrier encoded by *SLC25A19* (MIM*606521) (**Figure 1**). It is located on chromosome 17q25.1 and is ubiquitously expressed (Dolce et al 2001).

Excretion of thiamine species is mostly by urine as free thiamine, but there are small quantities of TMP and TPP. TMP can also be recycled to free thiamine (Turck et al 2016). Thiamine is also eliminated by faeces (from gut microflora unrelated to the quantity of thiamine intake), sweat (5-15% of the thiamine intake) (Alexander et al 1946) and breast milk (mostly as TMP, suggesting that folate carrier-1 could be responsible for this excretion) (Stuetz et al 2012).

2. Acquired conditions leading to thiamine deficiency

Thiamine deficiency may cause neurological and cardiovascular disease in vulnerable populations. Infantile beriberi and Wernicke's encephalopathy are rare life-threatening and reversible causes of acquired thiamine deficiency that occur in children with predisposing factors.

2.1. Infantile Beriberi

Beriberi occurs in infants that are breastfed by mothers with inadequate intake of thiamine, or fed with low thiamine content formulas (Barennes et al 2015, Mimouni-Bloch et al 2014, Nogueira et al 2016, Wani et al 2016). Infantile beriberi occurs in

developing countries with reduced food thiamine sources, such as milled white cereals, including polished rice (the rich thiamin envelop is removed by polishing) and wheat flour, and where other key sources of thiamine (meat, fish, and vegetables) are infrequently consumed. In developed countries, infantile thiamine deficiency outbreaks have been described due to thiamine deficient soy formula, with a high fatality rate and long term sequelae (Mimouni-Bloch et al 2014, Nogueira et al 2016).

Thiamine deficiency can develop within 2 to 3 months from a deficient intake. Infants present with neurological, systemic, cardiovascular and respiratory symptoms. Three phenotypes have been described: the pure cardiac form or wet thiamine deficiency, the aphonic form, and the neurologic or dry form. The more severe form is called Shoshin beriberi and presents as cardiac failure and lactic acidosis. Beriberi poses difficult diagnostic issues, as clinical manifestations such as tachypnea, respiratory distress, tachycardia and cardiomegaly can suggest other diagnoses. Mothers suspected of thiamine deficiency were treated with vitamin B1 tablets 100mg, twice daily for 20 days, and infants with suspected thiamine deficiency were treated with vitamin B1 tablets, 30 mg per day for 20 days. Patients with acute symptomatic thiamine deficiency received an intramuscular or slow intravenous injection of thiamine (100mg IM for mothers and 50mg for infants).

2.2. Wernicke's encephalopathy

Wernicke's encephalopathy occurs in children that suffer from malnutrition or malabsorption conditions in the context of gastrointestinal surgical procedures, prolonged total parenteral nutrition with low contents of thiamine, malignancies, organ

transplantations, pancreatitis, etc (Saeki et al 2010, Perko et al 2012, Benidir et al 2014, Park et al 2014). A minority of children presents with the triad of ataxia, ophtalmoplegia and decreased consciousness (Ortigoza-Escobar et al 2017). Most commonly, mental status changes are present in isolation at the beginning of symptoms. Uncommon presenting symptoms include hypotension and tachycardia, related to a defect in efferent sympathetic outflow; hypothermia, caused by involvement of the hypothalamic regions; and seizures, resulting from excessive glutamatergic activity. Mortality ranges from 10 to 20%. The diagnosis of Wernicke's encephalopathy is challenging due to non specificity of symptoms. The most sensitive diagnostic test is magnetic resonance imaging, with typical abnormalities being increased T2-weighted symmetrical signal intensity in the medial (periventricular) thalami, mammillary bodies, tectal plate, and periaqueductal area of the midbrain (Benidir et al 2014, Perko et al 2012). Authors report complete remission of symptoms within hours to days after thiamine supplementation and improvement of brain lesions on MRI in a few weeks. Thiamine doses reported range from 50 to 500 mg/day.

3. Inborn errors of metabolism leading to thiamine dysfunction syndromes.

Defects in genes encoding proteins with relevant functions in thiamine transport and metabolism cause inborn errors of metabolism leading to thiamine metabolism dysfunction syndromes. Currently, there are five genetic phenotypes caused by mutations in *SLC19A2, SLC19A3, SLC25A19* and *TPK1* (**Table 2**). While *SLC19A2* defects lead to diabetes mellitus, megaloblastic anaemia and sensory-neural hearing

loss, *SLC19A3*, *SLC25A19* and *TPK1* genetic defects cause severe encephalopathy in patients with otherwise normal systemic metabolism. Clinical, radiological and biochemical diagnosis criteria for inherited defects in thiamine transport and metabolism with prominent neurological involvement are stated in Table 3 (from Ortigoza-Escobar et al 2017).

3.1. Thiamine metabolism dysfunction syndrome 1 (Thiamine-responsive megaloblastic anemia syndrome) (OMIM 249270)

3.1.a. Clinical features

Rogers' syndrome (Porter et al 1969) also known as Thiamine metabolism dysfunction syndrome 1 or thiamine-responsive megaloblastic anemia (TRMA) syndrome, is caused by mutations in the thiamine transporter type 1 (THTR1) encoded by *SLC19A2* (OMIM 603941). This syndrome is characterized by a clinical triad: 1) megaloblastic anemia 2) non-autoimmune diabetes mellitus and 3) sensorineural deafness. At onset, some patients may not present the complete triad (Bergmann et al 2009, Onal et al 2009, Mathews et al 2009, Agladioglu et al 2012, Liu et al 2014, Cao et al 2016).

More than a hundred cases have been reported, all of them presenting with symptoms in childhood or adolescence (Ortigoza-Escobar et al 2016). Diabetes and anemia can appear as early as the neonatal period and require the administration of insulin and multiple blood transfusions. Deafness is usually the last manifestation to develop and requires cochlear implantation or hearing aids. Habeb et al 2018, reported 32 individuals harboring *SLC19A2* mutations. In this cohort, age at diabetes onset ranged

from 6 weeks to 8 years, age at anemia onset between birth and 7.5 years and age at sensorineural deafness between birth and 4.5 years.

Other symptoms associated with this disorder are (Bergmann et al 2009, Mikstiene et al 2015, Akbari et al 2014, Mozzillo et al 2013):

1) Neurological symptoms: seizures, ataxia, developmental delay, stroke-like episodes, spastic quadriplegia, and cerebral atrophy.
2) Ophthalmological symptoms: pigmentary retinopathy, abnormalities of the optic nerve, cone–rod dystrophy, Leber's congenital amaurosis, squint, macular degeneration.
3) Endocrinological symptoms: short stature, cryptorchidism, and polycystic ovarian syndrome.
4) Cardiological symptoms: congenital cardiac malformations with conduction defects (atrial fibrillation, secundum atrial septal defect, Ebstein anomaly, endocardial cushion defect, atrial dysrhythmia and supraventricular tachycardia), cardiomyopathy and situs inversus. Discontinuation of thiamine treatment appears to trigger supraventricular tachycardia episodes at puberty (Argun et al 2018).
5) Gastroenterological symptoms: hepatomegaly, gastroesophageal reflux.
6) Hematological symptoms: thrombocytopenia and neutropenia.
7) Other symptoms: immune thyroiditis, vocal cord nodules, and talipes.

Brain MRI of patients with TRMA can show hemorrhagic/ischemic stroke involving the middle cerebral artery (MCA) region in a minority of cases, with still unknown disease-

causing mechanisms (Scharfe et al 2000, Villa et al 2000, Karimzadeh et al 2018). Recurrent strokes alternating between right and left MCA have been reported (Karimzadeh et al 2018).

Biochemically, low plasma thiamine (14.64 pmol/ml, Reference Value (RV): 27.1±2.1 pmol/ml) and TMP (14.11 pmol/ml, RV: 37.9±1.9 pmol/ml) levels were found in some patients (Ozdemir et al 2002, Ye_ilkaya et al 2009, Agladioglu et al 2012). These patients do not usually present elevated lactate levels in blood or CSF, neither abnormal excretion of organic acids in urine.

3.1.b. Treatment.

The first line therapy for patients with TRMA syndrome is thiamine supplementation (25-100 mg/d) (Karimzadeh et al 2018). Habeb et al 2018 reported that thiamine therapy improved diabetes control in more than 70% of children, with some of them managing to discontinue insulin treatment. The best predictive factors for a good glycemic response to thiamine therapy were early diabetes diagnosis, early referral for genetic testing and early initiation of thiamine treatment. The exact dose of thiamine required to achieve clinical benefit is unknown; however, in the cohort of Habeb et al 2018, there seemed to be no additional clinical benefit with thiamine doses >150 mg/day. It is important to alert parents that, as with other children with diabetes, individuals with TRMA syndrome can develop diabetic ketoacidosis. Previous reports (Rickets et al 2006, Valerio et al 1988) indicate that thiamine responsiveness decreases after puberty and adults with TRMA syndrome may become transfusion-dependent and require insulin treatment despite early and adequate thiamine supplementation.

Thiamine supplementation cannot prevent complications as stroke (Karimzadeh et al 2018) or short stature.

3.1.c. *SLC19A2*: Genetic defects and functional studies.

SLC19A2 is a 6 exons gene of approximately 22.5kb length, which encodes thiamine transporter type 1 (ThTR-1), a high affinity, saturable thiamine transporter (Diaz et al 1999). Human ThTR-1 is a 497 amino acid length protein containing 12 transmembrane domains with cytoplasmic NH2 and COO terminus regions and two N-glycosylation sites (Dutta B 1999, Ganapathy et al 2004).

Disruption of this gene by homozygous or compound heterozygous mutations leads to autosomal recessive thiamine-responsible megaloblastic anemia (TRMA) (Diaz GA 1999). About 136 TRMA patients have been reported carrying 58 different mutations, 48, 3% of them affecting exon 2 (**Figure 2**). Truncating variants produced by nonsense mutations, frameshift mutations or gross deletions are more frequent than missense variants or inframe indels (58, 6% vs. 37, 9% respectively). Only two splicing variants have been described in a few cases.

Several studies were performed to show experimental evidence of ThTR-1 function and functional alterations in patients' cells. Flemming et al 1999 did the first thiamine uptake assay in fibroblasts of patients carrying the homozygous mutations c.1074G>A and c.885delT, and compared them with control cells. They demonstrated that mutant cells had a reduction of thiamine uptake capability, and that the TRMA causal gene was involved in thiamine transport. Later, Scharfe et al 2000 studied fibroblasts from a

patient with homozygous c.1074G>A mutation. These authors demonstrated that supplementation with high doses of thiamine resulted in restoration of complex I activity. In 2001, a KO mouse was generated targeting Slc19a2 gene. This animal model reproduced the human phenotype as mice were affected by diabetes mellitus, sensorineural deafness and megaloblastosis (Oishi et al 2001). Finally, in order to further study relevant domains in the transporter protein, mutagenesis assays were developed in several cell lines. These experiments concluded that transmembrane backbone and NH2-terminal residues are relevant for protein trafficking to the cell membrane instead of N-glycosylation positions or C-terminal region (Balamurugan and Said 2002, Subramanian et al 2003)

Several studies have been done to demonstrate variants pathogenicity (Gritli et al 2001, Balamurugan and Said 2002, Subramanian et al 2007, Manimaran et al 2016). All of them proved a severe impairment of thiamine cell uptake. Moreover, RNA and protein expression and cell localization studies have been also analyzed by some authors (Balamurugan and Said 2002; Subramanian et al 2007; Manimaran et al 2016) describing three pathophysiological mechanism causing thiamine transport dysfunction: (1) variants impairing RNA translation resulting in the absence or infraexpression of the protein (c.277G>C, c.1074G>A and c.1147delGT); (2) variants retaining the protein within intracellular compartments such as endoplasmatic reticulum (c.473C>G); and (3) variants which enable proteins to get cell membrane but resulting in a functional impairment (c.428C>T, c.515G>A, c.152C>T and c.1232delT). Finally, latest bioinformatics softwares have been used to model variant effects on protein structure in

comparison to wild-type THTR-1 in order to infer functional consequences (Manimaran et al 2016, Xian et al 2018).

3. 2. Thiamine metabolism dysfunction syndrome 2 (biotin- or thiamine-responsive encephalopathy type) (OMIM 607483)

3.2.a. Clinical features.

Biotin- or thiamine-responsive encephalopathy type or thiamine metabolism dysfunction syndrome 2 (THMD2), formerly known as biotin responsive basal ganglia disease (Ozand et al 1998) is an autosomal recessively inherited disease caused by mutations in thiamine transporter type 2 (ThTR-2), encoded by *SLC19A3* (#606152) (Zeng et al 2005). Phenotypes linked to SLC19A3 deficiency include Leigh encephalopathy and Wernicke encephalopathy (Kono et al 2009, Serrano et al 2012, Kevelam et al 2013, Gerards et al 2013, Pérez-Dueñas B et al 2013, Distelmaier et al 2014, Haack et al 2014). Yamada et al 2010 reported four Japanese patients who presented with epileptic spasms in early infancy, severe psychomotor retardation, brain atrophy and bilateral thalamic and basal ganglia lesions. These patients could be classified as Leigh Syndrome and not as a different phenotype (Yamada et al 2010). Early infantile Leigh syndrome is the most severe *SLC19A3*-related phenotype. Currently, 26 patients are known with this phenotype, all manifesting few days or weeks after delivery with feeding difficulties, lethargy, seizures and respiratory distress. Most infants with early infantile Leigh syndrome carry nonsense or frameshift variants predicting loss of function effects (Alfadhel 2017). In these infants, MRI lesions may be limited to the basal ganglia and the peri-rolandic cortex (Pérez-

Dueñas B et al 2013) or affect the whole brain with severe swelling and diffuse T2-hyperintensity of the cerebral and cerebellar white, basal ganglia and brainstem (Kevelam et al 2013). On the other end of the spectrum, Sgobbi de Souza et al 2016 reported an adult patient presenting with lethargy, dystonia and MRI abnormalities characterized by diffuse leukoencephalopathy and sparing of the basal ganglia, who improved after thiamine supplementation. Up to date, more than 130 *SLC19A3*-mutated patients have been reported with any of these phenotypes.

Our group has described the clinical and genetic characterization of 70 patients with *SLC19A3* deficiency (Ortigoza-Escobar et al 2017). Patients usually showed normal psychomotor development until the first episode of encephalopathy. The median age at disease onset was 3 years (range 1 month – 34 years), and in the majority of cases disease onset was triggered by infections, trauma, profuse exercise and vaccination. About 40% of these patients experienced more than one episode of encephalopathy before diagnosis. Interestingly, a minority of patients had an insidious onset of symptoms characterized by psychomotor regression, hyperactivity and attention deficit, unsteady gait, toe walking or stiffness of the limbs. Other symptoms observed during episodes of encephalopathy or as sequelae included: dystonia or status dystonicus, hypotonia, spasticity, seizure (myoclonic jerks, epileptic spasms, focal and generalized seizure, *epilesia partialis continua* and status epilepticus), dysphagia, ataxia, chorea, tremor, dysarthria, ophtalmoplegia, diplopia, nystagmus, strabismus, ptosis, opisthotonus, respiratory failure, weight loss, vertigo, rigidity, rhabdomyolysis, liver disease and jaundice. Biochemically, some patients showed elevated lactate in blood

(range 2.1-8.6 mmol/L) and CSF (range 2.1-7.1 mmol/L). Remarkably, younger patients had significantly higher lactate elevations. The excretion of organic acids was variable, with high concentrations of the following: isobutyric, 2-OH-isovaleric, 2, 4-di-OH-butyric, 3-OH-butyric, alpha-ketoglutaric, 2-OH-glutaric, glutaric, succinic, 2 keto adipic and 4-OH-phenyllactic acids (Ortigoza-Escobar et al 2017). In the majority of these patients, no abnormalities in respiratory chain complex activities were found. Additionally, our group described a profound decrease of free-thiamine in the CSF and fibroblasts of *SLC19A3*-mutated patients. This deficiency can be used as a biomarker for diagnosis and monitoring of treatment (Ortigoza-Escobar et al 2016).

Brain MRI is abnormal in all symptomatic cases and presents symmetrically distributed brain lesions in caudate nuclei, putamen, and medial thalami and, less frequently, cerebral cortex, brainstem and cerebellum (Ozand et al 1998, Kevelam et al 2013, Gerards et al 2013, Ortigoza-Escobar et al 2017). The changes are hyperintense on T2 and FLAIR images, and when MRI is performed in the acute phase, they generally exhibit a swelling appearance and diffuse restriction on ADC maps. Increased lactate levels can be observed at the time of MR spectroscopy. Lesions in the globus pallidum and brainstem have been significantly associated with a poor outcome (Ortigoza-Escobar et al 2017).

3.2. b. Treatment.

THMD2 is a treatable condition if recognized early and managed appropriately. For this reason, children presenting with unexplained encephalopathy and MRI abnormalities including bilateral signal alteration of caudate nucleus and putamen should raise the

suspicion of THMD2 and be started immediately on biotin and thiamine regimen since the prognosis of the disease is affected by the timing of treatment initiation. In this sense, extended family study is crucial to diagnose pre-symptomatic siblings and those with subtle neurological symptoms (Aljabri et al 2016).

Our group has previously demonstrated that thiamine supplementation during the acute encephalopathic episodes has a rapid benefit in alertness, improves feeding, controls seizures, and most patients gradually recover previously acquired milestones. Moreover, it prevents the occurrence of further encephalopathic episodes and increases survival. Importantly, disability measured with the Burke-Fahn-Marsden dystonia rating scale correlates with the time from disease onset to thiamine initiation. (Ortigoza-Escobar et al 2017). On the other hand, patients with the early infantile Leigh phenotype have a poor prognosis with a markedly reduced lifespan. Only a few patients have shown a good recovery after thiamine supplementation (Haack et al 2014, Pérez-Dueñas B et al 2013).

Thiamine doses are very variable but generally within the range of 10–40 mg/kg/day (Ortigoza-Escobar et al 2016). Toxicity studies reported minor adverse reactions after endovenous administration such as transient local irritation, and only one major reaction consisting of generalized pruritus (Wrenn et al 1989). However, no side effects have been described in patients with inherited defects of thiamine transport and metabolism treated with thiamine. Maximum reported therapeutic doses of thiamine are 1500 mg/day. Higher doses are not recommended as absorption mechanisms may be saturable. Thiamine supplementation is a long-term therapy that should not be

interrupted, as metabolic crisis have been reported within 30 days of thiamine withdrawal (Kono et al 2009). Tonduti et al 2018 described a patient who did not present any additional episode of encephalopathy over a period of 16 years after having stopped thiamine supplementation at the age of 20 years. However, adult onset presentations have been recently described, suggesting that thiamine is important during the entire life course in *SLC19A3* mutated patients.

Thiamine supplementation in *SLC19A3*-mutated patients restores CSF and intracellular thiamine levels (Ortigoza-Escobar et al 2016). It also normalizes lactic acid concentrations and organic acid profile in urine. Radiologically, thiamine supplementation leads to a significant reduction in the extension of brain lesions. In some cases, lesions are completely reversed, while in other cases residual atrophy and necrosis can be observed (Pérez-Dueñas et al 2013, Alfadhel et al 2013, Kassem et al 2014). Suzuki et al 2017 analyzed the therapeutic effects of high-dose thiamine treatment in knock-in and knock-out Slc19a3-deficient mice. They demonstrated and increase in survival and a stabilization of brain lesions, concluding that high doses of thiamine prevented acute neurodegeneration in Slc19a3-deficient mice.

The majority of patients with SLC19A3 deficiency are treated with a combination of thiamine and biotin. However, the administration of biotin is controversial. Some reported patients did not improve with biotin, as opposed to the initial description by Ozand et al 1998. Moreover, one-third of patients treated with biotin therapy alone showed a recurrence of acute crisis (Alfadhel et al 2013). After the addition of thiamine, crisis did not recur in these cases. Tabarki et al 2015 demonstrated that the combination

of biotin and thiamine was not superior to thiamine alone in the number of recurrences, neurological sequel, or brain MR changes for at least a 30-month period.

Doses of biotin vary from 5 mg/kg/day to 5–10 mg/day (Ortigoza Escobar et al 2016). Authors hypothesize that biotin can increase the expression levels of ThTR-2 mutants with some residual activity (Haack et al 2014).

3.2.c. *SLC19A3*: Genetic defects and functional studies.

SLC19A3 consists of 6 exons generating a predicted open-reading frame of 1488bp starting at exon 2 and finishing at exon 6. It encodes a 496 amino acid thiamine receptor (ThTR-2) of 56Kda. (Eudy et al 2000, Subramanian et al 2006). As other members of the same transporter family, the protein is formed by 12 transmembrane domains flanked by cytoplasmic N and C-terminal regions (Ganapathy et al 2004) (**Figure 3**).

Loss-of-function mutations affecting this gene disrupt thiamine transporter function leading to THMD2 (Yamada et al 2010). Up to date, 38 different mutations have been reported in *SLC19A3*, most of them combined in a compound heterozygous state in affected individuals. The majority of reported mutations are missense variants (60.5%) and only 34.2% are truncating variants (nonsense or frameshift mutations) (**Figure 3**). Also, two gross deletions affecting the gene promoter (exon 1 and flanking intronic regions) have been reported (Flønes et al 2016; Whitford et al 2017). The most prevalent genetic alteration in patients carrying *SLC19A3* defects is NM_025243: c.1264A>G; p.Thr422Ala. This mutation is present in homozygosity in patients with Arab ethnic backgrounds (Ortigoza-Escobar et al 2017).

Thiamine uptake and cellular localization assays have been performed using cell lines carrying experimental mutations in *SLC19A3* introduced by mutagenesis. Anionic residues potentially relevant for ThTR-2 function were mutated showing a decreased expression of the transporter at the apical domain (E120A and E320A) and a thiamine uptake reduction (E120A, E320A, E346A). The results demonstrate the importance of these residues for protein transport and function, especially those amino acids placed within TM4 or TM9 protein domains. Similar experiments were performed with N45Q and N166Q mutants, affecting potential glycosylation sites, but results suggested that N-glycosylation is not involved neither in protein targeting or thiamine uptake (Subramanian et al 2006).

A spontaneous canine model of Alaskan Husky Encephalopathy carrying homozygous loss-of-function mutations in *SLC19A3.1* presented with recurrent encephalopathic episodes with multifocal central nervous system deficits (Vernau et al 2013). The cerebral cortex and thalamus of affected dogs were severely deficient in TPP-dependent enzymes accompanied by decreases in mitochondrial mass and oxidative phosphorylation (OXPHOS) capacity, and increases in oxidative stress (Vernau et al 2015).

Moreover, KO and KI (for E320Q equivalent mice position) mice models have been generated (Reidling et al 2010; Suzuki et al 2017). These mice models showed a reduction in intestinal thiamine uptake associated with a depletion of thiamine levels in blood when fed with a thiamine-restricted diet. KI mice showed prolonged survival due to residual transporter activity compared with KO. Both models showed similar

pathological brain findings to patients consisting of neurodegeneration and astrogliosis. Finally, using primary rat hippocampal neuronal cultures, studies of knock down regulation of the expression of *SLC19A3* showed that thiamine metabolism defects can induce neuronal changes such as dendritic arbors growth inhibition and soma size reduction leading to a smaller brain size and neuronal degeneration (Liu et al 2017).

Further studies have been performed in order to functionally validate variants carried by patients of different cohorts (Subramanian et al 2006; Kono et al 2009; Debs et al 2010; Gerards et al 2013; Schänzer et al 2014). All of them were proven as pathogenic due to total or partial thiamine uptake reduction which can be explained by two main mechanisms: (1) the absence of ThTR-2 within the cell membrane due to an incorrect protein processing and trafficking (c.1179-3992_131+41del, c.130A>G) or (2) a protein placed in the cell membrane with functional impairment (c.68G>T; c.1264A>G, c.958G>C, c.280T>C). Interestingly, only a splicing variant has been reported in several patients (c.980-14A>G), which leads to a final truncated protein (p.Gly327Aspfs*8). The *in vitro* analysis of aberrant pre-messenger RNA splicing due to the c.980-14A>G allele showed the total exclusion of exon 4 and a predicted severe impairment of hTHTR2 function (Ortigoza-Escobar et al 2016).

3.3. Thiamine metabolism dysfunction syndrome 3 (Microcephaly Amish type) (OMIM 607196) and Thiamine metabolism dysfunction syndrome 4 (Bilateral striatal degeneration and progressive polyneuropathy type) (OMIM 613710)

3.3.a. Clinical features.

Clinical phenotypes associated with *SLC25A19* (#606521) mutations are: (1) Amish Lethal Microcephaly (MCPHA, OMIM 607196), (2) bilateral striatal degeneration and progressive polyneuropathy (OMIM 613710), characterized by episodes of encephalopathy triggered by fever or infections, flaccid weakness and slowly progressive axonal polyneuropathy in patients with normal psychomotor development (Spiegel et al 2009, Ortigoza-Escobar et al 2017].

MCPHA is characterized by severe congenital microcephaly, profound global developmental delay, CNS malformations (lissencephaly, corpus callosum dysgenesis, spinal dysraphia) and episodic encephalopathy (Kelley et al 2002, Siu et al 2010). All reported patients with MCPHA have been homozygous for the same p.G177A mutation and have had Amish origins, and manifest a homogeneous phenotype characterized by (1) severe microcephaly, similar to other cases of congenital microcephaly observed in children infected with the Zika virus; (2) profound developmental delay, progressive irritability, seizures and poor life span; (3) episodic encephalopathy associated with lactic acidosis and intermittent excretion of 2-ketoglutaric acid in urine. At least 61 affected infants have been born to 33 nuclear families in the Amish community from Pennsylvania, where incidence is approximately one in 500 births (Biesecker 2017).

Thiamine metabolism dysfunction syndrome 4 phenotype is a rare disorder, with four consanguineous Arabic patients from Israel (homozygous for c.373G>A; Spiegel et al 2009) and one German patient (homozygous for c.580T>C; Ortigoza-Escobar et al 2017) being described so far. These children presented between the age of 20 month and 6.5 years with recurrent episodes of encephalopathy and weakness, frequently triggered

by febrile illnesses. On evolution, these children developed slowly progressive axonal polyneuropathy, with distal weakness and contractures, dystonia, dysphagia, seizures and attention deficit disorder (Ortigoza-Escobar et al 2017).

Biochemically, Amish microcephaly patients show high excretion of alpha-ketoglutaric aciduria. Lactic acidosis and elevated CSF lactate (2.9–4.2 mmol/l) during acute decompensations are characteristic in both phenotypes (Kelley et al 2002, Siu et al 2010). The biochemical phenotype may be attributable to decreased activity of the three mitochondrial enzymes that require TPP as a cofactor: PDH, 2-oxoglutarate dehydrogenase, and branched-chain alpha-keto acid dehydrogenase.

MRI abnormalities in Amish microcephaly are characterized by a simplified gyral pattern, brainstem and cerebellar hypoplasia, and corpus callosum hypoplasia (Siu et al 2010). Patients with bilateral striatal degeneration and progressive polyneuropathy show T2-hyperintensities restricted to the caudate and putamen, (Spiegel et al 2009). Progression to cavitation is characteristic, described as T2-hyperintensity and T1-hypointensity in the neostriatum (Ortigoza-Escobar et al 2017).

3.3. b. Treatment.

Prognosis of Amish Lethal Encephalopathy is poor with most patients dying in infancy. The patient reported by Siu et al 2010 was treated with thiamine supplementation (100mg/day) and a high fat diet. This treatment resulted in a reduction of lactic acid. Surprisingly, authors found an inverse relationship between the production of lactic acid and alpha-ketoglutaric acid, which could be explained by reduced pyruvate

dehydrogenase activity during a metabolic crisis, resulting in lactic acidosis and a decline of acetyl-CoA entering the tricarboxylic acid cycle, with a consequent decreased production of alpha-ketoglutaric acid.

The five patients with thiamine metabolism dysfunction syndrome 4 were treated with thiamine supplementation (400–600mg/day), which led to a substantial improvement in peripheral neuropathy and gait in early treated patients, supporting the efficacy of thiamine treatment in preventing further disease progression. All patients are currently alive (Ortigoza-Escobar et al 2017). A pregnant patient with this defect has required an increase in thiamine dose of 400 to 1500 mg due to the appearance of neurological symptoms.

3.3.c. *SLC25A19*: Genetic defects and functional studies.

Thiamine mitochondrial carrier is encoded by *SLC25A19*. The gene is formed by 9 exons; exons 4 to 9 are part of the coding sequence, while exons 1 to 3 are placed in the 5' un-translated region. Thiamine mitochondrial carrier has a tripartite structure, similar to other mitochondrial carriers, which consists of three tandem repeats folded each one within two trans-membrane ±-helices resulting in a six trans-membrane domains protein linked through long extracellular hydrophilic loops and shorter cytoplasmic loops and flanked by intracellular N- and C- terminal domains (Iacobazzi et al 2001).

Three different missense mutations have been found affecting this gene, and at the moment, there is a strong genotype-phenotype correlation: c.530G>C appears only in MCPHA patients (Rosemberg et al 2002) while patients affected by striatal necrosis and

progressive polyneuropathy carry c.373G>A (Spiegel et al 2009) or c.580T>C (Ortigoza-Escobar et al 2017) (**Figure 4**). The explanation for these differential phenotypes according to the genetic variants remains unknown.

Functional studies were performed to better understand the pathophysiological mechanism of the disease. In vitro studies comparing wild-type DNC and c.530G>C showed an ablation of dATP/ADP exchange in the mutant suggesting a defect in the transport activity (Rosenberg et al 2002). In the light of these results, it was proposed that a defect in mitochondrial nucleotide transport leads to an impairment of mitochondrial DNA synthesis resulting in energy metabolism failure (Korf 2003). However, further analysis suggested that deoxyribonucleotide transport was not the primary function for SLC25A19. A high sequence identity with the yeast mitochondrial transporter for Thiamine Pyrophosphate (ThPP) indicated the potential function of DNC as a thiamine transporter (Kang and Samuels 2008). In 2006, Lindhurst et al generated a KO mouse model of Slc25a19, which has a reduction of mitochondrial ThPP. *In vitro* assays were also performed showing not only a reduction in thiamine transport in mutant cells compared to wild-type but also a lower activity in mitochondrial ThPP-dependent enzyme complexes PDH and KGDH. This work postulated *SLC25A19* gene as a carrier of mitochondrial thiamine pyrophosphate (MTPPT) (Lindhurst et al 2006). Latest studies performed by Liu et al 2016, correlated neurodegeneration and smaller brain size with a disruption of normal thiamine metabolism.

Sabui et al 2016 performed *in vitro* studies in HepG2 cells in order to describe which residues were important for the protein function. Mutagenesis for different positively-

charged residues involved in other membrane carriers that transport negative substrates was done and consequences were studied through mitochondria isolation, thiamine uptake measurement and both RNA and protein expression assays. Results showed that (1) a polar residue is required at position 34 for normal function of the transporter protein; (2) Ile33, Asp37, His137 and Lys291 are crucial to mitochondrial delivery of MTPPT; (3) RNA and protein expression results suggested that mutations affecting Ile33 and Asp37 may change translational efficiency and/or protein stability (Sabui et al 2016).

Finally, functional pathogenic validation was necessary to associate *SLC25A19* c.373G>A mutation with striatal necrosis patients phenotype. With that aim, human wild-type and mutant *SLC25A19* were over-expressed in a deleted TPC1 yeast model. Using thiamine depleted growth medium, authors demonstrated a total complementation in wild-type transfected yeast colonies while mutant colonies suffered a partial complementation, proving variant pathogenic effect (Spiegel et al 2009).

3.4. Thiamine metabolism dysfunction syndrome 5 (episodic encephalopathy type) (OMIM 614458)

3.4.a. Clinical phenotype:

Thiamine pyrophosphokinase deficiency (TPK1; #606370) is associated with episodic encephalopathy triggered by infections or dehydration. Since the first description of five individuals from three families reported by Mayr et al 2011, a total of fifteen patients have been reported (Mayr et al 2011, Fraser et al 2014, Banka et al 2014, Mahajan and

Sidiropoulos 2017, Invernizzi et al 2017, Huang et al 2018). All described patients had onset of symptoms in childhood (range 1 month – 4 years and 8 months). Children may exhibit a normal or delayed psychomotor development until they present with recurrent episodes of encephalopathy, ataxia, dysarthria, dystonia, seizures, ophtalmoplegia, nystagmus and psychomotor regression. A pair of sibs was reported manifesting subacute onset generalized dystonia without episodes of encephalopathy (Mahajan and Sidiropoulos 2017). One patient was initially misdiagnosed as acute disseminated encephalomyelitis and received corticosteroid and intravenous gamma globulins. However, this patient showed signal abnormalities within the putamina and dentate nuclei and high lactate levels in plasma and CSF. Thiamine supplementation prevented further encephalopathic episodes in this case (Invernizzi et al 2017).

Brain MRI abnormalities described in TPK1 deficient patients were localized in the cerebellum and dentate nuclei (100%), striatum (75%), Globus pallidus (50%) and spinal cord (25%) (Ortigoza-Escobar et al 2017, Invernizzi et al 2017, Mahajan and Sidiropoulos 2017).

Biochemically, lactic acidosis (range: 2.3-6.2 mmol/l, reference values (RV) 0.5-2.2 mmol/l) and elevated CSF lactate (range 2.4-3.3 mmol/l, RV 1.1-2.4 mmol/l) can be observed during episodes of encephalopathy. Likewise, there is a variable elevation of multiple organic acids, such as 2-ketoglutaric acid, 3-hydroxyisovaleric acid, fumaric acid, glutaric acid and 3, 4-dihydroybutryate. Plasma thiamine level can be normal (Mayr et al 2011) or slightly reduced (32 ng/l, RV 38–122 ng/l) (Mahajan and Sidiropoulos 2017), but characteristically, there is a decrease in blood TPP (range 46.6-

96,9 mmol/l, RV: 132-271 mmol/l) and muscle TPP (8.8-9.5 nmol/g protein, RV: 41.6–81.6 nmol/g protein) in *TPK1* patients (Mayr et al 2011).

3.4.b. Treatment.

Thiamine supplementation (100–500 mg/day) in TPK1 deficient patients has led to clinical improvement and even normal neurodevelopment in early treated patients (Mayr et al 2011). It has also proven to prevent further metabolic decompensations (Invernizzi et al 2017) and ameliorate brain MRI lesions (Banka et al 2014, Invernizzi et al 2017). Authors conclude that dosage of thiamine should be sufficient to provide adequate substrate concentration for residual TPK activity and to prevent any depletion of this vitamin. Recently, Huang et al 2018 reported a Chinese girl with a novel homozygous *TPK1* mutation (p.L28S) who was treated with thiamine early in disease evolution. The patient experienced a significant clinical and radiological improvement of brain MRI abnormalities, and blood TPP levels increased up to the lower limit of reference range after thiamine supplementation. These authors associated the onset of symptoms with TPP blood levels below 20% of healthy controls (Huang et al 2018). Supplying excess thiamine could overcome decreased thiamine binding affinity of TPK caused p.S160L (c.479C>T) and p.W202G (c.604T>G) mutations and allow normal production of TPP (Huang et al 2018).

The implementation of a ketogenic diet has shown controversial results, with one patient manifesting clinical improvement (Fraser et al 2014) and other patient presenting clinical deterioration (Banka et al 2014). Deep pallidal stimulation in a

patient with TPK1 deficiency and generalized dystonia had a minor beneficial effect (Mahajan and Sidiropoulos 2017).

3.4.c. *TPK1*: Genetic defects and functional studies.

Thiamine phosphokinase 1 is encoded by *TPK1*, a gene with 8 coding exons followed by a large 3'UTR region (Zhao et al 2001).

Recessive defects within *TPK1* sequence result in thiamine metabolism dysfunction due to a thiamine pyrophosphokinase deficiency (Mayr et al 2011). Up to date, eleven different variants have been reported (Mayr et al 2011, Fraser et al 2014, Banka et al 2014, Invernizzi et al 2017, Huang et al 2018). Most of them are missense variants but there is also a frameshift variant which truncates the protein (c.179_182delGAGA), two deletions of exon 3 and 4, and the splicing variant c.501+4A>T that results in a complete deletion of exon 6 (**Figure 5**).

Different authors have performed functional studies to prove pathogenicity for reported mutations and to better understand involved mechanisms causing the disease. Metabolic flux, mitochondrial enzyme and cofactor levels analysis from muscle biopsies of the first five patients described demonstrated a defect in mitochondrial pyruvate oxidation route and thiamine metabolism. Moreover, protein level analysis from muscle extracts showed a decrease of full-length TPP protein in affected individuals (Mayr et al 2011). Banka et al 2014 showed a reduction in TPK activity in cells transfected with *TPK1* mutants c.479C>T and c.664G>C compared to wild-type. Protein quantification from patients muscle biopsies showed lower protein levels than controls in all patients except

those carrying the c.479C>T variant. These results suggest that a reduction in protein levels is associated with a reduction of TPK activity in the majority of patients. However, c.479C>T should be affecting the enzyme activity through a different novel unknown mechanism (Banka et al 2014).

A crystal structure of TKP1 protein has been published recently (PDB 3S4Y), showing two crucial domains: dimerization domain and thiamine binding domain with its active site. In fact, binding site is constituted by the dimerization of two TPK1 molecules. Huang et al 2018 performed several studies to validate a new mutation (c.83A>G) and further studies for previously reported variants. First of all, the comparison between mutated protein models and wild-type crystal structure showed that Ser160 and Trp202 were crucial to allow TPP binding to TPK1. Then, thiamine binding assays confirmed that variants c.479C>T (p.Ser160Leu) and c.604T>G (p.Trp202Gly) produce a partial or total impairment, respectively, of thiamine binding and a reduced affinity to the product TPP. The enzyme activity was also measured and, although most of the mutants, especially c.148A>C (p.Asn50His), have a reduced activity compared to wild-type, variants c.479C>T (p.Ser160Leu) and c.604T>G (p.Trp202Gly) resulted in a higher enzymatic activity (Huang et al 2018). These experiments demonstrate that pathogenicity can be caused by a reduction or gain of enzymatic TPK1 activity. Finally, protein stability was assayed measuring the melting temperature with differential scanning calorimetric method. A huge range of results were obtained, however more instable mutants where those affecting residues within the C-terminus domain of TPK1:

c.479C>T (p.Ser160Leu), c.604T>G (p.Trp202Gly), c.656A>G (p.Asn219Ser) and c.664G>C (p.Asp222His).

All the biochemical assays performed to date revealed that mutations in *TPK1* cause thiamine metabolism dysfunction through three different mechanisms: enzymatic activity alteration, thiamine affinity reduction and decreased protein stability (Huang et al 2018).

4. Conclusion

Genetic defects of thiamin transport and metabolism should be considered in all patients with episodes of recurrent encephalopathy and / or dystonia, increased blood lactate or CSF or increased alpha-ketoglutarate in urine, and in patients with radiological injury of basal ganglia and thalami. Rogers' syndrome should be suspected in children with megaloblastic anemia, non-immune diabetes mellitus and sensorial deafness. Suspicion is essential since early treatment has been shown to improve prognosis in most patients. Functional work will allow a better understanding of pathogenic mechanisms leading to thiamine deficiency, which is essential to optimize treatment strategies and improve prognosis. At the same time, the use of next generation sequencing will expand the spectrum of genotypes and phenotypes of these genetic defects.

5. References

Agladioglu S, Aycan Z, Bas VN et al (2012) Thiamine-responsive megaloblastic anemia syndrome: a novel mutation. *Genet Couns* 23(2):149-56.

Akbari MT, Zare Karizi S, Mirfakhraie R, Keikhaei B (2014) Thiamine-responsive megaloblastic anemia syndrome with Ebstein anomaly: a case report. *Eur J Pediatr* 173(12):1663-5.

Alexander B, Landwehr G, Mitchell F (1946) Studies of thiamine metabolism in man. II. Thiamine and pyrimidine excretion with special reference to the relationship between injected and excreted thiamine in normal and abnormal subjects. *J Clin Invest*. 25(3):294-303.

Alfadhel M (2017) Early Infantile Leigh-like SLC19A3 Gene Defects Have a Poor Prognosis: Report and Review. *J Cent Nerv Syst Dis* 27(9):1179573517737521.

Alfadhel M, Almuntashri M, Jadah RH (2013) Biotin-responsive basal ganglia disease should be renamed biotin-thiamine-responsive basal ganglia disease: a retrospective review of the clinical, radiological and molecular findings of 18 new cases. *Orphanet J Rare Dis* 8:83.

Aljabri MF, Kamal NM, Arif M, AlQaedi AM, Santali EY (2016) A case report of biotin-thiamine-responsive basal ganglia disease in a Saudi child: Is extended genetic family study recommended? *Medicine* 95(40):e4819.

Argun M, Baykan A, Hatipo lu N et al (2018) Arrhythmia in thiamine responsive megaloblastic anemia syndrome. *Turk J Pediatr* 60(3):348-351.

Balamurugan K, Said HM (2002) Functional role of specific amino acid residues in human thiamine transporter SLC19A2: mutational analysis. *Am J Physiol Gastrointest Liver Physiol* 283(1):G37-43.

Banka S, de Goede C, Yue WW et al (2014) Expanding the clinical and molecular spectrum of thiamine pyrophosphokinase deficiency: a treatable neurological disorder caused by TPK1 mutations. *Mol Genet Metab* 113(4):301-6.

Barennes H, Sengkhamyong K, Rene JP, Phimmasane M (2015) Beriberi (thiamine deficiency) and high infant mortality in northern Laos. *PLoS Negl Trop Dis* 9:e0003581.

Benidir AN, Laughlin S, Ng VL (2014) Visual disturbances in total parenteral nutrition dependent liver transplant pediatric patient. *Gastroenterology* 146:e10–e11.

Bennett WP, Wang X, Hollstein M et al (1994) The p53 tumor suppressor gene: Clues to cancer etiology and molecular pathogenesis. *Lung Cancer* 11:126-127.

Bergmann AK, Sahai I, Falcone JF et al (2009) Thiamine-responsive megaloblastic anemia: identification of novel compound heterozygotes and mutation update. *J Pediatr* 155(6): 888-892.e1.

Beshlawi I, Al Zadjali S, Bashir W, Elshinawy M, Alrawas A, Wali Y (2014) Thiamine responsive megaloblastic anemia: the puzzling phenotype. *Pediatr Blood Cancer* 61(3):528-31.

Biesecker LG (2017) Amish Lethal Microcephally. *GeneReviews*

Burkholder PR, McVeigh I (1942) Synthesis of Vitamins by Intestinal Bacteria. *Proc Natl Acad Sci USA* 28(7):285-9.

Cao B, Gong C, Wu D et al (2016) Genetic Analysis and Follow-Up of 25 Neonatal Diabetes Mellitus Patients in China. *J Diabetes Res* 2016:6314368

Debs R, Depienne C, Rastetter A et al (2010) Biotin-Responsive Basal Ganglia Disease in Ethnic Europeans With Novel SLC19A3 Mutations. *Arch Neurol* 67(1):126–130.

Diaz GA, Banikazemi M, Oishi K, Desnick RJ, Gelb BD (1999) Mutations in a new gene encoding a thiamine transporter cause thiamine-responsive megaloblastic anaemia syndrome. *Nat Genet* 22(3):309-12.

Distelmaier F, Huppke P, Pieperhoff P et al (2014) Biotin-responsive basal ganglia disease: a treatable differential diagnosis of leigh syndrome. *JIMD Rep* 13: 53–7.

Dolce V, Fiermonte G, Runswick MJ, Palmieri F, Walker JE (2001) The human mitochondrial deoxynucleotide carrier and its role in the toxicity of nucleoside antivirals. *Proc Natl Acad Sci USA* 98(5):2284-8

Dutta B, Huang W, Molero M et al (1999) Cloning of the Human Thiamine Transporter, a Member of the Folate Transporter Family. *J Biol Chem* 274(45):31925-9.

Eudy JD, Spiegelstein O, Barber RC, Wlodarczyk BJ, Talbot J, Finnell RH (2000) Identification and characterization of the human and mouse SLC19A3 gene: a novel member of the reduced folate family of micronutrient transporter genes. *Mol Genet Metab* 71(4):581-90.

Ferreira-Vieira TH, de Freitas-Silva DM, Ribeiro AF, Pereira SR, Ribeiro ÂM (2016) Perinatal thiamine restriction affects central GABA and glutamate concentrations and motor behavior of adult rat offspring. *Neurosci Lett* 617:182-7.

Fleming JC, Tartaglini E, Steinkamp MP, Schorderet DF, Cohen N, Neufeld EJ (1999) The gene mutated in thiamine-responsive anaemia with diabetes and deafness (TRMA) encodes a functional thiamine transporter. *Nat Genet* 22(3)305-8.

Flønes I, Sztromwasser P, Haugarvoll K et al (2016) Novel SLC19A3 Promoter Deletion and Allelic Silencing in Biotin-Thiamine-Responsive Basal Ganglia Encephalopathy. *PLoS ONE* 11(2):e0149055.

Fraccascia P, Sniekers M, Casteels M, Van Veldhoven PP (2007) Presence of thiamine pyrophosphate in mammalian peroxisomes. *BMC Biochem* 27;8:10.

Fraser JL, Vanderver A, Yang S et al (2014) Thiamine pyrophosphokinase deficiency causes a Leigh Disease like phenotype in a sibling pair: identification through whole exome sequencing and management strategies. *Mol Genet Metab Rep* 1:66-70.

Fujiwara T, Harigae H (2013). Pathophysiology and genetic mutations in congenital sideroblastic anemia. *Pediatr Int*. 55(6):675-9.

Ganapathy V, Smith SB, Prasad PD (2004) SLC19: the folate/thiamine transporter family. *Pflugers Arch* 447(5):641-6.

Gerards M, Kamps R, van Oevelen J et al (2013) Exome sequencing reveals a novel Moroccan founder mutation in SLC19A3 as a new cause of early childhood fatal Leigh Syndrome. *Brain* 136: 882–90.

Goyer A (2010) Thiamine in plants: aspects of its metabolism and functions. *Phytochemistry* 71(14-15):1615-24.

Gritli S, Omar S, Tartaglini E et al (2001) A novel mutation in the SLC19A2 gene in a Tunisian family with thiamine-responsive megaloblastic anaemia, diabetes and deafness syndrome. *Br J Haematol* 113(2):508-13

Haack TB, Klee D, Strom TM et al (2014) Infantile leigh-like syndrome caused by SLC19A3 mutations is a treatable disease. *Brain* 137: e295.

Habeb AM, Flanagan SE, Zulali MA et al (2018) Pharmacogenomics in diabetes: outcomes of thiamine therapy in TRMA syndrome. *Diabetologia* 61(5):1027-1036.

Huang HM, Chen HL, Gibson GE (2010) Thiamine and oxidants interact to modify cellular calcium stores. *Neurochem Res* 35(12):2107-16.

Huang W, Qin J, Liu D et al (2018) Reduced thiamine binding is a novel mechanism for TPK deficiency disorder. *Mol Genet Genomics* 294(2):409-416

Iacobazzi V, Ventura M, Fiermonte G, Prezioso G, Rocchi M, Palmieri F (2001) Genomic organization and mapping of the gene (SLC25A19) encoding the human mitochondrial deoxynucleotide carrier (DNC). *Cytogenet Cell Genet* 93(1-2):40-2.

Invernizzi F, Panteghini C, Chiapparini L et al (2017) Thiamine-responsive disease due to mutation of tpk1: Importance of avoiding misdiagnosis. *Neurology* 89(8): 870-871.

Jones PT, Anderson R (1983) Oxidative inhibition of polymorphonuclear leukocyte motility mediated by the peroxidase/H2O2/halide system: studies on the reversible nature of the inhibition and mechanism of protection of migratory responsiveness by ascorbate, levamisole, thiamine and cysteine. *Int J Immunopharmacol* 5(5):377-89.

Hang J, Samuels DC (2008) The evidence that the DNC (SLC25A19) is not the mitochondrial deoxyribonucleotide carrier. *Mitochondrion* 8(2):103-8.

Karimzadeh P, Moosavian T, Moosavian H (2018) Recurrent Stroke in a Child with TRMA Syndrome and SLC19A2 Gene Mutation. *Iran J Child Neurol* 12(1): 84-88.

Kassem H, Wafaie A, Alsuhibani S, Farid T (2014) Biotin-responsive basal ganglia disease: neuroimaging features before and after treatment. *AJNR Am J Neuroradiol* 35(10):1990-5.

Ke ZJ, Calingasan NY, DeGiorgio LA, Volpe BT, Gibson GE (2005) CD40-CD40L interactions promote neuronal death in a model of neurodegeneration due to mild impairment of oxidative metabolism. *Neurochem Int* 47(3):204-15.

Kelley RI, Robinson D, Puffenberger EG et al (2002) Amish lethal microcephaly: a new metabolic disorder with severe congenital microcephaly and 2-ketoglutaric aciduria. *Am J Med Genet* 112:318–26.

Kevelam SH, Bugiani M, Salomons GS et al (2013) Exome sequencing reveals mutated SLC19A3 in patients with an early-infantile, lethal encephalopathy. *Brain* 136: 1534–43.

Kono S, Miyajima H, Yoshida K et al (2009) Mutations in a thiamine-transporter gene and Wernicke's-like encephalopathy. *N Engl J Med* 360(17):1792–1794

Korf BR (2003) What's new in Neurogenetics? Amish microcephaly. *Eur J Paed Neurol* 7(6):393-4

Labay V, Raz T, Baron D et al (1999) Mutations in SLC19A2 cause thiamine-responsive megaloblastic anaemia associated with diabetes mellitus and deafness. *Nat Genet* 22(3):300-4.

Lindhurst MJ, Fiermonte G, Song S (2006) Knockout of Slc25a19 causes mitochondrial thiamine pyrophosphate depletion, embryonic lethality, CNS malformations, and anemia. *Proc Natl Acad Sci USA* 103(43):15927-32

Liu G, Yang F, Han B, Liu J, Nie G (2014) Identification of four SLC19A2 mutations in four Chinese thiamine responsive megaloblastic anemia patients without diabetes. Blood *Cells Mol Dis* 52(4):203-4.

Liu H, Sang S, Lu Y, Wang Z, Yu X, Zhong C (2017) Thiamine metabolism is critical for regulating correlated growth of dendrite arbors and neuronal somata. *Sci Rep* 7(1):5342.

Losa R, Sierra MI, Fernández A, Blanco D, Buesa JM (2005) Determination of thiamine and its phosphorylated forms in human plasma, erythrocytes and urine by HPLC and fluorescence detection: a preliminary study on cancer patients. *J Pharm Biomed Anal* 37(5):1025-9.

Mahajan A, Sidiropoulos C (2017) TPK1 mutation induced childhood onset idiopathic generalized dystonia: Report of a rare mutation and effect of deep brain stimulation. *J Neurol Sci* 376:42-43.

Manimaran P, Subramanian VS, Karthi et al (2016) Novel nonsense mutation (p.Ile411Metfs*12) in the SLC19A2 gene causing Thiamine Responsive Megaloblastic Anemia in an Indian patient. *Clin Chim Acta* 452:44-3.

Manzetti S, Zhang J, van der Spoel D (2014) Thiamin function, metabolism, uptake, and transport. *Biochemistry* 53(5):821-35.

Mathews L, Narayanadas K, Sunil G (2009) Thiamine responsive megaloblastic anemia. *Indian Pediatr* 46(2):172-4.

Mayr JA, Freisinger P, Schlachter K et al (2011) Thiamine pyrophosphokinase deficiency in encephalopathic children with defects in the pyruvate oxidation pathway. *Am J Hum Genet* 89: 806–12.

Mielgo-Ayuso J, Aparicio-Ugarriza R, Olza J et al (2018) Dietary Intake and Food Sources of Niacin, Riboflavin, Thiamin and Vitamin B_6 in a Representative Sample of the Spanish Population. The Anthropometry, Intake, and Energy Balance in Spain (ANIBES) Study †. *Nutrients* 29;10(7).

Mikstiene V, Songailiene J, Byckova J et al (2015) Thiamine responsive megaloblastic anemia syndrome: a novel homozygous SLC19A2 gene mutation identified. *Am J Med Genet A* 167(7): 1605-9.

Mimouni-Bloch A, Goldberg-Stern H, Strausberg R et al (2014) Thiamine deficiency in infancy: long-term follow-up. *Pediatr Neurol* 51:311–316.

Mkrtchyan G, Aleshin V, Parkhomenko Y et al (2015) Molecular mechanisms of the non-coenzyme action of thiamin in brain: biochemical, structural and pathway analysis. *Sci Rep* 5:12583.

Mozzillo E, Melis D, Falco M et al (2013) Thiamine responsive megaloblastic anemia: a novel SLC19A2 compound heterozygous mutation in two siblings. *Pediatr Diabetes* 14(5):384-7.

Nabokina SM, Ramos MB, Valle JE, Said HM (2015) Regulation of basal promoter activity of the human thiamine pyrophosphate transporter SLC44A4 in human intestinal epithelial cells. *Am J Physiol Cell Physiol* 308(9):C750-7.

Nogueira RJ, Godoy JE, Souza TH (2016) Acute abdominal pain as a presenting symptom of beriberi in a pediatric patient. *J Trop Pediatr* 62:490–495.

Oishi K, Hirai T, Gelb BD, Diaz GA (2001) Slc19a2: Cloning and characterization of the murine thiamin transporter cdna and genomic sequence, the orthologue of the human TRMA gene. *Mol Genet Metab* 73(2):149-59.

Ozdemir MA, Akcakus M, Kurtoglu S, Gunes T, Torun YA (2002) TRMA syndrome (thiamine-responsive megaloblastic anemia): a case report and review of the literature. *Pediatr Diabetes* 3(4):205-9.

Park SW, Yi YY, Han JW, Kim HD, Lee JS, Kang HC (2014) Wernicke's encephalopathy in a child with high dose thiamine therapy. *Korean J Pediatr* 57:496–499.

Perko R, Harreld JH, Helton KJ, Sabin ND, Haidar CE, Wright KD et al (2012). What goes around comes around? Wernicke encephalopathy and the nationwide shortage of intravenous multivitamins revisited. *J Clin Oncol* 30:e318–e320.

Pérez-Dueñas B, Serrano M, Rebollo M et al (2013) Reversible lactic acidosis in a newborn with thiamine transporter-2 deficiency. *Pediatrics* 131(5):e1670-5.

Porter FS, Rogers LE, Sidbury JB Jr (1969) Thiamine-responsive megaloblastic anemia. *J Pediatr* 74(4):494-504.

Reidling JC, Lambrecht N, Kassir M, Said HM et al (2010) Impaired intestinal vitamin B1 (thiamin) uptake in thiamin transporter-2 deficient mice. *Gastroenterology* 138(5)

Reidling JC, Nabokina SM, Balamurugan K, Said HM (2006) Developmental maturation of intestinal and renal thiamin uptake: studies in wild-type and transgenic mice carrying human THTR-1 and 2 promoters. *J Cell Physiol* 206(2):371-7.

Reidling JC, Said HM (2005) Adaptive regulation of intestinal thiamin uptake: molecular mechanism using wild-type and transgenic mice carrying hTHTR-1 and -2 promoters. *Am J Physiol Gastrointest Liver Physiol* 288(6):G1127-34.

Ricketts CJ, Minton JA, Samuel J et al (2006) Thiamine-responsive megaloblastic anaemia syndrome: long-term follow-up and mutation analysis of seven families. *Acta Paediatr* 95:99–104.

Rosenberg MJ, Agarwala R, Bouffard G (2002) Mutant deoxynucleotide carrier is associated with congenital microcephaly. *Nat Genet* 32(1):175-9.

Sabui S, Subramanian VS, Kapadia R, Said HM (2016) Structure - function characterization of the human mitochondrial thiamin pyrophosphate transporter (hMTPPT; SLC25A19): important roles for Ile33, Ser34, Asp37, His137 and Lys291. *Biochim Biophys Acta* 1858(8):1883-1890

Saeki K, Saito Y, Komaki H et al (2010) Thiamine-deficient encephalopathy due to excessive intake of isotonic drink or overstrict diet therapy in Japanese children. *Brain Dev* 32:556–563.

Said HM, Balamurugan K, Subramanian VS, Marchant JS (2004) Expression and functional contribution of hTHTR-2 in thiamin absorption in human intestine. *Am J Physiol Gastrointest Liver Physiol* 286(3):G491-8.

Said HM, Ortiz A, Kumar CK, Chatterjee N, Dudeja PK, Rubin S (1999) Transport of thiamine in human intestine: mechanism and regulation in intestinal epitelial cell model Caco-2. Am J Physiol 277(4):C645-51.

Schänzer A, Döring B, Ondrouschek M et al (2014) Stress-Induced Upregulation of SLC19A3 is Impaired in Biotin-Thiamine-Responsive Basal Ganglia Disease. *Brain Pathology* 24:270–279

Scharfe C, Hauschild M, Klopstock T et al (2000) A novel mutation in the thiamine responsive megaloblastic anaemia gene SLC19A2 in a patient with deficiency of respiratory chain complex I. *J Med Genet* 37:669-673

Serrano M, Rebollo M, Depienne C et al (2012) Reversible generalized dystonia and encephalopathy from thiamine transporter 2 deficiency. *Mov Disord* 27:1295–8

Sgobbi de Souza PV, Bortholin T, Vieira de Rezende Pinto WB, Bulle Oliveira AS (2016) Teaching NeuroImages: An extremely rare cause of treatable acute encephalopathy. *Neurology* 87(11):e116.

Siu VM, Ratko S, Prasad AN et al (2010) Amish microcephaly: Long-term survival and biochemical characterization. *Am J Med Genet A* 152A(7):1747-3.

Spiegel R, Shaag A, Edvardson S et al (2009) SLC25A19 mutation as a cause of neuropathy and bilateral striatal necrosis. *Ann Neurol* 66(3):419-24

Subramanian VS, Marchant JS, Parker I, Said HM (2003) Cell biology of the human thiamine transporter-1 (hTHTR1). Intracellular trafficking and membrane targeting mechanisms. *J Biol Chem* 278(6):3976-84.

Subramanian VS, Marchant JS, Said HM (2006) Biotin-responsive basal ganglia disease-linked mutations inhibit thiamine transport via hTHTR2: biotin is not a substrate for hTHTR2. *Am J Cell Physiol* 291:C851-859.

Subramanian VS, Marchant JS, Said HM (2007) Targeting and intracellular trafficking of clinically relevant hTHTR1 mutations in human cell lines. *Clin Sci (Lond)* 113(2):93-102.

Suzuki K, Yamada K, Fukuhara Y, Tsuji A,Shibata K, Wakamatsu N (2017) High-dose thiamine prevents brain lesions and prolongs survival of Slc19a3-deficient mice. *PLoS ONE* 12(6): e0180279

Stuetz W, Carrara VI, McGready R, Lee SJ, Biesalski HK, Nosten FH (2012) Thiamine diphosphate in whole blood, thiamine and thiamine monophosphate in breast-milk in a refugee population. *PLoS One* 7(6):e36280.

Tabarki B, Alfadhel M, AlShahwan S, Hundallah K, AlShafi S, AlHashem A (2015) Treatment of biotin-responsive basal ganglia disease: Open comparative study between the combination of biotin plus thiamine versus thiamine alone. *Eur J Paediatr Neurol* 19(5):547-52.

Tittmann K (2009) Reaction mechanisms of thiamin diphosphate enzymes: redoxreactions. *FEBS J* 276(9):2454-68.

Tonduti D, Invernizzi F, Panteghini C et al (2018) SLC19A3 related disorder: Treatment implication and clinical outcome of 2 new patients. *Eur J Paediatr Neurol* 22(2):332-335.

Tuck D, Bresson JL, Burlingame B et al (2016) Dietary reference values for thiamin. *EFSA J* 14(12):4653

Valerio G, Franzese A, Poggi V, Tenore A (1998) Long-term follow-up of diabetes in two patients with thiamine-responsive megaloblastic anemia syndrome. *Diabetes Care* 21:38–41.

Vernau K, Napoli E, Wong S et al (2015) Thiamine Deficiency-Mediated Brain Mitochondrial Pathology in Alaskan Huskies with Mutation in SLC19A3.1. *Brain Pathol* 25(4):441-53.

Vernau KM, Runstadler JA, Brown EA et al (2013) Genome-Wide Association Analysis Identifies a Mutation in the Thiamine Transporter 2 (SLC19A3) Gene Associated with Alaskan Husky Encephalopathy. *PLoS ONE* 8(3): e57195

Vigil FA, Oliveira-Silva Ide F, Ferreira LF, Pereira SR, Ribeiro AM (2010) Spatial memory deficits and thalamic serotonergic metabolite change in thiamine deficient rats. *Behav Brain Res* 210(1):140-2.

Villa V, Rivellese A, Di Salle F, Iovine C, Poggi V, Capaldo B (2000) Acute Ischemic Stroke in a Young Woman with the Thiamine-Responsive Megaloblastic Anemia Syndrome *J Clin Endocrinol Metab* 85(3):947-9.

Wani NA, Qureshi UA, Jehangir M, Ahmad K, Ahmad W (2016) Infantile encephalitic beriberi: magnetic resonance imaging findings. *Pediatr Radiol* 46:96–103.

Whitford W, Hawkins I, Glamuzina E et al (2017) Compound heterozygous SLC19A3 mutations further refine the critical promoter region for biotin-thiamine-responsive basal ganglia disease. *Cold Spring Harb Mol Case Stud* 3(6)

Wrenn KD, Murphy F, Slovis CM (1989) A toxicity study of parenteral thiamine hydrochloride. *Ann Emerg Med* 18(8):867-70.

Xian X, Liao L, Shu WA (2018) Novel Mutation of SLC19A2 in a Chinese Zhuang Ethnic Family with Thiamine- Responsive Megaloblastic Anemia. *Cell Physiol Biochem* 47(5):1989-1997

Yadav UC, Kalariya NM, Srivastava SK, Ramana KV (2010) Protective role of benfotiamine, a fat-soluble vitamin B1 analogue, in lipopolysaccharide-induced cytotoxic signals in murine macrophages. *Free Radic Biol Med* 48(10):1423-34.

Yamada K, Miura K, Hara K et al (2010) A wide spectrum of clinical and brain MRI findings in patients with SLC19A3 mutations. *BMC Med Genet* 11:171.

Ye_ilkaya E, Bideci A, Temizkan M et al (2009) A novel mutation in the SLC19A2 gene in a Turkish female with thiamine-responsive megaloblastic anemia syndrome. *J Trop Pediatr* 55(4):265-7.

Zeng WQ, Al-Yamani E, Acierno JS Jr et al (2005) Biotin-responsive basal ganglia disease maps to 2q36.3 and is due to mutations in SLC19A3. *Am J Hum Genet* 77: 16–26.

Zhao R, Gao F, Goldman ID (2001) Molecular cloning of human thiamin pyrophosphokinase. *Biochim Biophys Acta* 1517(2):320-2.

Tables:

Table 1. Recommended dietary allowances (RDAs) of thiamine

Gender	Age / Condition	Thiamine RDA
Female/Male	0-6 months	0.2mg
Female/Male	7-12 months	0.3mg
Female/Male	1-3 years	0.5mg
Female/Male	4-8 years	0.6mg
Female/Male	9-13 years	0.9mg
Male	> 14 years	1.2mg
Female	14-18 years	1mg
Female	> 18 years	1.1mg
Female	Pregnancy	1.4mg
Female	Breast feeding	1.5mg

Table 2. Thiamine metabolism dysfunction syndromes nomenclature

Gene	Dysfunction syndrome	Disorder
SLC19A2	Thiamine metabolism dysfunction syndrome 1	Thiamine-responsive megaloblastic anemia syndrome
SLC19A3	Thiamine metabolism dysfunction syndrome 2	Biotin- or thiamine-responsive encephalopathy type
SLC25A19	Thiamine metabolism dysfunction syndrome 3	Microcephaly Amish type
	Thiamine metabolism dysfunction syndrome 4	Bilateral striatal degeneration and progressive polyneuropathy type
TPK1	Thiamine metabolism dysfunction syndrome 5	Episodic encephalopathy type

Table 3. Suggested Criteria for the Diagnosis of Inherited Thiamine Defects With Prominent Neurological Involvement (modified from Ortigoza-Escobar et al 2017)

Required
1. Clinical criteria
a. ***SLC19A3***: Acute or recurrent episodes of encephalopathy (decreased consciousness, irritability) with two or more of the following: (1) dystonia, (2) hypotonia, (3) bulbar dysfunction, (4) ataxia, and (5) seizures. Of note, 16% of patients may have an insidious onset of symptoms (psychomotor regression, clumsy or abnormal gait, and stiff limbs).
b. ***SLC25A19***: Acute or recurrent episodes of encephalopathy with: (1) progressive peripheral neuropathy or (2) severe congenital microcephaly with brain malformations.
c. ***TPK1***: Acute or recurrent episodes of encephalopathy, with two or more of the following: (1) dystonia, (2) hypotonia, (3) ataxia, (4) seizures, and (5) developmental delay. Of note, some patients may have a nonepisodic early-onset global developmental delay.
2. Biochemical criteria
a. Normal total thiamine blood levels
b. Low free-thiamine in CSF and/or fibroblasts (SLC19A3)
c. Low TPP in blood, muscle, and/or fibroblasts (TPK1)
d. High excretion of alpha-ketoglutaric acid in urine (common in TPK1 and SLC25A19, rare in SLC19A3).
3. Radiological criteria
a. MRI pattern compatible with Leigh's syndrome (SLC19A3, SLC25A19, TPK1) or Wernicke's encephalopathy (SLC19A3)
i. ***SLC19A3***: Symmetrical T2W hyperintensity of caudate, putamen, cortico/subcortical areas, and/or ventromedial thalamus. No involvement of mammillary bodies. Diffuse T2W hyperintensity of brain white matter (single adult patient reported).
ii. ***SLC25A19***: Symmetrical T2W hyperintensity in the caudate and putamen.
iii. ***TPK1***: Symmetrical T2W hyperintensity in basal ganglia and cerebellum (dentate nuclei).
4. Therapeutic criteria
a. Clinical improvement after thiamine supplementation.
Supportive
1. Consanguinity
2. Trigger event (infection, vaccination, trauma, intense physical activity, etc.).
3. Absence of predisposing factors of beriberi or Wernicke's encephalopathy.

4. Absence of systemic features of mitochondrial disease (cardiomyopathy, arrhythmia/conduction defects, renal tubulopathy, or dysmorphic features).
5. Increased lactate in blood and/or CSF, or presence of a lactate peak on MRS.
6. Normal OXPHOS and PDHc activity in muscle and fibroblast.

CSF = cerebrospinal fluid; TPP = thiamine pyrophosphate; MRI = magnetic resonance imaging; T2W = T2 weighted; OXPHOS = oxidative phosphorylation; PDHc = pyruvate dehydrogenase complex; MRS = magnetic resonance spectroscopy.

Figure Legends:

Figure 1: Thiamine transport and metabolism pathways. Three of the four thiamine vitamers are represented: free thiamine (T, blue balls), thiamine monophosphate (TMP, purple balls), thiamine pyrophosphate (TPP, green balls) and thiamine triphosphate (TTP, brown balls). Thiamine absorption takes place through passive diffusion, at high concentration, or through different carriers: SLC19A2 (thiamine transporter-1); SLC19A3 (thiamine transporter-2); SLC19A1 (folate carrier); SLC22A1 (OCT1, organic cation transporter 1); SLC35F3 (solute carrier) and SLC44A44 (human TPP carrier). In the cytosol, T is phosphorylated by TPK1 (thiamine pyrophosphokinase) into TPP. There, TPP enters the mitochondrial through SLC25A19 carrier. TPP, as the active thiamine species, acts as a cofactor in multiple enzyme reactions in cytosol: TK (transketolase); in the mitochondria: PDHc (pyruvate dehydrogenase complex), OGDHC (oxoglutarate dehydrogenase complex), BCQDC (branched chain 2-oxo acid dehydrogenasecomplex); and in peroxisome: HACL1 (2-hydroxyacyl-CoA lyase 1). G=glucose; G-6P=glucose-6-phosphate;

NADPH=nicotinamide adenine dinucleotide phosphate; TCA cycle=tricarboxylic acid cycle; ±-CG=alpha-ketoglutarate; GABA=gamma-aminobutiric acid.

Figure 2: *SLC19A2* structure including all described TRMA patients' variants. Homozygous variants in black, compound heterozygous variants in blue and variants reported both homozygous and compound heterozygous in green. Variants which have been studied functionally *in vitro* or computationally appear in bold. Variants represented with * are those variants only reported as a protein change for which the cDNA variant is currently unknown due to different nucleotide combination possibilities (in order from 5' to 3': p.Trp30*, p.Trp302* and p.Trp387*).

Figure 3: *SLC19A3* gene structure including all described patients' variants. Homozygous variants in black, compound heterozygous variants in blue and variants reported both homozygous and compound heterozygous in green. Variants which have been studied functionally *in vitro* appear in bold.

Figure 4: *SLC25A19* gene structure including all described patients' variants. Homozygous variants causing THMD4 in black and homozygous variant in orange cause a different phenotype (MCPHA). Variants which have been studied functionally *in vitro* appear in bold.

Figure 5: *TPK1* gene structure including all described patients' variants. Homozygous variants in black and compound heterozygous variants in blue. Variants which have been studied functionally *in vitro* appear in bold.

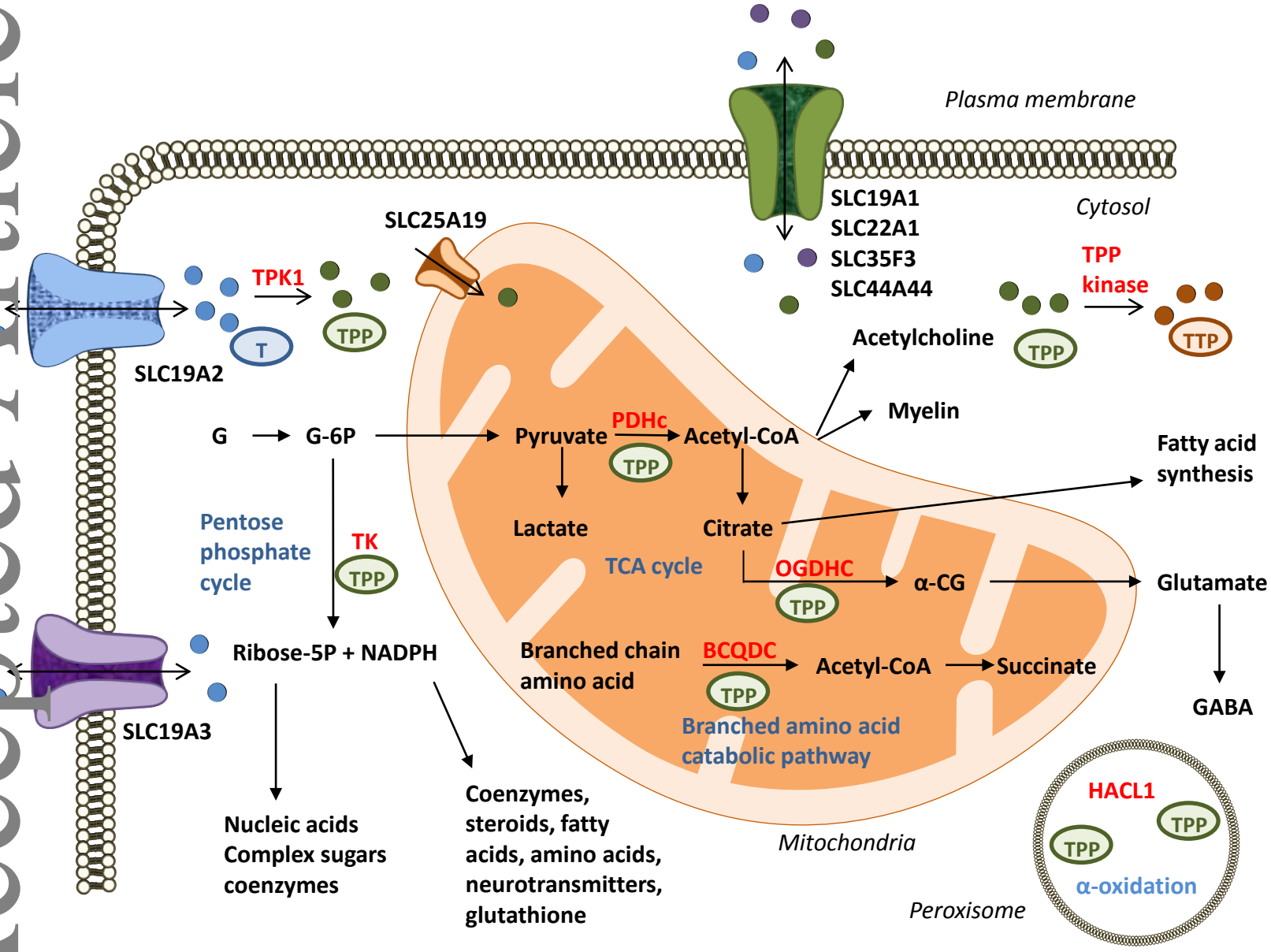

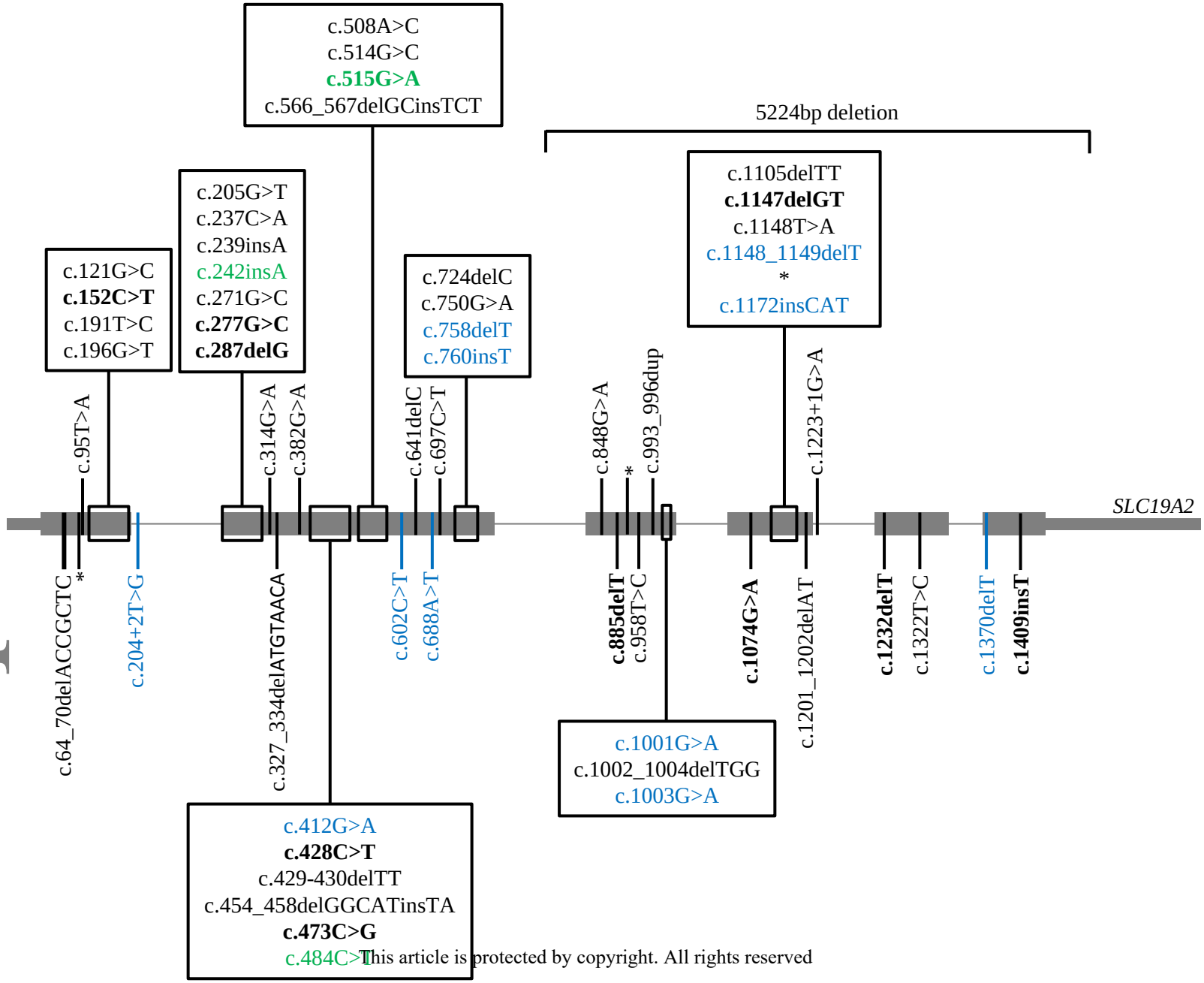

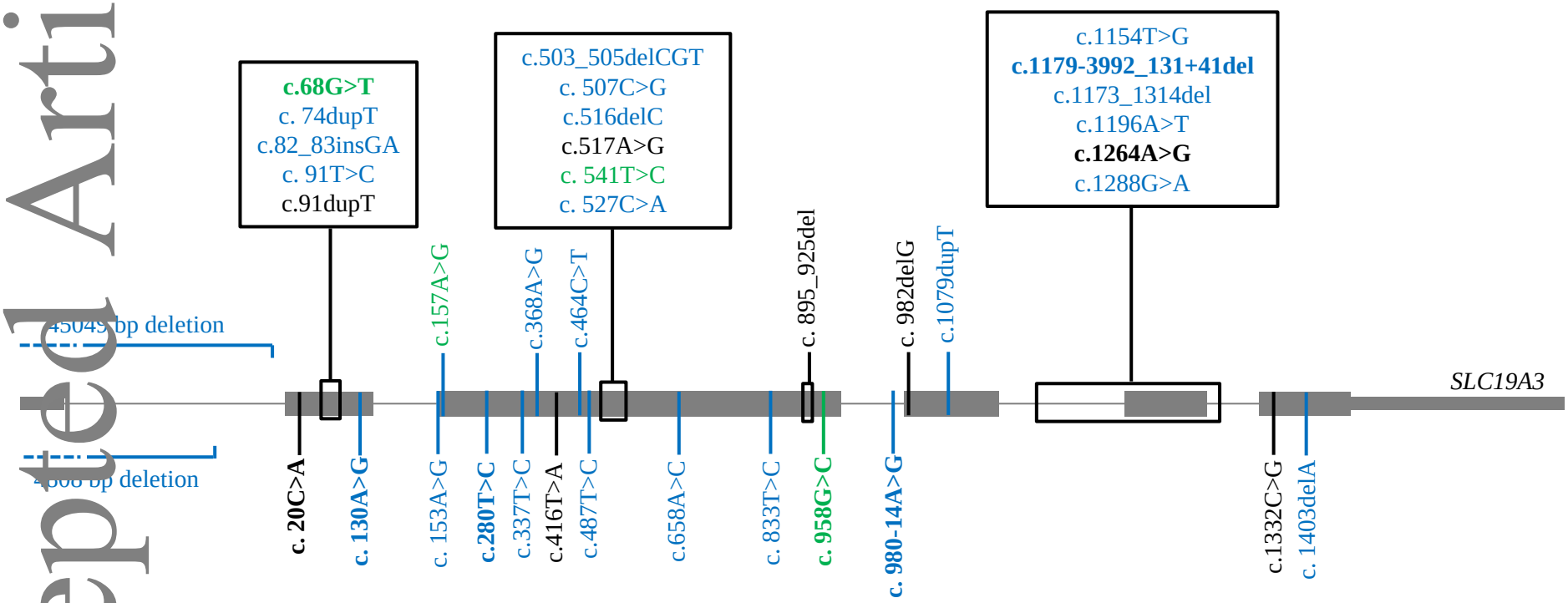

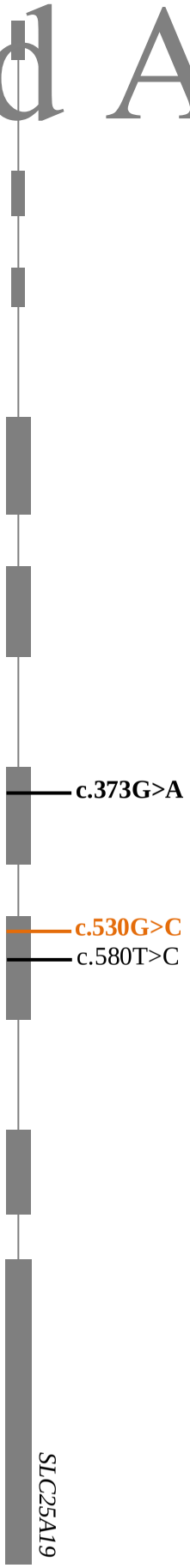

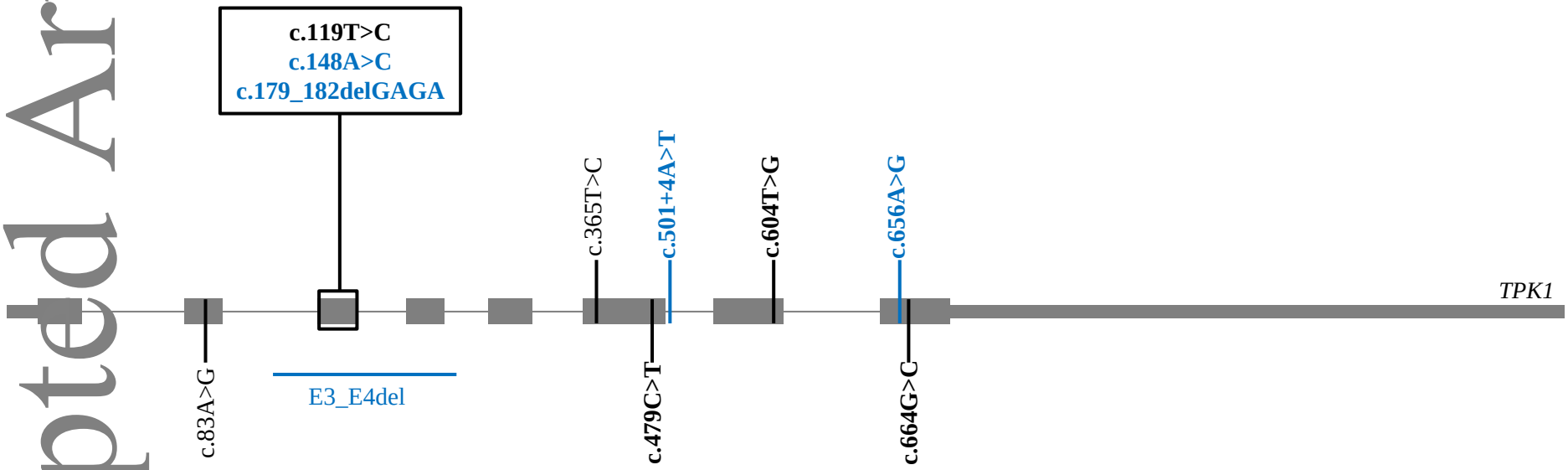

Publicación 3

Título:

Hypermanganesemia due to mutations in SLC39A14: further insights into Mn deposition in the central nervous system.

Autores:

L Marti-Sanchez, JD Ortigoza-Escobar, A. Darling, M. Villaronga, H Baide-Mairena, M Molero-Luis, M Batllori, MI Vanegas, J Muchart, L Aquino, R Artuch, A Macaya, MA Kurian , B Pérez-Dueñas

Referencia:

Marti-Sanchez L, Ortigoza-Escobar JD, Darling A, et al. Hypermanganesemia due to mutations in SLC39A14: further insights into Mn deposition in the central nervous system. *Orphanet J Rare Dis*. 2018;13(1):28. Published 2018 Jan 30. doi:10.1186/s13023-018-0758-x

Resumen:

Los genes *SLC39A14*, *SLC30A10* y *SLC39A8* están involucrados en la homeostasis del manganeso (Mn) en humanos. Los niveles de Mn en plasma y orina son herramientas útiles para el reconocimiento temprano de estos trastornos. En este estudio, hemos analizado varios biomarcadores de deposición de Mn en el sistema nervioso central en dos hermanos que se presentan con distonía aguda e hipermanganesemia debido a mutaciones en *SLC39A14*. Estos biomarcadores pueden ayudar a establecer un diagnóstico más rápido y preciso y a monitorizar la progresión de la enfermedad tras la administración de una terapia con agentes quelantes. Estos pacientes portaban el cambio c.311G> T (p.Ser104Ile) en homozigosis y presentaron a la edad de 10 meses una distonía aguda y regresión motora. Las concentraciones de Mn revelaron niveles elevados de Mn en plasma, orina y LCR en el caso índice en comparación con los pacientes control. Los valores de Mn fueron 3 veces mayores en LCR que en plasma. Por otro lado, se cuantificó el índice palidal del paciente mediante resonancia magnética cerebral encontrando valores significativamente más altos comparado con los controles. Estos valores aumentaron durante un período de 10 años, lo que sugiere la incesante acumulación palidal de Mn a nivel de sistema nervioso central. Tras la confirmación genética, un ensayo con el quelante de Mn $Na_2CaEDTA$ redujo los niveles plasmáticos de Mn, zinc y selenio. Sin

embargo, los padres informaron sobre un empeoramiento de la distonía cervical, irritabilidad y dificultades para dormir y se suspendió la terapia de quelación. Con este estudio se amplió las pocas descripciones de pacientes con mutaciones en *SLC39A14*. Reportamos por primera vez la elevación de Mn en el LCR de pacientes con mutaciones *SLC39A14*, lo que respalda la hipótesis de que el cerebro es un órgano importante de deposición de Mn en la enfermedad relacionada con este gen. El índice palidal es un método indirecto y no invasivo que se puede utilizar para evaluar la progresión de la enfermedad en las RMC de seguimiento. Finalmente, se propuso que los pacientes con defectos hereditarios del transporte de manganeso se traten inicialmente con dosis bajas de Na2CaEDTA seguido de una escalada gradual de la dosis, junto con una monitorización de los oligoelementos sanguíneos, para evitar efectos secundarios identificados en nuestro caso.

Marti-Sanchez et al. Orphanet Journal of Rare Diseases (2018) 13:28
DOI 10.1186/s13023-018-0758-x

Orphanet Journal of Rare Diseases

RESEARCH Open Access

Hypermanganesemia due to mutations in *SLC39A14*: further insights into Mn deposition in the central nervous system

L. Marti-Sanchez[1], J. D. Ortigoza-Escobar[2], A. Darling[2], M. Villaronga[3], H. Baide[2], M. Molero-Luis[1], M. Batllori[1], M. I. Vanegas[2], J. Muchart[4], L. Aquino[5], R. Artuch[1], A. Macaya[6], M. A. Kurian[7] and Pérez Dueñas[2,6*]

Abstract

Background: The *SLC39A14*, *SLC30A10* and *SLC39A8* are considered to be key genes involved in manganese (Mn) homeostasis in humans. Mn levels in plasma and urine are useful tools for early recognition of these disorders. We aimed to explore further biomarkers of Mn deposition in the central nervous system in two siblings presenting with acute dystonia and hypermanganesemia due to mutations in *SLC39A14*. These biomarkers may help clinicians to establish faster and accurate diagnosis and to monitor disease progression after chelation therapy is administered.

Results: A customized gene panel for movement disorders revealed a novel missense variant (c.311G > T; p.Ser104Ile) in *SLC39A14* gene in two siblings presenting at the age of 10 months with acute dystonia and motor regression. Mn concentrations were analyzed using inductively coupled mass spectrometry in plasma and cerebrospinal fluid, disclosing elevated Mn levels in the index case compared to control patients. Surprisingly, Mn values were 3-fold higher in CSF than in plasma. We quantified the pallidal index, defined as the ratio between the signal intensity in the globus pallidus and the subcortical frontal white matter in axial T1-weighted MRI, and found significantly higher values in the *SLC39A14* patient than in controls. These values increased over a period of 10 years, suggesting the relentless pallidal accumulation of Mn. Following genetic confirmation, a trial with the Mn chelator $Na_2CaEDTA$ led to a reduction in plasma Mn, zinc and selenium levels. However, parents reported worsening of cervical dystonia, irritability and sleep difficulties and chelation therapy was discontinued.

Conclusions: Our study expands the very few descriptions of patients with *SLC39A14* mutations. We report for the first time the elevation of Mn in CSF of *SLC39A14* mutated patients, supporting the hypothesis that brain is an important organ of Mn deposition in SLC39A14-related disease. The pallidal index is an indirect and non-invasive method that can be used to rate disease progression on follow-up MRIs. Finally, we propose that patients with inherited defects of manganese transport should be initially treated with low doses of $Na_2CaEDTA$ followed by gradual dose escalation, together with a close monitoring of blood trace elements in order to avoid side effects.

Keywords: Manganese homeostasis, *SLC39A14*; *SLC30A10*, Dystonia, Pallidum, Hypermanganesemia

Background

Manganese (Mn) is a trace metal with a key role as a co-factor of multiple enzymes, including hydrolases, lyases, glycosyltransferases, arginase, glutamine synthase and superoxide dismutase (SOD), in the synthesis of hormones and neurotransmitters [1] and during inflammatory events of the central nervous system [2].

Mn deposition in the brain can occur due to acquired causes (such as environmental exposure), as well as inherited defects in Mn transport and metabolism. Mn intoxication has been described in miners, welders, individuals working or living near ferro-alloy factories or in those drinking contaminated water, as well as in patients receiving total parenteral nutrition or those with acquired

* Correspondence: belen.perez@vhir.org
[2]Department of Child Neurology, Institut de Recerca - Hospital Sant Joan de Déu, University of Barcelona, Barcelona, Spain
[6]Pediatric Neurology Research Group, Vall d'Hebron Research Institute (VHIR), Universitat Autònoma de Barcelona, Passeig de la Vall d'Hebron, 119-129, 08035 Barcelona, Catalonia, Spain
Full list of author information is available at the end of the article

hepatocerebral degeneration [3]. Patients with severe Mn exposure may develop an extrapyramidal syndrome termed manganism, with rigidity, bradykinesia and dystonia [3]. Mn dyshomoeostasis may also result from inherited genetic defects in one of the transporters implicated in Mn homeostasis, namely *SLC39A8*, *SLC30A10* and *SLC39A14*. Recently, several in vitro and in vivo models have elucidated their role in the transport of Mn and other divalent metals [2, 4–10]. *SLC39A8* (MIM608732) encodes ZIP8, a Mn and Zn transporter that localizes to the hepatocyte canalicular membrane and reclaims Mn from bile [7]. Knock out ZIP8 mice showed markedly decreased Mn levels in multiple organs and whole blood, increased bile levels, and decreased activity of Mn-dependent enzymes, such as arginase and β-1, 4-galactosyltransferase [7]. Biallelic mutations in this gene lead to severe Mn depletion and a secondary congenital disorder of glycosylation (CDG) syndrome. Patients manifest developmental delay and intellectual disability, dwarfism, craniosynostosis, cerebellar atrophy, seizures and Leigh-like syndrome [11, 12].

SLC30A10 (also known as ZnT10) (MIM611146) and *SLC39A14* (also known as ZIP14) (MIM608736) are efflux and influx transporters, respectively, that cooperatively regulate Mn homeostasis in humans. Recently, Liu et al. 2017 generated knockout (KO) mice models lacking *SLC30A10*, *SLC39A14* and both transporters (double knockouts) demonstrating high blood and brain Mn levels in the three mice models, but only high liver Mn levels in the single *SLC30A10* KO model. These findings are in agreement with those observed in patients with recessive mutations in *SLC30A10* and *SLC39A14*, showing cerebral Mn deposition as a consequence of increased systemic Mn load in both disorders [13], but only polycythemia and liver cirrhosis in *SLC30A10* [14].

Animal models demonstrated that SLC30A10 and SLC39A14 localized to the canalicular and basolateral domains of hepatocytes, respectively, thereby mediating Mn biliary excretion synergistically [8]. Moreover, *SLC39A14* KO mice showed reduce Mn transport into enterocytes at the basolateral membrane, thereby decreasing Mn excretion via the gastrointestinal tract [4].

Patients with *SLC30A10* and *SLC39A14* defects show a progressive dystonia-parkinsonism syndrome as a consequence of Mn toxicity to the basal ganglia. Chelation therapy in both disorders increases Mn urinary excretion and decreases plasma Mn concentrations with variable clinical improvement [14–17]. *SLC39A14* KO mice suffer from Mn brain deposition and motor dysfunction, thus recapitulating the disease in humans [4, 10].

In this study, we present two siblings with homozygous *SLC39A14* mutations causing hypermanganesemia, progressive dystonia, severe disability and early death. Our study reports a likely novel pathogenic variant in *SLC39A14*, thereby expanding the reported mutations in this gene. We examine the levels of Mn and other trace elements in plasma and cerebrospinal fluid (CSF), as potential biomarkers for diagnosis and treatment monitoring. We also describe serial magnetic resonance imaging (MRI) abnormalities over time, confirming progressive changes with pallidal Mn deposition.

Methods

The index case was born to healthy consanguineous Senegalese parents. Detailed delineation of the patient's history, disease course and clinical examination was undertaken, as well as molecular genetics, radiological and biochemical studies. Family history revealed a similarly affected older brother for whom a stored DNA sample was available. Parental DNA was also obtained. The study was approved by the ethics committee at Sant Joan de Déu Hospital and parents gave written informed consent for study participation.

We also performed a literature review on genetic causes of Mn dysregulation, by searching MEDLINE (through PubMed) the following keywords: #1 *SLC30A10*, #2 *SLC39A14*, #3 *SLC39A8*, #4 hypermanganesemia and #5 manganese homeostasis. A total of 12 clinical studies were finally selected (Table 1) [11, 12, 15–25].

Biochemical studies

CSF and plasma samples were analyzed with an Agilent 7500ce inductively coupled plasma mass spectrometer (Agilent Technologies, Waldbronn, Germany). The instrument uses a collision/reaction cell with hydrogen for selenium (Se) determination, and helium for zinc (Zn) and Mn. Briefly, after ionization of plasma or CSF samples in the plasma torch and elimination of interference in the collision/reaction cells, element concentrations were determined by mass spectrometry, as previously reported [26, 27]. Hemolysed plasma samples were excluded to avoid blood contamination that can significantly increase Zn and Mn values.

Plasma samples preparation: 25 μL of plasma samples were diluted (1:40; V:V) in 25 μL of distilled water and 950 μL of a solution containing 0.7 mmol/L EDTA (Merck, Darmstadt, Germany), 0.07% Triton-X-100 (Merck), 2% butanol, 0.5% ammoniac (Merck) and germanium as internal standard (Merck).

CSF samples preparation: 50 μL of CSF samples were diluted (1:20; V: V) in a 2% nitric solution and 10 μg/L of germanium as internal standard (Merck).

MRI studies

The pallidal index (PI), defined as the ratio between the signal intensity in the globus pallidus (SIGP) and the subcortical frontal white matter (SIFW) in axial T1-weighted MRI [28] was calculated in our patient on MRIs undertaken at age 11 months, 8 and 10 years. Values were

Table 1 Characteristics of patients with *SLC30A10*, *SLC39A14*, and *SLC39A8* mutations

Phenotypes	*SLC30A10*	*SLC39A14*	*SLC39A8*
	Early-onset dystonia, polycythemia and hepatopathy, adult-onset parkinsonism and spastic paraparesis	Rapidly progressive childhood-onset parkinsonism-dystonia	Type II congenital disorder of glycosylation with Leigh syndrome and autosomal recessive intellectual disability with cerebellar atrophy
Number of patients reported	39	10	12
References	[16–24]	[15] current paper	[11, 12, 25]
First described in	2000	2016	2015
Age at onset, median (IQR)	7.1 (1–57 years)	15.8 (7–36 months)	Birth to 1 year of age
Sex	20F/19M	6F/4M	8F/4M
Death and cause	4 death (3 cirrhosis-related complications and 1 pneumonia)	4 death (2 respiratory infections and 2 unknown cause)	1 death (infection)
Parental Consanguinity (N)	34	10	10
Main neurological signs and symptoms	Focal and generalized dystonia, gait disturbances "cock-walk gait" and Parkinsonism	Generalized dystonia and Parkinsonism	Profound hypotonia
Other neurological signs and symptoms	Central hypotonia, behavioral changes, developmental delay, dysphagia, ataxia, spastic paraparesis and sensory motor axonal polyneuropathy	Spasticity, developmental delay, bulbar dysfunction	Dystonia, opisthotonus, severe intellectual disability, strabismus, nystagmus, hearing impairment, apnea/hypopnea episodes, axonal neuropathy, generalized and myoclonic seizures and infantile spasm
Abnormal head growth / skull deformity	Normal head circumference	Microcephaly ($N = 4$), macrocephaly ($N = 1$), Craniosynostosis (N = 1)	Normal head circumference, craniosynostosis in 1 patient
Blood Mn levels (nmol/L)	Increased 3345.7 ± 2575.3 (RV: <320)	Increased 2898 ± 2532(RV: <320)	Decreased 16.4 ± 5.8 (RV: 5.3–40.8)
Urinary Mn levels	Increased 11.3 ± 4.8 mcg/L (RV: 0.5–4)	Not reported (increased in our patient: 8.2 mcg/L; RV:0.4–0.9)	Increased 56.5 ± 73.2 nmol/L (RV: 1.3–9.1)
Systemic involvement and others biochemical abnormalities	Hepatopathy: Hepatomegaly in 14 patients, liver cirrhosis in 8 patients and increased transaminases in 41%: ALT: 107.1 ± 50.7 (RV <55) Polycythemia in 21% of patients: haematocrit 52.8 ± 6.4% (RV: 34–40)	Not reported	Dysmorphic features[a], dwarfism with short limbs and scoliosis Increased transaminases in 2 patient (AST: 441 UI/L (RV < 80), ALT: 102 and 113 UI/L (RV < 55)) and impaired blood coagulation 1 patient High blood lactate (8.7 mmol/L) and CSF lactate (4.2 mmol/L) in 1 patient (RV: <1.9) Abnormal glycosylation pattern in 7 patients
Brain MRI	T1 W hyperintensity Basal ganglia 38 Thalamus 20 Brainstem 13 Cerebellum 21 Pituitary gland 6	T1 W hyperintensity Basal ganglia 10 Pituitary gland 8 Cerebral white matter 10	T2 W hyperintensity Basal ganglia 2
	Brainstem atrophy 1	Diffuse cerebral and cerebellar atrophy 4	Diffuse cerebellar atrophy 10 Frontal lobes atrophy 1
Genetics findings	Missense 5 Stop gained 3 Deletion 11 Splicing 1	Missense 8 Stop gain 1 Deletion 1	Missense 14
	Homozygous 37 Heterozygous 0	Homozygous 10 Heterozygous 0	Homozygous 10 Heterozygous 2
Chelation therapy	Disodium calcium edetate, calcium ethylenediaminetetra-acetic acid, D-penicilamina and 2,3 mercaptosuccinic acid	Disodium calcium edetate	

Table 1 Characteristics of patients with *SLC30A10*, *SLC39A14*, and *SLC39A8* mutations *(Continued)*

Phenotypes	*SLC30A10*	*SLC39A14*	*SLC39A8*
	Early-onset dystonia, polycythemia and hepatopathy, adult-onset parkinsonism and spastic paraparesis	Rapidly progressive childhood-onset parkinsonism-dystonia	Type II congenital disorder of glycosylation with Leigh syndrome and autosomal recessive intellectual disability with cerebellar atrophy
Other Treatments	Iron oral supplementation 19 Zinc, vitamins C and D supplementation, manganese free-diet, L-dopa, pramiprexole and intratechal baclofen		Galactose, manganese, CoQ10, thiamine, pyridoxine and glucocorticoid

F Female, *M* Male, *Mn* Manganese, *IQR* Interquartile range, *RV* Reference values
[a]Dysmorphic features include a broad forehead, mid-face hypoplasia, small jaw, hirsutism, anteverted nostrils, thin lips and a smooth philtrum

compared to nine age-matched control patients. The MRIs in control patients were obtained as part of a diagnostic protocol for patients with chronic headache, and were classified as normal by expert neuroradiologists.

Genetic analysis

A customized gene panel for movement disorders was design by Sure Design Tool (Agilent Technologies, Santa Clara, CA, USA). This panel included 78 genes causing basal ganglia disease which were classified in four groups: Aicardi-Goutières syndrome, thiamine metabolism, mitochondrial disorders and other neurometabolic disorders, including *SLC30A10* and *SLC39A14* related to Mn dysregulation. Library construction was performed according to manufacturer's protocol using HaloPlex technology. Sequencing was carried out on MiSeq sequencer (Illumina, San Diego, CA, USA). Data processing, variant calling and variant annotation were done by DNAnexus platform and Variant Studio software. The average of mean-coverage in the sample gene panel was 95% for a read depth of 20X. Filtering was performed by minor allele frequency < 1% and possible pathogenicity based on mutation effects (frameshift, insertions deletions, missense, stop gain and splice site regions). Variant validation and segregation studies were done by PCR with Sanger sequencing using the Big Dye Terminator Cycle Sequencing System (Applied Biosystems). Primers for validation of the identified change in *SLC39A14* were forward primer 5'-GAAGGCTGAGTAGGTTGCTG- 3′ and reverse primer 5'-CTCCT CGTTTTCCTGGTTCT-3′.

Results

Clinical presentation

The proband was born from consanguineous healthy Senegalese parents, after an uneventful pregnancy and delivery. He had a normal perinatal period and early neurodevelopmental milestones were on average. At 11 months he developed acute generalized dystonia and neurological regression following an intercurrent viral respiratory infection. On neurological examination there was evidence of skull deformity with normal head circumference, dystonic tetraparesis, oromandibular dystonia and opisthotonos. A plain skull radiogram revealed multiple-suture craniosynostosis. Metabolic investigations in blood, CSF and urine were normal at that moment, except for a mild decrease in 5-hydroxyindolacetic acid concentrations (104 nmol/L, reference values (RV): 170–490). The family moved to Senegal and they returned to our hospital at the age of 9 years. At this time, the patient had developed microcephaly (head circumference 51 cm, 6th percentile), severe dystonic tetraparesis, anarthria, dysphagia and malnutrition. He required enteral tube feeding and received baclofen, diazepam and gabapentin for symptomatic control of dystonia.

On reviewing the family history, it became apparent that there was a similarly affected older brother, born in 1997, who developed acute dystonic tetraparesis associated with rigidity, hypokinesia and pyramidal signs, following a viral illness at the age of 10 months. Brain MRI revealed bilateral pallidal T2-hypointensity and pallidal and cerebral and cerebellar white matter T1-hyperintensity. His clinical status remained unchanged until age 21 months, when he died in Senegal of unknown cause.

The clinical picture of these siblings was analyzed in the context of the existing literature on 46 patients previously identified with genetic defects leading to Mn dysregulation (Table 1).

Biochemical studies

Biochemical studies in the proband detected normal full blood count, liver function, Fe metabolism, Zn, Se and copper (Cu) concentrations in plasma. We also found elevated plasma Mn (10.5 μg/L, RV: 0.4–0.9 μg/L) and extremely elevated CSF Mn concentrations (34 μg/L, RV: 0.5–1.7 μg/L).

MRI analysis

Brain MRI of the patient at 11 months showed a symmetrical high-T1 and low T2 signal in both the pallidum and dentate nuclei. White matter signal intensity of the cerebrum, cerebellum and brainstem was also very high in T1 (Fig. 1a). Follow-up MRI at 10 years showed persistent T1-hyperintensity of the globi pallidi, volume loss, gliosis and atrophy of the dentate nuclei and moderate atrophy

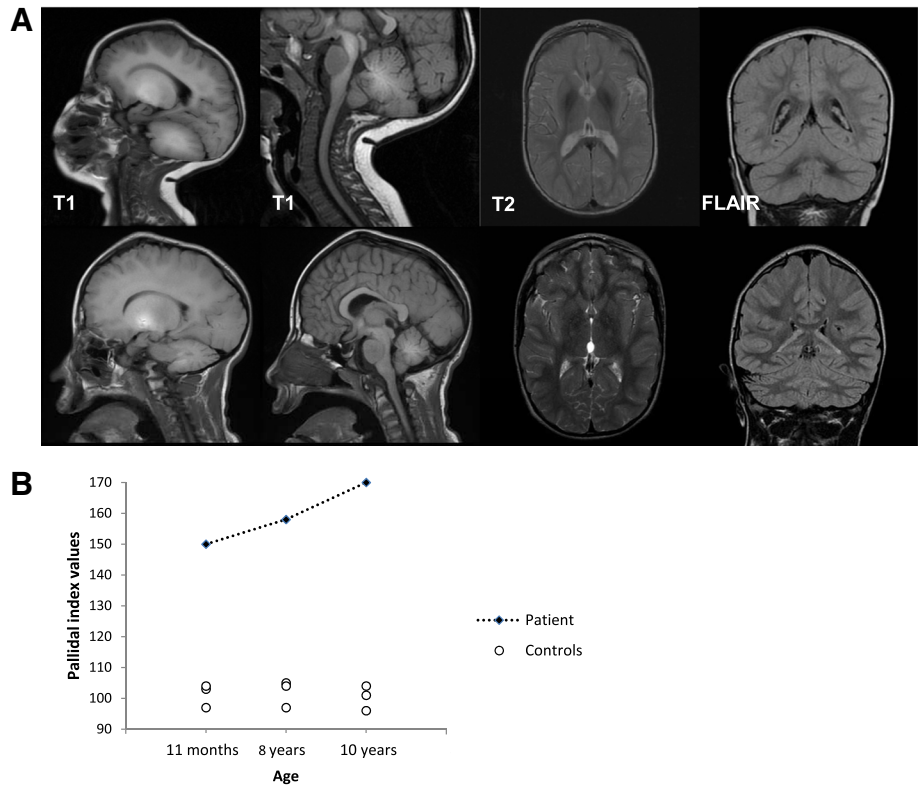

Fig. 1 Radiological findings from the patient. **a**: Brain MRI of the patient at 11 months (first line) shows a high-T1 and low T2 signal in the pallidi and dentate nuclei. MRI at 10 years (second line) shows persistent T1-hyperintensity of the globi pallidi, volume loss, gliosis and atrophy of the dentate nuclei and moderate atrophy of cerebellar folia. **b**: Distribution of individual PI scores in patient and controls

of cerebellar folia. Moreover, quantitative assessments of the PI was significantly higher in the patient at age 11 months, 8 and 10 years as compared to nine age-matched controls (U = 0.000; $p = 0.009$, Mann-Whitney U test). We also observed slightly increased signal intensity over time (Fig. 1b).

Genetic analysis

We identified a homozygous missense variant (c.311G > T; p.Ser104Ile) in exon 3 of *SLC39A14* (NM_001128431), which was confirmed by Sanger sequencing in both the patient and his affected brother. Both parents were heterozygous carriers of this variant (Fig. 2). Unfortunately, DNA samples from three unaffected siblings were not available for the analysis. This novel variant was not found in HGMD, dbSNP, 1000 Genome project, ExAC database or CIBERER Spanish Variant Server. This variant affected a highly conserved amino acid residue, located in the N-terminus extracellular loop, studied by UCSC browser and Clustal Omega software and it was categorized as pathogenic by SIFT (0.002), PROVEAN (−3.03) and Mutation Taster (142), and as possibly damaging by PolyPhen-2 (0.664).

Treatment

Following genetic confirmation, we instigated compassionate treatment with the Mn chelator, $Na_2CaEDTA$, 1 g/m2/day in two divided oral doses for a five-day course. This protocol was initially proposed for lead intoxication and has more recently been used in patients with *SLC30A10* and *SLC39A14* deficiency [14, 15]. No clinical side effects were recorded during the administration. On the fifth day, we observed a reduction of plasma Mn (from 10.5 to 4.5 μg/L, 57% reduction, RV: 0.4–0.9 μg/L), Zn (from 1260 to 381 ng/L, 69.8% reduction, RV: 628–1200 ng/L) and Se (from 84 to 58 ng/L, 31.5% reduction, RV: 67–104 ng/L) (Fig. 3), and therefore he was supplemented with Zn acetate (10 mg/day) and Se (50 mg every 2 days). There was also a mild decrease in plasma Cu and Fe but values remained within the normal range. Two weeks after treatment, the family referred worsening of cervical dystonia, irritability and sleep difficulties, which improved with incremental doses of diazepam. The family decided to discontinue chelation therapy. Neurological examination 3 weeks later was comparable to baseline.

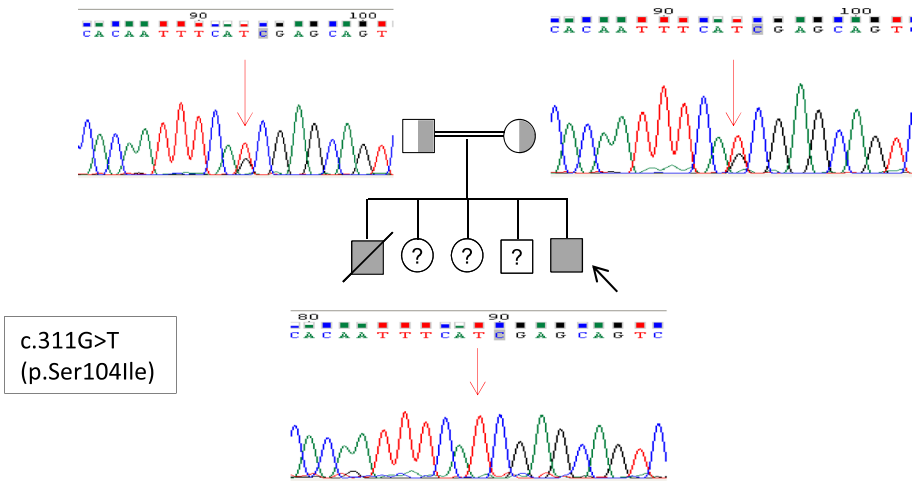

Fig. 2 The figure shows segregation of the novel variant by Sanger sequencing in the index case and family members. Footnote: The proband is marked with an arrow. The consanguinity is represented by a double line. Filled and unfilled symbols indicate affected and unaffected individuals, respectively. The parents are represented as a carrier status

Discussion

We present two siblings with a homozygous missense variant in *SLC39A14*, manifesting a rapidly progressive generalized dystonia in infancy and hypermanganesemia, similar to a cohort of eight *SLC39A14* mutated children reported [15]. Our patient did not show polycythemia or liver disease, as observed in SLC30A10-deficient patients (Table 1). We measured plasma and CSF Mn, both showing very high values comparing to our control patients and literature reference ranges [29]. Importantly, Mn values were 3-fold higher in CSF than in plasma; in keeping with the finding that brain Mn levels are four to 20-fold higher in *slc39a14* mutant zebra fish [15] and knockout mice [4, 6] compared to wild-type. Our findings support the hypothesis that brain is likely to be the main organ of Mn deposition in SLC39A14 deficiency.

Previously, Chang et al., 2009 reported a correlation between pallidal index (PI) and plasma Mn concentrations of 43 manganese-exposed welders and concluded that high PI might be attributed to Mn brain deposition [30]. We used PI to quantify pallidal Mn accumulation in our patient, and observed significantly higher values than in controls. Furthermore, our patient had higher PI values compared to occupationally Mn exposed workers [31]. These values slightly increased over time, suggesting the relentless pallidal accumulation of Mn in SLC39A14 deficiency.

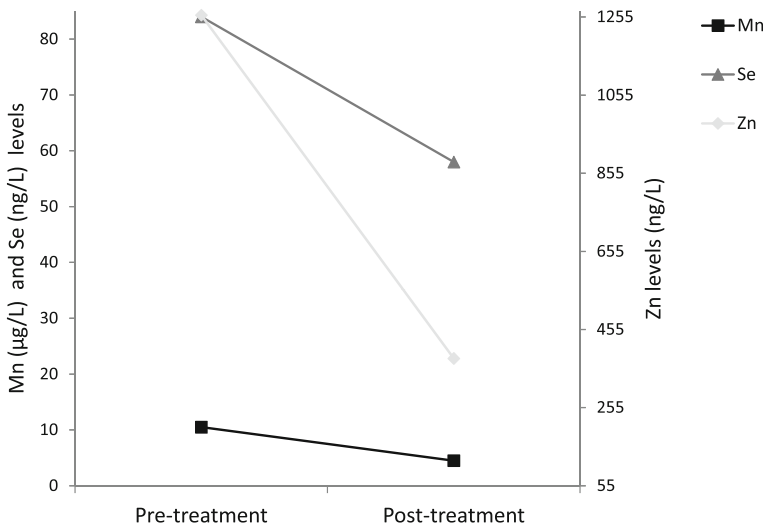

Fig. 3 Biochemical analysis before and after treatment. Footnote: Graph shows a reduction of plasma Mn, Zn and Se five days after $Na_2CaEDTA$ therapy

$Na_2CaEDTA$ is a chelating agent that combines with metal ions to form stable and soluble complexes that are excreted in the urine. It ameliorated dystonia and parkinsonism in *SLC30A10* mutated patients [18, 22], and its efficacy proved to be persistent over time is some cases with long-term follow-up [22, 32]. More recently, two *SLC39A14* patients received $Na_2CaEDTA$, one, given chelation early in the disease course showed clinical improvement, whereas the other (older) patient continued to deteriorate despite treatment [15]. Interestingly, two *SLC39A14* KO mice models recently demonstrated a positive effect with two different chelators: a zinc-supplemented diet significantly decreased brain Mn uptake [4], and the metal chelator Na2CaEDTA reduced serum Mn levels and rescued motor deficits [10].

The administration of $Na_2CaEDTA$ in our patient led to the reduction of not only plasma Mn values, but also Se and Zn, which are cofactors of important enzymes such as SOD and selenoproteins, and hence, they were supplemented in our patient. Even though Se is not a cation, the decrease might be an effect of EDTA on renal tubules during chelation therapy [33]. Unfortunately, worsening of dystonia resulted in discontinuation of $Na_2CaEDTA$ and the long-term efficacy of this treatment could not be tested in this patient.

Conclusions

In this study we present two infants presenting with dystonia and hypermanganesemia caused by a homozygous missense variant in *SLC39A14*, a recently recognized gene involved in Mn homeostasis in humans, thus expanding the very few descriptions of this disorder. We also report for the first time the elevation of Mn in CSF of *SLC39A14* mutated patients, supporting the hypothesis that brain is an important organ of Mn deposition in SLC39A14-related disease. The measurement of PI values on MRI is a non-invasive method that may help monitor Mn pallidal deposition over time. Finally, we propose that patients with inherited defects of manganese transport should be initially treated with low doses of $Na_2CaEDTA$ followed by gradual dose escalation, together with a close monitoring of blood trace elements in order to avoid side effects.

Abbreviations

CDG: Congenital disorder of glycosylation; CSF: Cerebrospinal fluid; Cu: Copper; Mn: Manganese; MRI: Magnetic resonance imaging; PI: Pallidal index; RV: Reference values; Se: Selenium; SIFW: Subcortical frontal white matter; SIGP: Signal intensity in the globus pallidus; SOD: Superoxide dismutase; Zn: Zinc

Acknowledgements

Not applicable.

Fundings

This work is funded by the Plan Nacional de I + D + I and Instituto de Salud Carlos III- Subdirección General de Evaluación y Fomento de la Investigación Sanitaria, project PI15/00287, the European Regional Development Fund (FEDER) and the Fundació La Marató TV3 (20,143,130 to BPD). LMS has a grant from Fundació Sant Joan de Déu. JD Ortigoza-Escobar has a grant from Rio Hortega, Instituto de Salud Carlos III (CM16/00084). MAK holds a Wellcome Intermediate Clinical Fellowship.

Available of data and materials

The biochemical, radiological and genetic data analysed during the current study are available from the corresponding author on reasonable request.

Authors' contributions

LMS participated in the study design, acquisition, analysis and interpretation of data, and drafting of the manuscript. LMS, MML, MB and RA participated in the analysis and interpretation of biochemical and molecular genetic studies. JDOE, MIV, HB, AD, LA, JM and AM performed the analysis and interpretation of clinical and radiological studies. MAK, JDOE, RA and AM participated in the analysis and interpretation of data, and in the drafting and revision of the manuscript. BPD conceived the idea for the study, designed study, supervised study, interpreted data, drafted and revised manuscript content. All authors read and approved the final manuscript.

Ethics approval and consent to participate

The study was approved by the ethics committee at Sant Joan de Déu Hospital (PIC-158-15) and parents gave written informed consent for study participation.

Consent for publication

Written informed consent was obtained from the patient's parents for publication of this case report and any accompanying images. A copy of the written consent is available for review by the Editor-in-Chief of this journal.

Competing interests

Authors disclose no financial or personal relationships with other people or organisations that could inappropriately influence the present work.

Publisher's Note

Author details

[1]Department of Biochemistry, Institut de Recerca - Hospital Sant Joan de Déu, University of Barcelona, Barcelona, Spain. [2]Department of Child Neurology, Institut de Recerca - Hospital Sant Joan de Déu, University of Barcelona, Barcelona, Spain. [3]Department of Pharmacy, Institut de Recerca - Hospital Sant Joan de Déu, University of Barcelona, Barcelona, Spain. [4]Department of Radiology, Institut de Recerca - Hospital Sant Joan de Déu, University of Barcelona, Barcelona, Spain. [5]Deparment of Pediatrics, Hospital de Mataró, Barcelona, Spain. [6]Pediatric Neurology Research Group, Vall d'Hebron Research Institute (VHIR), Universitat Autònoma de Barcelona, Passeig de la Vall d'Hebron, 119-129, 08035 Barcelona, Catalonia, Spain. [7]Molecular Neurosciences, Developmental Neurosciences Programme, UCL-Great Ormond Street Institute of Child Health, London, UK.

Received: 22 March 2017 Accepted: 3 January 2018
Published online: 30 January 2018

References

1. Santos D, Batoreu MC, Almeida I, Ramos R, Sidoryk-Wegrzynowicz M, Aschner M, et al. Manganese alters rat brain amino acids levels. Biol Trace Elem Res. 2012;150(1–3):337–41.
2. Fujishiro H, Yoshida M, Nakano Y, Himeno S. Interleukin-6 enhances manganese accumulation in SH-SY5Y cells: implications of the up-regulation of ZIP14 and the down-regulation of ZnT10. Metallomics. 2014;6(4):944–9.
3. Chen P, Parmalee N, Aschner M. Genetic factors and manganese-induced neurotoxicity. Front Genet. 2014;5:265.
4. Aydemir TB, Kim MH, Kim J, Colon-Perez LM, Banan G, Mareci TH, et al. Metal transporter Zip14 (Slc39a14) deletion in mice increases manganese deposition and produces Neurotoxic signatures and diminished motor activity. J Neurosci. 2017;37(25):5996–6006.
5. Girijashanker K, He L, Soleimani M, Reed JM, Li H, Liu Z, et al. Slc39a14 gene encodes ZIP14, a metal/bicarbonate symporter: similarities to the ZIP8 transporter. Mol Pharmacol. 2008;73(5):1413–23.

6. Hutchens S, Liu C, Jursa T, Shawlot W, Chaffee BK, Yin W, et al. Deficiency in the manganese efflux transporter SLC30A10 induces severe hypothyroidism in mice. J Biol Chem. 2017;292(23):9760–73.
7. Lin W, Vann DR, Doulias PT, Wang T, Landesberg G, Li X, et al. Hepatic metal ion transporter ZIP8 regulates manganese homeostasis and manganese-dependent enzyme activity. J Clin Invest. 2017;127(6):2407–17.
8. Liu C, Hutchens S, Jursa T, Shawlot W, Polishchuk EV, Polishchuk RS, et al. Hypothyroidism induced by loss of the manganese efflux transporter SLC30A10 may be explained by reduced thyroxine production. J Biol Chem in press https://doi.org/10.1074/jbc.M117.804989.
9. Pinilla-Tenas JJ, Sparkman BK, Shawki A, Illing AC, Mitchell CJ, Zhao N, et al. Zip14 is a complex broad-scope metal-ion transporter whose functional properties support roles in the cellular uptake of zinc and nontransferrin-bound iron. Am J Physiol Cell Physiol. 2011;301(4):C862–71.
10. Xin Y, Gao H, Wang J, Qiang Y, Imam MU, Li Y, et al. Manganese transporter Slc39a14 deficiency revealed its key role in maintaining manganese homeostasis in mice. Cell Discov. 2017;3:17025.
11. Riley LG, Cowley MJ, Gayevskiy V, Roscioli T, Thorburn DR, Prelog K, et al. A SLC39A8 variant causes manganese deficiency, and glycosylation and mitochondrial disorders. J Inherit Metab Dis. 2017;40(2):261–9.
12. Park JH, Hogrebe M, Grüneberg M, DuChesne I, von der Heiden AL, Reunert J, et al. SLC39A8 deficiency: a disorder of manganese transport and Glycosylation. Am J Hum Genet. 2015;97(6):894–903.
13. Aschner M, Erikson KM, Herrero Hernández E, Tjalkens R. Manganese and its role in Parkinson's disease: from transport to neuropathology. NeuroMolecular Med. 2009;11(4):252–66.
14. Tuschl K, Mills PB, Parsons H, Malone M, Fowler D, Bitner-Glindzicz M, et al. Hepatic cirrhosis, dystonia, polycythaemia and hypermanganesaemia - a new metabolic disorder. J Inherit Metab Dis. 2008;31(2):151–63.
15. Tuschl K, Meyer E, Valdivia LE, Zhao N, Dadswell C, Abdul-Sada A, et al. Mutations in SLC39A14 disrupt manganese homeostasis and cause childhood-onset parkinsonism-dystonia. Nat Commun. 2016;7:11601.
16. Tuschl K, Clayton PT, Gospe SM Jr, Gulab S, Ibrahim S, Singhi P, et al. Syndrome of hepatic cirrhosis, dystonia, polycythemia, and hypermanganesemia caused by mutations in SLC30A10, a manganese transporter in man. Am J Hum Genet. 2012;90(3):457–66.
17. Zaki MS, Issa MY, Elbendary HM, El-Karaksy H, Hosny H, Ghobrial C, et al. Hypermanganesemia with dystonia, polycythemia and cirrhosis in 10 patients: six novel SLC30A10 mutations and further phenotype delineation. Clin Genet. 2017; https://doi.org/10.1111/cge.13184.
18. Quadri M, Federico A, Zhao T, Breedveld GJ, Battisti C, Delnooz C, et al. Mutations in SLC30A10 cause parkinsonism and dystonia with hypermanganesemia, polycythemia, and chronic liver disease. Am J Hum Genet. 2012;90(3):467–77.
19. Quadri M, Kamate M, Sharma S, Olgiati S, Graafland J, Breedveld GJ, et al. Manganese transport disorder: novel SLC30A10 mutations and early phenotypes. Mov Disord. 2015;30(7):996–1001.
20. Gospe SM Jr, Caruso RD, Clegg MS, Keen CL, Pimstone NR, Ducore JM, et al. Paraparesis, hypermanganesaemia, and polycythaemia: a novel presentation of cirrhosis. Arch Dis Child. 2000;83(5):439–42.
21. Brna P, Gordon K, Dooley JM, Price V. Manganese toxicity in a child with iron deficiency and polycythemia. J Child Neurol. 2011;26(7):891–4.
22. Stamelou M, Tuschl K, Chong WK, Burroughs AK, Mills PB, Bhatia KP, et al. Dystonia with brain manganese accumulation resulting from SLC30A10 mutations: a new treatable disorder. Mov Disord. 2012;27(10):1317–22.
23. Lechpammer M, Clegg MS, Muzar Z, Huebner PA, Jin LW, Gospe SM Jr. Pathology of inherited manganese transporter deficiency. Ann Neurol. 2014;75(4):608–12.
24. Mukhtiar K, Ibrahim S, Tuschl K, Mills P. Hypermanganesemia with Dystonia, Polycythemia and cirrhosis (HMDPC) due to mutation in the SLC30A10 gene. Brain and Development. 2016;38(9):862–5.
25. Boycott KM, Beaulieu CL, Kernohan KD, Gebril OH, Mhanni A, Chudley AE, et al. Autosomal-recessive intellectual disability with Cerebellar atrophy syndrome caused by mutation of the manganese and zinc transporter gene SLC39A8. Am J Hum Genet. 2015;97(6):886–93.
26. Heitland P, Köster HD. Biomonitoring of 37 trace elements in blood samples from inhabitants of northern Germany by ICP-MS. J Trace Elem Med Biol. 2006;20(4):253–62.
27. Wahlen R, Evans L, Turner J, Hearn R. The use of collision/reaction cell ICP-MS for the simultaneous determination of 18 elements in blood and serum samples. Santa Clara: Agilent Technologies. 2005. http://www.agilent.com/chem. Accesed 28 Ago 2009.
28. Krieger D, Krieger S, Jansen O, Gass P, Theilmann L, Lichtnecker H. Manganese and chronic hepatic encephalopathy. Lancet. 1995;346(8970):270–4.
29. Harrington JM, Young DJ, Essader AS, Sumner SJ, Levine KE. Analysis of human serum and whole blood for mineral content by ICP-MS and ICP-OES: development of a mineralomics method. Biol Trace Elem Res. 2014;160(1):132–42.
30. Chang Y, Kim Y, Woo ST, Song HJ, Kim SH, Lee H, et al. High signal intensity on magnetic resonance imaging is a better predictor of neurobehavioral performances than blood manganese in asymptomatic welders. Neurotoxicology. 2009;30(4):555–63.
31. Li SJ, Jiang L, Fu X, Huang S, Huang YN, Li XR, et al. Pallidal index as biomarker of manganese brain accumulation and associated with manganese levels in blood: a meta-analysis. PLoS One. 2014;9(4):1–7.
32. Di Toro Mammarella L, Mignarri A, Battisti C, Monti L, Bonifati V, Rasi F, et al. Two-year follow-up after chelating therapy in a patient with adult-onset parkinsonism and hypermanganesaemia due to SLC30A10 mutations. Neurol. 2014;261(1):227–8.
33. Elmer M. Cranton MD. A Textbook on EDTA Chelation Therapy. 2nd ed. Hampton Roads Publishing Company, Inc. 2001.

DISCUSIÓN

Esta tesis es el resultado de un proyecto traslacional ligado al ámbito clínico cuya prioridad es el diagnóstico genético de los pacientes con alteraciones en los ganglios basales con el fin de personalizar el tratamiento y obtener una mejora clínica, radiológica y bioquímica. Por ello, el objetivo general de la tesis es el diagnóstico molecular de estos pacientes y la búsqueda de biomarcadores específicos.

Para el estudio genético de los pacientes de esta cohorte, se han utilizado distintas tecnologías. En lo referente a paneles de genes, mediante el panel HaloPlex se ha obtenido un porcentaje de diagnóstico (39%, 7/18) elevado respecto a estudios previos reportados, como un estudio de epilepsia que utiliza la misma tecnología en 87 pacientes obteniendo una tasa diagnóstica del 19.5% (17 pacientes)[133]. Estos estudios son comparables ya que ambas enfermedades son desórdenes clínica y genéticamente heterogéneos de inicio precoz. A pesar de las limitaciones de la tecnología de este panel, en concreto en este proyecto nos permitió diagnosticar obtener un porcentaje diagnóstico mayor de lo esperado, teniendo en cuenta la heterogeneidad de la enfermedad y el bajo número de genes incluidos en el panel (76 genes). Esto puede ser debido a una buena selección fenotípica de los pacientes. El cambio a tecnología SureSelect, a pesar de ser la tecnología mejor valorada principalmente por su uniformidad de captura en estudios previos[112], no conllevó un incremento en la tasa diagnóstica (33%, 3/9). Este porcentaje es similar a estudios reportados anteriormente[134]. Esto puede ser debido a la limitación de los paneles en cuanto a número de genes nucleares y la falta de genes mitocondriales. A posteriori se incorporó a la estrategia de diagnóstico la secuenciación completa del ADN mitocondrial en los pacientes con patologías en ganglios basales donde cuatro de los nueve (44%) pacientes estudiados con este panel portaban cambios patológicos mitocondriales.

La tasa de diagnóstico obtenida mediante WES (45.2%) es comparable a la reportada en la literatura[20,113], pero no es tan elevada como se esperaba. Esto puede ser debido a que parte de los pacientes estudiados por WES (26%, 8/31) habían tenido un resultado negativo previo por los paneles. La secuenciación mediante WES trío (paciente y progenitores) facilita el análisis gracias a la posibilidad de añadir datos de segregación familiar que contribuyen a filtrar según la posible herencia. En este proyecto 12 de los pacientes estudiados por WES fueron trío, pero, a pesar de facilitar el filtrado y rebajar mucho el coste de las validaciones de variantes candidatas, en este proyecto no ha resultado en una tasa diagnóstica mayor. Aproximadamente, la mitad de los pacientes estudiados por las estrategias de NGS quedan sin diagnóstico genético específico[135]. En

nuestro caso, esto puede ser debido a la falta de medios para estudiar variantes candidatas en nuevos genes no asociados previamente a enfermedad y a la limitación del WES para analizar variantes intrónicas profundas, en zonas reguladoras o variantes estructurales CNV[113]. Hasta 2016 se había reportado un total de 185 mutaciones intrónicas localizadas como mínimo a 100 pares de bases del sitio de *splicing* más cercano, en 77 genes distintos causantes de patología, que conducen a un pseudo-exón debido a la activación/inactivación de sitios de *splicing* no canónicos o cambios en los elementos reguladores de *splicing*[117].

En el análisis de ADN mitocondrial, el porcentaje de éxito obtenido en este proyecto (28.6%) concuerda con estudios previos de pacientes con síndrome de Leigh donde el 29% de los pacientes portaban mutaciones en el ADN mitocondrial[20].

En nuestra cohorte, después de las subunidades estructurales o de ensamblaje de la cadena respiratoria mitocondrial, dos genes (*ECHS1* y *HIBCH*) que codifican para enzimas encargadas del catabolismo de la valina constituyeron por sí solas el segundo grupo más representativo de esta serie de pacientes con síndrome de Leigh (Figura 4). En un estudio publicado recientemente en 106 pacientes con síndrome de Leigh, los genes más representativos fueron *SURF1* (5 pacientes), *NDUFAF6* (5 pacientes) y *ECHS1* (4 pacientes)[20]. A pesar de no coincidir con nuestros datos, en su cohorte también hay una gran representación de genes que codifican factores de ensamblaje de complejos de la cadena respiratoria mitocondrial. Cabe destacar, tanto en nuestra cohorte como en publicadas anteriormente[20], la alta representación de los genes implicados en el catabolismo de la valina.

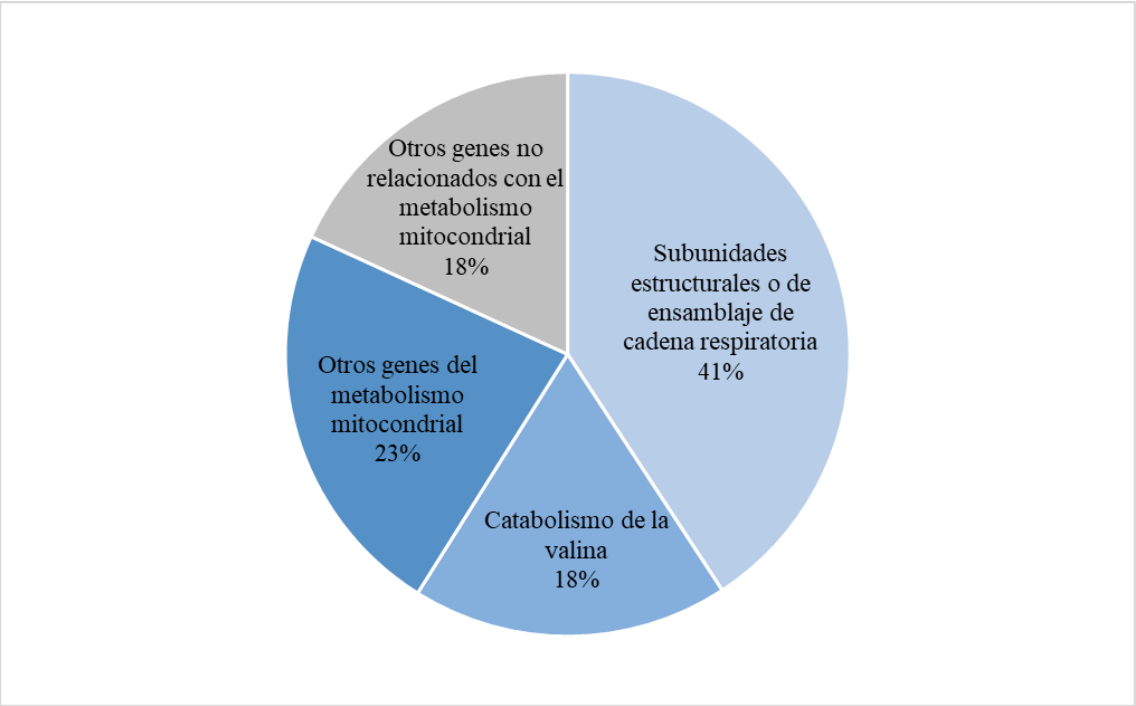

Figura 4: Porcentaje de genes de los 38 pacientes de nuestra serie con síndrome de Leigh clasificados según su función.

Este proyecto de tesis ha permitido reportar 19 nuevos pacientes con defectos en el catabolismo de la valina. Con este estudio se ha podido definir unos criterios clínicos, radiológicos y bioquímicos de estas patologías a fin de tener en cuenta estos dos genes en el diagnóstico de pacientes con síndrome de Leigh, debido a su prevalencia. En estos defectos destaca una gran heterogeneidad genética. En el caso del gen *HIBCH*, la variante c.913A>G se encuentra representada con una frecuencia alélica del 23% mientras que el resto de mutaciones están entre 2-9%, por lo que podemos considerarla una mutación prevalente en este gen. Por otro lado, en el gen *ECHS1* el 72% de las mutaciones reportadas están presentes únicamente en uno o dos alelos.

En este proyecto se ha estudiado en profundidad sobre el metabolismo de la tiamina, solo encontrando una paciente con mutaciones en el gen *SLC25A19*. Curiosamente, este es el gen menos representado de los pertenecientes al transporte y metabolismo de la tiamina, únicamente hay ocho pacientes reportados en la literatura hasta el momento, todos ellos con cambios en homozigosis. Desde el primer caso reportado en 2002[136] hasta el 2019 únicamente habían reportadas tres mutaciones, dos de ellas asociadas al síndrome de Leigh y la otra asociada a microcefalia Amish. Después de la publicación de la revisión incluida en esta tesis[11], en 2019, se amplió el espectro genético con tres cambios *missense*,

en tres pacientes con síndrome de Leigh[137,138]. El cambio c.530G>C, el único asociado a microcefalia Amish hasta el momento, es una mutación *missense* que se encuentra en el mismo exón que otras dos mutaciones asociadas a síndrome de Leigh, una de ellas en el mismo dominio transmembrana[**11**,137,138]. El mecanismo por el cual causa un fenotipo distinto es desconocido, pero no se ha podido asociar ni a la localización ni al tipo de mutación. Por otro lado, la mutación más frecuente c.1264A>G (p.Thr422Ala) del *SLC19A3* se ha reportado como mutación fundadora de la población saudita en un estudio con 3000 recién nacidos sanos[139]. Todos los pacientes reportados con este defecto provenientes de Arabia Saudí (52% del total de casos), portan esta variante patogénica[140]. Curiosamente, otro estudio similar con 7101 individuos de este mismo país reporta una alta frecuencia de portadores de cambios patológicos en *CYP1B1* y *HBB*, pero en su cohorte no hay ningún portador del cambio patológico en *SLC19A3*[141]. Estos estudios son de gran utilidad desde el punto de vista de personalizar en cada país el cribado neonatal, sobretodo en enfermedades con clínica tratable como el déficit de SLC19A3 donde un tratamiento precoz con cofactores como la tiamina y la biotina pueden evitar una clínica y radiología grave en el paciente.

En el caso de los 25 pacientes diagnosticados con mutaciones nucleares, todas esas variables se encontraban en una región bien cubierta en el WES, incluyendo aquellos cambios diagnosticados por panel. Todos ellos hubiesen sido detectados por WES, no siendo así en el caso de los paneles por falta de genes y cobertura. Además, actualmente es posible analizar conjuntamente el exoma completo y el ADN mitocondrial[142]. La tecnología óptima para estos pacientes sería esta opción, englobando los casos con mutaciones en genes nucleares y mitocondriales, en este proyecto se habrían diagnosticado 31 de los 53 pacientes (58.5%) con una solo técnica. Por otro lado, a nivel de coste-beneficio esta opción sería más rentable. Hoy en día, un WES que cubra al 99% todos los genes más ADN mitocondrial a una cobertura de 90X tiene un coste menor a 400€. En su momento, con el tamaño de los genes añadidos, el coste de los paneles por paciente era mayor, y algunos de esos pacientes hay que añadirles el coste de un WES y de la secuenciación completa del ADN mitocondrial. El avance de las tecnologías de NGS y el abaratamiento de costes tan competitivo que está habiendo estos últimos años en estas técnicas agilizará el diagnóstico de estos pacientes en el futuro.

1. Retos de la NGS

A pesar de haber diagnosticado más de la mitad de los pacientes de nuestra cohorte, hay un 41% de ellos que han quedado sin diagnóstico definitivo. Uno de los principales retos que existen en la NGS es como considerar las variantes de significado incierto[143], es decir, como valorar el efecto que producen en la proteína aquellos cambios que no han sido descritos anteriormente y no está clara su patogenicidad. Otro de los retos de la NGS serán las distintas aproximaciones que podemos utilizar para poder diagnosticarlos.

1.1 Variantes de significado incierto

La posibilidad de estudiar un gran número de genes mediante las nuevas técnicas de NGS ha permitido aumentar el número de genes asociados al síndrome de Leigh[20]. Por consiguiente, con estas técnicas se analizan muchos cambios genéticos para valorar su patogenicidad.

De las 38 mutaciones encontradas en los 22 genes en este proyecto, 10 de ellas (26.3%) eran noveles, incluyendo los cuatro cambios reportados por nuestro grupo**[97]** o colaboraciones[129,130]. Los cambios noveles suelen ser comunes en la secuenciación de WES, con publicaciones con más de la mitad de cambios reportados noveles (50.5%) en patologías mitocondriales[135]. Con las herramientas básicas *in silico*, junto con el estudio y correlación clínica, hemos podido considerar patológicas de acuerdo con los criterios de la ACMG el 90% de los cambios noveles de este proyecto. En el resto se ha podido estudiar su patogenicidad con estudios funcionales, estudiando el patrón de *splicing* y los niveles de proteína en fibroblastos, analizando su localización en la proteína a partir de una cristalografía de rayos X**[144]**, o mediante estudios bioquímicos y radiológicos**[97]**.

En el análisis de NGS de los pacientes, en ocasiones, se encuentran cambios patológicos que explican parcialmente el fenotipo. En estos casos se puede optar por dar el caso como resuelto (si explica el fenotipo principal que presenta el paciente) o como no resuelto (si explica un fenotipo secundario). Recientemente, se ha reportado un paciente que porta dos cambios patológicos en el gen *SLC19A2* y otro en el gen *SAMD9*, siendo el primer caso que comparte el síndrome de anemia megaloblástica sensible a tiamina (TRMA, siglas en inglés) provocado por las mutaciones en *SLC19A2* junto con el síndrome MIRAGE provocado por los cambios en *SAMD9*[145]. No es común encontrar dos enfermedades mendelianas en un mismo paciente, pero es una situación que habría que tener en cuenta a la hora de diagnosticar a los pacientes.

El estudio de mosaicismos también podría servir para valorar la patogenicidad de un cambio. En los últimos 10 años se han reportado una media de 417 casos al año de mosaicismos relacionados con enfermedades (Pubmed, acceso en agosto del 2020). En este proyecto, analizamos una familia con dos hijos afectos y padres sanos, donde encontramos una mutación ya reportada (c.3086T>G; p.Met1029Arg) en el gen *ADCY5* en heterozigosis. Este cambio se encontraba en ambos pacientes y en la madre. En el gen *ADCY5* se han reportado varios casos de mosaicismo[146,147], por lo que analizamos la muestra de la madre mediante una PCR alelo específica en sangre periférica. Desafortunadamente, no encontramos cambios en la carga alélica de madre comparada con la de los hijos y no fue posible estudiar otros tejidos, por lo que no pudimos determinar la presencia de mosaicismos. Se debe tener en cuenta la presencia de mosaicismos frente a WES negativos, con la limitación de tener que estudiar varios tejidos para su validación.

Por último, podría ocurrir que un paciente portase cambios patológicos en una proteína que no se relacione con su clínica, pero esté afectando otra proteína cuya función sí se hay relacionado con la enfermedad presente en el paciente. Una herramienta útil en estos casos es el programa STRING[148], que te permite ver las interacciones entre proteínas. Hoy en día, son muy utilizados como herramientas de diagnóstico softwares que te permiten comparar la clínica de tu paciente con otros pacientes que tengan mutaciones en el mismo gen. Una de las más utilizadas es la plataforma GeneMatcher[149]. A nivel de Cataluña, desde el 2016 se impulsó el proyecto URDCat que ha permitido obtener una plataforma con estas características. Estas herramientas son muy útiles en las enfermedades raras ya que te permiten conectar con otros investigadores y médicos para poder identificar nuevos genes asociados a una enfermedad, que de otra forma sería complicado debido al reducido número de pacientes.

A pesar de lo útil que puede resultar todas las herramientas anteriores, las variantes de significado incierto, para ser clasificadas como patológicas, deberían ser validadas funcionalmente a fin de comprobar su contribución real.

1.2. Casos negativos

El reanálisis de los datos cada cierto tiempo es importante ya que se van mejorando los algoritmos de anotación y se van asociado nuevos genes y mutaciones a patologías. El reanálisis consiste en volver a anotar las variables[150] con la información de las bases de

datos genéticas, detección de deleciones e inserciones y las clasificaciones fenotípicas actualizadas. La posibilidad de realizar un reanálisis es una de las ventajas del WES y WGS[113,114]. Recientemente, se ha reportado que el reanálisis de los datos puede aumentar el diagnóstico un 6% más frente a los datos iniciales[151]. El hecho de reanalizar los datos clínicamente y radiológicamente también puede aumentar el porcentaje de éxito. Este reanálisis conllevaría el seguimiento y revisión de la historia clínica del paciente teniendo en cuenta los nuevos fenotipos que se van asociando a distintos genes. En este proyecto este fenotipado ha permitido dar diagnóstico definitivo a ocho pacientes al comprobar que la causa de las alteraciones en los ganglios basales era adquirida. Tres de estos pacientes habían presentado una lesión en los ganglios basales asociada al tratamiento con vigabatrina, dos de ellos presentaban las alteraciones tras una infección y los otros tres pacientes habían presentado una encefalopatía, encefalopatía hipóxico-isquémica y Kernicterus. Por ello, es imprescindible un equipo multidisciplinar formado por clínicos, radiólogos, bioquímicos, genetistas y bioinformáticos para mejorar la tasa de diagnóstico total. El desarrollo de una sospecha clínica clara implicará un mejor enfoque a la hora de buscar genes causantes a través del análisis bioinformático.

Una primera aproximación para abordar las limitaciones de la WES y diagnosticar los casos negativos sería el WGS, ya que te permite analizar los cambios intrónicos profundos que pierdes con el WES. Además, es una herramienta más certera a la hora de analizar aberraciones cromosómicas, pequeñas deleciones o inserciones o CNVs, ya que la cobertura es más homogénea. El análisis de mosaicismos podría abordarse mediante WES o WGS[152]. Otras técnicas que complementan el WES en casos negativos serían el análisis del ARN mediante RNA-seq o el *array* CGh. El RNA-seq nos permitiría estudiar los patrones de expresión de los genes, pudiendo detectar cambios en el patrón de *splicing*. En un estudio reciente se han diagnosticado un 7.5% de los pacientes de su cohorte con esta técnica, teniendo candidatos en genes asociados al fenotipo de los pacientes en un 16.5% de los casos[153]. Por otro lado, el *array* CGH permite detectar grandes deleciones/inserciones que con las técnicas de NGS pasarían inadvertidas. En estudios anteriores con 1280 pacientes con sospecha de enfermedad mitocondrial o metabólica se diagnosticaron 40 pacientes (3%) mediante esta técnica. La combinación de diferentes "ómicas" mejorará aún más el diagnóstico de los pacientes con enfermedades raras no resueltos en un futuro.

Los casos que se han quedado como no resueltos en este proyecto siguen analizándose utilizando estas herramientas que hemos nombrado de forma que puedan llegar a ser positivos.

2. Estudio de biomarcadores

En esta tesis, se han estudiado posibles biomarcadores para las deficiencias de SCEH y HIBCH implicadas en el catabolismo de la valina, las deficiencias del transporte y metabolismo de la tiamina y en la hipermanganesia por mutaciones en el gen *SLC39A14*.

2.1. Deficiencias de SCEH y HIBCH implicadas en el catabolismo de la valina

En estas deficiencias se han estudiado tres posibles biomarcadores: el ácido 2,3-dihidroxi-2-metilbutirato, los metabolitos del metacrilato y la carnitina 3-hidroxi-isobutirilcarnitina**[144]**.

El ácido 2,3-dihidroxi-2-metilbutirato se ha relacionado sobre todo con pacientes con déficit de SCEH, ya que su elevación ha sido reportada en un 41% de los pacientes mientras que sólo tres pacientes (11%) con deficiencia en HIBCH presentaban esa anomalía. Un artículo con pacientes con desórdenes de depleción de ADN mitocondrial reporta una elevación de este metabolito en el 85% de los pacientes estudiados con síndrome de Pearson y el 29% de los pacientes con síndrome de Kearns-Sayre[154]. Este hecho y contando que más de la mitad de los pacientes con deficiencias de SCEH no presenten elevación de este ácido hace que no podamos considerarlo como buen biomarcador para estas patologías.

Los metabolitos del metacrilato (S-2-carboxypropyl cysteamine, S-2-carboxypropyl cysteine y N-acetyl-S-2-carboxypropyl) solo han sido reportados para pacientes con déficit de SCEH, encontrándose elevados en el 83% de los pacientes[16,20,162–171,88,172,155–161], incluyendo las formas más leves con fenotipo de distonía paroxística[163]. Solo un paciente HIBCH presentaba esta elevación**[144]**, además de no haber sido reportados en ninguna otra patología. Podríamos considerar estos metabolitos como buenos biomarcadores para la detección de una deficiencia de SCEH, pero, se debe destacar que estos metabolitos se analizan con el estudio de aminoácidos en orina. Este análisis no se realiza en los laboratorios de forma rutinaria por lo que podría ser que otras patologías también tuvieran estos metabolitos elevados y no estuviese reportado y que no fuese tan específico, y se necesitaría una sospecha previa de estas patologías para su análisis.

La 3-hidroxi-isobutiril carnitina está presente en un 75% de los pacientes con HIBCH[173,174,183–186,175–182] y un 21% en pacientes con SCEH[16,20,162–171,88,172,155–161]. Tampoco se ha reportado elevación de esta carnitina en ninguna otra patología y, a contrario del caso anterior, sí se analiza en el perfil de carnitinas. Este análisis se realiza a aquellos pacientes con sospecha de enfermedad metabólica, que englobaría estos pacientes. Podría considerarse un biomarcador para estas patologías, pero no diferenciaría entre una deficiencia de HIBCH y una deficiencia de SCEH ya que el porcentaje de los pacientes con déficit de SCEH y una elevación de la carnitina 3-hidroxi-isobutiril es considerable.

2.2. Deficiencias del transporte y metabolismo de la tiamina

Se han reportado patrones específicos de la alteración de las distintas isoformas de tiamina en los diferentes defectos[**11**,187,188], excepto en los pacientes con mutaciones en el *SLC25A19*. En este caso, una deficiencia de este transportador disminuye la actividad de las enzimas que utilizan como cofactor la TPP, por lo que se esperaría una disminución de esta isoforma en sangre total. El estudio de las distintas isoformas en varias matrices puede llegar a ser un biomarcador eficaz para estas deficiencias que, junto con la clínica, dirigiera los genes a estudiar. Hay que tener en cuenta que se han reportado otras enfermedades que cursan con déficit de tiamina como es la ataxia de Friedrich[189] y enfermedades cardiovasculares[190], siendo esta deficiencia un hallazgo común en estos pacientes, la clínica difiere mucho a los déficits de tiamina. Por otro lado, destacar la importancia de mantener unos niveles de tiamina adecuados. Un déficit de tiamina se ha asociado a cáncer[191] y produce una disminución del número de neuronas[189], lo que conlleva una mayor probabilidad de padecer enfermedades neurodegenerativas como son la demencia o el Alzheimer[192].

2.3. Hipermanganesemia por mutaciones en el gen *SLC39A14*

El gen *SLC39A14* se asoció por primera vez a una patología en 2016[12]. En este proyecto se diagnosticó el segundo grupo de pacientes (dos hermanos)[**97**] con mutaciones en este gen. Actualmente, únicamente hay dos publicaciones más con pacientes con esta deficiencia[193,194]. Para validar la mutación novel c.311G>T presente en los dos hermanos de este proyecto se realizó el análisis de manganeso en orina, plasma y LCR en uno de ellos, poniendo a punto esta última determinación. Los niveles de manganeso en LCR en este paciente eran treinta veces mayores comparado con pacientes control. Únicamente se ha reportado un aumento de manganeso en LCR en pacientes con esclerosis lateral

amiotrófica[110], cuya clínica es distinta de los pacientes con hipermanganesemia. Estos hechos validan la elevación de manganeso en LCR como buen biomarcador para detectar pacientes con estas deficiencias. Hay que destacar que el análisis en LCR realizado en nuestro laboratorio se ha realizado mayormente de forma cualitativa, ya que los valores de manganeso en controles sanos es muy bajo (en torno a 1 µg/L)[195], por lo que una deficiencia de manganeso no se detectaría.

La realización de una punción lumbar es un procedimiento invasivo y hay que tratar de minimizar su uso sobretodo en población pediátrica ya que existen complicaciones asociadas importantes: dolor local, cefalea, vómito, hematomas epidural o subdural, radiculitis, fístula de LCR, deterioro rostrocaudal por herniación o infecciones[196]. Por ello, se ha validado un método no invasivo como biomarcador para esta enfermedad, el índice palidal. En nuestro estudio, el paciente presentaba un índice palidal 1.6 veces mayor que los controles sanos. Estos datos, junto con ya reportados en trabajadores expuestos a altos niveles de manganeso[108], sugieren el índice palidal como posible biomarcador de enfermedades de acúmulo de manganeso. Para su validación, habría que estudiar más casos ya que se este estudio incluye únicamente un paciente**[97]**. Por otro lado, además de ser una técnica no invasiva y de no estar reportado hasta el momento, podría utilizarse en otras enfermedades de acúmulo de metales como las enfermedades neurodegenerativas con acúmulo cerebral de hierro que crean una hiperintensidad en secuencia T2 por los depósitos de hierro en el pálido[95].

Un diagnóstico precoz es importante para ofrecer al paciente un tratamiento con quelantes de metales antes de que la clínica se agrave, ya que podría ser eficaz pero no revierte los daños[197]. La utilización del quelante $Ca_2NaEDTA$ estudiado en este proyecto, a pesar de que la familia reportaba un empeoramiento de la clínica del paciente, bioquímicamente fue muy eficaz ya que disminuyó la cantidad de manganeso en plasma un 62%. Posteriormente a la publicación del artículo, se volvió a pautar una dosis del tratamiento, sin mejoría clínica. Este quelante ha sido utilizado en otros pacientes con mutaciones en el *SLC39A14* con mejoría clínica en un paciene[198] y sin ella en dos casos[199]. También presentó una mejoría de la distonía y una disminución de manganeso en suero un paciente con cambios en el gen *SLC30A10*, asociado también a defectos de acumulo de manganeso[109]. Recientemente, se ha reportado que unas posibles causas de la ineficacia del tratamiento en el caso de pacientes con mutaciones en *SLC39A14* pueden ser la severidad de la enfermedad o su genotipo. Es probable que el tratamiento no sea eficaz

en aquellos pacientes donde la neurodegeneración haya progresado y sea irreversible. Por otro lado, el único caso con excelente respuesta al tratamiento es portador de mutaciones que solo afectan a una isoforma de la proteína transportadora, por lo que el genotipo podría desempeñar un papel en la eficacia del tratamiento[197]. Tanto en nuestro paciente como en otros pacientes está reportado la disminución de otros metales[199], consecuencia directa del tratamiento. La orina es un medio eficaz para la monitorización de metales durante el tratamiento, además de ser un método no invasivo y fácil de recoger. Esto ayudará a llevar un seguimiento de los niveles de metales adaptando las suplementaciones según el requerimiento del paciente y confirmando su eficacia con la disminución de manganeso.

3. Correlaciones fenotipo-genotipo en pacientes con lesiones en los ganglios basales

Los resultados de esta tesis han permitido establecer nuevas correlaciones entre el genotipo y el fenotipo de los pacientes.

3.1. Correlaciones fenotipo-genotipo y estudios de historia natural en los defectos del metabolismo de valina

Las correlaciones fenotipo-genotipo realizadas en esta tesis en pacientes con defectos en el metabolismo de valina pueden ser de gran utilidad a la hora de predecir el progreso de la enfermedad y por lo tanto de dar tratamiento y seguimiento al paciente. Por un lado, se ha estudiado la relación entre el cambio c.518C>T en el gen *ECHS1* y el fenotipo distonía paroxística obteniendo una correlación muy significativa**[144]**. Este fenotipo es mucho más leve que los otros dos fenotipos presentados en dicha deficiencia, por lo que diagnosticar precozmente un paciente con este cambio podría indicar un buen pronóstico de la enfermedad y un fenotipo de distonía paroxística.

Por otro lado, se ha hecho un estudio de supervivencia comparando pacientes con mutaciones situadas cerca del centro catalítico y variantes que se encuentran en la superficie en homozigosis de la proteína HIBCH encontrando que los pacientes con mutaciones en el centro catalítico tienen una menor supervivencia. Datos similares se habían sugerido en artículos reportados previamente[182]. Esto es muy relevante ya que un diagnóstico temprano podría predecir el progreso de la enfermedad. Gracias a estos resultados en las correlaciones fenotipo-genotipo, según la variante genética que porte el

paciente podemos predecir el progreso de la enfermedad, por lo que es muy importante el diagnóstico precoz para poder dirigirlo de la mejor forma posible para el paciente.

3.2. Correlación entre bioquímica y genética para el diagnóstico de pacientes con lesiones en los ganglios basales

La disponibilidad de biomarcadores en las enfermedades ayuda a incrementar la tasa de éxito en el diagnóstico molecular. Un estudio con 146 pacientes con errores congénitos del metabolismo reportó que en los pacientes con enfermedades con un biomarcadores específico el porcentaje diagnóstico aumentaba a un 78% frente al 15.4% en enfermedades sin biomarcador[200].

En este proyecto, en cuatro pacientes con lesiones en los ganglios basales, a pesar de presentar un fenotipo de síndrome de Leigh de acuerdo con los criterios diagnósticos actuales[8,201], se identificaron variantes en genes no relacionados con dicho síndrome (*SCN2A* y *GNAO1* asociados con encefalopatía epiléptica de debut precoz; *PRKRA* asociado con distonía-parkinsonismo, y *ADAR* relacionado con el síndrome de Aicardi-Goutières). Por este motivo, se clasificaron finalmente como genocopias de síndrome de Leigh. Las proteínas codificadas por estos genes se han estudiado utilizando el programa STRING (Figura 5). Mediante el estudio de sus vías metabólicas y las proteínas relacionadas hemos encontrado una asociación de dichos genes con la patología presente en estos pacientes. Se ha reportado previamente pacientes con enfermedad mitocondrial y mutaciones en el gen *SCN2A,* donde se relaciona este gen con lesiones en los ganglios de la base[135]. Además, el gen *SCN4B,* que tiene una relación directa con el *SCN2A*, se localiza y tiene una función en los ganglios basales[202] y actúa en la misma ruta metabólica[203] (Figura 5A).

En el caso de los genes relacionados con *GNAO1,* se ha observado que algunos de ellos realizan su función en los ganglios basales (*GNB1*[204], *GNB3*[205], *GNB4*[206], *GNB5*[207] y *OPRM1*[208]), además las proteínas codificadas por GNB1 y GNAO1 actúan ambas en la vía del AMP y regulando la fusión de vesículas sinápticas y neurotransmisores, interaccionando entre ellas (Figura 5B). Varios genes (*DICER, AGO1, AGO2*) relacionados directamente con *PRKRA* (Figura 5C) tienen funciones en los ganglios basales[209]. Por otro lado, regula directamente la proteína DICER en la vía de micro ARNs[210] y EIF2AK2 en la respuesta a estrés y la regulación del ciclo celular[211], actuando conjuntamente en las mismas vías metabólicas. Por último, el gen ADAR está asociado

previamente a una necrosis estriatal bilateral[212], presente en los tres pacientes de este proyecto que presentaban un síndrome de Leigh y mutaciones en este gen.

Estos estudios *in silico* han permitido asociar los cambios patológicos encontrados en el paciente a su enfermedad ya que, aunque la proteína no esté asociada actualmente con el síndrome de Leigh, puede estar modificando otra proteína que se encuentre en la misma vía metabólica y con la que conecta directamente y ésta realizar una función errónea en los ganglios basales.

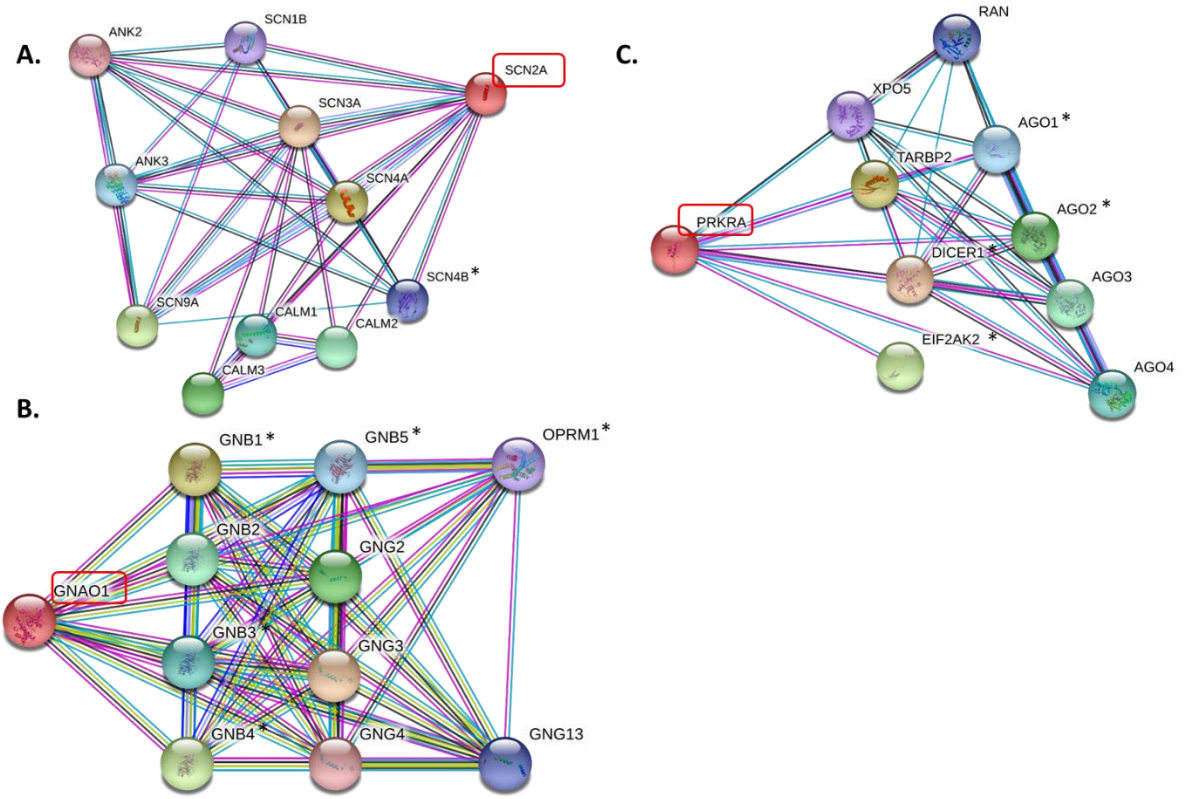

Figura 5: Redes de proteínas relacionadas directamente entre sí de los distintos genes que se asocian por primera vez enfermedades mitocondriales: (A) SCN2A, once nodos, enriquecimiento PPI *p_valor*= 3.46e-13; (B) *GNAO1*, once nodos, enriquecimiento PPI *p_valor*= 1.13e-10; y (C) *PRKRA;* diez nodos, enriquecimiento PPI *p_valor*= 7.17e-12. Se ha considerado que los nodos no son al azar cuando *p_valor*<0.01. Leyenda de los colores de las líneas, origen de la información para realizar esas relaciones: azul claro: bases de datos, morado: determinado experimentalmente, azul oscuro: genes co-ocurrentes, negro: coexpresión, amarillo (en el caso de GNAO1): extracción de textos. *: Proteínas asociadas con una clínica o función en los ganglios de la base (ver texto).

Para agilizar y asegurar un diagnóstico genético en un paciente es importante poder contar con un equipo interdisciplinar. El hecho realizar esta tesis en un laboratorio de un hospital, y en concreto, en un laboratorio de bioquímica, ha permitido abordar tanto una aproximación genética como bioquímica. Esta ventaja ha sido beneficiosa a la hora de diagnosticar a los pacientes, ya que ha permitido integrar los distintos resultados de los pacientes correlacionando la genética y la bioquímica. Por otro lado, la cercanía de profesiones clínicos y radiólogos también ha sido una gran ventaja. Una sinergia entre la bioquímica, genética, clínica y radiológica robusta, como ha permitido esta tesis mantener, mejora los resultados y permite formarse en aspectos importantes a la hora de analizar y realizar un diagnóstico a un paciente.

Como conclusión general, los resultados más relevantes de esta tesis han sido la asociación de distintos genes y nuevas mutaciones en los pacientes pediátricos con patologías de los ganglios basales, los estudios que han podido correlacionar el fenotipo y el genotipo en pacientes con cambios en *HIBCH* y *ECHS1* y, los avances en cuanto a biomarcadores con el análisis de metales y tiamina en LCR.

CONCLUSIONES

1. Los pacientes pediátricos con trastornos del movimiento y alteraciones en los ganglios basales presentan una gran heterogeneidad clínica, radiológica y genética, lo que dificulta su diagnóstico.
2. La secuenciación de exoma completo junto con la secuenciación del ADN mitocondrial ha resultado la herramienta más eficaz para diagnosticar pacientes con alteraciones en los ganglios basales.
3. La secuenciación por paneles génicos puede ser una herramienta eficaz en pacientes con fenotipos y genotipos bien definidos como aquellos que presentan calcificaciones en los ganglios basales.
4. Las deficiencias de SCEH y HIBCH, enzimas de la vía del catabolismo de la valina, son una de las causas genéticas más comunes en los pacientes con síndrome de Leigh. Los pacientes con un déficit en el SCEH presentan un gran rango de severidad, incluyendo pacientes con un fenotipo leve de distonía paroxística, relacionados estadísticamente con el cambio genético c.518C>T. Los estudios de expresión proteica han resultado de gran utilidad a la hora de diagnosticar pacientes con mutaciones en el gen *ECHS1* que presentan este fenotipo más leve.
5. La visualización *in silico* de las mutaciones *missense* en un modelo virtual de la proteína HIBCH ha permitido realizar una posible correlación genotipo-fenotipo, hecho que posibilitará el conocimiento de la prognosis del paciente y ayudará a realizar un mejor seguimiento.
6. El análisis de manganeso en líquido cefalorraquídeo ha permitido verificar el diagnóstico y reforzar la hipótesis del acúmulo de manganeso en cerebro en un paciente con mutaciones en el gen *SLC39A14*. Asimismo, la medida del índice palidal en la resonancia magnética cerebral ha facilitado la monitorización de los

efectos en cuanto al depósito de manganeso cerebral del tratamiento con el quelante $Na_2CaEDTA$. Este tratamiento ha resultado ser eficaz a nivel bioquímico, debe suministrarse empezando con dosis bajas, así como tener un seguimiento tanto de manganeso como de otros elementos traza.

7. En aquellos pacientes con episodios recurrentes de encefalopatías y/o distonía, lactato elevado en sangre y/o líquido cefalorraquídeo o incremento de alfa-cetoglutarato en orina y lesiones en el tálamo y los ganglios basales hay que tener en cuenta una deficiencia en el transporte o metabolismo de tiamina. El diagnóstico precoz en estos pacientes es importante ya que el tratamiento temprano mejora notablemente la prognosis de muchos de ellos.
8. La detección de las distintas isoformas de tiamina en sangre total y/o líquido cefalorraquídeo permite tanto el diagnóstico como la monitorización del tratamiento en pacientes con alteraciones en el transporte o metabolismo de la tiamina.
9. Un equipo interdisciplinar con clínicos, radiólogos, bioquímicos y genetistas ha sido fundamental a la hora del diagnóstico de los pacientes con alteraciones en los ganglios basales.

BIBLIOGRAFÍA

1. Lanciego JL, Luquin N & Obeso JA. (2012) Functional neuroanatomy of the basal ganglia. *Cold Spring Harb. Perspect. Med.* 2(12):a009621.

2. Hendelman WJ. (2006) *Atlas of Functional Neuroanatomy*. (Taylor and Francis Group).

3. Barha CK, Nagamatsu LS & Liu-Ambrose T. (2016) *Atlas of neuroanatomy and neurophysiology*. *Handbook of Clinical Neurology*. 138.

4. Lake NJ, Compton AG, Rahman S & Thorburn DR. (2016) Leigh syndrome: One disorder, more than 75 monogenic causes. *Ann. Neurol.* 79(2):190–203.

5. Sofou K, De Coo IF, Isohanni P, et al. (2014) A multicenter study on Leigh syndrome: Disease course and predictors of survival. *Orphanet J. Rare Dis.* 9:52.

6. Tonduti D, Chiapparini L, Moroni I, et al. (2016) Neurological Disorders Associated with Striatal Lesions: Classification and Diagnostic Approach. *Curr. Neurol. Neurosci. Rep.* 16(6):54.

7. Cavanagh JB & Harding BN. (1994) Pathogenic factors underlying the lesions in leigh's disease: Tissue responses to cellular energy deprivation and their clinico-pathological consequences. *Brain.* 117 (Pt 6):1357-1376.

8. Lake NJ, Bird MJ, Isohanni P & Paetau A. (2015) Leigh Syndrome: Neuropathology and Pathogenesis. *J. Neuropathol. Exp. Neurol.* 74(6):482-492.

9. Batla A & Gaddipati C. (2019) Neurodegeneration with Brain Iron Accumulation. *Ann. Indian Acad. Neurol.* 22(3):267–276.

10. Livingston JH, Lin JP, Dale RC, et al. (2014) A type i interferon signature identifies bilateral striatal necrosis due to mutations in ADAR1. *J. Med. Genet.* 51(2):76–82.

11. Marcé-Grau A, Martí-Sánchez L, Baide-Mairena H, Ortigoza-Escobar JD & Pérez-Dueñas B. (2019) Genetic defects of thiamine transport and metabolism: A review of clinical phenotypes, genetics, and functional studies. *J. Inherit. Metab. Dis.* 42(4):581–597.

12. Tuschl K, Meyer E, Valdivia LE, et al. (2016) Mutations in SLC39A14 disrupt manganese homeostasis and cause childhood-onset parkinsonism–dystonia. *Nat.*

Commun. 7:11601.

13. Hamilton EM, Polder E, Vanderver A, et al. (2014) Hypomyelination with atrophy of the basal ganglia and cerebellum: Further delineation of the phenotype and genotype-phenotype correlation. *Brain.* 137(Pt 7):1921–1930.

14. Purdon-Martin J. (1927) Hemichorea resulting from a local lesion of the brain (the syndrome of the body of Luys.). *Brain.* 50:637–651.

15. Leigh D. (1951) Subacute necrotizing encephalomyelopathy in an infant. *J Neurol Neurosurg Psychiatry.* 14(3):216–21.

16. Aretini P, Mazzanti CM, La Ferla M, et al. (2018) Next generation sequencing technologies for a successful diagnosis in a cold case of Leigh syndrome. *BMC Neurol.* 18(1):99.

17. Rahman J, Noronha A, Thiele I, Rahman S. (2017) Leigh map: A novel computational diagnostic resource for mitochondrial disease. *Ann. Neurol.* 81(1):9–16.

18. Kaur P, Sharma S, Kadavigere R, Girisha KM, Shukla A. (2020) Novel variant p.(Ala102Thr) in SDHB causes mitochondrial complex II deficiency: Case report and review of the literature. *Ann. Hum. Genet.* 84(4):345-351.

19. Friederich MW, Elias AF, Kuster A, et al. (2020) Pathogenic variants in SQOR encoding sulfide:quinone oxidoreductase are a potentially treatable cause of Leigh disease . *J. Inherit. Metab. Dis.* 10.1002/jimd.12232.

20. Ogawa E, Shimura M, Fushimi T, et al. (2017) Clinical validity of biochemical and molecular analysis in diagnosing Leigh syndrome: a study of 106 Japanese patients. *J. Inherit. Metab. Dis.* 40(5):685–693.

21. Chang X, Wu Y, Zhou J, Meng H, Zhang W, Guo J. (2020) A meta-analysis and systematic review of Leigh syndrome: clinical manifestations, respiratory chain enzyme complex deficiency, and gene mutations. *Medicine (Baltimore).* 99(5):e18634.

22. Sofou K, de Coo IFM, Ostergaard E, et al. (2018) Phenotype-genotype correlations in leigh syndrome: New insights from a multicentre study of 96 patients. *J. Med. Genet.* 55(1):21–27.

23. Lee JS, Kim H, Lim BC, et al. (2016) Leigh syndrome in childhood: Neurologic progression and functional outcome. *J. Clin. Neurol.* 12(2):181–187.

24. Ma YY, Wu TF, Liu YP, et al. (2013) Genetic and biochemical findings in Chinese children with Leigh syndrome. *J. Clin. Neurosci.* 20(11):1591–1594.

25. Fang F, Liu Z, Fang H, et al. (2017) The clinical and genetic characteristics in children with mitochondrial disease in China. *Sci. China Life Sci.* 60(7):746–757.

26. Alagia M, Cappuccio G, Torella A, et al. (2020) Cavitating and tigroid-like leukoencephalopathy in a case of NDUFA2 -related disorder . *JIMD Rep.* 52(1):11–16.

27. D'Gama AM, Brucker WJ, Zhang T, et al. (2020) A phenotypically severe, biochemically "silent" case of HIBCH deficiency in a newborn diagnosed by rapid whole exome sequencing and enzymatic testing. *Am. J. Med. Genet. Part A.* 182(4):780–784.

28. Halperin D, Drabkin M, Wormser O, et al. (2020) Phenotypic variability and mutation hotspot in COX15-related Leigh syndrome. *Am. J. Med. Genet.* 182(6):1506-1512.

29. Yang H, Yu D. (2020) Clinical, biochemical and metabolic characterization of patients with short-chain enoyl-CoA hydratase(ECHS1) deficiency: Two case reports and the review of the literature. *BMC Pediatr.* 20(1):50.

30. Koenig MK. (2008) Presentation and Diagnosis of Mitochondrial Disorders in Children. *Pediatr. Neurol.* 38(5):305–313.

31. Baertling F, Rodenburg RJ, Schaper J, et al. (2014) A guide to diagnosis and treatment of Leigh syndrome. *J. Neurol. Neurosurg. Psychiatry.* 85(3):257–265.

32. Gorman GS, Chinnery PF, DiMauro S, et al. (2016) Mitochondrial diseases. *Nat. Rev. Dis. Prim.* 2:16080.

33. Morava E, van den Heuvel L, Hol F, et al. (2006) Mitochondrial disease criteria: diagnostic applications in children. *Neuorology.* 67(10):1823–1826.

34. Witters P, Saada A, Honzik T, et al. (2018) Revisiting mitochondrial diagnostic criteria in the new era of genomics. *Genet. Med.* 20(4):444–451.

35. Skladal D, Sudmeier C, Konstantopoulou V, et al. (2003) The clinical spectrum of mitochondrial disease in 75 pediatric patients. *Clin. Pediatr. (Phila).* 42(8):703–710.

36. Gorman GS, Schaefer AM, Ng Y, et al. (2015) Prevalence of nuclear and mitochondrial DNA mutations related to adult mitochondrial disease. *Ann. Neurol.* 77(5):753–759.

37. Russell OM, Gorman GS, Lightowlers RN, Turnbull DM. (2020) Mitochondrial Diseases: Hope for the Future. *Cell.* 181(1):168–188.

38. Thompson K, Collier JJ, Glasgow RIC, et al. (2020) Recent advances in understanding the molecular genetic basis of mitochondrial disease. *J. Inherit. Metab. Dis.* 43(1):36–50.

39. Frazier AE, Thorburn DR, Compton AG. (2019) Mitochondrial energy generation disorders: Genes, mechanisms, and clues to pathology. *J. Biol. Chem.* 294(14):5386–5395.

40. Manzetti S, Zhang J, van der Spoel D. (2014) Thiamin function, metabolism, uptake, and transport. *Biochemistry.* 53(5):821–835.

41. Stuetz W, Carrara VI, McGready R, Lee SJ, Biesalski HK, Nosten FH. (2012) Thiamine diphosphate in whole blood, thiamine and thiamine monophosphate in breast-milk in a refugee population. *PLoS One*. 7(6): e36280.

42. Burkholder PR, McVeigh I. (1942) Synthesis of Vitamins by Intestinal Bacteria. 28(7)**:**285–289.

43. Said HM, Balamurugan K, Subramanian VS, Marchant JS. (2004) Expression and functional contribution of hTHTR-2 in thiamin absorption in human intestine. *Am. J. Physiol. Gastrointest. Liver Physiol.* 286(3):G491-G498.

44. Turck D, Bresson JL, Burlingame B. (2016) Dietary reference values for thiamin. *EFSA J.* 14(12):4653.

45. Alexander B, Landwehr G, Mitchell F. (1946) Studies of thiamine metabolism in man; thiamine and pyrimidine excretion with special reference to the relationship between injected and excreted thiamine in normal and abnormal subjects. *J. Clin. Invest.* 25(3):294–303.

46. Nogueira RJ, Godoy JE, Souza TH. (2016) Acute abdominal pain as a presenting symptom of beriberi in a pediatric patient. *J. Trop. Pediatr.* 62(6):490-495.

47. Saeki K, Saito Y, Komaki H, et al. (2010) Thiamine-deficient encephalopathy due to excessive intake of isotonic drink or overstrict diet therapy in Japanese children. *Brain Dev.* 32(7):556–563.

48. Park JH, Hogrebe M, Grüneberg M, et al. (2015) SLC39A8 Deficiency: A Disorder of Manganese Transport and Glycosylation. *Am. J. Hum. Genet.* 97(6):894–903.

49. Wani NA, Qureshi UA, Jehangir M, Ahmad K, Ahmad W. (2016) Infantile encephalitic beriberi: magnetic resonance imaging findings. *Pediatr. Radiol.* 46(1):96–103.

50. Benidir AN, Laughlin S, Ng VL. (2014) Visual disturbances in total parenteral nutrition dependent liver transplant pediatric patient. *Gastroenterology.* 146(5):e10-e11.

51. Perko R, Harreld JH, Helton KJ, Sabin ND, Haidar CE, Wright KD. (2012) What Goes Around Comes Around ? Wernicke Encephalopathy and the Nationwide Shortage. *J. Clin. Oncol.* 30(31):e318–e320.

52. Pitel AL, Zahr NM, Jackson K, et al. (2011) Signs of preclinical wernicke's encephalopathy and thiamine levels as predictors of neuropsychological deficits in alcoholism without korsakoff's syndrome. *Neuropsychopharmacology.* 36(3):580–588.

53. Harper CG, Giles M, Finlay-Jones R. (1986) Clinical signs in the Wernicke-Korsakoff complex: A retrospective analysis of 131 cases diagnosed at necropsy. *J. Neurol. Neurosurg. Psychiatry.* 49(4):341–345.

54. Mantero V, Rifino N, Costantino G, et al. (2020) Non-alcoholic beriberi, Wernicke encephalopathy and long-term eating disorder: case report and a mini-review. *Eat. Weight Disord.* 10.1007/s40519-020-00880-0.

55. Shible AA, Ramadurai D, Gergen D, Reynolds PM. (2019) Dry beriberi due to thiamine deficiency associated with peripheral neuropathy and wernicke's encephalopathy mimicking guillainbarré syndrome: A case report and review of the literature. *Am. J. Case Rep.* 20:330–334.

56. Ozand PT, Gascon GG, Al Essa M, et al. (1998) Biotin-responsive basal ganglia disease: A novel entity. *Brain.* 121(Pt7):1267–1279.

57. Sen A, Pillay RS. (2011) Striatal necrosis in type 1 glutaric aciduria: Different stages

in two siblings. *J. Pediatr. Neurosci.* 6(2):146–148.

58. Strauss KA, Lazovic J, Wintermark M, Morton DH. (2007) Multimodal imaging of striatal degeneration in Amish patients with glutaryl-CoA dehydrogenase deficiency. *Brain.* 130(Pt 7):1905–1920.

59. Gascon GG, Ozand PT, Brismar J. (1994) Movement disorders in childhood organic acidurias. Clinical, neuroimaging, and biochemical correlations. *Brain.* 16 Suppl:94–103.

60. Korman SH, Jakobs C, Darmin PS, et al. (2007) Glutaric aciduria type 1: Clinical, biochemical and molecular findings in patients from Israel. *Eur. J. Paediatr. Neurol.* 11(2):81–89.

61. Claerhout H, Witters P, Régal L, et al. (2018) Isolated sulfite oxidase deficiency. *J. Inherit. Metab. Dis.* 41(1):101–108.

62. Tian M, Qu Y, Huang L, et al. (2019) Stable clinical course in three siblings with late-onset isolated sulfite oxidase deficiency: A case series and literature review. *BMC Pediatr.* 19(1):510.

63. Sass JO, Gunduz A, Araujo Rodrigues Funayama C, et al. (2010) Functional deficiencies of sulfite oxidase: Differential diagnoses in neonates presenting with intractable seizures and cystic encephalomalacia. *Brain Dev.* 32(7):544–549.

64. Basel-Vanagaite L, Muncher L, Straussberg R, et al. (2006) Mutated nup62 causes autosomal recessive infantile bilateral striatal necrosis. *Ann. Neurol.* 60(2):214–222.

65. Nizon M, Ottolenghi C, Valayannopoulos V, et al. (2013) Long-term neurological outcome of a cohort of 80 patients with classical organic acidurias. *Orphanet J. Rare Dis.* 8:148.

66. Valdés Hernández Mdel C, Maconick LC, Tan EM, Wardlaw JM. (2012) Identification of mineral deposits in the brain on radiological images: A systematic review. *Eur. Radiol.* 22(11):2371–2381.

67. Miklossy J, Mackenzie IR, Dorovini-Zis K, et al. (2005) Severe vascular disturbance in a case of familial brain calcinosis. *Acta Neuropathol.* 109(6):643–653.

68. Donzuso G, Mostile G, Nicoletti A, Zappia M. (2019) Basal ganglia calcifications

(Fahr's syndrome): related conditions and clinical features. *Neurol. Sci.* 40(11):2251–2263.

69. Quintáns B, Oliveira J, Sobrido MJ. (2018) Primary familial brain calcifications. Handb Clin Neurol. 147:307-317.

70. Savino E, Soavi C, Capatti E, et al. (2016) Bilateral strio-pallido-dentate calcinosis (Fahr's disease): Report of seven cases and revision of literature. *BMC Neurol.* 16(1):165.

71. Nicolas G, Charbonnier C, Campion D, Veltman JA. (2018) Estimation of minimal disease prevalence from population genomic data: Application to primary familial brain calcification. *Am. J. Med. Genet. Part B Neuropsychiatr. Genet.* 177(1):68–74.

72. Yao XP, Cheng X, Wang C, et al. (2018) Biallelic Mutations in MYORG Cause Autosomal Recessive Primary Familial Brain Calcification. *Neuron.* 98(6):1116-1123.e5.

73. Cen Z, Chen Y, Chen S, et al. (2020) Biallelic loss-of-function mutations in JAM2 cause primary familial brain calcification. *Brain.* 143(2):491–502.

74. Arkadir D, Lossos A, Rahat D, et al. (2019) MYORG is associated with recessive primary familial brain calcification. *Ann. Clin. Transl. Neurol.* 6(1):106–113.

75. Chelban V, Carecchio M, Rea G, et al. (2020) MYORG -related disease is associated with central pontine calcifications and atypical parkinsonism . *Neurol. Genet.* 6(2):e399.

76. Chen Y, Fu F, Chen S, et al. (2019) Evaluation of MYORG mutations as a novel cause of primary familial brain calcification. *Mov. Disord.* 34(2):291–297.

77. Ferreira LD, de Oliveira JRM. (2019) New homozygous indel in MYORG linked to brain calcification, thyroidopathy and neuropathy. *Brain.* 142(9):e51.

78. Forouhideh Y, Müller K, Ruf W, et al. (2019) A biallelic mutation links MYORG to autosomal-recessive primary familial brain calcification. *Brain.* 142(2):e4.

79. Grangeon L, Wallon D, Charbonnier C, et al. (2019) Biallelic MYORG mutation carriers exhibit primary brain calcification with a distinct phenotype. *Brain* 142(6):1573–1586.

80. Peng Y, Wang P, Chen Z, Jiang H. (2019) A novel mutation in MYORG causes primary familial brain calcification with central neuropathic pain. *Clin. Genet.* 95(3):433–

435.

81. Saranza G, Grütz K, Klein C, Westenberger A, Lang AE. (2020) Primary brain calcification due to a homozygous MYORG mutation causing isolated paroxysmal kinesigenic dyskinesia. *Brain.* 143(5):e36.

82. Taglia I, Kuipers DJS, Breedveld GJ, et al. (2019) Primary familial brain calcification caused by MYORG mutations in an Italian family. *Park. Relat. Disord.* 67:24–26.

83. Ramos EM, Roca A, Chumchim N, et al. (2019) Primary familial brain calcification caused by a novel homozygous MYORG mutation in a consanguineous Italian family. *Neurogenetics.* 20(2):99–102.

84. Schottlaender LV, Abeti R, Jaunmuktane Z, et al. (2020) Bi-allelic JAM2 Variants Lead to Early-Onset Recessive Primary Familial Brain Calcification. *Am. J. Hum. Genet.* 106(3):412–421.

85. Chen Y, Cen Z, Chen X, et al. (2020) MYORG mutation heterozygosity is associated with brain calcification. *Mov. Disord.* 35(4):679–686.

86. Crow YJ. (2016) Aicardi-Goutières Syndrome Summary. *Gene reviews.* 1–29.

87. Adang L, Gavazzi F, De Simone M, et al. (2020) Developmental Outcomes of Aicardi Goutières Syndrome. *J. Child Neurol.* 35(1):7–16.

88. Al Mutairi F, Alfadhel M, Nashabat M, et al. (2018) Phenotypic and Molecular Spectrum of Aicardi-Goutières Syndrome: A Study of 24 Patients. *Pediatr. Neurol.* 78:35–40.

89. Garau J, Cavallera V, Valente M, et al. (2019) Molecular Genetics and Interferon Signature in the Italian Aicardi Goutières Syndrome Cohort: Report of 12 New Cases and Literature Review. *J. Clin. Med.* 8(5):750.

90. Rice GI, Park S, Gavazzi F, et al. (2020) Genetic and phenotypic spectrum associated with IFIH1 gain-of-function. *Hum. Mutat.* 41(4):837–849.

91. Videira G, Malaquias MJ, Laranjinha I, Martins R, Taipa R, Magalhães M. (2020) Diagnosis of Aicardi-Goutières Syndrome in Adults: A Case Series. *Mov. Disord. Clin. Pract.* 7(3):303–307.

92. Rice G, Patrick T, Parmar R, et al. (2007) Clinical and molecular phenotype of Aicardi-Goutières syndrome. *Am. J. Hum. Genet.* 81(4):713–725.

93. Crow YJ. (2005) Aicardi-Goutières Syndrome Summary. *Gene Rev.* 1–29.

94. Crow YJ, Manel N. (2015) Aicardi-Goutières syndrome and the type I interferonopathies. *Nat. Rev. Immunol.* 15(7):429–440.

95. Hogarth P. (2015) Neurodegeneration with Brain Iron Accumulation : Diagnosis and Management. 8(1):1–13.

96. Scheiber IF, Brůha R, Dušek P. (2017) Pathogenesis of Wilson disease. *Handb Clin Neurol.* 142:43–55.

97. Marti-Sanchez L, Ortigoza-Escobar JD, Darling A, et al. (2018) Hypermanganesemia due to mutations in SLC39A14: Further insights into Mn deposition in the central nervous system. *Orphanet J. Rare Dis.* 13(1):28.

98. Majid DS, Aron AR, Thompson W, et al. (2011) Basal ganglia atrophy in prodromal Huntington's disease is detectable over one year using automated segmentation. *Mov Disord.* 26(14):2544–2551.

99. Saint-Val L, Courtin T, Charles P, et al. (2019) GJA1 variants cause spastic paraplegia associated with cerebral hypomyelination. *Am. J. Neuroradiol.* 40(5):788–791.

100. La Piana R, Tonduti D, Gordish Dressman H, et al. (2014) Brain Magnetic Resonance Imaging (MRI) Pattern Recognition in Pol III-related Leukodystrophies. *J Child Neurol.* 29(2):214–220.

101. Biomarkers Definitions Working Group. (2001) Biomarkers and surrogate endpoints: Preferred definitions and conceptual framework. *Clin. Pharmacol. Ther.* 69(3):89–95.

102. Strimbu K, Tavel JA. (2010) What are biomarkers?. *Curr Opin HIV AIDS*. 5(6):463-466.

103. Ortigoza-Escobar JD, Molero-Luis M, Arias A, et al. (2016) Free-thiamine is a potential biomarker of Thiamine transporter-2 deficiency: A treatable cause of Leigh syndrome. *Brain.* 139(Pt 1):31–38.

104. Mayr JA, Freisinger P, Schlachter K, et al. (2011) Thiamine pyrophosphokinase deficiency in encephalopathic children with defects in the pyruvate oxidation pathway. *Am. J. Hum. Genet.* 89(6):806–812.

105. Rice GI, Kasher PR, Forte GM, et al. (2012) Mutations in ADAR1 cause Aicardi-Goutières syndrome associated with a type I interferon signature. *Nat Genet.* 44(11):1243–1248.

106. Molero-Luis M, Fernández-Ureña S, Jordán I, et al. (2013) Cerebrospinal fluid neopterin analysis in neuropediatric patients: Establishment of a new cut off-value for the identification of inflammatory-immune mediated processes. *PLoS One.* 8(12):e83237.

107. Dale RC, Brilot F, Fagan E, Earl J. (2009) Cerebrospinal fluid neopterin in paediatric neurology: A marker of active central nervous system inflammation. *Dev. Med. Child Neurol.* 51(4):317–323.

108. Li SJ, Jiang L, Fu X, et al. (2014) Pallidal index as biomarker of manganese brain accumulation and associated with manganese levels in blood: A meta-analysis. *PLoS One.* 9(4):e93900.

109. Stamelou M, Tuschl K, Chong WK, et al. (2012) Dystonia with brain manganese accumulation resulting from SLC30A10 mutations: A new treatable disorder. *Mov. Disord.* 27(10):1317–1322.

110. Roos PM, Vesterberg O, Syversen T, Flaten TP, Nordberg M. (2013) Metal concentrations in cerebrospinal fluid and blood plasma from patients with amyotrophic lateral sclerosis. *Biol. Trace Elem. Res.* 151(2):159–170.

111. Krieger D, Krieger S, Jansen O, Gass P, Theilmann L, Lichtnecker H. (1995) Manganese and chronic hepatic encephalopathy. *Lancet.* 346(8970):270-274.

112. Samorodnitsky E, Datta J, Jewell BM, et al. (2015) Comparison of custom capture for targeted next-generation DNA sequencing. *J. Mol. Diagnostics.* 17(1):64–75.

113. Dillon OJ, Lunke S, Stark Z, et al. (2018) Exome sequencing has higher diagnostic yield compared to simulated disease-specific panels in children with suspected monogenic disorders. *Eur. J. Hum. Genet.* 26(5):644–651.

114. Sun Y, Ruivenkamp CA, Hoffer MJ, et al. (2015) Next-Generation Diagnostics:

Gene Panel, Exome, or Whole Genome?. *Hum. Mutat.* 36(6):648–655.

115. Endris V, Buchhalter I, Allgäuer M, et al. (2019) Measurement of tumor mutational burden (TMB) in routine molecular diagnostics: in silico and real-life analysis of three larger gene panels. *Int. J. Cancer*. 144(9):2303–2312.

116. Lionel AC, Costain G, Monfared N, et al. (2018) Improved diagnostic yield compared with targeted gene sequencing panels suggests a role for whole-genome sequencing as a first-tier genetic test. *Genet. Med.* 20(4):435–443.

117. Vaz-Drago R, Custódio N, Carmo-Fonseca M. (2017) Deep intronic mutations and human disease. *Hum. Genet.* 136(9):1093–1111.

118. Pfundt R, Del Rosario M, Vissers LELM, et al. (2017) Detection of clinically relevant copy-number variants by exome sequencing in a large cohort of genetic disorders. *Genet. Med.* 19(6):667–675.

119. Enomoto Y, Tsurusaki Y, Yokoi T, et al. (2020) CNV analysis using whole exome sequencing identified biallelic CNVs of VPS13B in siblings with intellectual disability. *Eur. J. Med. Genet.* 63(1):103610.

120. Wang Z, Gerstein M, Snyder M. (2009) RNA-Seq: a revolutionary tool for transcriptomics. *Nat Rev Genet.* 10(1):57–63.

121. Richards CS, Bale S, Bellissimo DB, et al. (2008) ACMG recommendations for standards for interpretation and reporting of sequence variations: Revisions 2007. *Genet. Med.* 10(4):294–300.

122. Li Q, Wang K. (2017) InterVar: Clinical Interpretation of Genetic Variants by the 2015 ACMG-AMP Guidelines. *Am. J. Hum. Genet.* 100(2):267–280.

123. Kopanos C, Tsiolkas V, Kouris A, et al. (2019) VarSome: the human genomic variant search engine. *Bioinformatics.* 35(11):1978–1980.

124. Rentzsch P, Witten D, Cooper GM, Shendure J, Kircher M. (2019) CADD: Predicting the deleteriousness of variants throughout the human genome. *Nucleic Acids Res.* 47(D1):D886–D894.

125. Schwarz JM, Cooper DN, Schuelke M, Seelow D. (2014) Mutationtaster2: Mutation

prediction for the deep-sequencing age. *Nat. Methods.* 11(4):361–362.

126. Choi Y, Chan AP. (2015) PROVEAN web server: A tool to predict the functional effect of amino acid substitutions and indels. *Bioinformatics.* 31(16):2745–2747.

127. Adzhubei I, Jordan DM, Sunyaev SR. (2013) Predicting functional effect of human missense mutations using PolyPhen-2. *Curr Protoc Hum Genet.* Chapter 7:Unit7.20.

128. Desmet FO, Hamroun D, Lalande M, Collod-Béroud G, Claustres M, Béroud C. (2009) Human Splicing Finder: An online bioinformatics tool to predict splicing signals. *Nucleic Acids Res.* 37(9):e67.

129. Rice GI, Kitabayashi N, Barth M, et al. (2017) Genetic, Phenotypic, and Interferon Biomarker Status in ADAR1-Related Neurological Disease. *Neuropediatrics* 48(3):166–184.

130. Baide-Mairena H, Gaudó P, Marti-Sánchez L, et al. (2019) Mutations in the mitochondrial complex I assembly factor NDUFAF6 cause isolated bilateral striatal necrosis and progressive dystonia in childhood. *Mol. Genet. Metab.* 126(3):250–258.

131. Ortigoza-Escobar JD, Molero-Luis M, Arias A, et al. (2016) Treatment of genetic defects of thiamine transport and metabolism. *Expert Rev. Neurother.* 16(7):755–763.

132. Ortigoza-Escobar JD, Alfadhel M, Molero-Luis M, et al. (2017) Thiamine deficiency in childhood with attention to genetic causes: Survival and outcome predictors. *Ann. Neurol.* 82(3):317–330.

133. Ortega-Moreno L, Giráldez BG, Soto-Insuga V, et al. (2017) Molecular diagnosis of patients with epilepsy and developmental delay using a customized panel of epilepsy genes. *PLoS One.* 12(11):e0188978.

134. Kim JH, Seo GH, Kim GH, et al. (2019) Targeted Gene Panel Sequencing for Molecular Diagnosis of Kallmann Syndrome and Normosmic Idiopathic Hypogonadotropic Hypogonadism. *Exp. Clin. Endocrinol. Diabetes.* 127(8):538–544.

135. Pronicka E, Piekutowska-Abramczuk D, Ciara E, et al. (2016) New perspective in diagnostics of mitochondrial disorders: Two years' experience with whole-exome sequencing at a national paediatric centre. *J. Transl. Med.* 14(1):174.

136. Rosenberg MJ, Agarwala R, Bouffard G, et al. (2002) Mutant deoxynucleotide carrier is associated with congenital microcephaly. *Nat. Genet.* 32(1):175–179.

137. Gowda VK, Srinivasan VM, Jehta K, Bhat MD. (2019) Bilateral Striatal Necrosis with Polyneuropathy with a Novel SLC25A19 (Mitochondrial Thiamine Pyrophosphate Carrier OMIMI*606521) Mutation: Treatable Thiamine Metabolic Disorder-A Report of Two Indian Cases. *Neuropediatrics.* 50(5):313–317.

138. Bottega R, Perrone MD, Vecchiato K, et al. (2019) Functional analysis of the third identified SLC25A19 mutation causative for the thiamine metabolism dysfunction syndrome 4. *J Hum Genet.* 64(11):1075–1081.

139. Alfadhel M, Umair M, Almuzzaini B, et al. (2019) Targeted SLC19A3 gene sequencing of 3000 Saudi newborn: a pilot study toward newborn screening. *Ann. Clin. Transl. Neurol.* 6(10):2097–2103.

140. Alfadhel M, Tabarki B. (2018) SLC19A3 Gene Defects Sorting the Phenotype and Acronyms: Review. *Neuropediatrics.* 49(2):83–92.

141. Abouelhoda M, Sobahy T, El-Kalioby M, et al. (2016) Clinical genomics can facilitate countrywide estimation of autosomal recessive disease burden. *Genet. Med.* 18(12):1244–1249.

142. Wagner M, Berutti R, Lorenz-Depiereux B, et al. (2019) Mitochondrial DNA mutation analysis from exome sequencing-A more holistic approach in diagnostics of suspected mitochondrial disease. *J Inherit Metab Dis*. 42(5):909-917.

143. Taylor JC, Martin HC, Lise S, et al. (2015) Factors influencing success of clinical genome sequencing across a broad spectrum of disorders. *Nat Genet.* 47(7):717-726.

144. Marti-Sanchez L, Baide-Mairena H, Marcé-Grau A, et al. (2020) Delineating the neurological phenotype in children with defects in the ECHS1 or HIBCH gene. *J. Inherit. Metab. Dis.* 10.1002/jimd.12288.

145. Zhang Y, Zhang Y, Zhang VW, Zhang C, Ding H, Yin A. (2019) Mutations in both SAMD9 and SLC19A2 genes caused complex phenotypes characterized by recurrent infection, dysphagia and profound deafness - A case report for dual diagnosis. *BMC Pediatr.* 19(1):364.

146. Mencacci NE, Erro R, Wiethoff S, et al. (2015) ADCY5 mutations are another cause of benign hereditary chorea. *Neurology.* 85(1):80–88.

147. Chen DH, Méneret A, Friedman JR, et al. (2015) ADCY5-related dyskinesia: Broader spectrum and genotype-phenotype correlations. *Neurology.* 85(23)2026–2035.

148. Szklarczyk D, Gable AL, Lyon D, et al. (2019) STRING v11: Protein-protein association networks with increased coverage, supporting functional discovery in genome-wide experimental datasets. *Nucleic Acids Res.* 47(D1):D607–D613.

149. Wang JZ, Du Z, Payattakool R, Yu PS, Chen CF. (2007) A new method to measure the semantic similarity of GO terms. *Bioinformatics.* 23(10):1274–1281.

150. Van der Auwera GA, Carneiro MO, Hartl C, et al. (2013) From FastQ data to high confidence variant calls: the Genome Analysis Toolkit best practices pipeline. *Curr Protoc Bioinformatics.* 43(1110):11.10.1-11.10.33.

151. Salfati EL, Spencer EG, Topol SE, et al. (2019) Re-analysis of whole-exome sequencing data uncovers novel diagnostic variants and improves molecular diagnostic yields for sudden death and idiopathic diseases. *Genome Med.* 11(1):83.

152. King DA, Sifrim A, Fitzgerald TW, et al. (2017) Detection of structural mosaicism from targeted and whole-genome sequencing data. *Genome Res.* 27(10):1704–1714.

153. Frésard L, Smail C, Ferraro NM, et al. (2019) Identification of rare-disease genes using blood transcriptome sequencing and large control cohorts. *Nat Med.* 25(6):911-919.

154. Semeraro M, Boenzi S, Carrozzo R, et al. (2018) The urinary organic acids profile in single large-scale mitochondrial DNA deletion disorders. *Clin. Chim. Acta.* 481:156–160.

155. Tetreault M, Fahiminiya S, Antonicka H, et al. (2015) Whole-exome sequencing identifies novel ECHS1 mutations in Leigh syndrome. *Hum. Genet.* 134(9):981–991.

156. Peters H, Buck N, Wanders R, et al. (2014) ECHS1 mutations in Leigh disease: A new inborn error of metabolism affecting valine metabolism. *Brain.* 137(Pt 11):2903–2908.

157. Sakai C, Yamaguchi S, Sasaki M, Miyamoto Y, Matsushima Y, Goto Y. (2015)

ECHS1 mutations cause combined respiratory chain deficiency resulting in leigh syndrome. *Hum. Mutat.* 36(2):232–239.

158. Haack TB, Jackson CB, Murayama K, et al. (2015) Deficiency of ECHS1 causes mitochondrial encephalopathy with cardiac involvement. *Ann. Clin. Transl. Neurol.* 2(5):492-509.

159. Yamada K, Aiba K, Kitaura Y, et al. (2015) Clinical, biochemical and metabolic characterisation of a mild form of human short-chain enoyl-CoA hydratase deficiency: Significance of increased n-acetyl-s-(2-carboxypropyl)cysteine excretion. *J. Med. Genet.* 52(10):691–698.

160. Ganetzky RD, Bloom K, Ahrens-Nicklas R, et al. (2016) ECHS1 Deficiency as a Cause of Severe Neonatal Lactic Acidosis. *JIMD Rep.* 30:33-37.

161. Ferdinandusse S, Friederich MW, Burlina A, et al. (2015) Clinical and biochemical characterization of four patients with mutations in ECHS1. *Orphanet J. Rare Dis.* 10:79.

162. Nair P, Hamzeh AR, Mohamed M, Malik EM, Al-Ali MT, Bastaki F. (2016) Novel ECHS1 mutation in an Emirati neonate with severe metabolic acidosis. *Metab. Brain Dis.* 31(5):1189–1192.

163. Olgiati S, Skorvanek M, Quadri M, et al. (2016) Paroxysmal exercise-induced dystonia within the phenotypic spectrum of ECHS1 deficiency. *Mov. Disord.* 31(7):1041–1048.

164. Bedoyan JK, Yang SP, Ferdinandusse S, et al. (2017) Lethal neonatal case and review of primary short-chain enoyl-CoA hydratase (SCEH) deficiency associated with secondary lymphocyte pyruvate dehydrogenase complex (PDC) deficiency. *Mol. Genet. Metab.* 120(4):342–349.

165. Huffnagel IC, Redeker EJW, Reneman L, Vaz FM, Ferdinandusse S, Poll-The BT. (2017) Mitochondrial Encephalopathy and Transient 3Methylglutaconic Aciduria in ECHS1 Deficiency: LongTerm Follow-Up. *JIMD Rep.* 39:83-87.

166. Balasubramaniam S, Riley LG, Bratkovic D, et al. (2017) Unique presentation of cutis laxa with Leigh-like syndrome due to ECHS1 deficiency. *J. Inherit. Metab. Dis.* 40(5):745–747.

167. Fitzsimons PE, Alston CL, Bonnen PE, et al. (2018) Clinical, biochemical, and genetic features of four patients with short-chain enoyl-CoA hydratase (ECHS1) deficiency. *Am. J. Med. Genet. A.* 176(5):1115–1127.

168. Mahajan A, Constantinou J, Sidiropoulos C. (2017) ECHS1 deficiency-associated paroxysmal exercise-induced dyskinesias: case presentation and initial benefit of intervention. *J. Neurol.* 264(1):185–187.

169. Carlston CM, Ferdinandusse S, Hobert JA, Mao R, Longo N. (2019) Extrapolation of Variant Phase in Mitochondrial Short-Chain Enoyl-CoA Hydratase (ECHS1) Deficiency. *JIMD Rep.*;43:103-109.

170. Uchino S, Iida A, Sato A, et al. (2019) A novel compound heterozygous variant of ECHS1 identified in a Japanese patient with Leigh syndrome. *Hum. Genome Var.* 6:19.

171. Stark Z, Tan TY, Chong B, et al. (2016) A prospective evaluation of whole-exome sequencing as a first-tier molecular test in infants with suspected monogenic disorders. *Genet. Med.* 18(11):1090–1096.

172. Korenke G, Nuoffer JM, Alhaddad B, Mayr H, Prokisch H, Haack TB. (2016) Paroxysmal Dyskinesia in ECHS1 Defect with Globus Pallidus Lesions. *Neuropediatrics.* 47:518.

173. Brown GK, Hunt SM, Scholem R, et al. (1982) beta-hydroxyisobutyryl coenzyme A deacylase deficiency: a defect in valine metabolism associated with physical malformations. *Pediatrics.* 70(4):532-538.

174. Loupatty FJ, Clayton PT, Ruiter JP, et al. (2007) Mutations in the gene encoding 3-hydroxyisobutyryl-CoA hydrolase results in progressive infantile neurodegeneration. *Am. J. Hum. Genet.* 80(1):195–199.

175. Ferdinandusse S, Waterham HR, Heales SJ, et al. (2013) HIBCH mutations can cause Leigh-like disease with combined deficiency of multiple mitochondrial respiratory chain enzymes and pyruvate dehydrogenase. *Orphanet J. Rare Dis.* 8:188.

176. Yamada K, Naiki M, Hoshino S, et al. (2014) Clinical and biochemical characterization of 3-hydroxyisobutyryl-CoA hydrolase (HIBCH) deficiency that causes Leigh-like disease and ketoacidosis. *Mol. Genet. Metab. Reports.* 1:455–460.

177. Reuter MS, Sass JO, Leis T, et al. (2014) HIBCH deficiency in a patient with phenotypic characteristics of mitochondrial disorders. *Am. J. Med. Genet. A.* 164A(12):3162–3169.

178. Yang HY, Wu LW, Deng XL, Yin F, Yang LF. (2018) Diagnosis and treatment of 3-hydroxyisobutyryl-CoA hydrolase deficiency: A case report and literature review. *Zhongguo Dang Dai Er Ke Za Zhi.* 20(8):647–651.

179. Peters H, Ferdinandusse S, Ruiter JP, Wanders RJ, Boneh A, Pitt J. (2015) Metabolite studies in HIBCH and ECHS1 defects: Implications for screening. *Mol Genet Metab.* 115(4):168–173.

180. Soler-Alfonso C, Enns GM, Koenig MK, Saavedra H, Bonfante-Mejia E, Northrup H. (2015) Identification of HIBCH gene mutations causing autosomal recessive Leigh syndrome: A gene involved in valine metabolism. *Pediatr. Neurol.* 52(3):361–365.

181. Stiles AR, Ferdinandusse S, Besse A, et al. (2015) Successful diagnosis of HIBCH deficiency from exome sequencing and positive retrospective analysis of newborn screening cards in two siblings presenting with Leigh's disease. *Mol. Genet. Metab.* 115(4):161–167.

182. Schottmann G, Sarpong A, Lorenz C, et al. (2016) A movement disorder with dystonia and ataxia caused by a mutation in the HIBCH gene. *Mov. Disord.* 31(11):1733–1739.

183. Reuter MS, Tawamie H, Buchert R, et al. (2017) Diagnostic yield and novel candidate genes by exome sequencing in 152 consanguineous families with neurodevelopmental disorders. *JAMA Psychiatry.* 74(3):293–299.

184. Tan H, Chen X, Lv W, Linpeng S, Liang D, Wu L. (2018) Truncating mutations of HIBCH tend to cause severe phenotypes in cases with HIBCH deficiency: A case report and brief literature review. *J. Hum. Genet.* 63(7):851–855.

185. Karimzadeh P, Saberi M, Sheidaee K, Nourbakhsh M, Keramatipour M. (2019) 3-Hydroxyisobutyryl-CoA hydrolase deficiency in an Iranian child with novel HIBCH compound heterozygous mutations. *Clin. Case Reports.* 7(2):375–380.

186. Candelo E, Cochard L, Caicedo-Herrera G, et al. (2019) Syndromic progressive

neurodegenerative disease of infancy caused by novel variants in HIBCH: Report of two cases in Colombia. *Intractable Rare Dis. Res.* 8(3):187–193.

187. Bugiardini E, Pope S, Feichtinger RG, et al. (2019) Utility of Whole Blood Thiamine Pyrophosphate Evaluation in TPK1-Related Diseases. *J. Clin. Med.* 8(7):991.

188. Ortigoza-Escobar JD, Serrano M, Molero M, et al. (2014) Thiamine transporter-2 deficiency: Outcome and treatment monitoring. *Orphanet J. Rare Dis.* 9:92.

189. Costantini A, Laureti T, Pala MI, et al. (2016) Long-term treatment with thiamine as possible medical therapy for Friedreich ataxia. *J. Neurol.* 263(11):2170–2178.

190. Eshak ES, Arafa AE. (2018) Thiamine deficiency and cardiovascular disorders. *Nutr Metab Cardiovasc Dis*. 28(10):965-972.

191. Lu'o'ng KV, Nguyễn LT. (2013) The role of thiamine in cancer: possible genetic and cellular signaling mechanisms. *Cancer Genomics Proteomics.* 10(4):169–185.

192. Gibson GE, Hirsch JA, Fonzetti P, Jordan BD, Cirio RT, Elder J. (2016) Vitamin B1 (thiamine) and dementia. *Ann N Y Acad Sci.* 1367(1):21–30.

193. Zeglam A, Abugrara A, Kabuka M. (2019) Autosomal-recessive iron deficiency anemia, dystonia and hypermanganesemia caused by new variant mutation of the manganese transporter gene SLC39A14. *Acta Neurol. Belg.* 119(3):379–384.

194. Juneja M, Shamim U, Joshi A, et al. (2018) A novel mutation in SLC39A14 causing hypermanganesemia associated with infantile onset dystonia. *J. Gene Med.* 20(4):e3012.

195. Du K, Liu MY, Pan YZ, Zhong X, Wei MJ. (2018) Association of circulating manganese levels with Parkinson's disease: A meta-analysis. *Neurosci Lett.* 665:92-98.

196. Báez LM. (2014) Punción lumbar. Condiciones e indicaciones en pediatría. *Acta Pediatr. Mex.* 35:423–427.

197. Anagianni S, Tuschl K. (2019) Genetic Disorders of Manganese Metabolism. *Curr. Neurol. Neurosci. Rep.* 19(6):33.

198. Tuschl K, Gregory A, Meyer E, et al. (2017) SLC39A14 Deficiency. *GeneReviews*.

199. Rodan LH, Hauptman M, D'Gama AM, et al. (2018) Novel founder intronic variant

in SLC39A14 in two families causing Manganism and potential treatment strategies. *Mol Genet Metab.* 124(2):161–167.

200. Yubero D, Brandi N, Ormazabal A, et al. (2016) Targeted next generation sequencing in patients with inborn errors of metabolism. *PLoS One.* 11(5):e0156359.

201. Rahman S, Blok RB, Dahl HH, et al. (1996) Leigh syndrome: Clinical features and biochemical and DNA abnormalities. *Ann. Neurol.* 39(3):343–351.

202. Miyazaki H, Oyama F, Inoue R, et al. (2014) Singular localization of sodium channel β4 subunit in unmyelinated fibres and its role in the striatum. *Nat. Commun.* 5:5525.

203. Pan X, Li Z, Huang X, et al. (2019) Molecular basis for pore blockade of human Na+ channel Nav1.2 by the μ-conotoxin KIIIA. *Science*. 363(6433):1309-1313.

204. Kitanaka N, Kitanaka J, Walther D, Wang XB, Uhl GR. (2003) Comparative inter-strain sequence analysis of the putative regulatory region of murine psychostimulant-regulated gene GNB1 (G protein beta 1 subunit gene). *DNA Seq.* 14(4):257–263.

205. Chen PS, Yeh TL, Lee IH, et al. (2011) Effects of C825T polymorphism of the GNB3 gene on availability of dopamine transporter in healthy volunteers--a SPECT study. *Neuroimage*. 56(3):1526-1530.

206. Li X, Carreria MB, Witonsky KR, et al. (2018) Role of Dorsal Striatum Histone Deacetylase 5 in Incubation of Methamphetamine Craving. *Biol Psychiatry*. 84(3):213-222.

207. Xie K, Masuho I, Brand C, Dessauer CW, Martemyanov KA. (2012) The Complex of G Protein Regulator RGS9-2/Gβ5 Controls Sensitization and Signaling Kinetics of Type 5 Adenylyl Cyclase. *Sci Signal.* 5(239):ra63.

208. Ray LA, Courtney KE, Hutchison KE, Mackillop J, Galvan A, Ghahremani DG. (2014) Initial evidence that Oprm1 genotype moderates ventral and dorsal striatum functional connectivity during alcohol cues. *Alcohol Clin Exp Res.* 38(1):78–89.

209. Mulligan MK, Dubose C, Yue J, Miles MF, Lu L, Hamre KM. (2013) Expression, covariation, and genetic regulation of miRNA biogenesis genes in brain supports their role in addiction, psychiatric disorders, and disease. *Front. Genet.* 4:126.

210. Li S, Zhu J, Fu H, et al. (2012) Hepato-specific microRNA-122 facilitates accumulation of newly synthesized miRNA through regulating PRKRA. *Nucleic Acids Res.* 40(2):884–891.

211. Meyer C, Garzia A, Mazzola M, Gerstberger S, Molina H, Tuschl T. (2018) The TIA1 RNA-Binding Protein Family Regulates EIF2AK2-Mediated Stress Response and Cell Cycle Progression. *Mol. Cell.* 69(4):622-635.e6.

212. Piekutowska-Abramczuk D, Mierzewska H, Bekiesińska-Figatowska M, et al. (2016) Bilateral striatal necrosis caused by ADAR mutations in two siblings with dystonia and freckles-like skin changes that should be differentiated from Leigh syndrome. *Folia Neuropathol*. 54(4):405-409.

ANEXOS

Tabla A1: Números MIM de los distintos fenotipos y genes relacionados con las alteraciones de los ganglios basales

Números MIM de los genes							
Gen	**MIM**	**Gen**	**MIM**	**Gen**	**MIM**	**Gen**	**MIM**
ABCD1	300371	FOXRED1	613622	NDP	300658	RNASEH2C	610330
ADAR	146920	FTL1	NR	NDUFA1	300078	RNF213	613768
AIFM1	300169	GALC	606890	NDUFA10	603835	RRM2B	604712
AQP2	107777	GCDH	608801	NDUFA12	614530	RTEL1	608833
ARSA	607574	GCM2	603716	NDUFA2	602137	SAMHD1	606754
ATN1	607462	GFAP	137780	NDUFA4	603833	SLC25A19	606521
ATP13A2	610513	GFM1	606639	NDUFA9	603834	SCO2	604272
ATP7B	606882	GFM2	606544	NDUFAF2	609653	SDHA	600857
AVP	192340	GJA1	121014	NDUFAF4	611776	SDHAF1	612848
AVPR2	300538	GNA11	139313	NDUFAF5	612360	SDHB	185470
BCS1L	603647	GNAS	139320	NDUFAF6	612392	SERAC1	614725
BOLA3	613183	GTF2H5	608780	NDUFAF8 (C17ORF89)	618461	SLC12A3	600968
BTD	609019	GTPBP3	608536	NDUFB8	602140	SLC19A2	603941
C12ORF65	613541	HEXA	606869	NDUFS1	157655	SLC19A3	606152
C19ORF12	614297	HEXB	606873	NDUFS2	602985	SLC20A2	158378
C1QB	120570	HIBCH	610690	NDUFS3	603846	SLC25A4	103220
CA2	611492	IARS2	612801	NDUFS4	602694	SLC25A46	610826
CASR	601199	IFIH1	606951	NDUFS6	603848	SLC30A10	611146
CLPB	616254	ISG15	147571	NDUFS7	601825	SLC39A14	608736
COASY	609855	JAM2	606870	NDUFS8	602141	SLC39A8	608732
COL4A1	120130	JAM3	606871	NDUFV1	161015	SLC46A1	611672
COL4A2	120090	LIAS	607031	NDUFV2	600532	SMARCAL1	606622
COQ9	612837	LIPT1	610284	NF1	613113	SPG7	602783
COX10	602125	LRPPRC	607544	NF2	607379	SQUOR	NR
COX15	603646	MFN2	608507	NHP2 (NOLA)	606470	STX16	603666
COX8A	123870	MGP	154870	NOP10 (NOLA3)	224230	SUCLA2	603921

Gen	MIM	Gen	MIM	Gen	MIM	Gen	MIM
CP	117700	MPLKIP	609188	NUBPL	613621	SUCLG1	611224
CTC1	613129	MPV17	137960	NUP62	605815	SUOX	606887
CYP2U1	610670	MRPS34	611994	NUP62	605815	SURF1	185620
DCAF17	612515	MRPS39	NR	OCLN	602876	SYNE1	608441
DDB2	600811	MTATP6	516060	PAH	612349	TACO1	612958
DHFR	126060	MTCO3	516050	PANK2	606157	TBCE	604934
DKC1	300126	MTFD1	NR	PCDH12	605622	TBX1	602054
DLAT	608770	MTFMT	611766	PDGFB	190040	TERC	602322
DLD	238331	MTHFR	607093	PDGFRB	173410	TERT	187270
DNM1L	603850	MTND1	516000	PDHA1	600502	TINF2	604319
EARS2	612799	MTND2	516001	PDHB	179060	TPK1	606370
ECHS1	602292	MTND3	516002	PDHX	608769	TREM2	605086
ERCC1	126380	MTND4	516003	PDSS2	610564	TREX1	606609
ERCC2	126340	MTND5	516005	PET100	614770	TRMU	610230
ERCC3	133510	MTND6	516006	PLA2G6	603604	TSC1	605284
ERCC4	133520	MTTC	590020	PNPT1	610316	TSC2	191092
ERCC5	133530	MTTH	590040	POLG	174763	TSFM	604723
ERCC6	609413	MTTI	590045	POLG2	604983	TTC19	613814
ERCC8	609412	MTTK	590060	POLH	603968	TUBB4A	602662
ETHE1	608451	MTTL1	590050	POLR3A	614258	TWNK	606075
FA2H	611026	MTTL2	590055	POLR3B	614366	TYROBP	604142
FAM111A	615292	MTTQ	590030	PSMB8	177046	UQCRQ	612080
FAM20C	611061	MTTS1	590080	PTH	168450	WDR45	300526
FARS2	611592	MTTS2	590085	QDPR	612676	WFS1	606201
FBXL4	605654	MTTV	590105	RANBP2	601181	WRAP53	612661
FGF23	605380	MTTW	590095	RNASEH1	604123	XPA	611153
FLVCR2	610865	MYORG	618255	RNASEH2A	606034	XPC	613208
FOLR1	136430	NARS2	612803	RNASEH2B	610326	XPR1	605237

Números MIM de los fenotipos			
Fenotipo	**MIM**	**Fenotipo**	**MIM**
Síndrome de Aicardi-Goutieres 1	255750	Hypermanganesemia con distonia 2	617013
Síndrome de Aicardi-Goutieres 2	610181	Enfermedad de Krabbe	245200
Síndrome de Aicardi-Goutieres 3	610329	Síndrome de Leigh	256000
Síndrome de Aicardi-Goutieres 4	610333	Microcefalia, tipo Amish	607196
Síndrome de Aicardi-Goutieres 5	612952	Enfermedad MoyaMoya	252350
Síndrome de Aicardi-Goutieres 6	615010	NBIA 1	234200
Síndrome de Aicardi-Goutieres 7	615846	NBIA 2A	256600
BGC, idiopática, 1	213600	NBIA 2B	610217
BGC, idiopática, 4	615007	NBIA 3	606159
BGC, idiopática, 5	615483	NBIA 4	614298
BGC, idiopática, 6	616413	NBIA 5	300894
BGC, idiopática, 7	618317	NBIA 6	615643
BGC, idiopática, 8	618824	Fenilcetonuria	261600
Enfermedad de Coat	300216	Deficiencia de sulfito oxidase	272300
Síndrome de Cockayne A	216400	Síndrome de disfunción del metabolismo de tiamina 2	607483
Síndrome de Cockayne B	133540	Síndrome de disfunción del metabolismo de tiamina 4	613710
Síndrome de DiGeorge	188400	Síndrome de disfunción del metabolismo de tiamina 5	614458
Glutaricaciduria, type I	231670	Síndrome de TRMA	249270
Hypermanganesemia con distonia 1	613280	Enfermedad de Wilson	277900

Abreviaturas utilizadas: BGC: calcificación de los ganglios basales; NBIA: Neurodegeneración con acúmulos cerebrales de hierro; TRMA: Anemia megaloblástica con respuesta a tiamina

Tabla A2: Correlación entre los síntomas clínicos y los HPO (Human Phenotype Oncology)

Síntoma clínico	HPO	Síntoma clínico	HPO
Ausencia de reflejos	HP:0001284	Enfermedad del hígado	HP: 0001392
Ataxia	HP: 0001251	Anemia megaloblástica	HP: 0001889
Polineuropatía axonal	HP:0007327	Microcefalia	HP: 0000252
Bradiquinesia	HP: 0002067	Neutropenia	HP: 0001875
Signos bulbares	HP: 0002483	Nistagmo	HP: 0000639
Cardiomegalia	HP: 0001640	Oftalmoplegia	HP: 0000602
Cardiovascular	HP: 0001626	Opisthotonus	HP: 0002179
Atrofia cerebral	HP: 0002054	Parkinsonismo	HP: 0001300
Corea	HP: 0002072	Neuropatía periférica	HP: 0009830
Deterioro cognitivo	HP: 0000543	Retraso psicomotor	HP: 0001263
Contracturas	HP: 0001371	Regresión psicomotora	HP: 0002376
Criptorquidia	HP: 0000028	Ptosis	HP: 0000508
Retraso del desarrollo global	HP:0001263	Dificultad respiratoria	HP: 0002098
Diplopia	HP: 0000651	Insuficiencia respiratoria	HP: 0002878
Disartria	HP: 0001260	Rabdomiolisis	HP: 0003201
Disfagia	HP: 0002015	Rigidez	HP: 0002063
Distonia	HP: 0001332	Convulsiones	HP: 0001250
Encefalopatía	HP: 0001298	Sordera neurosensoria	HP: 0000407
Epilepsia	HP: 0001250	Baja estatura	HP: 0004322
Dificultades de la marcha	HP: 0001288	Habla arrastrada	HP: 0001350
Reflujo gastroesofágico	HP: 0002020	Cuadriplegia espástica	HP: 0002510
Dolor de cabeza	HP: 0002315	Espasticidad	HP: 0001257
Hepatomegalia	HP: 0002240	Estrabismo	HP: 0000486
Hiperquinesia	HP: 0002487	Apoplejía	HP: 0002401
Hiperreflexia	HP: 0001347	Taquicardia	HP: 0001649

Síntoma clínico	HPO	Síntoma clínico	HPO
Hipomimia	HP: 0000338	Taquipnea	HP: 0002789
Hipotensión	HP: 0002615	Talipes	HP: 0001883
Hipotermia	HP: 0002045	Trombocitopenia	HP: 0001873
Hipotonia	HP: 0001290	Temblor	HP: 0001337
Tiroiditis autoinmune	HP:0011771	Marcha inestable	HP:0006962
Irritabilidad	HP: 0000737	Vértigo	HP: 0002321
Ictericia	HP: 0000952	Pérdida de peso	HP: 0001824

Figura A1: Algoritmo general del proyecto.

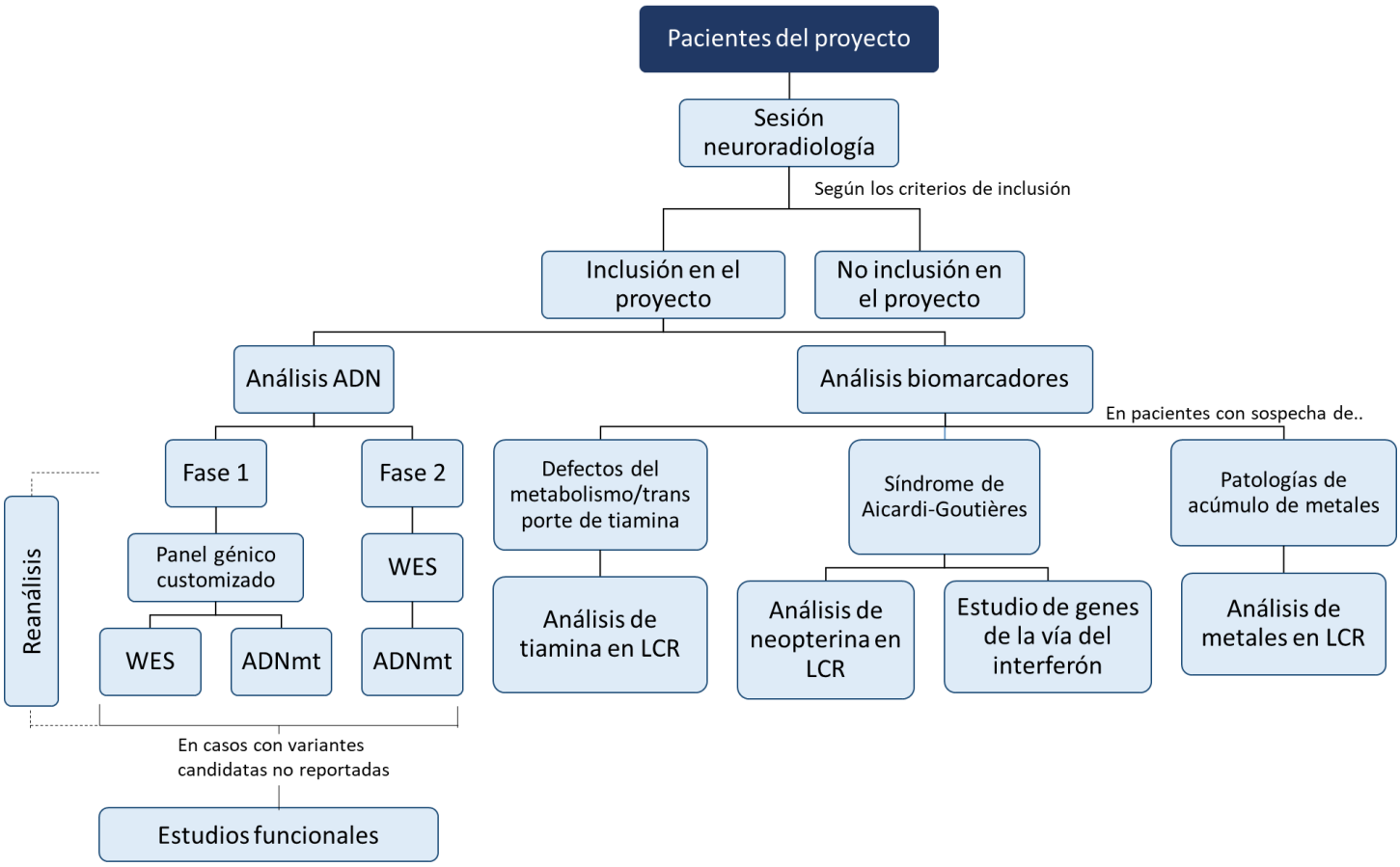

ADNmt: secuenciación completa de ADN mitocondrial. WES: secuenciación de exoma completo

Otras publicaciones

Vanegas MI, Marcé-Grau A, **Martí-Sánchez** L, Mellid S, Baide-Mairena H, Correa-Vela M, Cazurro A, Rodríguez C, Toledo L, Fernández-Ramos JA, Pons R, Aguilera-Albesa S, Martí MJ, Eiris J, Iglesias G, De Fabregues O, Maqueda E, Garriz-Luis M, Madruga M, Espinós C, Macaya A, Cabrera JC, Pérez-Dueñas B. Delineating the motor phenotype of SGCE-myoclonus dystonia syndrome. (2020) *Parkinsonism Relat Disord*. 80:165-174.

Ortigoza-Escobar JD, Alfadhel M, Molero-Luis M, Darin N, Spiegel R, de Coo IF, Gerards M, Taylor RW, Artuch R, Nashabat M, Rodríguez-Pombo P, Tabarki B, Pérez-Dueñas B, **Thiamine Deficiency Study Group**. Thiamine deficiency in childhood with attention to genetic causes: Survival and outcome predictors. (2017) *Ann Neurol*. 82(3):317-330.

Batllori M, Casado M, Sierra C, Salgado MC, **Marti-Sánchez L**, Maynou J, Fernandez G, Garcia-Cazorla A, Ormazabal A, Molero-Luis M, Artuch R. Effect of blood contamination of cerebrospinal fluid on amino acids, biogenic amines, pterins and vitamins. *Fluids Barriers CNS*. 2019;16(1):34.

Baide-Mairena H, Gaudó P, **Marti-Sánchez L**, Emperador S, Sánchez-Montanez A, Alonso-Luengo O, Correa M, Marcé-Grau A, Ortigoza-Escobar JD, Artuch R, Vázquez E, Del Toro M, Garrido-Pérez N, Ruiz-Pesini E, Montoya J, Bayona-Bafaluy MP, Pérez-Dueñas B. Mutations in the mitochondrial complex I assembly factor NDUFAF6 cause isolated bilateral striatal necrosis and progressive dystonia in childhood. *Mol Genet Metab*. 2019;126(3):250-258.

Rice GI, Kitabayashi N, Barth M, Briggs TA, Burton ACE, Carpanelli ML, Cerisola AM, Colson C, Dale RC, Danti FR, Darin N, De Azua B, De Giorgis V, De Goede CGL, Desguerre I, De Laet C, Eslahi A, Fahey MC, Fallon P, Fay A, Fazzi E, Gorman MP, Gowrinathan NR, Hully M, Kurian MA, Leboucq N, Lin JPSM, Lines MA, Mar SS, Maroofian R, **Martí-Sánchez L**, McCullagh G, Mojarrad M, Narayanan V, Orcesi S, Ortigoza-Escobar JD, Pérez-Dueñas B, Petit F, Ramsey KM, Rasmussen M, Rivier F, Rodríguez-Pombo P, Roubertie A, Stödberg TI, Toosi MB, Toutain A, Uettwiller F, Ulrick N, Vanderver A, Waldman A, Licingston JH, Crow YJ. Genetic, Phenotypic, and Interferon Biomarker Status in ADAR1-Related Neurological Disease. *Neuropediatrics*. 2017;48(3):166-184.

Darling A, Tello C, Martí MJ,Garrido C, Aguilera-Albesa S, Tomás-Vila M, Gastón I, Madruga M, González-Gutiérrez L, Ramos-Lizana J, Pujol M, Gavilán-Iglesias T, Tustin K, Lin JP, Zorzi G, Nardocci N, Martorell L, Lorenzo-Sanz G Gutiérrez F, García PJ, Vela L, Hernández-Lahoz C, Ortigoza-Escobar JD, **Martí-Sánchez L**, Moreira F, Coelho M, Correira-Guedes L, Castro-Caldas A, Ferreira J, Pires P, Costa C, Rego P, Magalhães M, Stamelou M, Cuadras-Pallejà D, Rodríguez-Blazquez C, Martínez-Martín P, Lupo V, Stefanis L, Pons R, Espinós C, Temudo T, Pérez-Dueñas B. Clinical rating scale for pantothenate kinase-associated neurodegeneration: A pilot study. *Mov Disord*. 2017;32(11):1620-1630.

Ortigoza-Escobar JD, Molero-Luis M, Arias A, **Martí-Sánchez L**, Rodríguez-Pombo P, Artuch R, Pérez-Dueñas B. Treatment of genetic defects of thiamine transport and metabolism. *Expert Rev Neurother*. 2016;16(7):755-763.